SCALE MODEL STUDIES OF DISPLACEMENT VENTILATION

by

GALIP MEHMET OKUTAN

B.S. , Mechanical Engineering
Middle East Technical University, Ankara, 1993

SUBMITTED TO THE DEPARTMENT OF ARCHITECTURE
IN PARTIAL FULFILLMENT OF THE REQUIREMENTS FOR THE DEGREE OF
MASTER OF SCIENCE IN BUILDING TECHNOLOGY
AT THE
MASSACHUSETTS INSTITUTE OF TECHNOLOGY
JUNE 1995

Signature of Author .....
Galip Mehmet Okutan, Department of Architecture
May 12, 1995

Certified by .....
Leon R. Glicksman, Professor of Building Technology
and Mechanical Engineering
Co-Thesis Supervisor

Certified by .....
Leslie K. Norford, Associate Professor of Building Technology
Co-Thesis Supervisor

Accepted by .....
Leon R. Glicksman
Chairman, Departmental Committee on Graduate Studies

Scale Model Studies of Displacement Ventilation

by
Galip Mehmet Okutan

Submitted to the Department of Architecture on May 12, 1995
in partial fulfillment of the requirements for the Degree of
Master of Science in Building Technology

Abstract

Displacement ventilation is an air conditioning method that provides conditioned air to indoor environments with the goal to improve air quality while reducing energy consumption. This study investigates the performance of displacement ventilation systems in open plan office environments, focusing on vertical temperature stratification. It explores the possibility of improving the performance of these systems by reducing the temperature stratification at lower levels and allowing them to operate with high cooling loads without exceeding thermal comfort limits.

An experimental setup consisting of a scale model of an open plan office room and equipment necessary to provide the experimental conditions was designed and constructed. Steady state experiments on displacement ventilation were conducted. The experiments simulated a variety of cases in terms of heat gain per area, air supply flow rate and slow mixing at lower levels. Temperature distributions in the model and fluid flow rates were measured. Flow visualization was performed to investigate the flow patterns in the office room.

The vertical temperature profiles for the considered cases were not linear. The vertical temperature stratification increased when the heat gain in the office increased. It was within the comfort limits for all simulated cases, except the case with the maximum heat gain ($38W/m^2$). The introduction of slow mixing at lower levels decreased the temperature differential in all experiments. This effect of slow mixing was more pronounced at lower heights. This suggested that displacement ventilation may accommodate higher cooling loads if slow mixing at the lower levels is provided. Flow visualization results indicated that the height of the stratification was about 1m above the floor. The plumes over the heat sources had different characteristics, implying the possible importance of the size, shape and spatial distribution of the heat sources.

Co-Thesis Supervisor: Leon R. Glicksman
Title: Professor of Building Technology and Mechanical Engineering

Co-Thesis Supervisor: Leslie K. Norford
Title: Associate Professor of Building Technology

To my parents

ACKNOWLEDGMENTS

First of all, I thank my advisors Leon Glicksman and Leslie Norford, for their enthusiasm and insight which made this study a more rewarding one for me. They have always provided me with the necessary guidance. Sadik Kakac, James Axley and my thesis reader Oral Buyukozturk have provided valuable direction.

Katherine Holden worked on the design and construction of the experimental setup. I am thankful for her cooperation and sharing of results. Annia Yiu and Peter Cho contributed to the preparation of the apparatus. Mark DeSimone and other friends at MIT have given valuable advice. Dorrit Schuchter has always helped when asked.

I thank Eda Akhunlar for her joy and her strong support that I needed. To Evren Unver, I give thanks for all his help and for being my editor. I thank Selin Sayek, Fethi Okyar, Emre Ozcan, Gonul Ozkul and Serpil Rosenfeld for their encouragement.

Finally, I thank my father and colleague Celal Okutan, for providing excellent advice and assistance throughout my studies. For my mother Oya Okutan and my sister Zeynep Okutan, I am very grateful for their continuous support of all my efforts and for being friends through difficult times.

TABLE OF CONTENTS

LIST OF TABLES

LIST OF FIGURES

NOMENCLATURE

υ	kinematic viscosity
β	coefficient of thermal expansion
ρ	density
α	specific heat
μ	dynamic viscosity
Π_1	first dimensionless parameter used in heat exchanger pressure drop calibration
Π_2	first dimensionless parameter used in heat exchanger pressure drop calibration
υ_m	kinematic viscosity in the model
ρ_m	density in the model
β_m	coefficient of thermal expansion in the model
υ_p	kinematic viscosity in the prototype
ρ_p	density in the prototype
β_p	coefficient of thermal expansion in the prototype
υ_r	kinematic viscosity scale ratio
ρ_r	density scale ratio
ΔT_m	temperature difference in the Grashof number for the model
ΔT_p	temperature difference in the Grashof number for the prototype
ΔT_r	temperature difference scale ratio
Ar	Archimedes number
c_p	specific heat
cp_m	specific heat in the model
cp_p	specific heat in the prototype
cp_r	specific heat scale ratio

g	gravitational acceleration
g'	modified gravitational acceleration term in the Archimedes number
g_m	gravitational acceleration in the model
g_p	gravitational acceleration in the prototype
Gr	Grashof number
Gr_m	Grashof number in the model
Gr_p	Grashof number in the prototype
k	conductivity
$K_{average}$	average of Ki values
Ki	constant relating heat exchanger pressure drop to the volumetric flow rate
L	characteristic length
L_m	length in the model
L_{model}	length in the model
L_p	length in the prototype
L_r	length scale ratio
P	pressure
P^*	dimensionless pressure
P_m	cooling in the model
P_p	cooling in the prototype
Pr	Prandtl number
P_r	cooling scale ratio
Q	volumetric flow rate in the heat exchanger
q_m	volumetric flow rate in the model
q_p	volumetric flow rate in the prototype
q_r	volumetric flow rate scale
Re	Reynolds number
Re_m	Reynolds number in the model
Re_p	Reynolds number in the prototype
T	temperature

T_∞ free stream temperature

T^* dimensionless temperature

T_{ref} reference temperature

T_s surface temperature

Tw_{real} total power consumption of the heat sources in the prototype

Tw_{scale} total power consumption of the heat sources in the model

u velocity in horizontal direction

u^* dimensionless velocity in the horizontal direction

V characteristic velocity

V_m velocity in the model

V_p velocity in the prototype

V_r velocity scale ratio

w velocity in the vertical direction

w_∞ free stream velocity in the vertical direction

w^* dimensionless velocity in the vertical direction

x horizontal coordinate

x^* dimensionless horizontal coordinate

z vertical coordinate

z^* dimensionless vertical coordinate

CHAPTER 1

INTRODUCTION

1.1. Commercial Buildings and the Indoor Environment

Buildings are structures constructed to be shelters for human. They offer protection from undesirable outside conditions and provide a comfortable and healthy indoor environment. They are integrated with mechanical equipment to help the building function efficiently. This equipment can range from elevators to refrigeration units, but in all cases they consume energy.

Building energy consumption constitutes an important fraction of the total energy consumption in the world, especially in developed countries where more comfortable and healthy indoor environments are demanded. In the United States, for example, residential and commercial building energy consumption accounts for 37% of the total national energy consumption. Commercial building energy consumption alone is 14% of the total, with approximately 90% of this energy derived from fossil fuels [1]. The fraction of the energy consumed in buildings in Britain is even larger, corresponding to nearly half of the total energy consumed there [2].

Building energy issues have assumed far greater importance as the limitations of the world's fossil fuel reserves have become increasingly apparent. The twenty years following the sharp increases in oil prices during 1970s, have been a period of intense change in the world energy balance. There has been a strong drive to reduce energy consumption. This

could be done in two fundamental ways, namely, austerity and efficiency [3]. Austerity stands for making do with less, whereas efficiency denotes efforts to provide the same level of service with less energy. An effective course of action may be some combination of both.

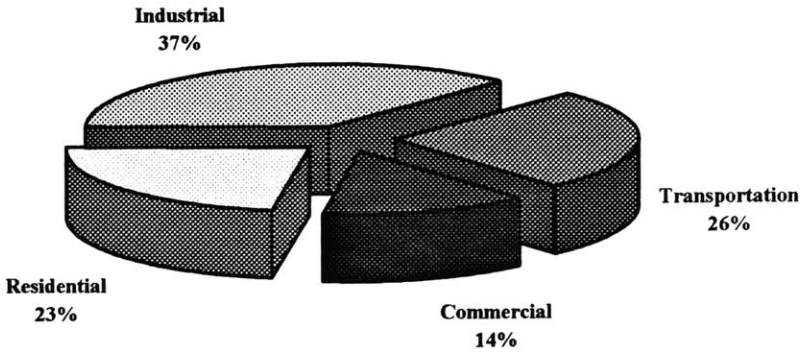

Figure 1.1. United States Energy Consumption in 1989, Principles of Heating, Ventilating, and Air Conditioning, Sauer et al., ASHRAE, 1989

Running parallel with the changing energy scene, there has been continuous investment in research and development into improved building mechanical equipment designs and into finding ways to improve existing buildings by reducing the energy consumption. Therefore, energy efficiency is no longer an optional extra in building systems, it has become a basic requirement. On the other hand, while considering austerity, one has to be very cautious, as thermal comfort and health requirements cannot be reckoned as simply luxury items. HVAC systems providing healthy and comfortable indoor environments are essential, although these systems do not necessarily consume more energy than unsuccessful ones.

Indoor air quality has become a most noted subject over the last decade. Sick building syndrome, a term that applies to buildings whose occupants complain of ailments ranging from frequent discomfort to serious chronic illnesses, is often attributed to inadequate

ventilation (cause of 52% of all cases as reported by Spoormaker) [4]. Inadequate ventilation may cause chemical and biological contamination of indoor environments giving way to complaints such as chronic illnesses, increasing respiratory problems, fatigue, headache, cancer and multiple chemical sensitivity. Therefore, research into innovative HVAC systems promising better indoor air quality and energy efficiency has gained much importance. Economics, a third factor overlapping the first two in terms of energy, medical, legal and insurance costs, must also be included.

Energy consumed by commercial buildings constitutes as much as 14% of the total United States energy consumption (see Figure 1.1). Commercial building energy consumption can be further divided into five groups. As can be seen in Figure 1.2, energy consumed by space heating and air conditioning comprises about 63% of the total [1]. This means that any efficient HVAC system with lower energy consumption could have a substantial effect on the total energy consumption. Furthermore, more people spend more of their time in office buildings. There is a shift from agricultural, construction and indoor factory work towards office work in developed countries where the economy is increasingly dependent on knowledge and services. For example, in 1990, about 2/3 of the American work force was employed in offices; this number is increasing [5].

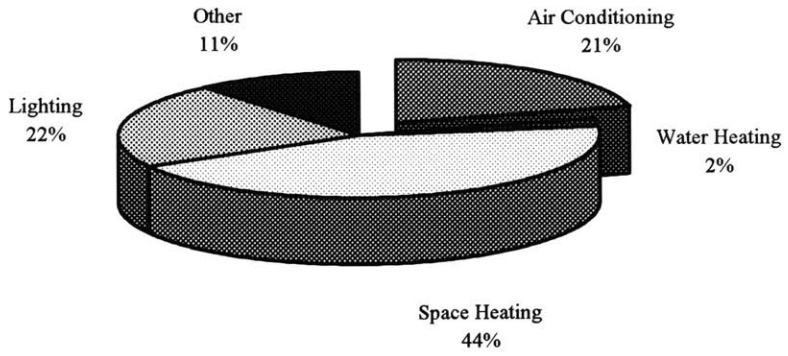

Figure 1.2. United States Energy Consumption in 1989, Principles of Heating, Ventilating, and Air Conditioning, Sauer et al., ASHRAE, 1989.

Several studies such as the Steelcase [6] and BOSTI [7] concluded that the indoor environment, including thermal comfort, has some effects on productivity. Moreover, Slone tested mental capability in relation to room air conditions and confirmed that people worked best and made less mistakes when they felt comfortable thermally. As any possible increase in productivity of the office work force could increase profits, a larger initial investment in a HVAC system to improve indoor air quality and energy consumption might also be more economically beneficial. Therefore, it is essential to improve existing HVAC systems and to search for innovative alternatives that may meet today's needs more efficiently.

1.2. Open Plan Offices

Closed offices (one room per person) may be the most acceptable working place for a single executive. They offer the greatest opportunities for arranging surroundings to suit individual preferences [8]. But on economic grounds they are not feasible as they take up a lot of floor space. Besides, in today's offices lots of equipment is being used and usually equipment is shared by many workers, as reported by Norford et al [9]. Closed offices make it harder to share equipment and manage the necessary electrical wiring. Additionally, closed offices are not flexible and they make communication between the workers more difficult.

Open plan office buildings are designed with large open spaces to be partitioned by the tenant, rather than providing numerous rooms with permanent walls. The open plan office is flexible, working positions can be regrouped as needed and communication routes can be changed without having to consider space restrictions. Open plan offices offer better sharing and utilization of electronic equipment and better wire management. Therefore,

open plan offices are becoming increasingly popular especially in developed countries where a substantial fraction of the work force is working in offices.

Comfort standards, set by ASHRAE, attempt to ensure a stable environment in which the majority of the occupants will find the conditions acceptable (ASHRAE, 1981). Air conditioning of open plan offices can sometimes be quite challenging as HVAC systems may not achieve these comfort standards uniformly in large spaces. Workers close to the supply diffusers may feel a draft; while those close to the exhaust diffusers may feel that the air is too stuffy. Several alternatives have been suggested for air conditioning of open plan offices. These include underfloor air distribution which supplies conditioned air from the floor diffusers distributed in the space, and task conditioning which provides each workstation with an individual source of conditioned air so that each occupant is allowed to control his own environment. Another interesting alternative suggested first by Scandinavian countries is displacement ventilation.

1.3. Displacement Ventilation

Displacement ventilation is a method that provides conditioned air to indoor environments with the goal to improve air quality while reducing energy usage [10]. These systems have been employed in industrial applications, notably in Scandinavia, for many years and have gained popularity in office building spaces in recent years.

Mechanical ventilation is traditionally based on the dilution of the contaminated air with fresh conditioned air and removing the polluted air from a suitable location. This method of design assumes a uniform thermally comfortable environment. In the best cases where this uniformity is actually achieved, indoor air quality is determined by even dilution of indoor pollutants by the fresh air supply. Alternatively, the conditioned air is supplied from one end of the room and allowed to sweep the pollutants in one direction across the space,

disposing of them at the opposite end of the room. This is the basic principle of displacement ventilation. Displacement ventilation is a promising candidate for air conditioning of open plan offices, as this type of office requires large spaces in buildings, usually interior zones where the main consideration is removing the heat generated by numerous occupants and equipment.

Displacement ventilation is based on the idea of an ideal flow pattern characterized mainly by buoyancy driven air flows. Instead of total mixing, the flow is unidirectional, with minimum spreading of pollutants. This ideal flow pattern is achieved by introducing the conditioned air at a low level, for instance from diffusers placed in the floor, at a temperature slightly lower than that of the occupied zone, and removing the hot polluted air at a higher level. Supply air enters the space from the diffusers at low velocities and moves along the floor creating a cool layer. At local heat sources such as people or equipment, the air temperature is raised. The natural buoyancy of heated air gives rise to plumes which create upward air currents. Cool air is then entrained into the plume and it replaces the warm and contaminated air (see Figure 1.3).

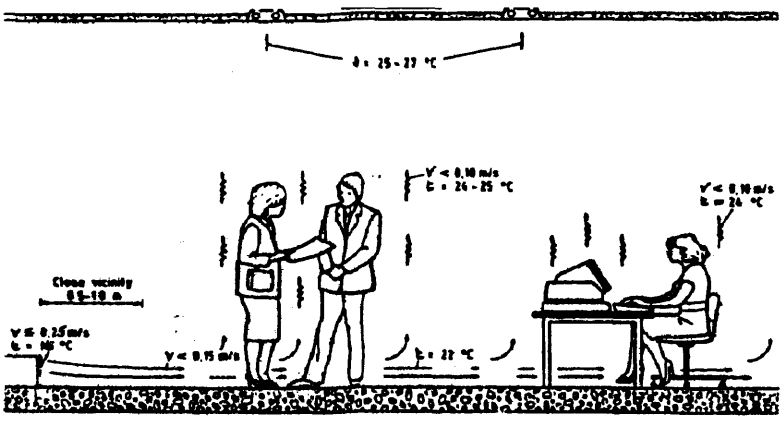

Figure 1.3. Displacement Ventilation, ARUP HVAC System Guide, ARUP, 1993

The air plumes created by heat sources carry contaminants and odors with a piston like flow pattern [11] and they spread out below the ceiling creating a contaminated layer which has to be assured by the designer to be above the occupied zone. The supply and exhaust are balanced to produce a boundary layer above which the air is contaminated and below which the air is considered to be clean and comfortable in the occupied zone [12] (see Figure 1.4).

Displacement ventilation is of interest because it may offer better air quality in the occupied zone due to reduced spreading of the contaminants within the room air. In addition, it may have lower running costs when compared to conventional systems, as supply volumes are reduced because of the increased ventilation effectiveness [12]. High supply temperatures associated with displacement ventilation may offer energy savings due to longer periods of economizer utilization as outside air can be used more effectively compared to conventional systems that operate with lower supply and exhaust temperatures. Higher supply and exhaust temperatures could also be advantageous for heat recovery possibilities. Due to low supply velocities, low turbulence intensity in the occupied zone is reported to reduce the risk of draft problems, a common problem in conventional office air conditioning methods [13].

Although displacement ventilation has substantial potential as a preferred alternative for open plan office air conditioning, there are some problems or disadvantages with these systems. First of all, there is temperature stratification in the vertical direction. Because cool air is supplied at lower levels at low velocity, the temperature difference between the floor level and the exhaust may be as high as 6°K. This means that there is a possibility of exceeding 3°K between ankle and head level, which is the limit for temperature stratification set by ASHRAE. This puts a restriction on the cooling load that can be handled by displacement ventilation systems, as greater cooling loads mean higher ankle to head temperature differences, especially when the ceiling height is below 3m.

Displacement ventilation is reported to have a maximum cooling capacity of around $40W/m^2$ while meeting the comfort requirements, as the vertical temperature stratification increases when the heat removed by conditioned air increases [12]. This value is below that reported for conventional systems ($80W/m^2$). Therefore, designers are seeking ways to integrate the displacement ventilation systems with supporting cooling systems such as cooled ceilings. Yet, this is another issue to be investigated thoroughly, as there is no substantial performance data on this type of systems.

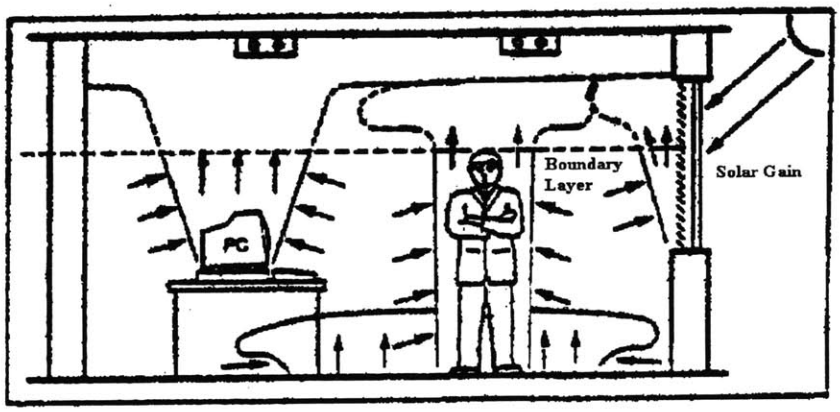

Figure 1.4. Plumes in Displacement Ventilation, ARUP HVAC Guide, ARUP, 1993

Another problem associated with displacement ventilation is 'draft' which is defined as the unwanted local cooling of the human body caused by air movement. Fanger and Pedersen recognized that fluctuations in the air velocity also contribute to the sensation of draft [14]. The typical fluctuations associated with the air velocity when the flow is turbulent may cause dissatisfaction due to draft. In displacement ventilation, as the plumes rising from the local heat sources gain height, turbulence intensity in the plume increases giving way to possibility of a draft sensation on the occupant. This depends on the relative locations of the heat sources. When wall mounted diffusers are used, the occupants close to the diffusers may feel draft [15]. When the diffusers are located at the floor, then the occupant may again be dissatisfied due to draft, depending on the type and closeness of the floor diffuser

Nevertheless, as displacement ventilation is reported to have a better ventilation efficiency in large open plan offices and is at least theoretically capable of substantial energy savings, it is worth investigating further. Most of the studies about displacement ventilation so far accept that, when designed and considered with care, it is feasible to use the whole potential of the displacement ventilation to provide good thermal climates. However, criteria for good displacement ventilation system design are not fully established and there are still many questions about performance of these systems.

1.4. Goals of this Study

Office building air conditioning is a large area of research that has been popular for the last decade. The Building Technology Program at MIT has been interested in the subject for the last few years, and has directed some research in alternative office building air conditioning methods. Displacement ventilation is a promising method of office room air conditioning that has recently acquired attention in the United States. One problem with displacement ventilation is the lack of a proper method to use it with high heat gains. This study aimed to answer some of the questions about the performance of this ventilation method. It focused on the maximum cooling loads that can be handled by displacement ventilation, the temperature stratification in the ventilated space, and the possibility to improve thermal comfort by providing slow mixing at lower levels.

One of the major objectives of this study is to design and implement an experimental setup that can be used to study displacement ventilation performance in open plan office spaces. Actual size office models are hard to accommodate and finance. Furthermore, they are not flexible, or in other words, they can not be modified easily for other configurations or other research. Scale modeling, however, allows for the investigation of large spaces, by using appropriate working fluids in scaled enclosures. It is relatively cheap and flexible. Therefore, the experiments are conducted with a setup containing a scale model.

Among the most important problems associated with displacement ventilation is the typical vertical temperature stratification, which is desirable as it allows for energy conservation, but is also undesirable when it exceeds the thermal comfort limits. The affect of the heat sources, their locations and diffuser layouts on the vertical temperature stratification has not been thoroughly studied. The amount of heat that can be effectively removed while keeping the temperature stratification within comfort limits is another issue that demands attention. This study aims to look at the vertical temperature stratification at a variety of situations which involve displacement ventilation in a typical open plan office room. It investigates the effect of small fans, located at a low level, on the vertical temperature stratification mainly in the occupied zone. It examines the possibility of reducing the stratification at lower occupied levels to comfort limits, without disturbing the stratification at higher levels needed to keep the exhaust temperatures high. This might promote comfort conditions allowing better performance of displacement ventilation systems at high cooling loads.

It is believed that the visual interpretation of the flow fields in displacement ventilation applications will be useful in understanding the method and its performance. Flow visualization is one of the ways to investigate the flow field and its interaction with the plumes in the office space considered. In this study, flow visualization is included.

In summary, this study aims to investigate the performance of displacement ventilation systems in open plan office environments, focusing on the vertical temperature stratification. It investigates the possibility to improve the performance of these systems by reducing the temperature stratification at lower levels and allowing the system to operate with high cooling loads. The goal is to obtain results which will enable application of displacement ventilation in open plan offices to meet comfort requirements and consume less energy.

CHAPTER 2

LITERATURE REVIEW

In the last ten years, displacement ventilation attracted attention as the market share of these systems in new office buildings started to increase especially in the Nordic countries. Displacement ventilation was first introduced about 15 years ago in industrial buildings and these systems were reported to operate quite successfully [13]. It gained considerable use in other buildings with large spaces such as theaters, concert halls, department stores and finally open plan offices. There is a wide range of literature about different applications of displacement ventilation systems and their performance along with the problems associated with thermal comfort. What is interesting is that their conclusions and remarks vary considerably.

This chapter gives a brief summary of the literature reviewed relevant to this study. The first section considers various applications of displacement ventilation focusing on three papers by Svensson, Kristenson et al. and Mathiesen. The second section concentrates on the problems with thermal comfort in displacement ventilation applications and performance of these systems. The last section gives a brief description of Olson's thesis that has been very useful during the research and the design of the experimental apparatus in this study.

2.1. Displacement Ventilation Applications

Svensson, in his paper 'Nordic Experiences of Displacement Ventilation Systems' [13], claims that the disadvantages of the system have often been neglected. He finds this rather natural as the research about these systems is somewhat limited. Svensson compares the application of displacement ventilation in industrial buildings and in office buildings. He asserts that the draft problems, unwanted local evaporative cooling of occupants due to high air velocities, in industrial building applications are much less than that in office buildings. He adds that this might be due to greater ceiling height of the former allowing a greater accumulation of heat on the upper zone of the spaces. He reports it is possible to remove heat gains of $30W/m^2$ in rooms with heights of 2.75m and $40W/m^2$ when the height is 3.4m, without exceeding the comfort limits. This is because temperature stratification increases when heat gains are greater. Cooled ceilings are one of the ways he suggests to back up displacement ventilation systems in removing larger loads. Svensson states that displacement ventilation has better ventilation efficiency (>100%) than mixing systems. He also points out the importance of the diffuser types and their location in the performance of these systems. This paper gives the view point of an engineer experienced in application of displacement ventilation, although the data that the conclusions are based on is not presented well.

Kristenson and Lindquist [16] study the application of displacement ventilation systems in industrial buildings. They claim that air showers mounted close to the occupants with the air introduced at a temperature equal to or slightly below the air temperature at the floor level, achieve a protective effect where most harmful pollutants are prevented from entering the area underneath the air inlet. The most successful results were obtained with the air showers mounted close to each other (four feet center to center). The geometry of the diffusers and the heights they were located are not clearly specified. Furthermore, when the air flow supply rate is equal to the total convective airflow inside the space, ventilation efficiency is reported to be significantly better than that of the conventional

systems. This is especially true if the pollutants are lighter than air and the convective airflow on the heat dissipating machinery is well predicted during the design of the system. Local ventilation index (the ratio between the pollutant concentration in the exhaust air and that at a certain point in the room) is found to be between 500% and 1000% whereas for conventional systems it is around 75%. Vertical temperature stratification is reported to have a linear distribution, somewhat typical of spaces with high ceilings, and to create draft at the lower levels.

Mathisen [17] looks at the performance of displacement ventilation in public rooms. Several cases were studied: a theater with air inlets along the walls, an auditorium, a cinema and an assembly hall with air inlets under the seats. It is pointed out that, although the second and third cases were very similar in terms of spatial geometry and the air supply terminal devices, the thermal comfort in the cinema was better than the auditorium. Mathisen claims that this is possibly because the air was carefully distributed in the cinema. There was a board forming an elevation at the edge of the steps that form the amphitheater which might have stopped the cool air from falling down from step to step and helped to maintain the upwards air motion associated with the plumes around seated people. It is also concluded that displacement ventilation had better ventilation efficiency than that of complete mixing systems.

2.2. Problems with Thermal Comfort

One of the most intriguing studies was that of Sandberg and Blomqvist [18]. They carried out velocity and temperature measurements in an office room to investigate the limits to the application of displacement ventilation. Four different types of low velocity diffusers very close to the floor were placed in an office module having the dimensions of 4.2m x 3.6m x 2.5m (L x W x H). Tests were carried out at two flow rates ($100m^3/s$ and $200m^3/s$) corresponding to two different cooling loads in winter and summer ($28W/m^2$ and

20W/m^2). At low air flow rates (0.5-1 room volumes/h) only 30% to 40% of the heat given off within the room was removed by the ventilation air. This behavior is explained by the high temperature of the ceiling due to the rising plumes transporting the heat to it. The floor temperature might have risen due to radiative heat exchange with the ceiling making its temperature higher than that of the supplied air. The heat was then transferred to the floor structure. At higher air flow rates, the velocity along the floor increased resulting in a greater fraction of the heat removed by air flow.

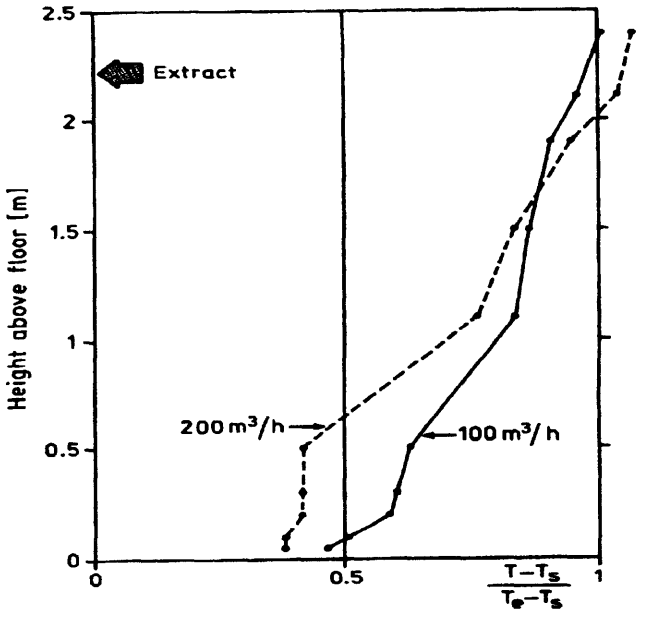

Figure 2.1. Non-dimensional Temperature Distribution over Height for 28W/m^2 (200m^3/h) and 20W/m^2 (100m^3/h), Sandberg M., C. Blomqvist, "Displacement Ventilation Systems in Office Rooms", ASHRAE, 1989.

In the same study, the vertical temperature stratification was found to have an almost linear pattern between the head and ankle level (see Figure 2.1), not exceeding the comfort temperature difference limit of 3°K (ISO/DIS7730) for cooling loads up to 25W/m^2. This situation did not depend on the type of the diffuser used. The temperature difference between room air at the floor level and the supply was less than half the

difference between the extract and the supply. It is also concluded that supply air diffusers should spread the air over a large sector to avoid complaints about draft associated with air motion.

Melikov and Nielsen [15] look at the local thermal discomfort due to draft and vertical temperature difference in rooms with displacement ventilation. The risk of local thermal discomfort is estimated by measurements of mean velocity, turbulence intensity and air temperature. It is concluded that there could be a high risk of draft and vertical temperature difference in the occupied space. These risks varied substantially within the zone, increasing when the occupant was closer to the outlets.

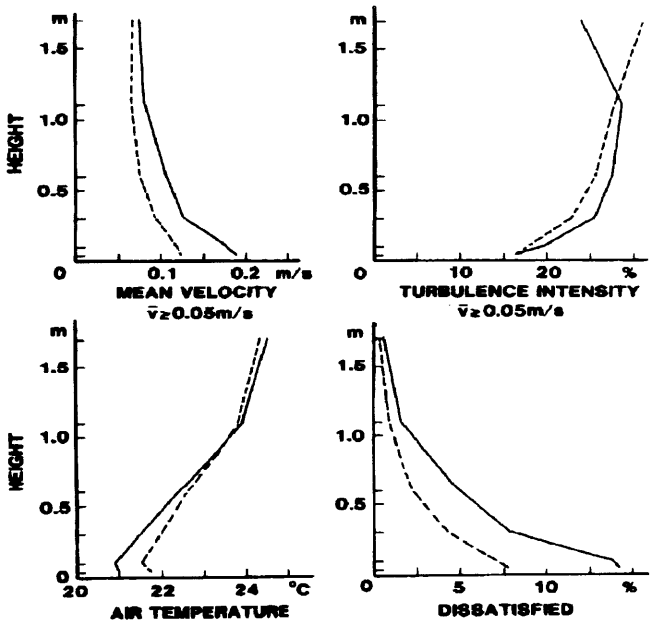

Figure 2.2. Vertical Profiles of Average Mean Velocity, Turbulence Intensity, Air Temperature and Percent Dissatisfied due to Draft in two Halves of the Room. (---) the half far from the outlets. Melikov A.K., J.B. Nielsen, "Local Thermal Discomfort Due to Draft and Vertical Temperature Difference in Rooms with Displacement Ventilation", ASHRAE, 1989.

In this study, 18 spaces with displacement ventilation were investigated, where the heat production in the rooms varied between $10W/m^2$ and $50W/m^2$. In one exceptional case the heat gain was $105W/m^2$. The exhaust and supply air temperature difference in the rooms ranged from 1.8°C to 8°C. A large percentage (40 %) of the locations within the occupied zone was found to have a vertical temperature difference of more than 3K, which is the standard limit. This result was based on statistical analysis of all cases considered. The temperature profiles corresponding to different cooling loads are not given. The non-uniformity of the occupied zone of the rooms was examined by considering the room in two halves, one near the outlets and the other far from them. The risk of vertical temperature stratification and draft was more pronounced in the half that was closer to the supply diffusers (see Figure 2.2). It is confirmed that when the air flow rate increases, the vertical temperature stratification decreases but because of the increased air velocities, there is a higher risk of draft.

Sandberg and Blomqvist [18] considered the effect of occupant motion on stratification. They found out that the stratification was not affected by a person walking into the test room. The temperature and the concentration profiles were not alike, the former was relatively smoother. In addition to these, it was confirmed that the comfort criteria about vertical temperature stratification puts a restriction on the maximum possible cooling load, in this experiment it was found to be $25W/m^2$.

The influence of physical activity on performance of displacement ventilation is also investigated by a recent study by Mattsson and Sandberg [19]. A mannequin was moved in a room with the dimensions of 4.2m x 3.6m x 2.5m. The mannequin was heated at 100W to simulate the heat dissipation by an office worker. Temperatures and trace gas concentration was measured. It was found that when the mannequin moved at a relatively small velocity (0.3m/s), ventilation efficiency increased, probably due to the naturally convected air around the mannequin being swept away and affecting the circulation

pattern in the upper zone, reducing the stagnation at some points. When the only heat source was the mannequin, the temperature stratification was greatly affected by its motion, but when heat gains increased the sensitivity of vertical temperature stratification to the motion of the mannequin vanished (see Figure 2.3).

Mattsson and Sandberg found that additional heat sources increased the temperature gradient in the room. When they were placed at higher levels such as the ceiling, the air exchange efficiency increased. On the other hand, when they were located at the lower levels, the efficiency increase tended to be diminished. This was explained by possible turbulent plumes in the latter case.

Mundt [20] looks at the convection flows from different heat sources in rooms with a vertical temperature stratification. This has not been studied thoroughly for displacement ventilation. Experiments included investigation of the temperature gradient when the heat dissipation in the rooms varied, the behavior of convection flows and plume size on different heat sources at different heat dissipation and supply air flow rate conditions. The relative rise of air temperature at the floor level was found to be very dependent on the ventilation rate. The plumes disintegrated before they reached the ceiling when the temperature gradient was of the size common in office rooms. Furthermore, different ventilation rates gave the same temperature gradient above the heat sources but different convection flows. The influence of the temperature gradient on the convection flows was less for heat sources giving higher initial velocities. In this study the deviation of the results between different experiments was quite large.

Mundt also presents a simplified method for calculating the rise in air temperature at floor level in rooms with displacement ventilation. The method does not include the induction of the supply air and the heat transfer at the ceiling, however the simplified method is shown to fit rather well with the test data of some other studies.

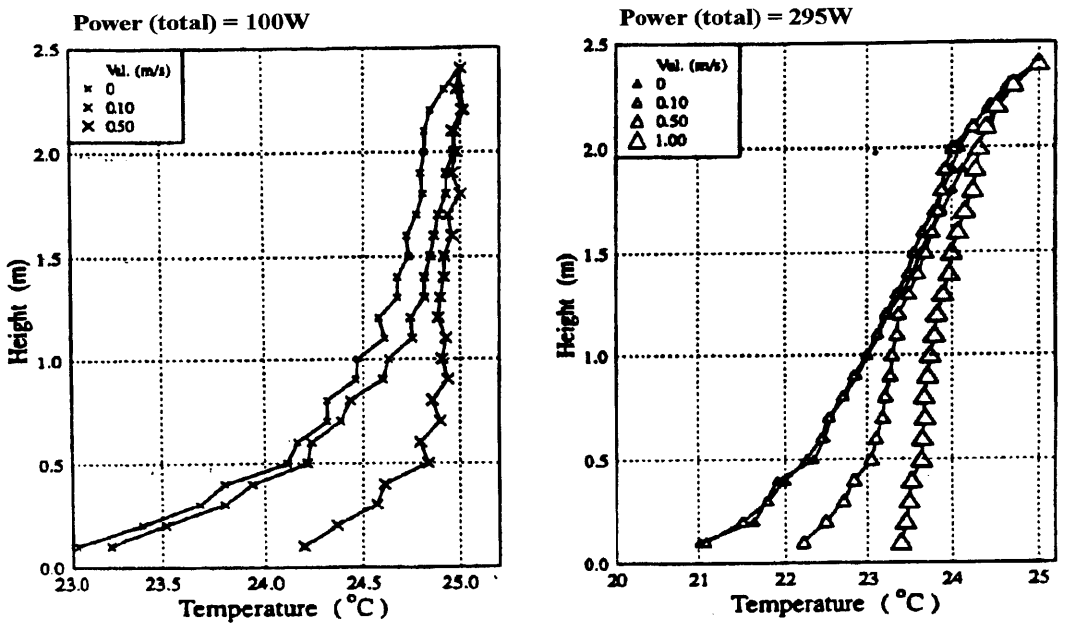

Figure 2.3. Vertical Temperature Stratification with Mannequin Moving at Different Speeds, (velocity of mannequin 0 to 1m/s), Mattsson M., M. Sandberg, "Displacement Ventilation-Influence of Physical Activity", Proceedings Roomvent 94, Poho, Volume 2, 1994.

The study by Sepannen et al. [11] compares the performance of displacement ventilation and conventional mixing systems in commercial buildings by means of the DOE-2.1C building simulation program. This study naturally involves many assumptions and simplifications associated with computer simulations. Because it makes relative comparisons only instead of finding actual performance values, it might be useful. Since the simulation programs were based on the assumption of uniform properties in the spaces and hence could not simulate displacement ventilation in the individual rooms, test data from a limited number of experiments were used as inputs and the simulation was basically for the central equipment. It is reported that displacement ventilation systems consume about the same energy with the conventional systems but the first cost of the former is higher due to required cooling panels when the cooling load exceeds

$40W/m^2$. It must however be noted that the experimental data used as input to the simulation is not available. The cost analysis included many simplifications and assumptions.

Alamderi et al. [10] conducted site measurements and computer simulations of air velocity and temperature to analyze the performance of displacement ventilation systems in office spaces. Alamderi et al. conclude that displacement ventilation systems are capable of providing the necessary thermal comfort in office spaces. They note, however, that there is a delicate balance between the interacting flow fields that are induced for example by secondary air motions resulting from cold surfaces and infiltration. The maximum heat gain considered in the study was about $30W/m^2$ so it is not surprising that the temperature gradient did not exceed the comfort limits. The results indicate that the temperature difference between the supply and the air at 0.1m height was 0.4 times the overall exhaust to supply temperature difference. It is claimed that the CFD models were capable of simulating the complex flow patterns generated within offices. The predicted temperature and velocity distributions are compared with averaged test values at various heights. Although the predicted temperature distribution is close to the measured data, there are significant differences between the predicted and measured velocity distributions. The deviation between predicted and measured quantities is even more pronounced when individual readings instead of averages are compared. This deviation is probably due to modeling assumptions inherent in CFD methods.

2.3. Olson

Douglas A. Olson studied scale modeling of natural convection in enclosures. He conducted natural convection experiments at $Ra \sim 10^{10}$ and $Pr \sim 0.8$ in an enclosure 47cm high, 136cm long and 68cm wide filled with refrigerant 114 gas and designed as a 1:5 scale model of a building interior space containing air. The opposing end walls were

heated and cooled isothermally, and the ceiling, floor and side walls were insulated. Temperature distributions, flow patterns and heat transfer were measured [25].

Olson includes a detailed explanation of the scaling analysis and the design of the experimental apparatus, along with the equipment used for temperature measurement and flow visualization. The scaling parameters appropriate for scaling natural convection in enclosures are derived from Grashof and Prandtl numbers. Refrigerant 114 was selected as the working fluid in the scale model. Experiments included steady-state experiments in an empty enclosure with and without partition, and transient natural convection in an empty enclosure. The scale model results agreed well with the published data for the full scale on which it was modeled, indicating R114 gas can accurately simulate natural convection of air, despite the differences in radiation absorption between the air and R114.

During this study, Olson's thesis proved to be a valuable reference. The reader will find detailed referring to Olson's study in Chapter 3.

CHAPTER 3

SCALING

3.1. Scaling of Displacement Ventilation

To start similitude analysis for scale modeling, one needs to determine what is to be simulated during the experiments [26]. After defining the important phenomena, the appropriate scaling parameters to be satisfied in modeling can be found. In this study, we want to build a model experiment which can simulate natural convection flow patterns and temperature distributions in a typical open plan office room.

The numerical value that is obtained by a test of the model depends on the independent variables involved in the phenomena. Complete similarity means that the same dependent dimensionless variables are determined when the same independent dimensionless variables are used for both the model and the prototype. Complete similarity between a prototype and a model can be achieved if laws of similitude (geometric similarity, kinematic similarity and geometric similarity) are satisfied. When it is not feasible to impose complete similarity in a model test, some of the independent dimensionless variables believed to have secondary influence may be allowed to deviate from their correct values [27]. Furthermore, if a phenomenon can be treated as an assembly of separate regions, each governed by its own set of laws, the prototype may be modeled regionally with appropriate justification of the assumptions involved. This is sometimes referred to as 'regional relaxation' [28].

In this study, 'displacement ventilation in open plan offices' is considered. Large open plan office spaces in commercial buildings are usually classified as interior zones. Instead of skin heat loss, the heat gain generated by the internal heat sources such as people, lights and equipment is of concern. Consequently the major HVAC consideration is cooling. The application of the displacement ventilation in open office spaces involves the supply of cold conditioned air at low velocities from diffusers close to the floor level. Cold supply air entering the space at low velocities constitutes a low temperature blanket which is distributed evenly on the floor. Air temperature increases when the supplied air reaches local heat sources such as computers or people. The natural buoyancy of heated air gives rise to plumes which are relied upon to create upward air currents.

The air motion at the diffusers and along the floor is mainly associated with the supply velocities. There are usually no important heat sources (0-0.3m) that may lead to notable density differences to affect the fluid motion at the floor level. Therefore we can conclude that the main driving phenomena for the motion of the air near the floor is the initial momentum of the fluid.

When we consider the motion of air at higher levels (0.3m-1.7m) where most of the heat sources are present, it is observed that the buoyancy effects are significant. As the supply velocity associated with the initial momentum of the air at the diffusers and the velocity at which the cold air moves on the floor is low, the effect of these are small in the vertical direction. Considering the velocity of the rising plumes around local heat sources, it is reasonable to say that the main driving phenomena is the density differences associated with natural convection at heat source surfaces. Accordingly buoyant forces seem to be important in displacement ventilation. Therefore, while determining the scaling parameters, natural convection is defined as the driving phenomena.

3.2. Similarity Considerations

In the next three sections, the scaling analysis complied from the three basic laws of similitude are explained.

3.2.1. Dimensional Similarity

Geometric similarity states that the prototype and the model must be identical in shape but differ in size. Therefore, ratios of the corresponding linear dimensions in the prototype and the model are to be kept the same. As corollaries of the geometric similarity, the area scale is defined as the square of the length scale and the volume scale as the cube of the length scale.

The experimental setup includes a box where a scale model of an office room is placed. This box was previously constructed by Olson to model an enclosure with the dimensions of 7.9m x 3.9m x 2.5m (L x W x H). Olson used refrigerant 114 which provided a scale of 1:5 over the full scale enclosure. Accordingly, the height of the box is 47cm. However, the prototype, or the office room, considered in this study has the dimensions of 8.03m in length and 4.02m in width. It has a height of 2.70m, and eventually a floor area of $32.3m^2$, and volume of $87.2m^3$. Besides, the scale model is designed to have a false floor and a false ceiling, each with a height of 3cm. Hence, it is necessary to simulate the prototype height with a model height of 41cm, leading to geometric scaling with a length scale ($L_r = L_{prototype}/ L_{model}$) of 6.6. The model dimensions then are;

Length: $$L_m = \frac{L_p}{L_r} = \frac{8.03}{6.6} = 1.22m$$

Width: $$\frac{4.02}{6.6} = 0.61m$$

Height: $\frac{2.70}{6.6} = 0.41\text{m}$

Hence the floor area in the model is scaled down to 0.75m^2 and the volume of the model is scaled down to 0.31m^3. The dimensions of the workstations and related equipment are also scaled down accordingly. The results can be found in Table 3.1.

Table 3.1. Actual and Scaled Dimensions of the Heat Sources.

Item	Real Dimensions in cm			Dimensions in cm		
Description	Height	Length	Width	Height	Length	Width
Screen	**46.0**	**35.5**	**27.2**	7.0	5.4	4.1
Tower	**66.9**	**37.6**	**37.6**	10.2	5.7	5.7
Table for screen	**100.3**	**66.9**	**83.6**	15.2	10.2	12.7
Occupant	**175**	**36**	**diameter**	26	5.5	diameter
Xerox	**50.1**	**83.6**	**35.5**	7.6	12.7	5.4
Table for Xerox	**66.9**	**83.6**	**50.1**	10.2	12.7	7.6

3.2.2. Kinematic Similarity

Kinematic similarity states that the flow fields in the prototype and the model must have geometrically similar sets of streamlines, indicating that between the prototype and the model, the velocities and the accelerations must be parallel and have the same ratio of magnitude between all corresponding sets of points under consideration. The motions of two systems are similar, if homogeneous particles lie at homogeneous points at homogeneous times [27]. If the quantity of mass is introduced into the study of space time relations, the problem becomes one of kinetics or so called dynamics [29]. In this analysis, kinematic similarity considerations are coupled with dynamic similarity considerations and the associated calculations are given in Section 3.3.

3.2.3. Dynamic Similarity

Dynamic similarity implies that the force distribution between the flow field of the prototype and the model is such that the identical types of forces are parallel at and have the same ratio of magnitude between all corresponding sets of points. At this point we need to consider the scaling related to heat transfer.

The quantity of energy contained in a body is related to the kinetic energy of the motion of the molecules. The dimensions of heat and work or energy are kept the same [30]. The heat transfer scale is based on natural convection parameters in this analysis. Temperature is not defined by specifying a unit which can be duplicated and a scale established by addition but rather each point on the entire scale has to be specified by reference to some physical phenomenon [31]. The temperature difference scale is chosen such that the heat flow is proportional to the temperature difference which is determined by Grashof number similarity.

3.3. Scaling Parameters

As indicated in the previous sections, both inertial and buoyant forces seem to be important in the consideration of displacement ventilation. Therefore, energy and momentum equations are to be investigated to determine the dimensionless parameters that must be matched. These parameters may be found by non-dimensionalization of the governing equations describing the fluid motion [32]. Assuming that the fluid motion is primarily in the direction normal to the supply diffusers (x) and in the vertical direction (z), that the fluid flow is steady with constant fluid properties and that the gravity acts in the negative z direction, the governing equations for mass, momentum and energy conservation can be given as:

mass conservation,

$$\frac{\partial w}{\partial z}+\frac{\partial u}{\partial x}=0 \tag{1}$$

momentum conservation in x direction,

$$u\frac{\partial u}{\partial x}+w\frac{\partial u}{\partial z}=-\frac{1}{\rho}\frac{\partial P}{\partial x}+\upsilon\left[\frac{\partial^2 u}{\partial z^2}+\frac{\partial^2 u}{\partial x^2}\right] \tag{2}$$

momentum conservation in z direction,

$$u\frac{\partial w}{\partial x}+w\frac{\partial w}{\partial z}=-\frac{1}{\rho}\frac{\partial P}{\partial z}+\upsilon\left[\frac{\partial^2 w}{\partial z^2}+\frac{\partial^2 w}{\partial x^2}\right]-g\left[1-\beta\left(T-T_{ref}\right)\right] \tag{3}$$

energy conservation,

$$w\frac{\partial T}{\partial z}+u\frac{\partial T}{\partial x}=\alpha\left[\frac{\partial^2 T}{\partial z^2}+\frac{\partial^2 T}{\partial x^2}\right] \tag{4}$$

where β is the volumetric thermal expansion coefficient.

Clearly radiation effects are neglected. Furthermore the fluid is assumed incompressible with one exception accounting for the effect of variable density in the buoyancy force which induces the fluid flow, as is common in natural convection analysis and so called the Boussinesq approximation.

The boundary conditions for the velocity field can be given as,

$$w(z,0) = 0 \qquad x(z,0) = 0 \qquad w(z,\infty) = w_\infty(z) \tag{5}$$

and for the temperature field;

$$T(z,0) = T_s \qquad T(z,\infty) = T_\infty \tag{6}$$

In order to non-dimensionalize these equations (1,2,3,4) it is possible to define a characteristic length 'L' and a characteristic velocity 'V'. Then one can introduce the dimensionless variables:

$$x^* \equiv x/L \qquad z^* \equiv z/L \qquad u^* \equiv u/V \qquad w^* \equiv w/V \qquad T^* \equiv (T - T_\infty)/(T_s - T_\infty)$$

and for the dimensionless pressure:

$$P^* = \frac{P}{\rho V^2}$$

Then equations (1), (2), (3) and (4) reduce to:

$$\frac{\partial w^*}{\partial z^*} + \frac{\partial u^*}{\partial x^*} = 0 \tag{7}$$

$$u^* \frac{\partial u^*}{\partial x^*} + w^* \frac{\partial u^*}{\partial z^*} = -\frac{\partial P^*}{\partial x^*} + \frac{\upsilon}{VL}\left[\frac{\partial^2 u^*}{\partial z^{*2}} + \frac{\partial^2 u^*}{\partial x^{*2}}\right] \tag{8}$$

$$u^* \frac{\partial w^*}{\partial x^*} + w^* \frac{\partial w^*}{\partial z^*} = -\frac{\partial P^*}{\partial z^*} + \frac{\upsilon}{VL}\left[\frac{\partial^2 w^*}{\partial z^{*2}} + \frac{\partial^2 w^*}{\partial x^{*2}}\right] + \frac{g\beta(T_s - T_\infty)L^3}{\upsilon^2} T^* \tag{9}$$

$$w^* \frac{\partial T^*}{\partial z^*} + u^* \frac{\partial T^*}{\partial x^*} = \frac{\alpha}{VL}\left[\frac{\partial^2 T^*}{\partial z^{*2}} + \frac{\partial^2 T^*}{\partial x^{*2}}\right] \tag{10}$$

The dimensionless boundary conditions then can be given as;

$$w^*(z^*,0) = 0 \qquad x^*(z^*,0) = 0 \qquad w^*(z^*,\infty) = w_\infty(z^*)/V \tag{11}$$

$$T^*(z^*,0) = 0 \qquad T^*(z^*,\infty) = 1 \tag{12}$$

As a result of this nondimensionalization three similarity parameters are important, namely the Reynolds number, Prandtl number and the Grashof number. This was expected as the modeling involves basically fluid flow in an enclosure and natural convection associated with the supplied air.

$$Re = \frac{VL}{\upsilon} = \frac{(m/s)\times(m)}{(m^2/s)} \tag{13}$$

$$Pr = \frac{\upsilon}{\alpha} = \frac{(m^2/s)}{(m^2/s)} \tag{14}$$

$$Gr = \frac{g\beta(T_s - T_\infty)L^3}{\upsilon^2} = \frac{(m/s^2)\times(1/K)\times(K)\times(m)^3}{(m^2/s)^2} \tag{15}$$

In the literature concerning investigations of displacement ventilation, it is popular to consider Archimedes number which may be derived from Grashof and Reynolds numbers. Proper scaling of these two would automatically satisfy Archimedes similarity.

$$Ar = \frac{Gr}{Re^2} = \frac{g\beta(T_s - T_\infty)L^3}{\upsilon^2} \times \frac{\upsilon^2}{V^2L^2} = g\frac{(T_s - T_\infty)}{T_\infty}\frac{L}{V^2} = g'\frac{L}{V^2} \qquad (16)$$

The appropriate scaling ratios for the small scale experiment are based on matching of these non-dimensionless parameters for both the scale model and the prototype under consideration.

3.3.a. Prandtl Similarity

Prandtl number arises in heat transfer whenever both temperature as well as velocity gradients are involved. Thus thermal conductivity becomes a relevant variable together with viscosity which effects the thickness of the boundary. The Prandtl number can be defined as the ratio of the momentum and the thermal diffusivities [33]. It provides a measure of the relative effectiveness of momentum and energy transport by diffusion in the velocity and thermal boundary layers.

In choosing the fluid that is to be used in the model, a fluid with a Prandtl number as close as possible to the Prandtl number for air was sought. If air is used there are problems with the verification of the other similarity parameters such as Grashof number. If water with a Prandtl number of around 7 is used then Prandtl number similarity is not insured which might lead to significant errors in the results [26].

The restriction of Prandtl number to be around 1 required that a gas be used a the working fluid. A dense gas such as Refrigerant 114 (R114) with Pr ~ 0.9, Refrigerant 227ea (R227ea) or Refrigerant RC318 with Pr ~ 0.92 were strong candidates. Scaling analysis for each of these gases was performed. The results are summarized in Table 3.5 for R227ea and RC318, and in Table 3.6 for R114. Temperature scale ratio (ΔT_{ratio} = $\Delta T_{prototype}$ / ΔT_{model}) was 0.34 for R227ea, 0.51 for RC318 and 0.38 for R114 . These scale

ratios were suitable. They allowed an actual air temperature difference of 4°K to be simulated with refrigerant gas temperature differences of 7.8°K to 11.5°K in the model with a length scale of 6.6. Finally R114 was chosen to be the working fluid as it was non-toxic (toxicity group 6), non-corrosive, non-flammable, with transparency close to that of air, thermally stable and considerably cheaper than R227ea (40 times) and RC318 (100 times). R114 required recovery when the experiments were completed. Since it damages the ozone layer, a refrigerant recovery and storage apparatus was used during the experiments. The properties of refrigerant R114 are summarized in Table 3.2 and Table 3.3.

Table 3.2. Properties of R114 Vapor State at 1 atm,
Thermophysical Properties of Refrigerants, ASHRAE, 1976.

T °C	ρ kg/m^3	μ kg/m/s	k W/m/°K	c_p J/kg/°K
5	7.790	10.89E-6	0.00921	686.1
10	7.673	11.05E-6	0.00951	693.2
15	7.491	11.21E-6	0.00980	700.0
20	7.350	11.37E-6	0.01010	706.7
25	7.214	11.53E-6	0.01039	713.2
30	7.083	11.70E-6	0.01067	719.6
35	6.958	11.86E-6	0.01096	725.7
40	6.837	12.03E-6	0.01124	731.8

Table 3.3. Thermodynamic Properties of R114 at 293°K, 1 atm.
(Saturation Temperature = 276.7°K), Fundamentals, ASHRAE , 1989.

Density	kg/m^3	7.35
Kinematic Viscosity	m^2/s	1.55E-6
Specific Heat	J/kg.K	706.70
Viscosity	kg/m.s	1.14E-5
Conductivity	W/m.K	1.01E-2
Thermal Diffusivity	dimensionless	1.94E-6
Thermal Expansion Coeffnt.	1/K	3.41E-3
Prandtl Number	dimensionless	0.80

Table 3.4. Thermodynamic Properties of Air at 293 K, 1 atm.

Density	kg/m^3	1.2
Kinematic Viscosity	m^2/s	1.51E-5
Specific Heat	J/kg.K	1005
Viscosity	kg/m.s	1.82E-5
Conductivity	W/m.K	2.61E-2
Thermal Diffusivity	dimensionless	2.16E-5
Thermal Expansion Coeffnt.	1/K	3.40E-3
Prandtl Number	dimensionless	0.71

3.3.b. Reynolds Similarity

Dimensionally the Reynolds number is proportional to the ratio of the inertial forces of an element of fluid to the viscous force acting on it. The design requirement that the Reynolds number of the model and the prototype is equivalent to requiring that the ratio of the inertial forces and the viscous forces be equal in the model and the prototype.

Having chosen the geometric length scale (L_r) for the working fluid it is possible to extend the analysis for other similarity ratios in terms of Reynolds similarity.

$$Re_p = \frac{V_p L_p}{\upsilon_p} = \frac{V_m L_m}{\upsilon_m} = Re_m$$

for the viscosity scale ratio,

$$\upsilon_r = \frac{\upsilon_p}{\upsilon_m} = \frac{1.51E-5}{1.55E-6} = 9.74 \qquad (17)$$

then the velocity scale ratio is

$$V_r = \frac{\upsilon_r}{L_r} = \frac{9.74}{6.59} = 1.48 \tag{18}$$

the density scale ratio is

$$\rho_r = \frac{\rho_p}{\rho_m} = \frac{1.2}{7.35} = 0.16 \tag{19}$$

and the specific heat scale ratio is

$$cp_r = \frac{cp_p}{cp_m} = \frac{1005}{707} = 1.42 \tag{20}$$

The volumetric flow rate scale ratio can be found as,

$$q_r = \frac{q_p}{q_m} = V_r \times L_r^{\,2} = 1.48 \times 6.59^2 = 64.15 \tag{21}$$

3.3.c. Grashof Similarity

The Grashof number represents an expression for the interaction of viscous, buoyancy and inertial forces. These forces need to be considered when a fluid is subjected to natural convection due to fluid temperature variations in a gravitational field, and when the fluid flow encounters viscous effects. The Grashof number is the ratio of buoyancy to viscous forces.

$$Gr_p = \frac{g_p \beta_p \Delta T_p L_p^3}{\upsilon_p^2} = \frac{g_m \beta_m \Delta T_m L_m^3}{\upsilon_m^2} = Gr_m$$

For equal values of Grashof number the temperature scale ratio becomes;

$$\Delta T_r = \frac{\Delta T_p}{\Delta T_m} = \frac{\upsilon_r^2}{L_r^3 \beta_r g_r} = \frac{9.74^2}{6.59^3 \times 0.91 \times 1} = 0.37 \qquad (22)$$

This result give us the ratio of the surface to fluid temperature difference of the prototype to that of the model and lead us to the power scale ratio. Choosing the temperature difference ratio for the exhaust and the supply the same as Grashof temperature difference scale ratio, the scaling ratio for cooling is;

$$P_r = \frac{P_p}{P_m} = q_r \times \rho_r \times cp_r \times \Delta T_r = 64.2 \times 0.16 \times 1.42 \times 0.37 = 5.48 \qquad (23)$$

Table 3.5. Scaling Analysis Results for R227ea and RC318.

Property	**Unit**	**Air**	**R227ae**	**RC318**
Density	kg/m^3	1.2	7.30	8.69
Viscosity	kg/m.s	1.82E-5	1.17E-5	1.10E-5
Specific Heat	J/kg.K	1005	813	796
Conductivity	W/m.K	0.0261	0.0126	0.0114
Thermal Exp. Coef.	1/K	3.40E-3	3.76E-3	3.41E-3
Prandtl Number	none	0.701	0.758	0.767
Grashof Number	none	1.15E10	1.15E10	1.15E10
Length Scale	none	1	6.6	6.6
Grashof ΔT	K	4	11.74	7.92
Temperature Scale	none	1	0.341	0.503

Then it was possible to extend the analysis to further scaling of the individual heat sources, so that they would dissipate scaled down versions of realistic amounts energy (see Table 4.1 for scaling of power for heat sources).

The results for the scaling analysis for Refrigerant 114 can be found in Table 3.6. These results were used in the design and operation of the experimental apparatus. The application of these can be found in more detail in Chapter 4 in which description of the design and implication of experimental apparatus is given.

Table 3.6. Summary of the Scaling Parameters for R114 for 40W/m^2 case.

Property	Unit	Full Scale (Air)	Ratio (p/m)	Model (R114)
Length	m	8.03	6.59	1.22
Width	m	4.02	6.59	0.61
Height	m	2.70	6.59	0.41
Floor Area	m^2	32.28	43.43	0.74
Volume	m^3	87.16	286.19	0.30
Density	kg/m^3	1.20	0.16	7.35
Kinematic Viscosity	m^2/s	1.51E-5	9.74	1.55E-6
Viscosity	kg/m.s	1.82E-5	1.60	1.14E-5
Specific Heat	J/kg.K	1005.00	1.42	706.70
Conductivity	W/m.K	0.03	2.58	0.01
Thermal Diffusivity	none	2.16E-5	11.13	1.96E-5
Thermal Expansion Cof.	1/K	3.40E-5	0.90	3.41E-3
Velocity	m/s	0.10	1.48	0.07
Supply Air Area	m^2	3.56	43.37	0.08
Volume Flow Rate	m^3/s	0.38	64.15	0.01
Mass Flow Rate	kg/s	0.43	10.47	0.04
Prandtl Number	none	0.71	0.90	0.79
Reynolds Number	none	17900	1.00	17900
Rayleigh Number	none	8.04E9	0.88	9.18E9
Archimedes Number	none	36.16	1.11	32.69
Grashof Number	none	1.15E10	1.00	1.15E10
Grashof ΔT	K	4	0.37	10.9
Required Cooling	W	1291.00	5.48	235.58
Heat Gains per Area	W/m^2	40.00	0.13	317.46

CHAPTER 4

DESIGN AND CONSTRUCTION OF THE EXPERIMENTAL APPARATUS

4.1. Design Problem and Objectives

The major objective of this study was to design and construct an experimental setup consisting of a scale model of an office room and equipment necessary to provide the experiment conditions for the model, to investigate the performance of displacement ventilation in open plan office environments. There were many points contemplated in the design of the full experimental apparatus. The initial approach consisted of the following goals.

The first consideration was to build up a small scale model of an open plan office with components which would function as heat sources and hence determine the flow of the working fluid inside the model. Thus it was necessary to have an enclosure that would allow to do a variety of experiments involving temperature measurements and flow visualization. It should also have enough flexibility to be modified for future research. Moreover, it was imperative for the enclosure to be well sealed, as the selected working fluid was refrigerant 114 reported to be environmentally hazardous. The second main requirement was equipment to function like a typical HVAC system, or in other words, condition the working fluid, supply it to the enclosure and then extract it and recirculate. This led to consideration of a gas circuit with a heat exchanger to cool the circulating fluid

and a fan to displace it at desired flow rates. A secondary circuit was necessary to provide means to transfer the heat extracted from working fluid to the environment.

Some means to supply power and control the heat sources in the enclosure was required. Furthermore, for flow visualization experiments, a smoke generating system, a filtering unit and a camera along with some equipment to provide adequate lighting conditions were needed. The integration of the flow visualization system components had to be simple for the sake of easy operation and possible future modifications. The smoke generating system had to inject smoke at a variety of locations inside the enclosure. Finally, some equipment for effective temperature measurement both in the enclosure and at some points in the small scale HVAC system elements was essential.

It was necessary to design and manufacture a number of components and integrate them to construct an experimental setup that would make it possible to simulate both displacement ventilation and some other air conditioning alternatives using forced or free flow in future research.

4.2. Experimental Setup

The need for an enclosure led to the use of a box. A box which was utilized during previous research at MIT was modified to serve the objectives of this study. The experimental setup in this study could be considered in two main parts, namely, 'inside the box' where the small scale open plan office was located, and 'outside the box' where the equipment that provides experimental conditions and takes temperature and flow rate measurements was established.

A scale model of a typical open plan office room consisting of three work stations was placed inside the box. Each work station contained scale models of an occupant, a

computer, a lamp and an office equipment such as a photocopier (see Figure 4.4). Each model had a power resistor placed inside so that it could dissipate heat at desired rates. Electrical connections for these power resistors extended from the box to a control board where the power resistors could be switched on or off and the voltage across them be regulated. In addition to these, in the box, a smoke injection probe was placed at the point of interest. The smoke was supplied to the probe by means of a smoke generating system located outside the box.

Outside the box, a gas circuit was constructed to condition the circulating working fluid. The circuit contained a fan and a heat exchanger to cool the recirculated gas. A filtering unit was placed at the fan housing to capture the smoke particles used for flow visualization. Additionally, a water circuit through the heat exchanger was constructed. It was designed to make use of the chilled water supply available at the laboratory. A pump and some other piping elements served to pressurize and regulate the flow of water in the circuit.

A laser and a slide projector were utilized to provide adequate lighting conditions for the flow visualization experiments. In addition to that, a camera system with necessary viewing and editing components was furnished. A temperature measurement system was built. This system consisted of a moving rake holding the thermocouple sensors inside the box and a data acquisition system which allowed the monitoring of the measurements.

The reader will find detailed description and drawings of each part of the experimental setup in the succeeding sections.

4.3. The Box

During his studies at MIT, Olson constructed and used a box to conduct experiments on small scale modeling of natural convection in enclosures at high Rayleigh number. The box was designed with a dimensional scale ratio of 1:5 as a model of the full scale enclosure used by Fern. The scale model inner dimensions were 69cm in width, 136cm in length and 47cm in height.

Olson, in his thesis, describes the wall construction details of the box as follows (see Figure 4.1) ;

> *Each vertical wall was a composite structure consisting of three sections of 0.6cm thick aluminum plate, stacked one above each other. Each aluminum plate was 11.7cm high. 2cm high closed cell polyurethane strips separated the plate sections. An additional strip of foam surrounded the outer perimeter of each wall to thermally isolate it from its neighbors. Aluminized mylar strips were glued on the inner facing side of the foam insulation strips to reduce the surface emissivity. The edges and corners were sealed with a soft, closed cell urethane gasket, coated with vacuum grease.*
>
> *Electrical resistance strip heaters were bolted to the back side of each wall section of four vertical walls, with a thin layer of thermal contact grease between the plates and the heaters. Besides, copper cooling tubes were soldered to the back side of the wall sections of the two side walls and one of the end walls. The tubes looped around the electric heaters. The aluminum plate assemblies with the heaters and the cooling coils connected to them were bolted to 0.6cm thick exterior grade plywood. The plywood was reinforced with slotted angle iron along the edges, which also served as the means of clamping the walls together [26].*

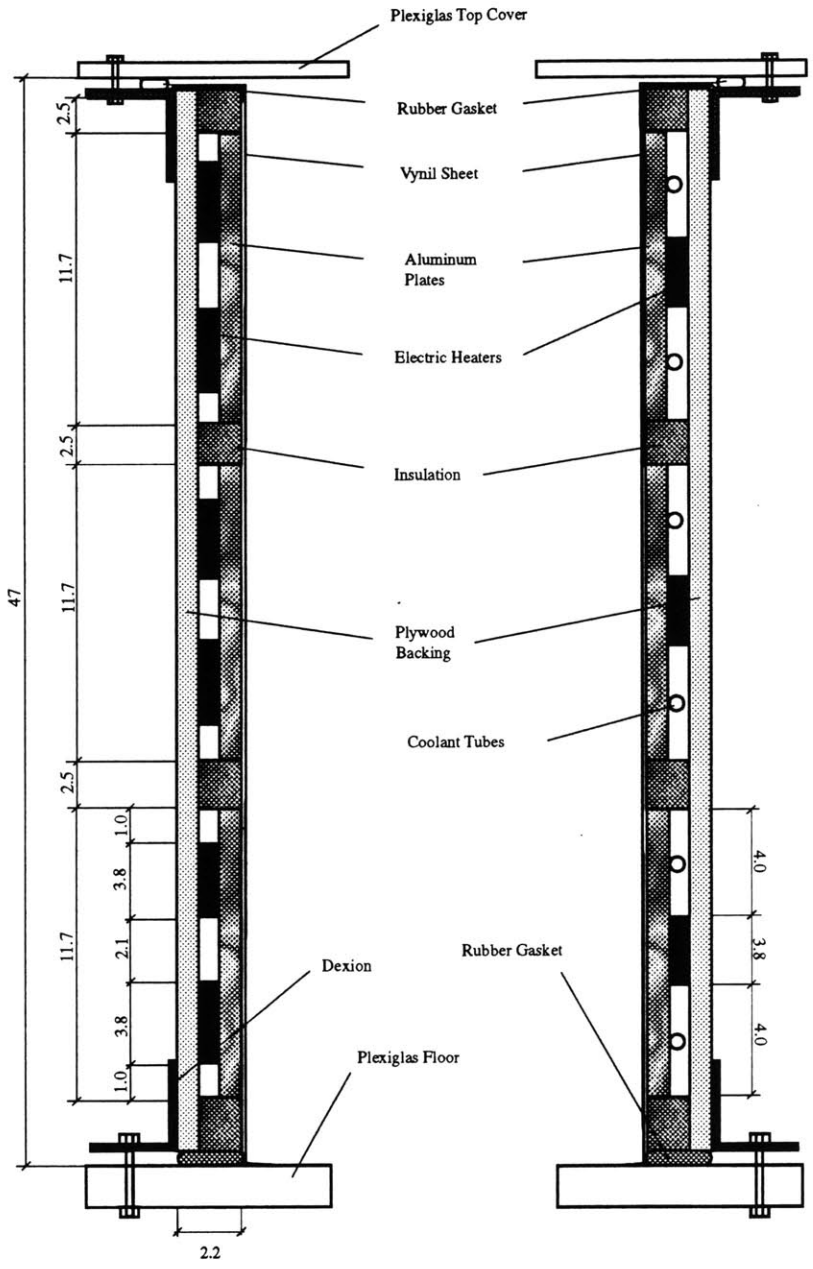

Figure 4.1. Wall Construction Details of Small Scale Experimental Apparatus. All Dimensions in Centimeters (26).

At the time of this study, the box was about 10 years old and it had been used during some other research. Accordingly, some sections of the walls, especially the top polyurethane strip were slightly damaged. It was necessary to smooth the top surface with a silicone glazing agent. Additionally, a continuos vinyl sheeting was wrapped along the side walls and connected to the bottom Plexiglas cover and the top dexion structure with RTV silicone sealing adhesive. This sheeting acted as a secondary barrier for possible leaks at the wall sections.

The floor of the box was made of Plexiglas, 1.2cm thick. Olson used a triple pane window in early experiments and later he used a double pane window made of Plexiglas, each piece separated by 2.5cm, as the ceiling. The Plexiglas ceiling permitted easier access to the inside of the box.

As mentioned above, the box had been used in some experiments after Olson's studies. Therefore, the ceiling and the walls were modified. For this study, a transparent and yet strong material was necessary for the ceiling, as the laser beam had to pass through it without significant deflection for flow visualization and there would be mechanical connections at the sides where the top cover of the box met the side walls. After checking the deflection characteristics of various transparent materials, it was decided that Plexiglas was the best alternative because of its light weight, relatively low cost and easy to machine form. A large sheet of Plexiglas, 0.64cm thick, served as the top cover for the box during this study. The Plexiglas floor of the box and the side walls were not changed. A few modifications took place at these locations for the necessary connections for the smoke injection probe, the thermocouple rake and the resistance wiring. These modifications are explained in detail in the following sections.

The geometric scaling ratio for this study was chosen to be 1:6.6 as mentioned in Chapter 3. Therefore, it was necessary to have a enclosure with a size smaller than that of the box,

so as to study an office with 4m x 8m floor area. It was decided to construct a smaller structure to be put in box. The other reason to prefer a structure inside the box was the ease of modification in terms of machining. Furthermore, the office model was designed to have a false floor and a false ceiling so that other supply and exhaust configurations could be studied in future research.

The structure was made of 0.64cm thick Plexiglas sheets. The prototype office had the dimensions of 8m in length, 4m in width and 2.7m in height. This meant a small scale office with dimensions of 1.22m in length, 0.61m in width and 0.41m in height. Because the box was previously constructed with a height of 0.47m, the remaining 6cm was used for the false floor and the false ceiling, each with a scaled height of 3cm.

The side wall of the structure was used as a false wall (see Figure 4.2 and Figure 4.3). The supply diffusers were placed at two openings with dimensions of 12.5cm x 12.5cm machined in this false wall. As the width of the new structure was 61cm whereas the box had a width of 68cm, the remaining 7cm allowed the space between the side wall of the box and the Plexiglas false wall to be used as a canal for the working fluid to flow from the main supply point at the top cover to the supply diffusers, functioning like a large duct. The Plexiglas structure components were assembled by means of iron brackets, with tapered bolt connections so that the flow in the enclosure was not disturbed by the bolt heads. The terminal strips used for electrical wiring for the power resistors were also located at the false wall

The false ceiling was designed to be an exhaust plenum. Two exhaust diffusers were placed on the openings machined at two symmetrical locations at the false ceiling Plexiglas surface. The exhaust diffusers had the dimensions of 4.5cm x 4.5cm. Both the supply and exhaust diffusers had screens made of perforated sheet grade 7, to provide flow uniformity at the discharge. The perforated sheets were connected to the Plexiglas surfaces in the same way as for the bracket connections with tapered holes so that the flow in the vicinity

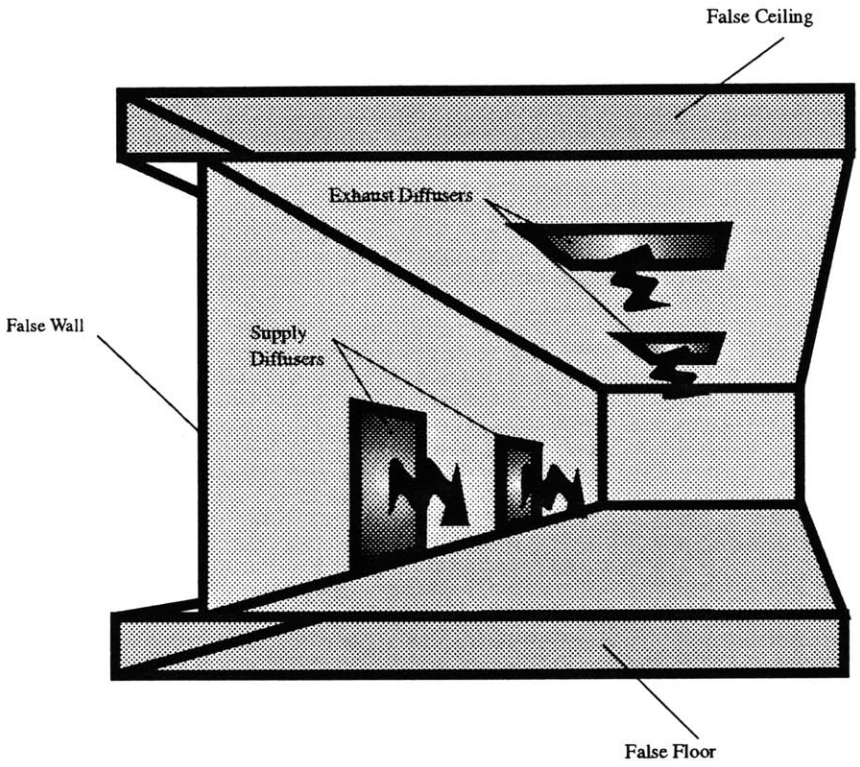

Figure 4.2. View of the Plexiglas Scale Model Structure.

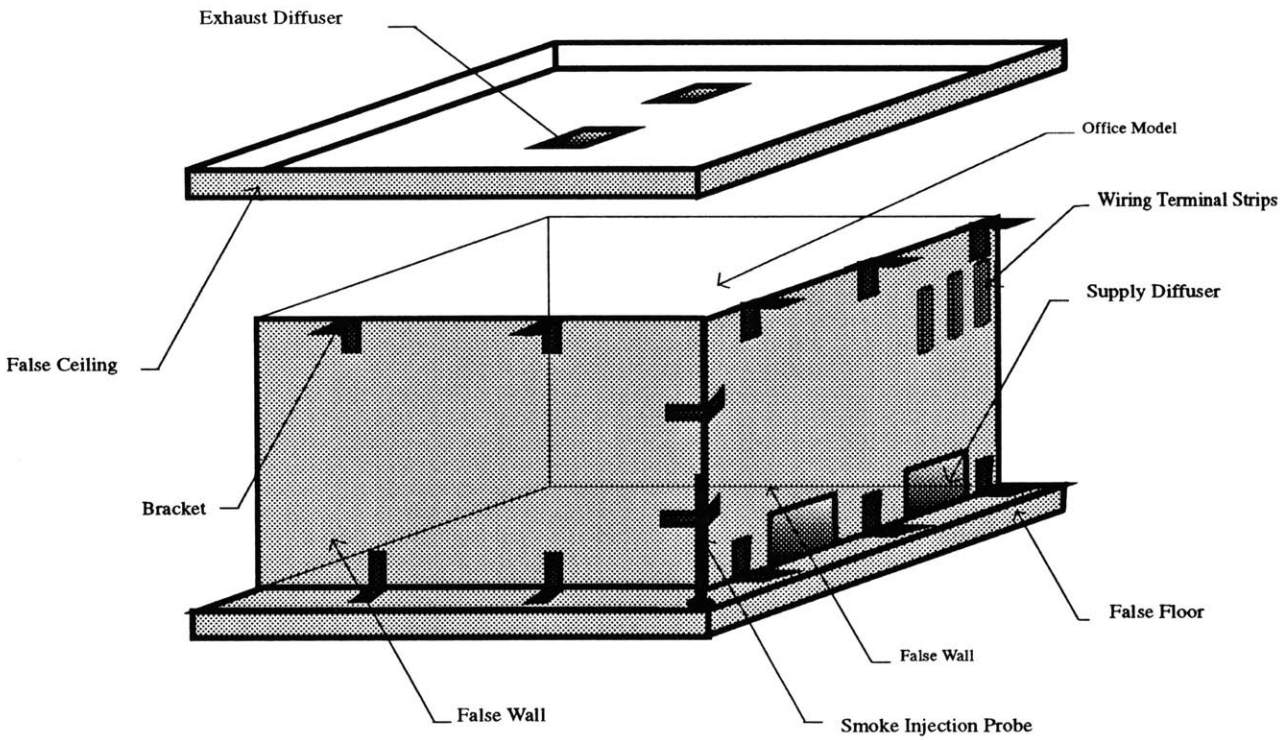

Figure 4.3. Scale Model Plexiglas Structure inside the Box.

of the diffusers was not affected. The false ceiling was connected directly to the suction side of the gas circuit. A PVC connection was placed at the false ceiling to ensure the passage of the supplied refrigerant to the space between false wall and the side wall of the box. The sides for the false ceiling were constructed such that the space between the side Plexiglas strips and the side wall of the box is minimum to maintain the possibility to put a secondary sealant at this location.

The false floor was a scaled down version of a typical underfloor air supply plenum with a height of 20cm reduced to 3cm in the model. The false floor was also designed to have the flexibility to be modified in the future to examine underfloor distribution air conditioning. In this study, it acted as a container for the resistance wiring extending from the terminal strips located at the false walls to the power resistors. It was connected to the side walls by means of brackets. The false floor surface had holes at necessary locations for the resistance wiring at the bottom to reach the power resistors. The side walls of the false floor were constructed in the same way like the sides of the false ceiling for the same reasons. The false floor was not connected to the bottom Plexiglas cover by any mechanical means. The structure supported itself inside the box by its own weight.

The top cover was basically a 0.64cm thick Plexiglas sheet. Two large holes were cut at opposing corners, one for the supply, the other for the exhaust connection. The supply line coming from the gas circuit was connected in terms of a threaded male fitting and a short PVC extension piping that goes through the false ceiling structure and reaches the space behind the false wall. An O ring and elastic removable rubber sealant was used to seal the connection. The exhaust line at the suction side of the gas circuit was connected in the same manner. But this time, there was no extension piping and as mentioned before exhaust line was connected directly to the false ceiling.

The assembly of the structure was realized in three steps every time the structure needed to be placed inside the box. First, the side walls and the false ceiling were connected to each other. Then the power resistors were placed in the structure and the wiring between the resistors and the terminal strips was connected by spade lugs. Next, this part of the structure was placed inside the box, and the sides where the Plexiglas sheets meet the box walls were sealed with removable rubber sealant. At that point, the electric wiring coming from the control panel and the thermocouple wiring coming from the data acquisition boards were connected to the wiring going to the power resistors and the wiring going to the thermocouple sensors at the structure walls respectively. For these connections the terminal strips located at the false wall were used. Then the thermocouple rake assembly was placed on the structure and the thermocouple sensors were placed on the rake. Later on, the wiring connection for the power resistors located at the false ceiling was made, and this was also connected to the terminal strips at false walls. Afterwards, the false ceiling was placed into the box, on top of the side walls of the structure. The supply extension piping was connected to the false ceiling. Then, the gas circuit exhaust and the supply piping were connected to the top cover. Finally, the top cover was placed on top of the whole assembly and it was connected to the box support structure tightly, compressing a rubber gasket between the dexion and the Plexiglas so that the box was tightly sealed.

A halogen detecting propane torch was used for leak tests. Tests indicted that the box was leaking. Therefore, the junctions at the side walls were sealed with RTV silicone sealant adhesive. Washers were placed at each bolt connection on the side walls. The wiring connections at the bottom were sealed again with sealing foam. A Plexiglas piece was placed on the side wall from the inside to eliminate the leaks at the camera window. Removable rubber sealant was used on the strip heater connections and at the top cover where piping penetrated the box. All corners were secured by duct tape to reduce possible leaks.

4.4. Interior Heat Sources

The office space in consideration had three work stations. In each work station there was an occupant, a computer monitor placed on a desk, a computer tower placed on the floor, a light source fixed at the ceiling and additional equipment such as a photocopier placed on a table close to the opposing wall where supply diffusers were located (see Figure 4.4). For the sake of flow investigation, two of the three occupants were standing and the remaining one sitting. Although the simulated office space was an interior space, the effect of an external heat gain was also considered, extending the analysis to an office space with external heat gain through the building skin.

As mentioned earlier, some means to simulate the heat dissipation by the people and the equipment inside an office space was needed. The heat sources were considered in five groups, namely the people, the lights, computers towers, computer monitors and some additional office equipment. In order to simulate these heat sources, power resistors of various capacity and cylindrical shape were used. These power resistors were regulated by means of transformers located at a control panel. The heat release by the power resistors were selected in accordance with the conventional heat dissipation values for the people and machines assumed in cooling load calculations. The assumed values are summarized in Table 4.1.

Table 4.1. Rating of Power Resistors (see Chapter 3 for calculation of power scale ratio).

Item Name	Real Heat Dissipation	Power Scale Ratio	Power Needed
People	100 W	5.48	18.5 W
Lights (each)	160 W	5.48	29.2 W
Screen (each)	110 W	5.48	20 W
Tower (each)	110 W	5.48	20 W
Other (each)	260 W (max.)	5.48	48 W (max.)

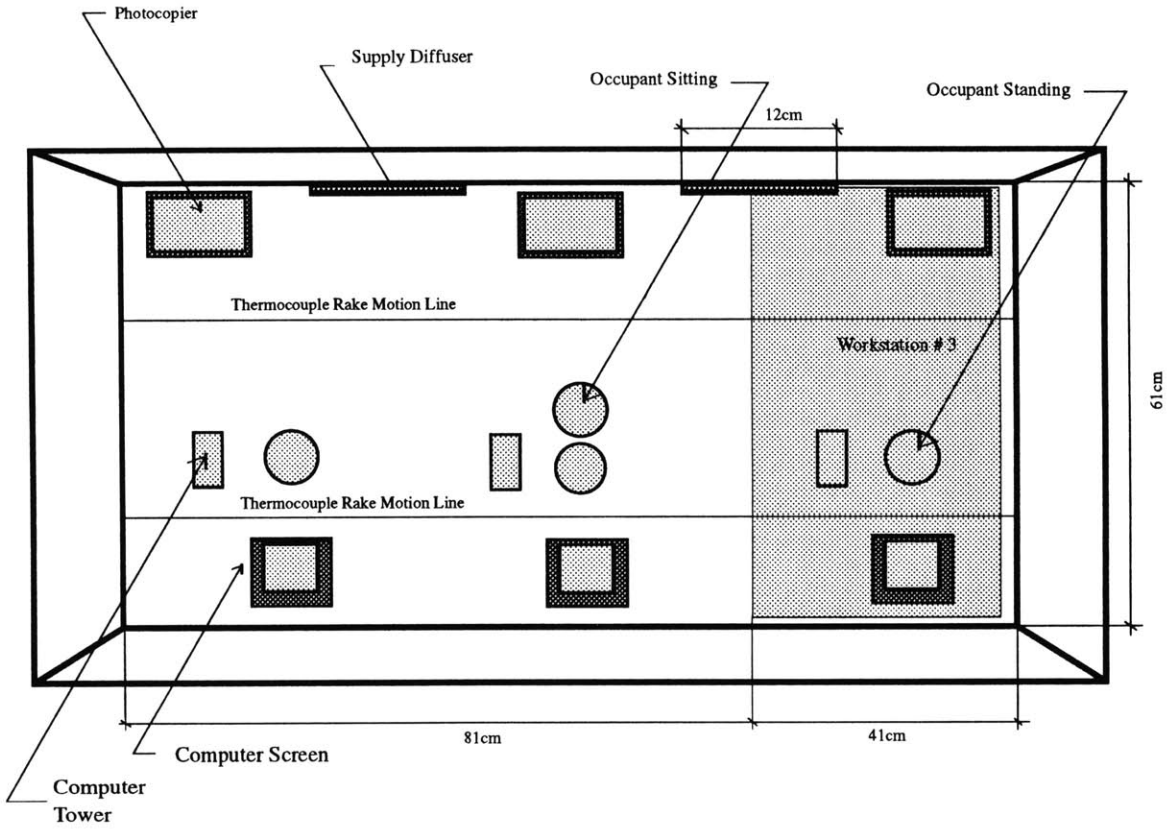

Figure 4.4. Layout of Heat sources and Workstations.

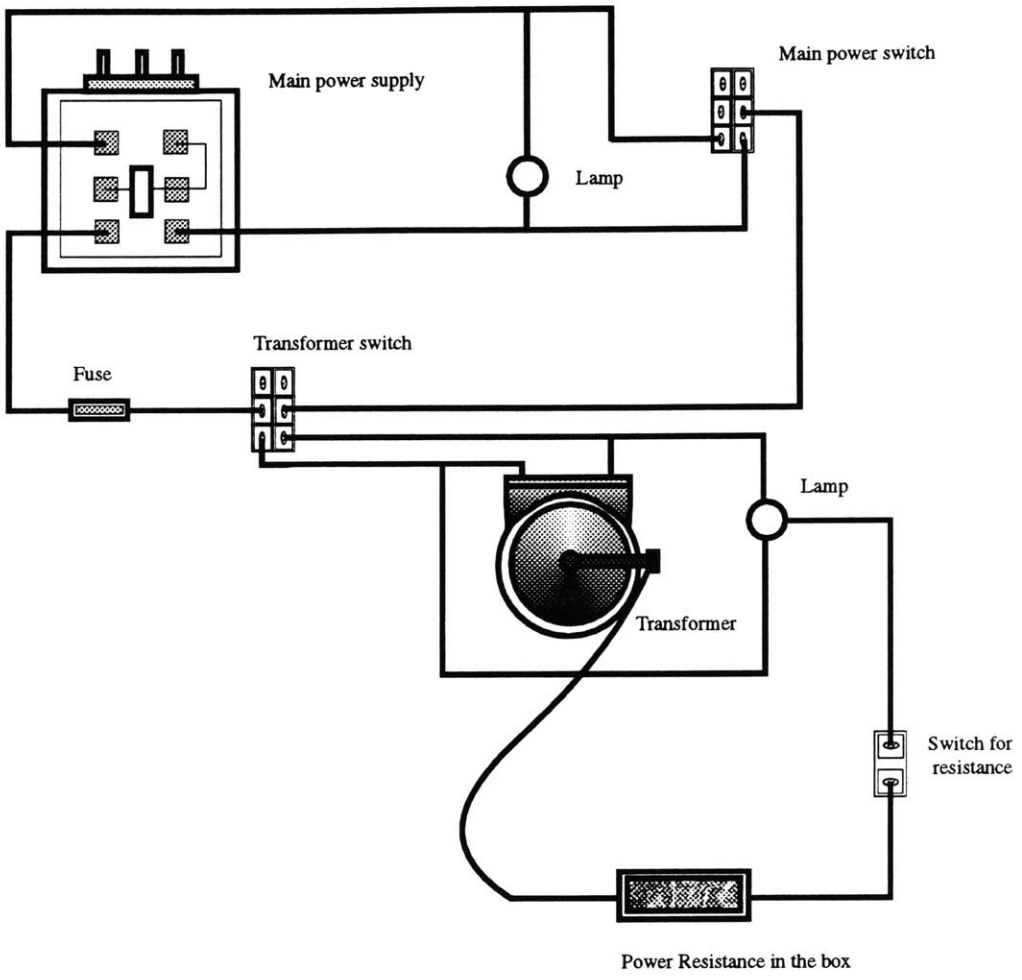

Figure 4.5. The Circuit Layout at the Control Board for Power Resistors.

Usually, the resistance of the power resistors were chosen to dissipate necessary power at an average voltage difference of around 50 Volts AC. Another consideration was the dimensions of the resistors, they had to fit inside the small scale models of the actual heat sources mentioned above. Besides, they had to be flexible to simulate other heat sources with different heat release values if desired. The selected power resistors are listed in Table 4.2.

Table 4.2. Summary of Power Resistor Selection.

Item	Necsry W	Max W	Ohms	Max Amps	Number	Name
Lights Upstairs	30	50	10	2.23	3	Ohmite type 270-50
People	20	100	150	0.82	2	Ohmite type 270-100
	10	50	75	1.15	2	Ohmite type 270-50
Equipment 1	25	25	150	0.41	6	Ohmite type 270-25
Equipment 2	50	50	150	0.58	3	Ohmite type 270-50
Additional	49	50	10	2.23	3	Ohmite type 270-50

where 'equipment 1' stands for the computer monitors and towers, and 'equipment 2' stands for the other possible equipment. 'Additional' stands for a possible power resistor that would be placed inside the box for the simulation of an external heat gain such as solar radiation. Later, it was decided to use the strip heaters placed by Olson on the side walls of the box to simulate external heat gain.

Circuit configuration for each heat source was set up for control and simplicity. The power resistors were connected such that there were six separate circuits for each type. The resistors simulating the lights were connected in series and the circuit had only one switch. The strip heaters on side walls of the box were connected in the same manner. Two resistors of 75Ω were used for the sitting occupant, one for the lower part of the body and the other for the upper part. One resistor of 150Ω was enough for each standing

occupant. The 75Ω resistors were connected in series, then they were connected in parallel with the 150Ω resistors. Each parallel line had its own switch so that different occupancy rates could be simulated. Resistors for the computer towers and computer monitors were connected in terms of two independent parallel circuits and each resistor had its own switch.. The circuit for the additional equipment (photocopiers) was constructed in the same way as for computer screens and towers.

Table 4.3. Scenarios for the Heat Dissipation in the Model.

Scenario 1 **80** **W/m2**

Item	Number on A	W real/p B	W model/p B/5.48	TW real C=A*B	TW scale C/5.48	W/m2 real C/32
Lights upstairs	3	160	29.2	480	88	15
People	3	107	19.5	321	59	10
Equipment1	6	100	18.2	600	109	19
Equipment2	3	120	21.9	360	66	11
Additional	3	267	48.7	801	146	25
Totals	18	754	137.6	2562	468	80

Scenario 2 **55** **W/m2**

Item	Number on A	W real/p B	W model/p B/5.48	TW real C=A*B	TW scale C/5.48	W/m2 real C/32
Lights upstairs	3	160	29.2	480	88	15
People	3	107	19.5	321	59	10
Equipment1	6	100	18.2	600	109	19
Equipment2	3	120	21.9	360	66	11
Additional	0	0	0.0	0	0	0
Totals	15	487	88.9	1761	321	55

Scenario 3 **40** **W/m2**

Item	Number on A	W real/p B	W model/p B/5.48	TW real C=A*B	TW scale C/5.48	W/m2 real C/32
Lights upstairs	3	160	29.2	480	88	15
People	3	107	19.5	321	59	10
Equipment1	6	80	14.6	480	88	15
Equipment2	0	0	0.0	0	0	0
Additional	0	0	0.0	0	0	0
Totals	12	347	63.3	1281	234	40

Each separate circuit contained a transformer, Staco 291 single phase model. The coil tapping arrangements at the transformers permitted an output voltage from 0 to line voltage, 110 VAC to each power resistor. There were six transformers placed on the control board for the six sets of power resistors. Each transformer had its own on off switch. Additionally, another switch was placed for safety reasons between the main power supply and each set of two transformers. The circuit schematic is given in Figure 4.5.

The heat gain for the prototype office was designed to vary between $40W/m^2$ and $80W/m^2$. It was possible to simulate any cooling load by means of the six separate power resistor circuits explained above. Three of the heat gain scenarios are summarized in Table 4.3. Different distributions for the heat gains were considered for different scenarios to investigate their effect on vertical temperature profiles during the experiments. External heat gain was included for the $80W/m^2$ as this much heat gain was not realistic for an interior zone office room.

Each of these power resistors were placed inside small scale models of the heat sources. In order to ensure a uniform heat distribution on the surfaces, a metal with high conductivity such as aluminum was preferred. Therefore, the power resistors were placed in aluminum boxes with the dimensions of the actual heat sources scaled down with a scaling ratio of 6.6 by brass brackets (see Figure 4.6). Aluminum cylinders were used to simulate the occupants. The dimensions of the aluminum enclosures and the assumed dimensions for the actual heat sources are listed in Table 4.4. The human body was idealized as a cylinder with an actual diameter of 40 cm and was modeled with an aluminum cylinder with a diameter of 5.5 cm.

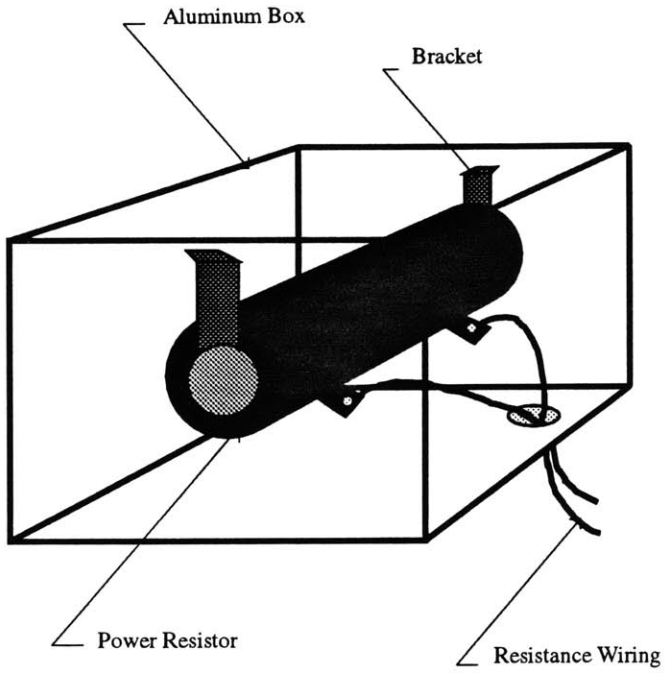

Figure 4.6. Example for the Scale Models of the Heat Sources.

Table 4.4. Dimensions of the Heat Sources.

Item Description	Real Dimensions in cm			Dimensions in cm			Dimensions in inches		
	Height	Length	Width	Height	Length	Width	Height	Length	Width
Screen	**46.0**	**35.5**	**27.2**	7.0	5.4	4.1	2.75	2.125	1.625
Tower	**66.9**	**37.6**	**37.6**	10.2	5.7	5.7	4	2.25	2.25
Table for screen	**100.3**	**66.9**	**83.6**	15.2	10.2	12.7	6	4	5
Occupant	**170**	**36**	diameter	26	5.5	diameter	10.2	2.2	diameter
Xerox	**50.1**	**83.6**	**35.5**	7.6	12.7	5.4	3	5	2.125
Table for Xerox	**66.9**	**83.6**	**50.1**	10.2	12.7	7.6	4	5	3

4.5. Small Scale HVAC System

A series of machinery to function like a typical HVAC system to condition the circulating working fluid in the experimental setup was necessary. The system in this study consisted of two major parts, namely, the gas circuit and the water circuit. In the next two sections the design and implementation of these circuits are described in detail.

4.5.1. The Gas Circuit

A gas circuit to condition and circulate the working fluid was constructed outside the box. The circuit resembled a small scale HVAC system. It consisted of an heat exchanger, a fan and a filtering unit. The fan and the filtering unit were located inside a housing made of Plexiglas (see Figure 4.7).

The refrigerant was pressurized inside the Plexiglas housing by means of the fan. Then it left the housing and entered the heat exchanger where it was cooled to the desired supply temperatures. The cooled refrigerant was supplied to the experiment box through the

supply connection located at the top cover of the box. In the box, flowing in the space between the false Plexiglas wall and the side wall of the box, the fluid entered the office model through the supply diffusers located at the false wall and reached the heat sources. The heated refrigerant went out of the model through the exhaust diffusers placed at the false ceiling and was extracted from the box by the exhaust connection at the top cover. The fluid then entered the fan housing and passed through the filter reaching the fan.

Among various heat gain scenarios considered during the design of the experimental apparatus, the most extreme one was $80W/m^2$ case. This corresponded to a cooling requirement of about 470W in the office model which could be handled with a R114 flow rate of 20cfm at a supply-exhaust temperature difference of 8°K. Based on a pressure drop calculation, the fan was selected to provide a static pressure of 1.5 inches of water at the design flow rate. The fan, Fasco Model A086 (OEM replacement for Rheem), was a centrifugal fan, preferred for the purposes of this study since it provided relatively more static pressures at the desired flow rates than the axial fans. It also had a variable speed control so that it could operate at a wide range of flow rates. It operated at 110VAC 60Hertz and its rated power was 0.04Hp. The operation characteristics for the fan working with a different gas than air was analyzed by using fan laws.

The filter unit was used to filter out any smoke particles in the gas stream. In selection of the filtering unit, the major concern was the pressure drop across the filter. The HEPA (high efficiency particulate air) filters and high efficiency fiberglass air filters were found have unacceptable pressure drops for our system. Additionally, they were expensive and standard sizes did not match the dimensions of the fan housing. Consequently, the filter unit selected was a glass fiber air filter cartridge with a thickness of 2.54cm. It was placed in the fan housing before the fan, so that the gas was filtered before it could reach the fan. The initial testing of the apparatus proved that the filter cartridge provided negligible pressure drop when compared to the system total pressure drop (about 6% of the total).

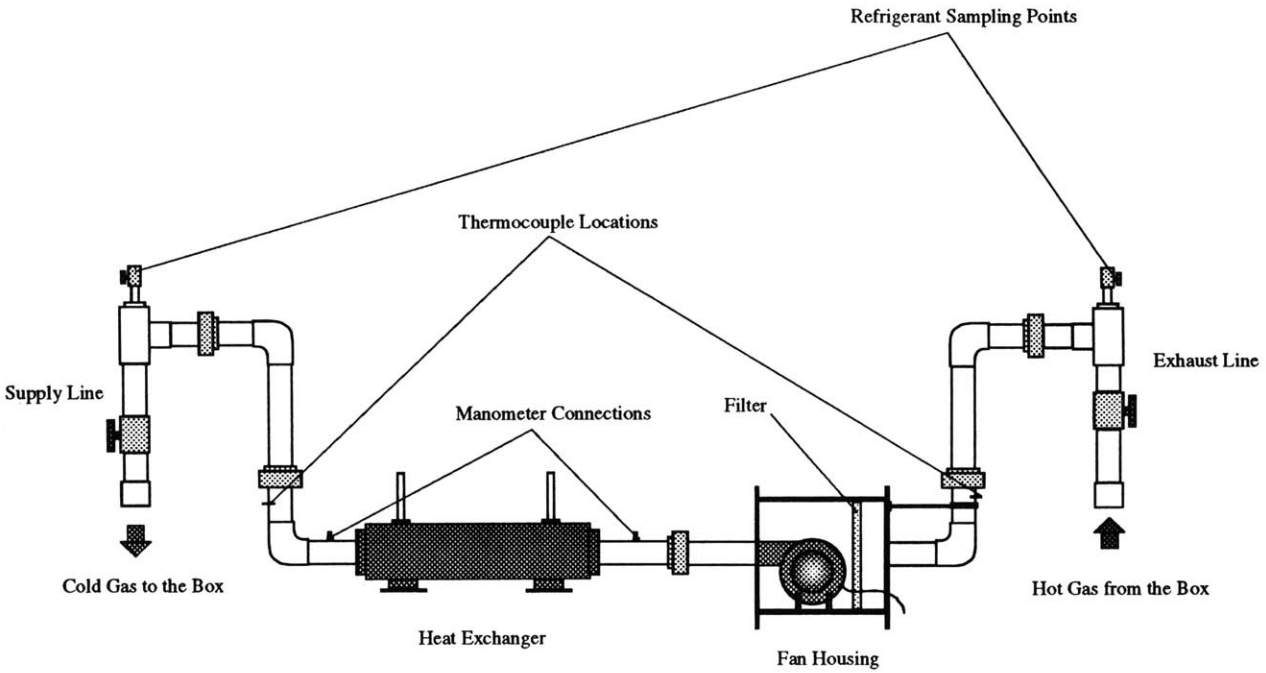

Figure 4.7. The Gas Circuit in the Experimental Setup.

The fan was mounted on a wooden frame structure which could be placed with a sliding motion into the fan housing. The filter was placed in the housing once the fan was inside. The fan housing was constructed out of Plexiglas sheets, 1.26cm thick. It had the dimensions of 30.5cm x 33.1cm x 33.1cm. Five sides of the housing were glued to each other by acrylic cement. The remaining side, which was connected to the piping coming out from the box, was connected to the glued parts by threaded rods extending to the opposing side. The removable side provided easy access to inside. The compression fitting connections necessary for the pressure measurements and filling the gas line were also located at this side.

The heat exchanger was located after the fan housing. A conventional heat exchanger, Basco shell and tube type 500 Size 05014 was selected. The unit had 80 copper tubes, each 36cm long, and one steel shell with a design pressure specification of 100psi. The flow configuration was chosen to be counterflow to ensure higher values of heat exchanger effectiveness. The heat exchanger performance was quoted to have the capacity to cool the refrigerant from 28°C to 20°C at a flow rate of 23 cfm. The water side specifications of the heat exchanger are given in Section 4.5.2.

The ducting system was constructed using 5.08cm (2inch) size, schedule 40 PVC piping. The main reason for the selection of PVC as the piping material was its chemical resistance to R114 and the easiness in machining. Besides it was relatively cheap and could be found easily. Piping of 6.35cm (2.5inch) size and 7.62cm (3inch) was also considered during the early stages of the design. The former was not readily available and the latter was too large. The major consideration in the construction of the piping system was to make well sealed connections. PVC Primer and PVC Cement was used to connect the socket type fittings. For the threaded connections at the heat exchanger inlet and outlet, Teflon tape was used to achieve good seals.

Two Teflon seal ball valves were used as flow regulating and shut off valves. One of them was located by the inlet to the box and the other was placed by the exhaust connection at the top cover. Both at the supply and the exhaust line, a branch made of 1.27cm (0.5inch) size piping was connected to the main line by means of a tee. These branches were used to take samples from the working fluid during the initial filling and extracting the refrigerant from the apparatus for recovery after experiments. These samples were monitored in terms of oxygen concentration which indicated the amount of air in the sample. Two small ball valves located at the end of these branches were closed during the experiments and opened when it was necessary to take samples or to let the air escape from the apparatus during filling the box with R114.

The piping could be disconnected at four points by means of union fittings placed to make it easy to move and modify the circuit if necessary. The unions had Teflon O ring gaskets to ensure a better seal when tightened. A leak test carried out with a halogen detecting propane torch confirmed that the piping system was leakproof at the operation pressure, about 500Pa gauge.

The flow rate was measured by calibration of the pressure drop across the heat exchanger which basically had the most appropriate geometry among the circuit components for calibration. Two compression fittings were placed on the piping at the inlet and outlet of the heat exchanger for manometer tubing connections. The details for the flow measurement can be found in Section 4.7.

4.5.2. Water Circuit

A second circuit to transfer the heat extracted at the heat exchanger to the environment was constructed. The working fluid for the secondary circuit was water. Initially the circuit was designed to have a barrel full of ice water to provide the necessary cooling (see

Figure 4.8). Later, when the experimental apparatus was moved to another laboratory where chilled water from MIT system was available, the circuit was modified to utilize the cooling available from MIT system (see Figure 4.9).

The circuit made use of the cooling available from MIT system via another heat exchanger so that it was independent of the primary circuit. The configuration had another heat exchanger, an expansion tank and an air purger in addition to the components in the initial design. The connection to the MIT heat exchanger was made so that it would be possible to use the heat exchanger for some other apparatus in terms of a parallel circuit. However, because the whole system did not involve a primary loop with its own pump, two circuits could not operate at the same time.

The chilled water left the MIT heat exchanger and went through an expansion tank that regulated the operation pressure in the system. Going through a strainer that removed possible debris in the system, water reached the pump and was pressurized. The drain was placed at the bottom of the circuit at the discharge side of the pump. Water coming out from the pump went through a gravity actuated vertical rotameter which indicated the flow rate in the main circuit. Then it reached a tee that connects the main circuit to the heat exchanger bypass loop. After the tee, water went through a second rotameter located at the inlet of the heat exchanger. Warm water coming out from the system heat exchanger went to the MIT heat exchanger to be cooled again.

There were two needle valves at the circuit. One of them was placed just after the pump to control the flow rate in the main circuit. The other was used to regulate the flow in the heat exchanger bypass loop. The circuit had three ball valves which were used to stop the flow at times of maintenance. Two three way valves connected the main circuit to the radiant panel loop which was used during experiments conducted by Holden.

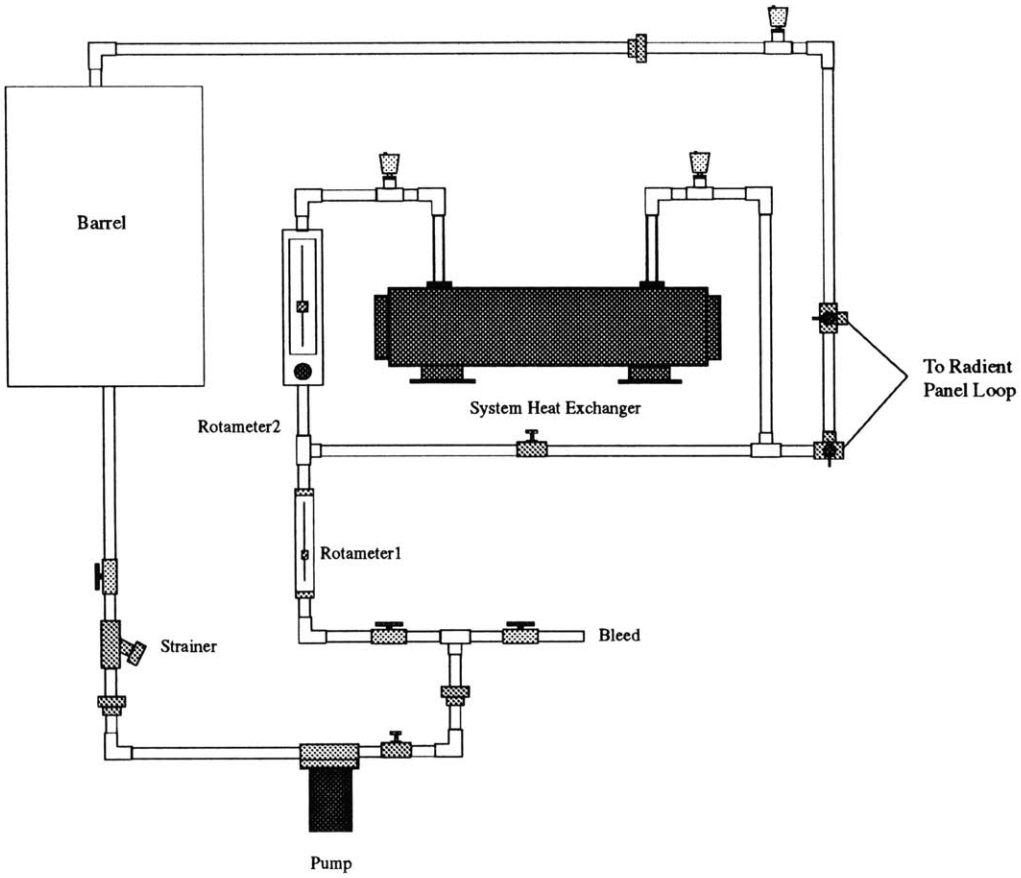

Figure 4.8. The Water Circuit in the Experimental Setup (Initial Design).

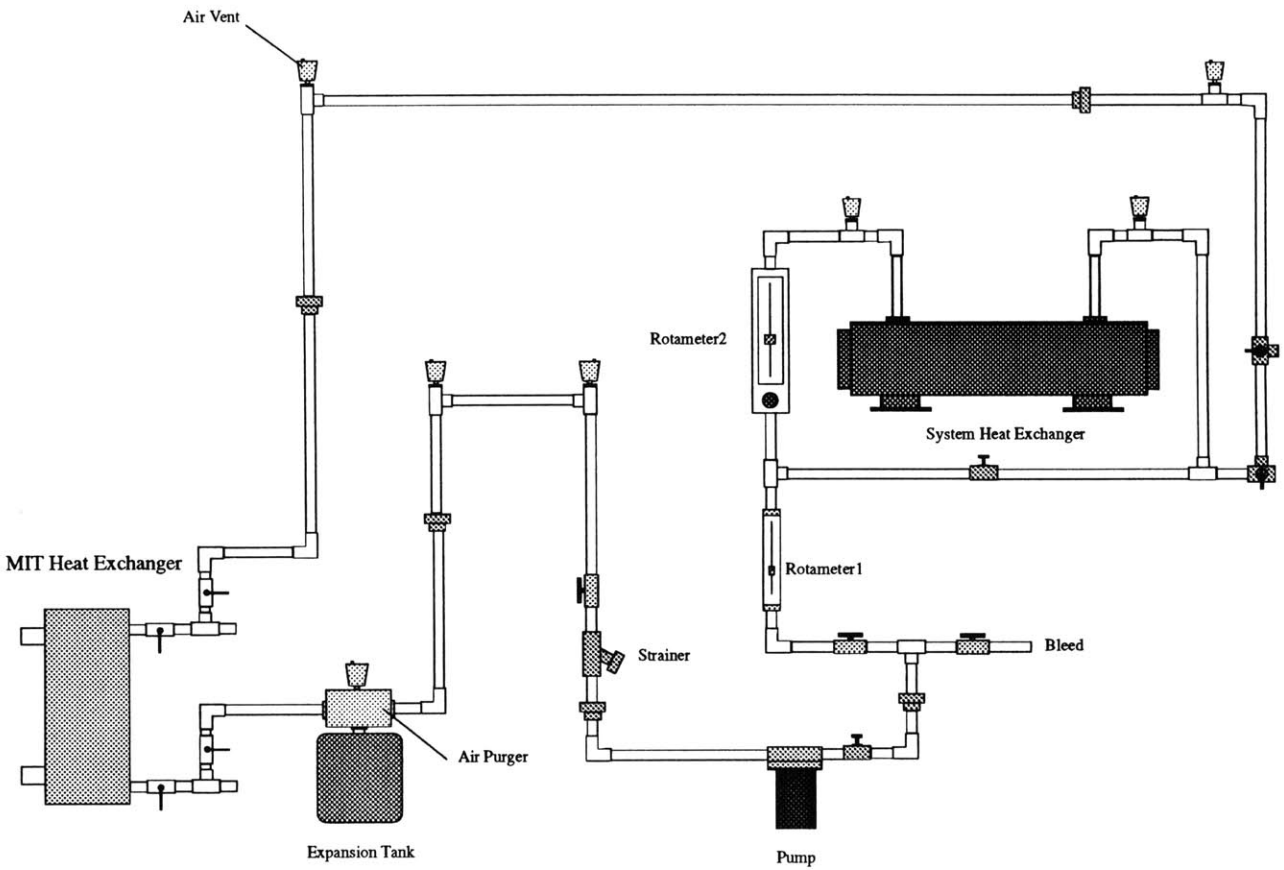

Figure 4.9. The Water Circuit in the Experimental Setup.

The pump selected was Laing brass Type SM-303. The maximum pump pressure was 6.5inches of water and it could provide 4gpm flow rate at a pressure drop of 2inches of water. It should be noted, however, that the selection was based on pressure drop calculations for the initial design. Therefore, when the circuit was modified pressure drop increased because of the additional components. Still, the pump was able to provide 0.8gpm flow rate which was sufficient for this study.

The expansion tank selected was rated at 12psig and could be adjusted if necessary. It was placed at the suction side of the circuit so that the circuit operated above atmospheric pressure. It was connected to the piping with an air purger which had specially contoured walls to remove air from the flow effectively. Besides, automatic air vents were placed at each additional riser.

The MIT heat exchanger was quoted to have a cooling capacity of 6166W for a maximum flow rate of 3gpm in our circuit corresponding to a pressure drop of 4.8inches of water. On the other side, the system heat exchanger was a Basco shell and tube type 500, as mentioned in section 4.5.1. It had enough capacity to provide cooling for the gas line at a water flow rate of 0.8gpm with a temperature difference of 3°K. The quoted pressure drop for the water side was 2.8inches of water at 0.8gpm.

The water circuit was constructed by 1.27cm (0.5inch) size schedule 40 PVC piping. PVC was chosen for the same reasons mentioned in the description of the gas circuit. The connections were typically socket type which were assembled by using PVC Primer and PVC Cement. Teflon tape was used to achieve good seals at threaded PVC connections. However, a small potion of the circuit close to the MIT heat exchanger was constructed with 1.27cm (0.5inch) size copper piping in the second configuration. 2.54cm (1inch) piping was connected the heat exchanger, and the 1.27cm (0.5inch) piping was taken off from this line by a reducing tee. Unions were placed at this location so as to make the

connection easy to modify for future use. Four ball valves were placed to regulate the flow in different branches. Copper piping connections were silver soldered. Rector seal was used at the threaded connections and unions to achieve good seal.

4.6. Flow Visualization System

A flow visualization system was constructed to investigate the flow of the refrigerant inside the office model. The system consisted of a smoke generating system, an illuminating system and a camera system. Flow motions were made visible by injecting light reflecting smoke into the box at the points of interest and illuminating the smoke with a planar light source. The flow motions were recorded by the camera system.

The use of heavy refrigerant gas imposed some requirements on the type of the smoke that could be employed. First of all, the injected smoke had to follow the flow motion of the refrigerant without affecting it as the result of its momentum associated with injection. Besides, the smoke particles had to be smaller than 1micron so that their settling speed would be small when compared to the gas velocities. One possibility was smoke from a combustible material such as tobacco which is sometimes used in natural convection experiments with air, but the combustion required oxygen which is not present in R114 gas. Additionally, because the refrigerant gas is much denser than the smoke particles and the gaseous combustion products, it was likely they would rise like a chimney plume after injection. More over, vaporization of liquid, which is used commonly in smoke generators in theaters and was used in some previous studies at MIT, required addition of heat which again would create a plume upon injection. It was desired to have a naturally buoyant system.

The smoke chosen was ammonium chloride (NH_3Cl), made in a smoke generator similar to the one used by Olson (see Figure 4.10). The generator consisted of two flasks, One of

them was 1/4 full of HCl and the other 1/4 full of NH_3OH. The flasks had inlet and outlet ports at the rubber stoppers on the flasks. R114 gas from the pressurized tank was allowed to pass at a low flow rate into the first flask containing acid, entraining the acid vapors. A rotameter was placed between the tank and the first flask, to monitor the flow rate. The flow rate could be adjusted by two valves at the tank and at the rotameter. The refrigerant then passed into the flask containing the ammonia through tygon tubing. In the second flask, the acid vapors reacted with the ammonia vapors to form the white smoke, NH_3Cl. The smoke laden refrigerant gas then left the flask and entered the box.

Initially, the system was designed to inject the smoke at the points of interest in the box by means of a probe made of 0.95cm diameter steel tubing. The probe was connected to the bottom Plexiglas cover of the box by an O ring compression fitting and its height could be adjusted. However, serious clogging problems were encountered during the first tests of the system. It was decided to replace the steel probe with 1.3cm size tygon tubing. The tubing end was placed between the two supply diffusers located at the side Plexiglas wall of the model structure. It was oriented in the direction of the flow. Typical injection velocities were kept smaller than 1cm/s.

The smoke within the box was illuminated with a vertical plane of light oriented parallel to the primary direction of the flow motions. In addition to a slide projector which was also used by Olson, an Argon laser was used for the illumination of the flow motions. The laser beam was produced at an Omnichrome Model 532 Argon laser machine placed at the top of the experiment box. The beam was projected horizontally on a special diffusive mirror, oscillating at a frequency set by a function generator coupled with an amplifier and was reflected at the desired angles as a vertical light plane. Observation, either visually or with the camera, was at right angles to the plane of light, looking through the camera window located at one of the sides of the box, and sometimes down through the ceiling. The field of view of camera and the lighting system was such that the entire cross section could be viewed at once (see Figure 4.11).

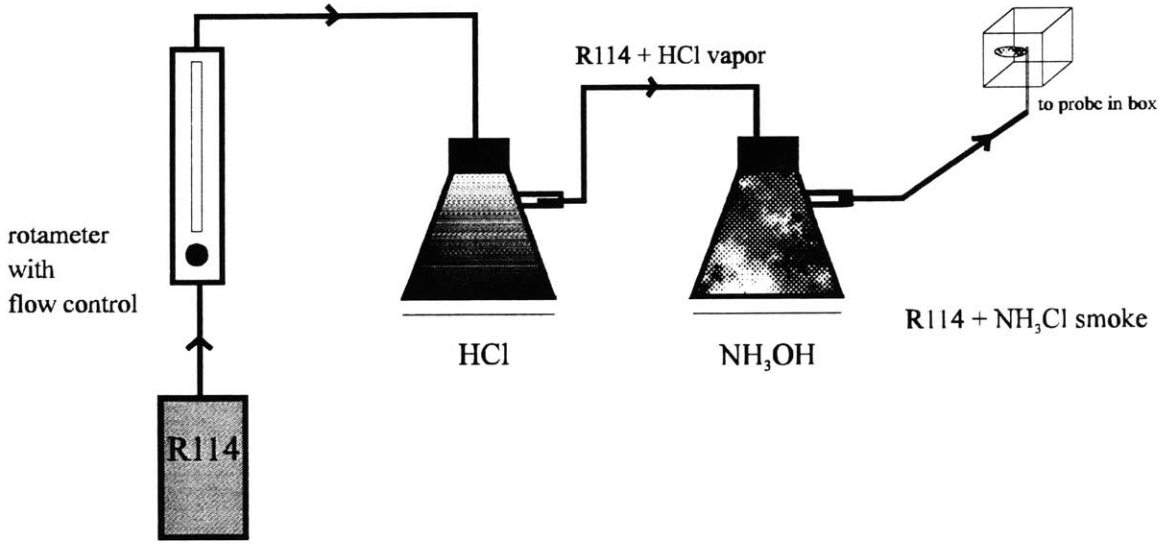

Figure 4.10. The Smoke Generation System.

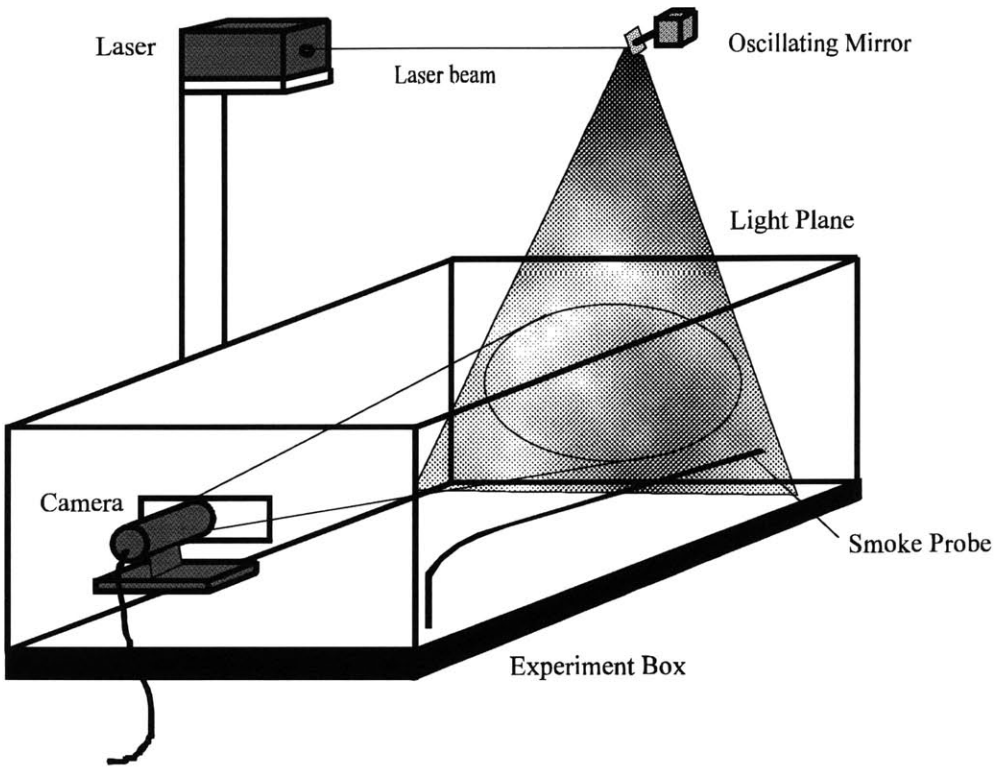

Figure 4.11. The Flow Visualization System.

The camera system consisted of a camera, a control unit and a computer which had a frame grabber board. The software permitted easy analysis of the captured images and saving them as files. The memory capacity of the computer allowed capture of 12 consecutive pictures. During the experiments a video recorder was also used at times, as it provided a continuos analysis and better view at some locations.

4.7. Flow Measurement in the Gas Circuit

It was necessary to measure the flow rate of the refrigerant in the gas circuit so that the supplied fluid to the model could be determined. The pressure drop across the heat exchanger was calibrated to determine the flow rate from the pressure drop. Tests at various flow rates were carried out with air and the pressure drop readings were taken. This flow rate and pressure drop data was converted to test data for R114 by dimensional analysis. The following dimensionless parameters were used :

$$\Pi_1 = \frac{P \times \rho \times L^2}{\mu^2} \qquad \text{and} \qquad \Pi_2 = \frac{Q \times \rho}{\mu \times L}$$

In these dimensionless parameters pressure and flow rate appear in different Pi's making it convenient for analysis. The test data and the converted data for R114 can be found in Table 4.5 and Figure 4.12. Using this R114 data, the constants relating the pressure drop to R114 flow rate were found.

Ki values given in Table 4.5 are the calibration constants for each case, according to the formula;

$$\Delta P = K_i \times Q^2$$

Table 4.5. Heat Exchanger Pressure Drop Calibration Data.

Test Data for Air			Converted Test Data for R114		
delta P (iwg)	Q (cfm)	Ki (iwg/cfm^2)	delta P (iwg)	Q (cfm)	Ki (iwg/cfm^2)
0.62	65.32	0.000145	0.040	6.68	0.000890
0.60	63.67	0.000148	0.038	6.51	0.000907
0.55	59.24	0.000157	0.035	6.06	0.000960
0.50	55.95	0.000160	0.032	5.72	0.000978
0.45	53.62	0.000157	0.029	5.48	0.000959
0.40	49.87	0.000161	0.026	5.10	0.000985
0.35	46.61	0.000161	0.022	4.77	0.000987
0.30	42.60	0.000165	0.019	4.36	0.001013

where ΔP is the pressure drop across the heat exchanger in inches of water and Q is the flow rate in cfm. Apparently, the test data for air corresponds to a limited range of flow rates for R114 (4.3cfm-6.7cfm). Because the experimental setup was designed for flow rates between 5cfm to 20cfm, it was necessary to extrapolate the test results for the experimental conditions.

For the extrapolation of the experimental results, Ki values were used. The difference in the Ki values for each case arises because of the dependence of Ki to the friction factor which is a function of Reynolds number, hence the flow rate. Although the pressure drop across the heat exchanger is both associated with sudden geometry change and the friction loss due to viscous effects in the tubes and Ki values represent both effects, the effect of the latter is assumed to be smaller for the range of flow rates required for the experiments. This assumption was verified by theoretical pressure drop calculations carried out and also the test data which reflects only a slight dependence of Ki values to the flow rate (see Figure 4.13).

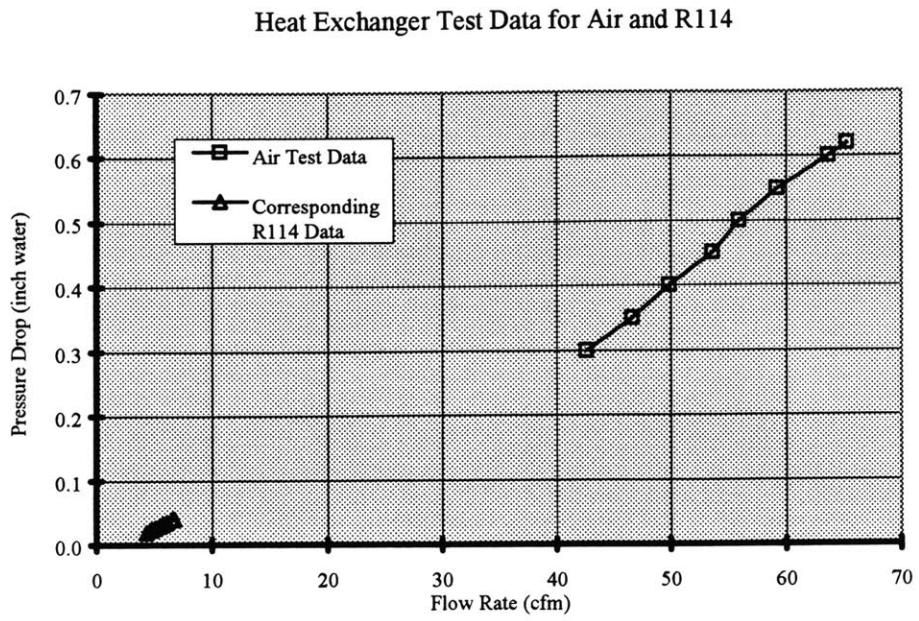

Figure 4.12. Heat Exchanger Pressure Drop Test Data for Air and R114.

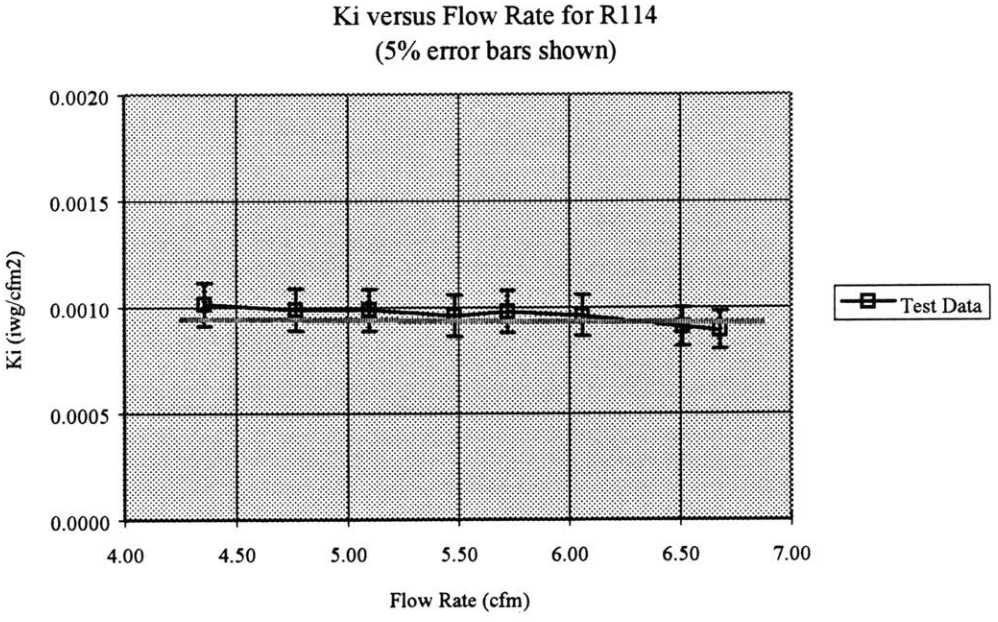

Figure 4.13. Dependence of Ki Values to the Flow Rate (R114 Operation).

The Ki values for R114 were averaged to find K values to be used for the extrapolation of the test results to experiment conditions. This value was;

K average R114 = 0.00095974 inch water/cfm^2

Using this K value, it was possible to determine R114 flow rate by the pressure drop readings across the heat exchanger. The results of the extrapolation is given in Figure 4.14.

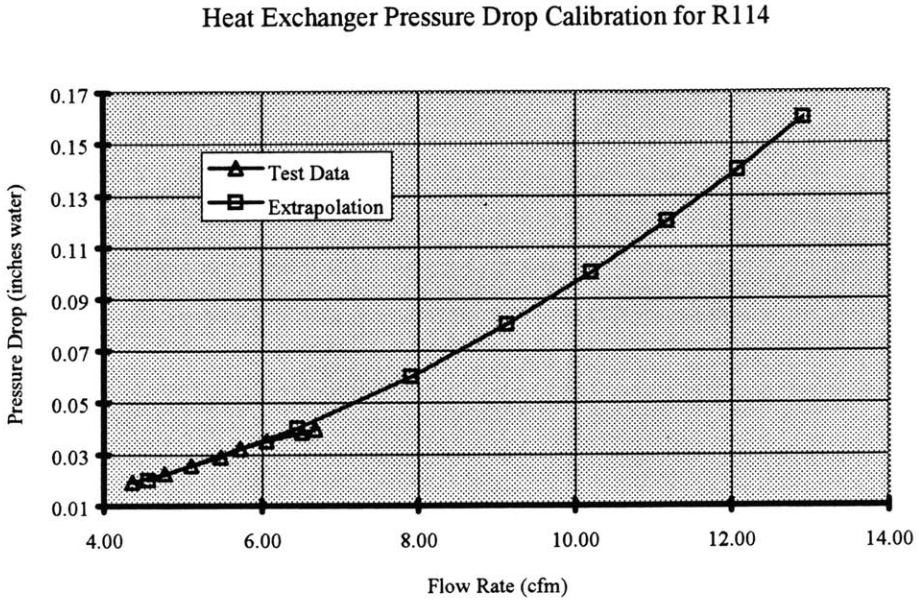

Figure 4.14. Heat Exchanger Pressure Drop Calibration for R114 Operation.

4.8. Temperature Measurement

Temperatures were measured at 32 locations in the experimental apparatus by means of various size thermocouples and a data acquisition system. 4 thermocouples were placed at the water and gas circuits. 16 of the remaining 28 thermocouples were put on a rake

structure inside the model, whereas the rest were used to measure temperatures on the walls of the office model.

The temperature of the refrigerant gas flowing in the office model were measured with a movable rake on which 16 type-T (copper-constantan) 38 WGA Teflon insulated thermocouples were located. The thermocouple bead size was typically 3 times the wire diameter, quoted to be the standard by the manufacturer. The rake consisted of four vertical rods placed in pairs on each side of an aluminum strip (see Figure 4.15). Plexiglas with considerably smaller conductivity than any metal was chosen for the rod material. It prevented the possible effect of conductive heat transfer along the rods exposed to a temperature difference of about 8K at ends, on the thermocouple readings. Each rod pair functioned as a structure to hold the thermocouple probes. In order to eliminate possible lead conduction errors, arising if the temperatures of the rods were different than the temperature of the gas, about 1cm of lead wire were arranged between the probe tip and the rod. On each rod pair, 8 thermocouple probes were placed at heights summarized in Table 4.6 (see Figure 4.16). These heights were selected after a survey of similar studies. The temperature measurement locations of these studies can be found in Table 4.7.

Table 4.6. Gas Temperature Measurement Locations.

Probe No	Height	Real Height	Explanation
1	15mm	10cm	Ankle level
2	45mm	30cm	Knee level
3	91mm	60cm	Gravity center of human body
4	129mm	85cm	Sandberg Study
5	167mm	110cm	Head level for sitting person
6	258mm	170cm	Head level for standing person
7	303mm	200cm	Above head
8	364mm	240cm	Exhaust diffuser level

The vertical Plexiglas rods were connected to an aluminum strip which could slide on two 0.9cm diameter hollow stainless steel tubes which extended from end wall to end wall and served as supports for the rake (see Figure 4.14). The motion of the rake on these tubes was controlled by a 1.2cm diameter hollow stainless steel tube which penetrated the experiment box through an O ring compression fitting located at one of the end walls. The thermocouple probe wires were fed out of the experiment box through the center of the tube. In order to eliminate the possible damage to the thin 38 WGA thermocouple, the wires coming out from the steel tube were connected to type-T 20 WGA Teflon insulated thermocouple lead wires by means of two terminal strips placed on the tubing. The larger lead wires extended to a data acquisition unit.

Table 4.7. Temperature Measurement Locations of Various Studies.

Name of Study	Height for temperature measurement (m)
Arens and Tanale	0.1, 0.6, 1.1, 1.7
Melikov	0.033, 0.1, 0.3, 0.6, 1.1, 1.7
Sandberg	5 below 0.5, 1, 1.5, 1.7, 2.2, 2.4
Shaw	0.48, 1.10, 1.44, 2.40
Bauman	0.1, 0.6, 1.1, 1.7, 2.0, 2.35

Temperatures of the wall, ceiling and floor surfaces of the model were measured by 9 type-T 38 WGA Teflon insulated and 3 type-T 30 WGA glass bead insulated thermocouples. The 30 WGA thermocouples were initially mounted by Olson in small holes drilled in the back side of the box wall sections such that their tips were 1.5mm from the inner surface. A dab of thermal grease was placed in the holes, assuring good thermal contact between the thermocouples and the aluminum [26]. 2 of 30 WGA thermocouples were placed on the side wall, one at the top section and the other at the middle. The remaining 30 WGA thermocouple was at the top section of the end wall through which the rake tubing penetrated the box.

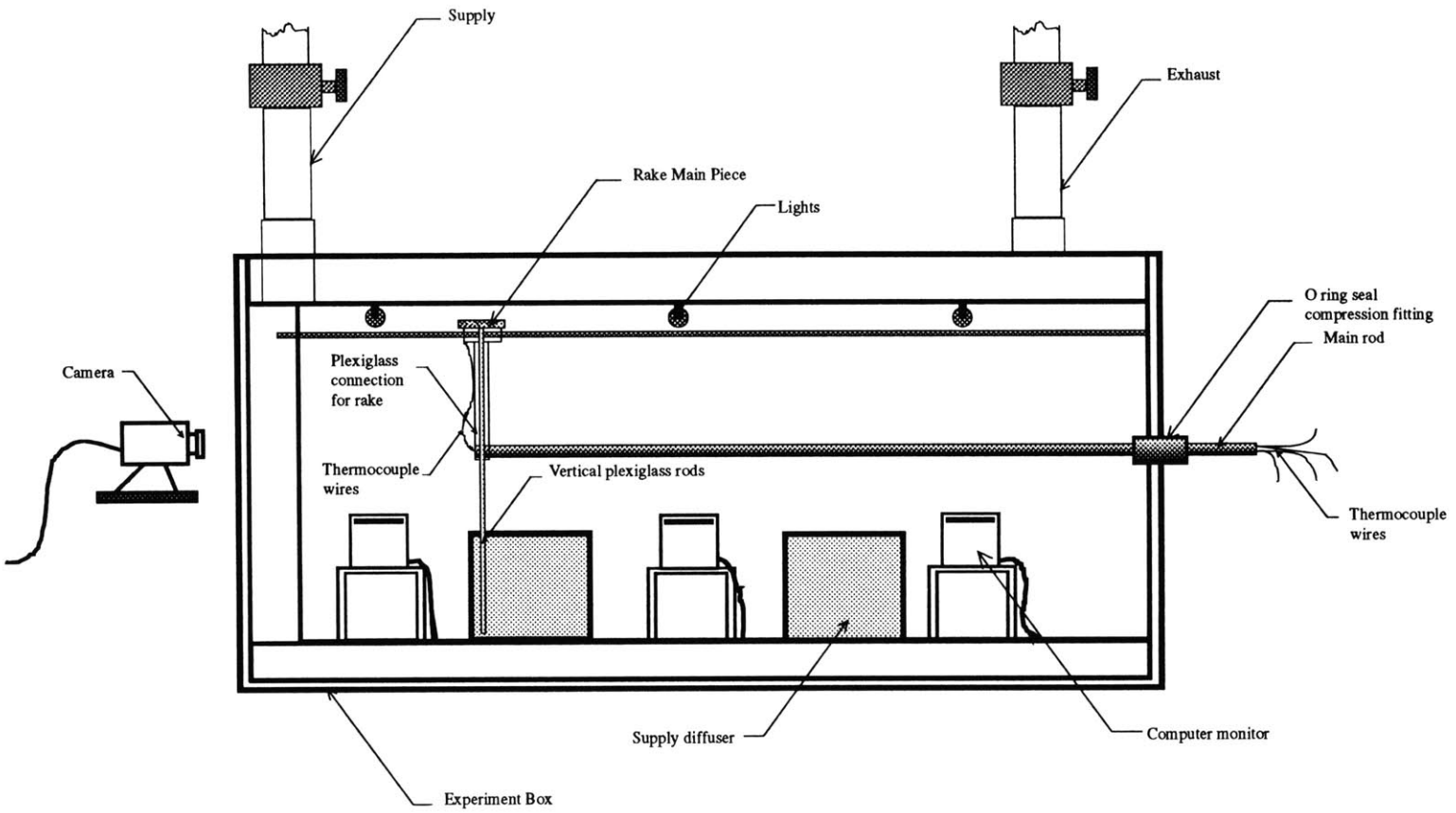

Figure 4.15. Thermocouple Rake Assembly and the Scale Model in the Experiment Box (Side View).

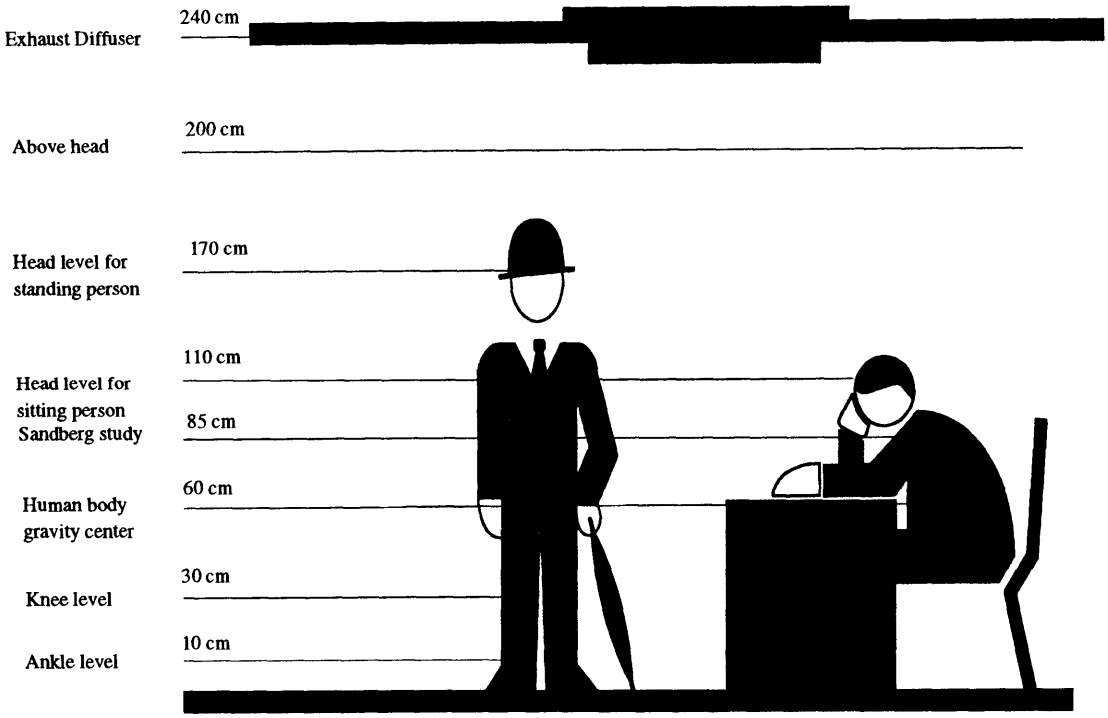

Figure 4.16. Vertical Temperature Measurement Locations on the Rake.

38 WGA thermocouples, however, were located on the Plexiglas side walls, ceiling and floor of the model structure in the box. 4 thermocouples were placed in pairs on the false ceiling and the false floor surfaces. On the side wall, two thermocouples were placed on the wall surface and one thermocouple was mounted on each diffuser. The last 38 WGA thermocouple was positioned on the end Plexiglas wall. Thermal grease was placed on the thermocouple probes to ensure good thermal contact between the probes and the Plexiglas. 38 WGA thermocouples were connected to 20 WGA thermocouple lead wires at the interface mounted on the side wall of the model structure. 20 WGA wiring went through the Plexiglas bottom cover of the box by a connection sealed with RTV silicone sealant adhesive and extended to the data acquisition unit.

In the gas circuit, temperature of the refrigerant gas was measured at the inlet to the box and at the exhaust line before the gas entered the fan housing, by type-T 20 WGA Teflon insulated thermocouples. These thermocouples were mounted in small holes drilled through PVC piping (see Figure 4.7). The beads were positioned at the centerline of the piping. The connection was sealed with high strength epoxy and RTV silicone sealant.

In the water circuit, temperature was measured at two locations, at the inlet and the outlet of the heat exchanger, again by type-T 20 WGA Teflon insulated thermocouples. These thermocouples, unlike the ones located at the gas side, were placed on the piping and were covered by insulation at the top. The large convection coefficient of the water flow inside the piping assures that the temperature at the piping surface was close enough to the water temperature, once the connection was well insulated.

All thermocouple wires were connected to two Keithley Metrabyte Exp-16 expansion multiplexer and amplifier systems. Each system multiplexed 16 different analog input channels into one analog output channel providing signal amplification and filtering. The systems included cold junction sensing and compensation circuitry. They were connected

to a computer in which data acquisition software was installed. The software was programmed to take and average readings at specified intervals, scale the temperatures with reference to a set temperature and print the results on file. Once the temperature measurement system was complete, thermocouples were calibrated by using an ice bath and water at precisely measured temperatures.

4.9. Filling and Emptying the Experiment Box

One end of the box was raised about 10cm, by using a car jack, in order to fill the experiment box with refrigerant gas. Refrigerant was added slowly at the lower corner of the floor at a rate about 1 experiment box volume per 2 hours. Because the refrigerant was seven times denser than air, air was trapped at the top of the box. Therefore. as the refrigerant was supplied to the box, air was periodically vented from the ball valve located at the top of the exhaust piping which was at that time the highest point in the system.

While filling the box, R114 concentration was monitored by measuring the oxygen concentration in samples taken from the air purging point at the top of the exhaust piping. When the oxygen concentration in the sample was low enough, indicating a low air concentration, the refrigerant flow was stopped and the box was ready for experiments. Olson, during his studies, had found that an air concentration up to about 10% did not effect the results significantly. Hence, during sample analysis, an oxygen concentration up to a maximum of 2%, roughly 10% air, was sought.

The two compression fitting connection located at the fan housing were used to fill the gas circuit. The refrigerant was supplied in the same manner described above through the fitting at the bottom corner of the removable side of the fan housing which was the lowest point in the system. At the same time, air was allowed to escape from the sampling locations at the supply and exhaust lines and also from a hole placed at the top corner of

the fan housing so as to prevent any air to be trapped inside. Oxygen concentration was monitored and no more refrigerant was supplied once the desired concentrations were reached. The gas circuit could be completely isolated from the experiment box in terms of ball valves supply and exhaust lines, so that each time the box was filled with air again, it was not necessary to empty the circuit.

When the experiments were finished, the box was filled with air and the refrigerant was stored in a tank to be recovered. The procedure was exactly the inverse of the one described above. Refrigerant was sucked from the tilted experiment box at the lower corner, by means of a recovery setup consisting of a vacuum recovery tank and a flow regulator operated by certified MIT staff. Oxygen concentration was monitored at the various locations in the box to ensure no more refrigerant was left inside. The gas circuit was evacuated in the same way, the recovery apparatus connected to the bottom compression fitting at the fan housing.

4.10. Small Fans

One of the major problems associated with the application of displacement ventilation in open plan office environments is the vertical temperature stratification which can sometimes exceed the comfort limits. Therefore, in displacement ventilation systems vertical temperature stratification puts a limit on the cooling load that can be handled, as stratification gets more pronounced when the heat generation in the space increases. However, as mentioned in Chapter 1, this temperature stratification can also be very useful in terms of reduced energy consumption and improved air quality as economizers utilizing outside fresh air can be used more often when the exhaust temperatures increase. Accordingly, if only it could be possible to achieve better mixing at lower levels in the office space where occupants are sitting (0m-1.1m) without effecting the stratification at the higher levels, the objective to save energy by displacement ventilation would be more

effectively achieved without exceeding comfort limits. In that case, the amount of cooling load that can be handled by displacement ventilation would increase. Furthermore, an economizer placed at the supply side could operate with outside fresh air whenever exhaust temperatures exceed outside air temperatures and higher exhaust temperatures promise to extend the times the economizer is utilized in summer months.

In this study, an office model where the supply diffusers were located on the side walls is considered. In order to achieve slow mixing at lower levels, three small fans were placed symmetrically on the floor. The dimensions of the suction opening and the discharge diffusers of the fans were designed such that the discharge velocity was low, close to the velocity at the supply diffusers on the wall. The fans sucked the cold air accumulated at the floor level and discharged it at a height of 7.5cm, corresponding to a real height of 52cm. The flow at the discharge diffuser was slightly angled towards the floor. Because the cold air was supplied at low velocities to the space and it immediately flowed down to constitute a uniform cold air blanket on the floor, in principle this configuration was not very different than a displacement ventilation application with floor diffusers. The case when the fans were operating to create slow mixing at lower levels could be compared to the displacement ventilation applications with swirl diffusers. However, the fans eliminate the need for a raised floor, needed will floor diffusers.

The fans were selected to be NMB Technologies Type 1606KL brushless DC axial fans. The reason to prefer DC fans were the easiness in the control of the voltage difference and the response of the fan to the changes in the voltage. The fans could operate at voltage difference between 4.3V to 13.5V. This was important as effects of different flow rates were planned to be investigated. The fans were connected in parallel and were controlled by a variable DC power supply. The fan casing was constructed out of cardboard. The cardboard pieces were then assembled by means of four long bolts which also functioned as supports to hold the structure vertically (see Figure 4.17).

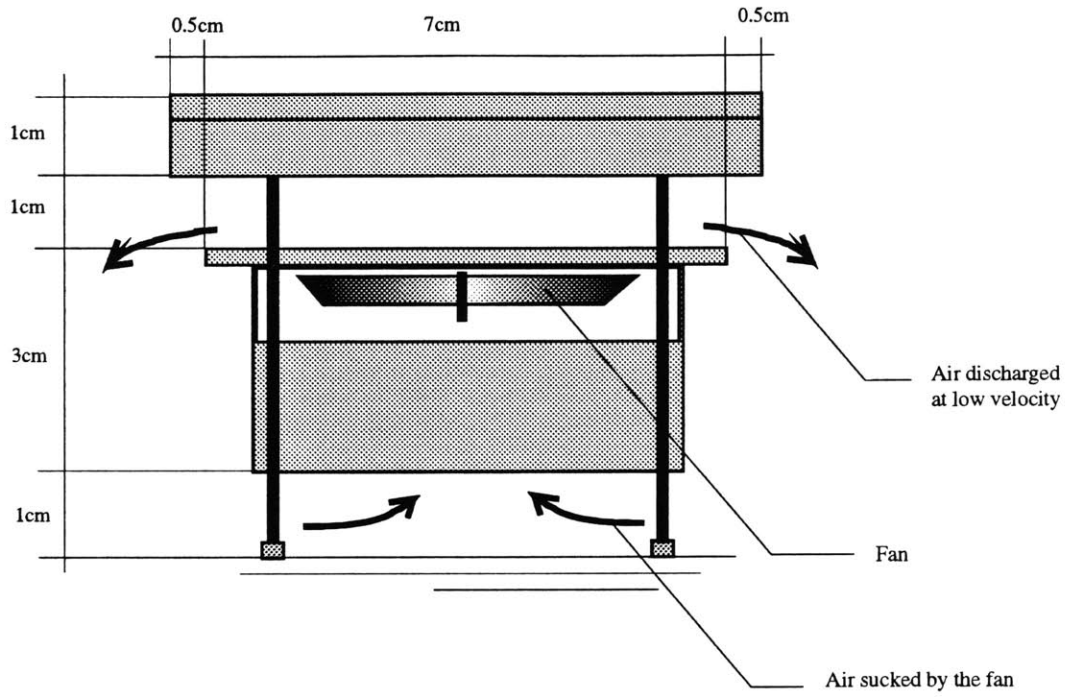

Figure 4.17. Small Fans at the Floor Level.

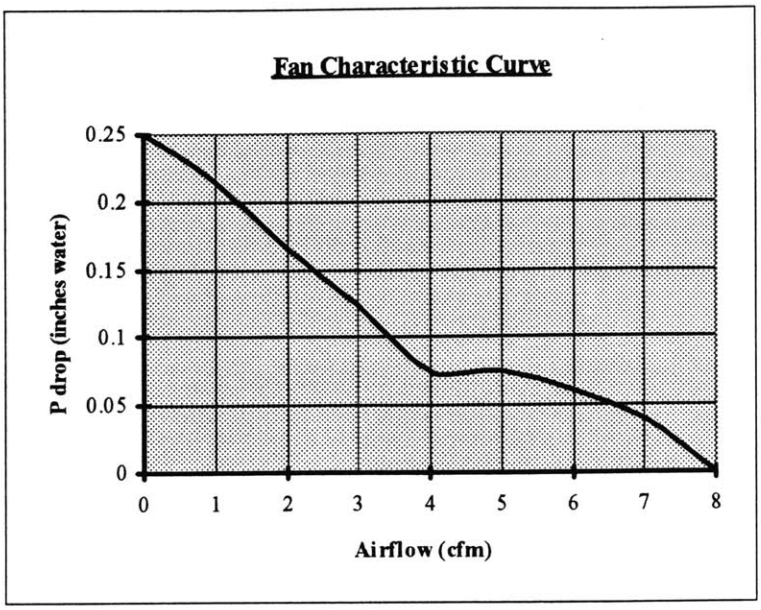

Figure 4.18. Fan Characteristic Curve for Air Operation for NMB 1606KL DC.

Table 4.8. Test Data for NMB 1606 KL DC.

Refrigerant 114 Test Data

Test No #	Voltage V	Current Amp	Power Watts	Vav inlet m/s	Flow rate m^3/s	Flow rate cfm	delta P inch water	Vav outlet m/s
1	13.2	0.08	1.06	0.86	0.0011	2.34	0.070	0.37
2	12.0	0.07	0.84	0.76	0.0010	2.06	0.075	0.32
3	11.1	0.07	0.77	0.67	0.0009	1.83	0.075	0.29
4	10.0	0.06	0.60	0.58	0.0007	1.58	0.080	0.25
5	9.0	0.05	0.45	0.55	0.0007	1.50	0.090	0.23
6	8.3	0.05	0.41	0.49	0.0006	1.32	0.110	0.21
7	7.6	0.05	0.38	0.42	0.0005	1.14	0.135	0.18
8	7.2	0.04	0.29	0.38	0.0005	1.02	0.145	0.16
9	7.0	0.04	0.28	0.34	0.0004	0.93	0.150	0.15
10	6.5	0.04	0.26	0.34	0.0004	0.92	0.150	0.14
11	6.0	0.03	0.18	0.28	0.0004	0.77	0.170	0.12
12	5.5	0.03	0.16	0.22	0.0003	0.60	0.180	0.09
13	5.1	0.03	0.15	0.20	0.0003	0.55	0.200	0.09
14	4.3	0.02	0.09	0.13	0.0002	0.35	0.220	0.05

The flow rate was controlled by varying the DC voltage difference across the fans. After the assembly of the diffusers, tests were carried out at various voltage differences for each unit. The velocities at the suction and the discharge cross sections were measured by a

sensitive velocity indicator. The velocities were averaged over the cross section to find the flow rates. The pressure drop in the unit was estimated according to the fan operation data supplied by the manufacturer (see Figure 4.18). Then it was possible to convert the air data to the case for refrigerant gas by fan laws. The converted test data for R114 operation is given in Table 4.8. The velocities at discharge section given in the last column of Table 4.8 are for R114 operation. Simulated velocities can be found by applying velocity scale ratio for these values.

4.11 Uncertainty in the Experimental Measurements

Table 4.9. summarizes the source and the magnitude of the uncertainties in the experimental measurements.

Table 4.9. Uncertainty in the Experimental Measurements

Measurement	Technique	Source of uncertainty	Magnitude of uncertainty
R114 temperature Model wall temperature	Type-T thermocouple	Radiation error and calibration	± 0.5°C measured ±0.15°C scaled
Box wall temperature	Type-T thermocouple	Spatial T non-uniformity, calibration	± 0.5°C measured ±0.15°C scaled
Water temperature	Type-T thermocouples	Calibration and conduction errors	± 0.8°C measured
R114 purity	O_2 monitor	Calibration	3% of R114 concentration
Rake position	Read meter,stick scale	Calibration	± 0.01m
Tmoermocouple height	Ruler	Bead, rake movement	± 0.003m
Flow rate (gas circuit)	Manometer readings	Calibration	5%
Flow rate(water circuit)	Rotameters	Calibration	3%
Heater voltage	AC voltmeter	Voltmeter accuracy	0.5%
Gas cooling rate	Enthalpy rise of R114	Flow rate and T rise	10%
Heat gain in model	Power at resistors	Voltmeter accuracy	0.5%
Velocity at diffusers	Mass continuity	Flow rate	10%

CHAPTER 5

STEADY STATE EXPERIMENTS ON DISPLACEMENT VENTILATION

Steady state experiments were conducted to investigate the performance of displacement ventilation in open plan offices. The experiments covered a variety of cases in terms of heat gain per area, air supply flow rates and operation of small fans located at floor level. The temperature distribution in the office model was determined. Measured quantities were analyzed to compare the performance of displacement ventilation at different conditions. Flow visualization was performed to investigate the nature of the fluid flows.

5.1. Objectives

This study investigated the performance of displacement ventilation systems in open plan office environments. It focused on the possibility of improving the performance of these systems by reducing the temperature stratification at lower levels and allowing the system to operate with high heat gains.

The major goal of the experiments was to look at the vertical temperature stratification corresponding to different heat gains and flow rates. Different heat gain scenarios and different heat source distributions had to be realized in the box. It was desired to determine the temperature field at the model for each case studied. The change in the vertical temperature profiles due to the small fans at floor level was investigated. It was

desired to compare the temperature profiles corresponding to different heat gains at the same supply flow rates. The effect of slow mixing at lower heights was to be compared for each heat gain. The character of the fluid flow in the model was to be explored by flow visualization.

5.1. Experimental Test Conditions

23 experiments corresponding to different heat gains, flow rates and small fan operations were performed. The working fluid used in the experiments was primarily R114 gas, but also contained small concentrations of air. The R114 concentration was different for each experiment. The highest R114 concentration achieved was 86% by volume. The experimental conditions were set according to a R114 concentration of 100% by volume. Therefore, the scaling ratios deviated from their designed values for experiments. The same method Olson [24] used was applied to calculate the thermophysical properties of the gas mixture in each experiment. Scaling ratios and manometer pressure drop calibration were corrected accordingly. It was found that, heat gains from $10W/m^2$ to $38W/m^2$ could be simulated. The supply air flow rates varied between $700m^3/h$ (8 ACH) and $1000m^3/h$ (11 ACH). Air supply temperatures were typically around 19°C. The flow through the small fans located on the floor varied between 0% to 86% of the supply flow rate. The cases simulated by experiments are summarized in Table 5.1. Unfortunately, no sufficient temperature data could be recorded for experiment 1.

Among 23 experiments, experiments 5 to 13 were performed consecutively and they had the highest R114 concentration. Supply air flow rate and supply air temperatures were approximately constant for experiments 5 to 13. This was convenient for comparison of the results. They corresponded to $20W/m^2$, $27W/m^2$, $38W/m^2$ heat gain, which were close to the cases considered by other studies. In experiments 5 to 13, the heat losses from the side walls the box to the outside were the smallest (0% for $20W/m^2$, 20% for $27W/m^2$ and

30% for 38W/m^2), hence the effect of heat dissipation on the temperature field was more realistic. For example, the temperature stratification in experiment 8 is more pronounced than that of experiment 17, although the heat gain was the same and the air supply flow rate was smaller for the latter. The heat sources were different for the two experiments. In experiment 17, strip heaters on the box side walls were used to simulate external heat gain. This was probably the reason for higher (53% of total) heat loss at the box side walls.

Table 5.1. Summary of Cases Considered by Experiments.

(the heat sources used in each experiment can be found in Appendix)

No	Case	R114 con.	Supply flow rate	Small fans flow rate	Velocity at supply diffusers	T Supply	T Exhaust	T (0.1m)	ΔT (0.1m - 1.1m)	ΔT (0.1m - 1.7m)
#	W/m^2	%total	cfm	%total	m/s	°C	°C	°K	°K	°K
1	**15**	0.68	513	0%	0.17	N/A	N/A	N/A	N/A	N/A
2	**25**	0.83	412	0%	0.13	19.0	20.7	19.7	0.6	1.7
3	**25**	0.83	412	39%	0.13	19.2	21.0	20.1	0.6	1.7
4	**25**	0.83	412	86%	0.13	19.3	21.1	20.6	0.5	1.3
5	**20**	0.86	596	0%	0.19	18.9	20.9	19.7	0.4	1.2
6	**20**	0.86	596	23%	0.19	18.9	20.8	20.0	0.2	0.8
7	**20**	0.86	596	16%	0.19	18.9	20.8	19.7	0.4	1.1
8	**27**	0.86	626	0%	0.20	18.9	20.8	19.7	0.9	2.3
9	**27**	0.86	626	50%	0.20	18.9	20.9	20.2	0.6	1.8
10	**27**	0.86	626	15%	0.20	18.9	20.9	19.9	0.9	2.3
11	**38**	0.84	615	0%	0.20	19.1	21.4	20.1	1.8	3.0
12	**38**	0.84	615	58%	0.20	19.1	21.6	21.0	1.1	2.2
13	**38**	0.84	615	22%	0.20	19.1	21.7	20.6	1.7	2.8
14	**10**	0.76	388	0%	0.13	19.4	20.1	19.6	0.2	0.3
15	**10**	0.76	388	22%	0.13	19.3	20.5	19.7	0.1	0.5
16	**10**	0.76	388	76%	0.13	19.2	20.3	19.9	0.1	0.3
17	**27**	0.74	465	0%	0.15	19.1	20.6	19.7	0.4	1.0
18	**27**	0.74	465	26%	0.15	19.1	20.7	19.8	0.4	1.1
19	**27**	0.74	465	70%	0.15	19.1	20.7	20.2	0.3	0.7
20	**31**	0.69	513	60%	0.17	19.2	20.6	20.3	0.6	1.0
21	**31**	0.69	629	0%	0.20	19.2	20.7	20.0	0.9	1.5
22	**31**	0.69	629	18%	0.20	19.3	20.9	20.2	0.7	1.3
23	**31**	0.69	629	49%	0.20	19.2	20.7	20.4	0.5	0.9

For experiments 5 to 13, temperature data could be recorded in full detail (224 readings for each experiment). The temperature data for experiments 15 to 23 was less detailed (96 - 128 readings) and R114 concentration was considerably lower (%69 to %76). Additionally, the supply flow rates were not constant. Therefore, it was decided to base the analysis on the results of experiments 5 to 13.

5.3. Description of the Experiments

Once the experiment box and the gas circuit were filled with refrigerant, oxygen concentration was measured at the fan housing and the sampling locations at the gas line. The heat sources were turned on in accordance with the scenarios considered. Water and gas circuits were put into operation. The water flow rate was measured by the rotameters in the circuit. The flow rate was adjusted if necessary so that the gas supply temperatures to the model corresponded to 19°C for air operation. The manometer pressure drop across the heat exchanger was used to measure the gas flow rate. The temperatures at 8 points in the box and the water circuit were monitored by the data acquisition system. When it was observed that at least 75% of the readings at 8 selected locations did not change by a tenth of a degree for at least 3 readings (average of 3x1000 readings over 60 seconds) , it was decided that steady state was achieved. The system achieved steady state in about 1/2 hour.

For each experiment, temperature readings were taken at seven sections in the model, by moving the thermocouple rake (see Figure 5.1). 3 of these sections were at the workstations. At every section, temperatures at heights mentioned in Chapter 4 were scanned. For each scan, temperatures at the walls, the floor, the ceiling, water circuit and the gas circuit were also measured (see Section 4.8 for the measurement locations). The data was captured by the data acquisition unit and printed on file. The data was then used

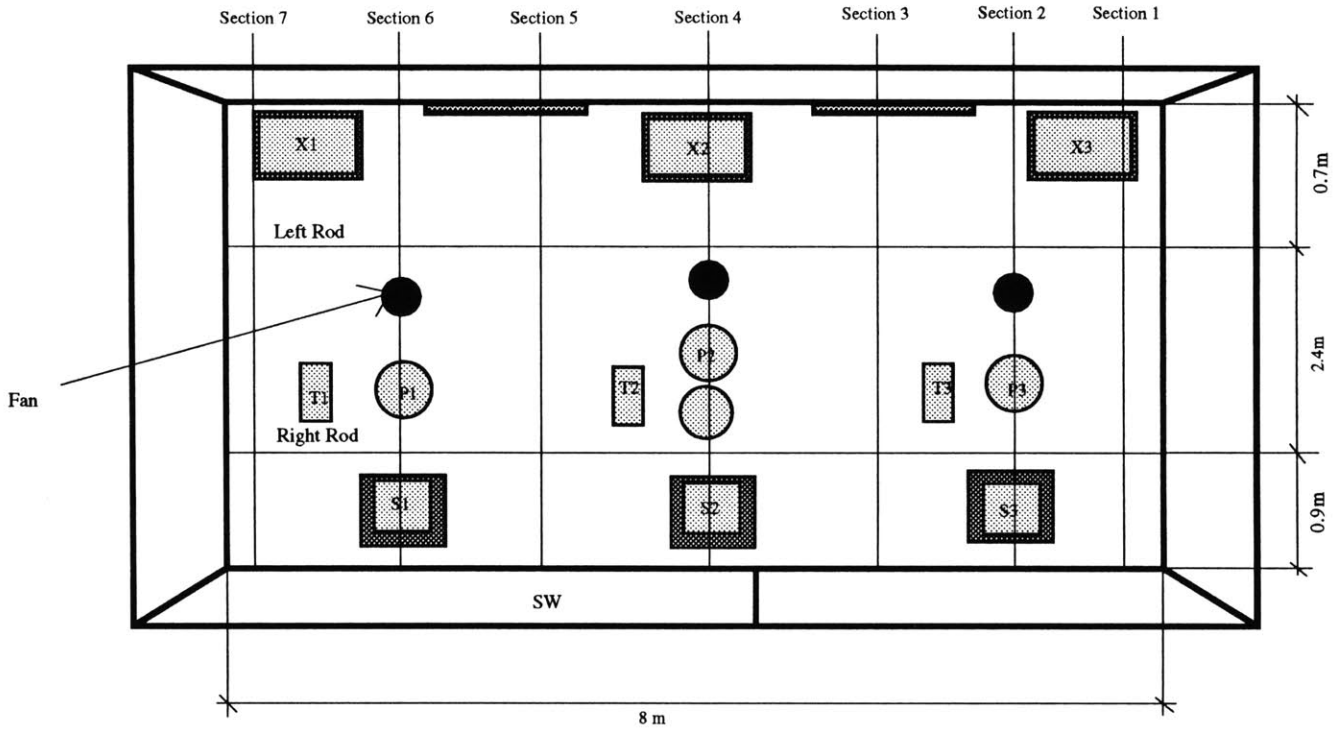

Section 1 0.15m, Section 2 1.7m, Section 3 2.75m, Section 4 3.6m, Section 5 4.7m, Section 6 5.5m, Section 7 7.2m from right end wall.

Figure 5.1. Distribution of Heat Sources and Temperature Measurement Locations.

as input to a spreadsheet. The spreadsheet averaged the two readings at each height at each section to find the section temperature distribution. Then it averaged the section profiles to find the average temperature profile in the model. The gas supply, gas exhaust, water inlet to heat exchanger, water outlet from the heat exchanger and model surface were averaged for seven scans. The spreadsheet also corrected the scaling ratios for the R114 and air mixture for that case, and used these ratios to convert the experiment data to air data. The calibration constants for the system fan and the small fans were corrected in the same manner to find the simulated air flow rates.

Once an experiment with no small fans was finished, two other experiments corresponding to the same heat gain and supply flow rate but with small fans operating were performed. Therefore, the 9 experiments analyzed can be considered as three sets corresponding to three different heat gains. Each set consisted of three experiments; one of them with no small fans, the other two with small fans at two different settings.

5.4. Displacement Ventilation for 20W/m^2 (Experiments 5,6,7)

In this set of experiments, a heat gain of 20W/m^2 was simulated with a supply air flow rate of 0.28m^3/s (596cfm, 8.8 L/s.m^2). The velocity at the supply diffusers was 0.19m/s. The total simulated cooling load in the model (8m x 4m floor area, 2.7m height) was 639W. The heat was dissipated by two occupants, two computer monitors, one photocopier and the lights at the ceiling. See Table 5.2. and Figure 5.1 for the location and the percentage of contribution of each heat source.

R114 concentration during these experiments was 86%. The corrected scaling ratios are summarized in Table 5.3.

Table 5.2. Heat Sources in Experiments 5,6,7 (20W/m^2).

Heat Source	Symbol	Heat Dissipated (W)	% of total
Occupant 1	P1	73	11%
Occupant 2	P3	73	11%
Monitor 1	S1	66	10%
Monitor 2	S3	66	10%
Photocopier	X2	120	19%
Lights	L	241	38%
Total		**639**	100%

Table 5.3. Scaling Ratios for Experiments 5,6,7 (20W/m2).

(Ratios are defined as prototype value / model value)

Geometric Scale Ratio	6.6
Temperature Difference Scale Ratio	0.26
Power Scale Ratio	3.65
Volumetric Flow Rate Scale Ratio	54.62
Mass Flow Rate Scale Ratio	10.18
Velocity Scale Ratio	1.26

The small fans located at the floor level were not used in experiment 5. In experiment 6, the flow through the small fans was 23% of the supply flow rate (air velocity at fan discharge was 0.15m/s). This figure was 16% for experiment 7 (air velocity at fan discharge was 0.10m/s).

The supply air temperature was 18.9°C for these experiments. The summary of the average temperature readings for these experiments can be found in Table 5.4.

EXPERIMENT 5

Case	20 W/m^2
Cooling Load	639 W
Heat Sources	P1,P3,S1,S3,X2,L
Flow at fans on floor	0% of total flowrate
Supply air flow rate	596 cfm 0.28 m^3/s
Velocity at diffusers	0.19 m/s

Average Temperature Field Summary	
T supply	18.9 C
T exhaust	20.9 C
T (0.1m)	19.7 C
T (1.1m)	20.1 C
T(1.7m)	20.9 C
delta T (0.1m-1.1m)	0.4 C
delta T (0.1m-1.7m)	1.2 C

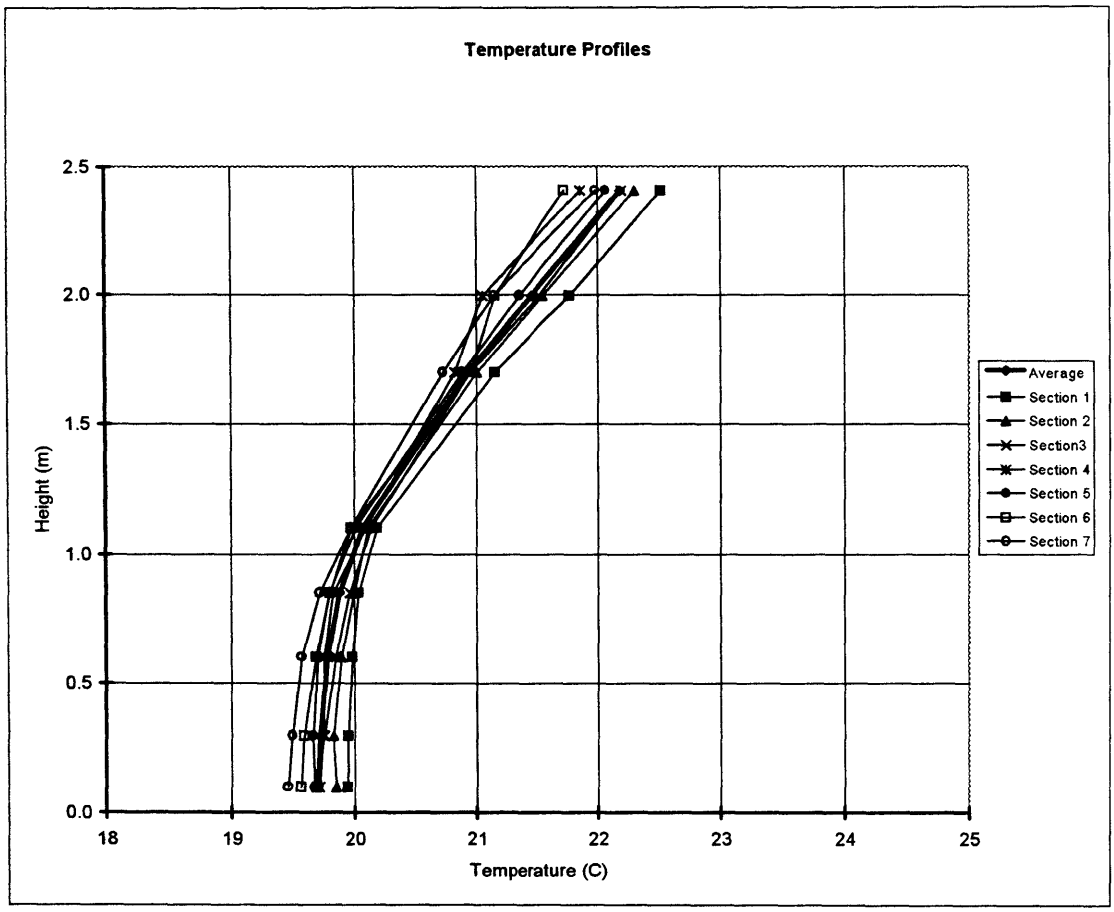

Figure 5.2. Temperature Profiles for Experiment 5 (20W/m^2, 596cfm, 0% fans).

EXPERIMENT 5

Case	20 W/m^2
Cooling Load	639 W
Heat Sources	P1,P3,S1,S3,X2,L
Flow at fans on floor	0% of total flowrate
Supply air flow rate	596 cfm 0.28 m^3/s
Velocity at diffusers	0.19 m/s

Average Temperature Field Summary	
T supply	18.9 C
T exhaust	20.9 C
T (0.1m)	19.7 C
T (1.1m)	20.1 C
T(1.7m)	20.9 C
delta T (0.1m-1.1m)	0.4 C
delta T (0.1m-1.7m)	1.2 C

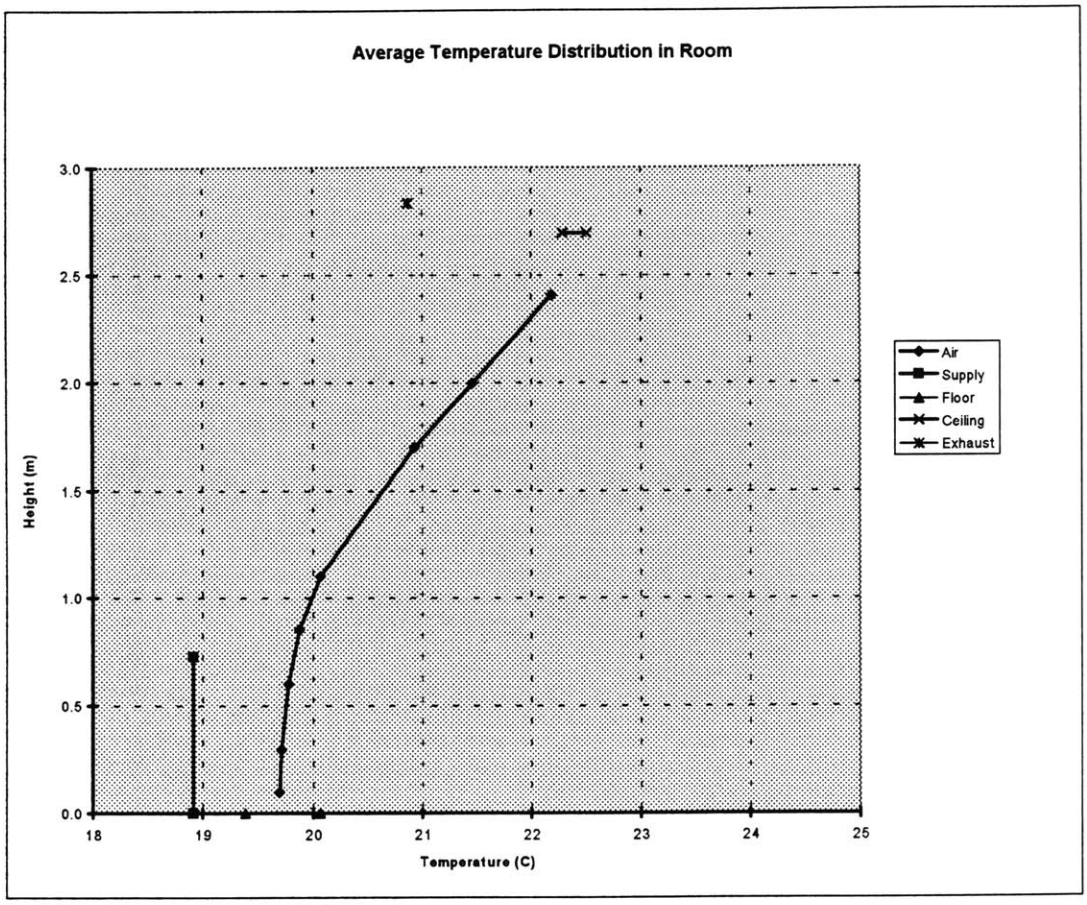

Figure 5.3. Average Temperature Distribution for Experiment 5 (20W/m^2, 596cfm, 0% fans).

EXPERIMENT 6

Case	20 W/m^2
Cooling Load	639 W
Heat Sources	P1,P3,S1,S3,X2,L
Flow at fans on floor	23% of total flowrate
Supply air flow rate	596 cfm 0.28 m^3/s
Velocity at diffusers	0.19 m/s

Average Temperature Field Summary	
T supply	18.9 C
T exhaust	20.8 C
T (0.1m)	20.0 C
T (1.1m)	20.2 C
T(1.7m)	20.9 C
delta T (0.1m-1.1m)	0.2 C
delta T (0.1m-1.7m)	0.8 C

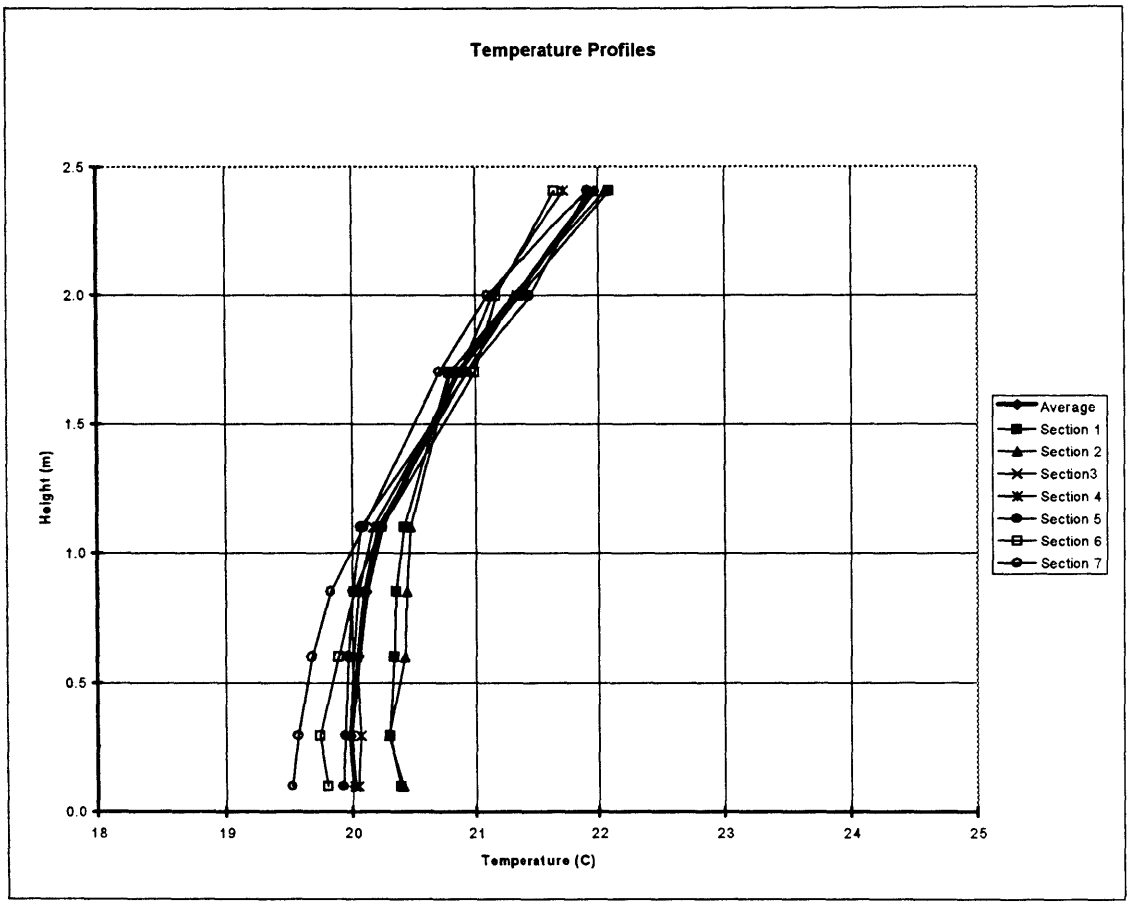

Figure 5.4. Temperature Profiles for Experiment 6 (20W/m^2, 596cfm, 23% fans).

EXPERIMENT 6

Case	20 W/m^2
Cooling Load	639 W
Heat Sources	P1,P3,S1,S3,X2,L
Flow at fans on floor	23% of total flowrate
Supply air flow rate	596 cfm 0.28 m^3/s
Velocity at diffusers	0.19 m/s

Average Temperature Field Summary	
T supply	18.9 C
T exhaust	20.8 C
T (0.1m)	20.0 C
T (1.1m)	20.2 C
T(1.7m)	20.9 C
delta T (0.1m-1.1m)	0.2 C
delta T (0.1m-1.7m)	0.8 C

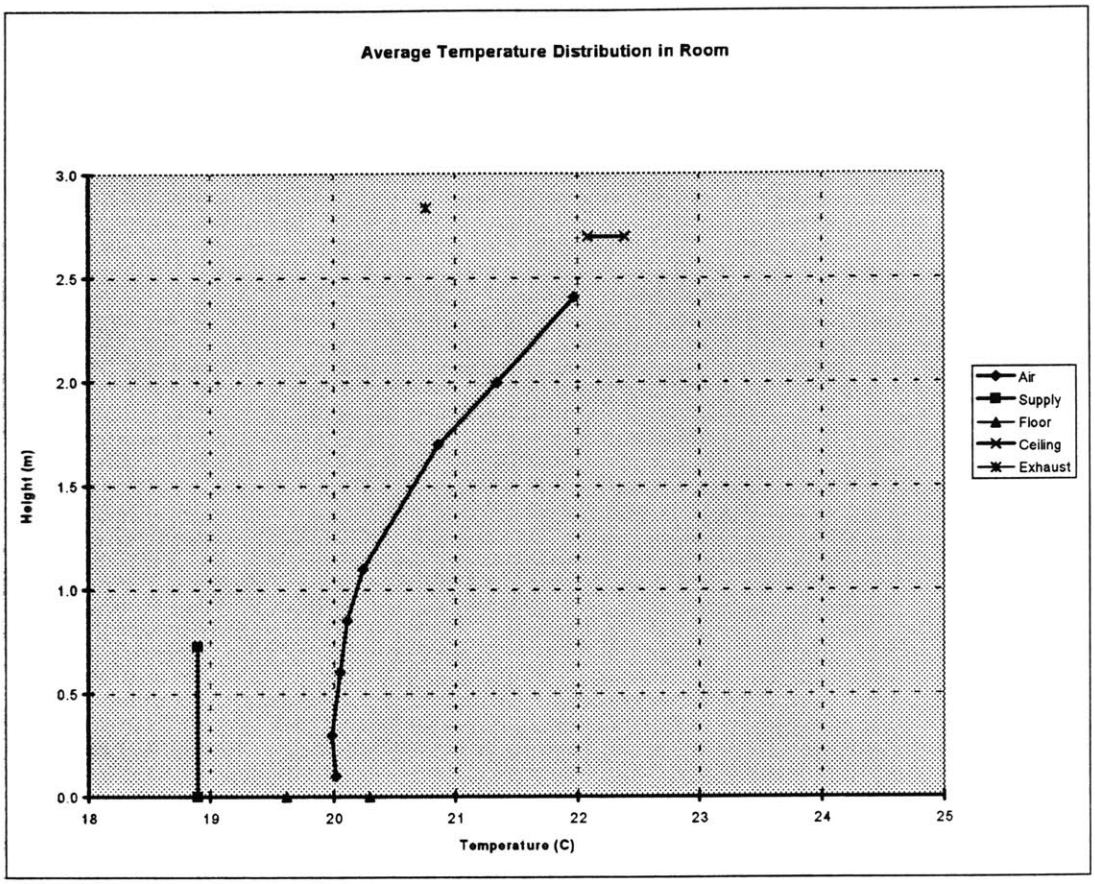

Figure 5.5. Average Temperature Distribution for Experiment 6 (20W/m^2, 596cfm, 23% fans).

EXPERIMENT 7

Case	20 W/m^2
Cooling Load	639 W
Heat Sources	P1,P3,S1,S3,X2,L
Flow at fans on floor	16% of total flowrate
Supply air flow rate	596 cfm 0.28 m^3/s
Velocity at diffusers	0.19 m/s

Average Temperature Field Summary	
T supply	18.9 C
T exhaust	20.8 C
T (0.1m)	19.7 C
T (1.1m)	20.1 C
T(1.7m)	20.8 C
delta T (0.1m-1.1m)	0.4 C
delta T (0.1m-1.7m)	1.1 C

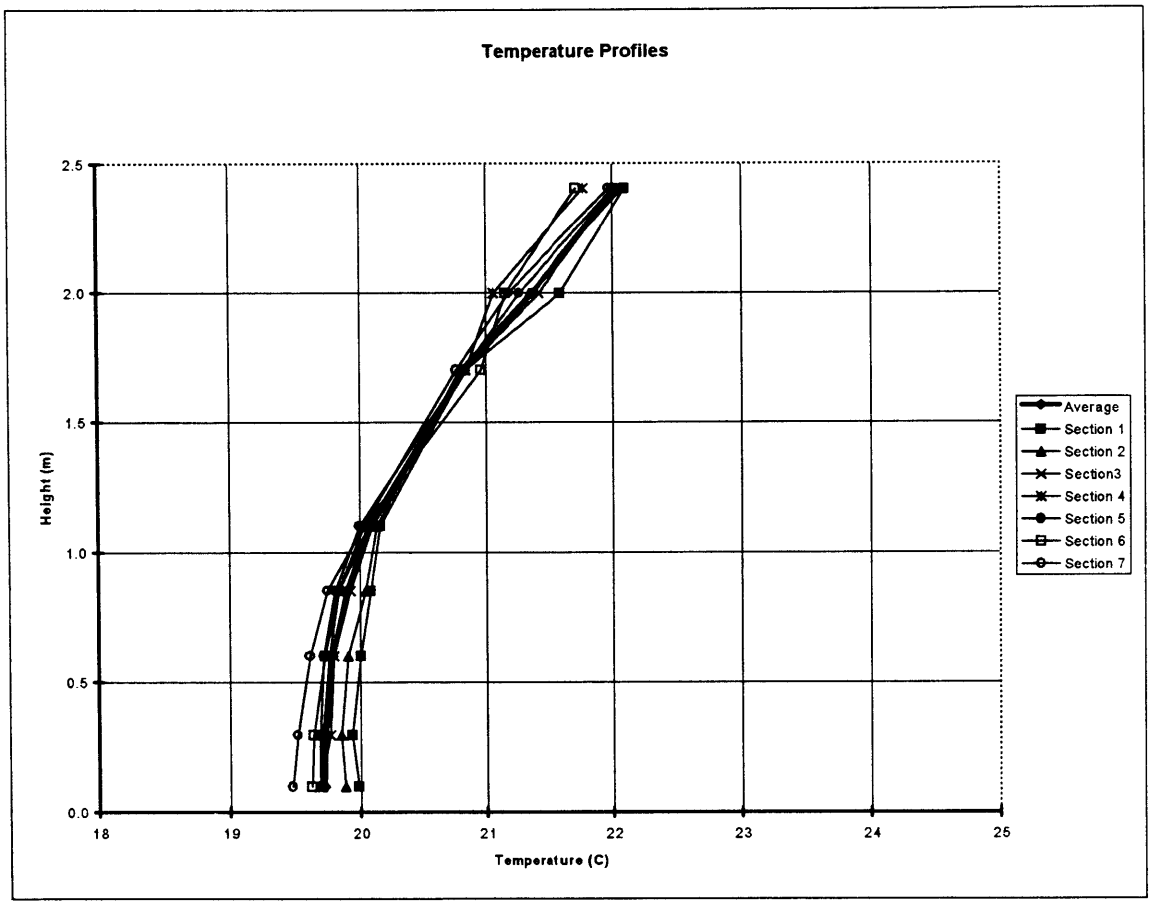

Figure 5.6. Temperature Profiles for Experiment 7 (20W/m^2, 596cfm, 16% fans).

EXPERIMENT 7

Case	20 W/m^2
Cooling Load	639 W
Heat Sources	P1,P3,S1,S3,X2,L
Flow at fans on floor	16% of total flowrate
Supply air flow rate	596 cfm 0.28 m^3/s
Velocity at diffusers	0.19 m/s

Average Temperature Field Summary	
T supply	18.9 C
T exhaust	20.8 C
T (0.1m)	19.7 C
T (1.1m)	20.1 C
T(1.7m)	20.8 C
delta T (0.1m-1.1m)	0.4 C
delta T (0.1m-1.7m)	1.1 C

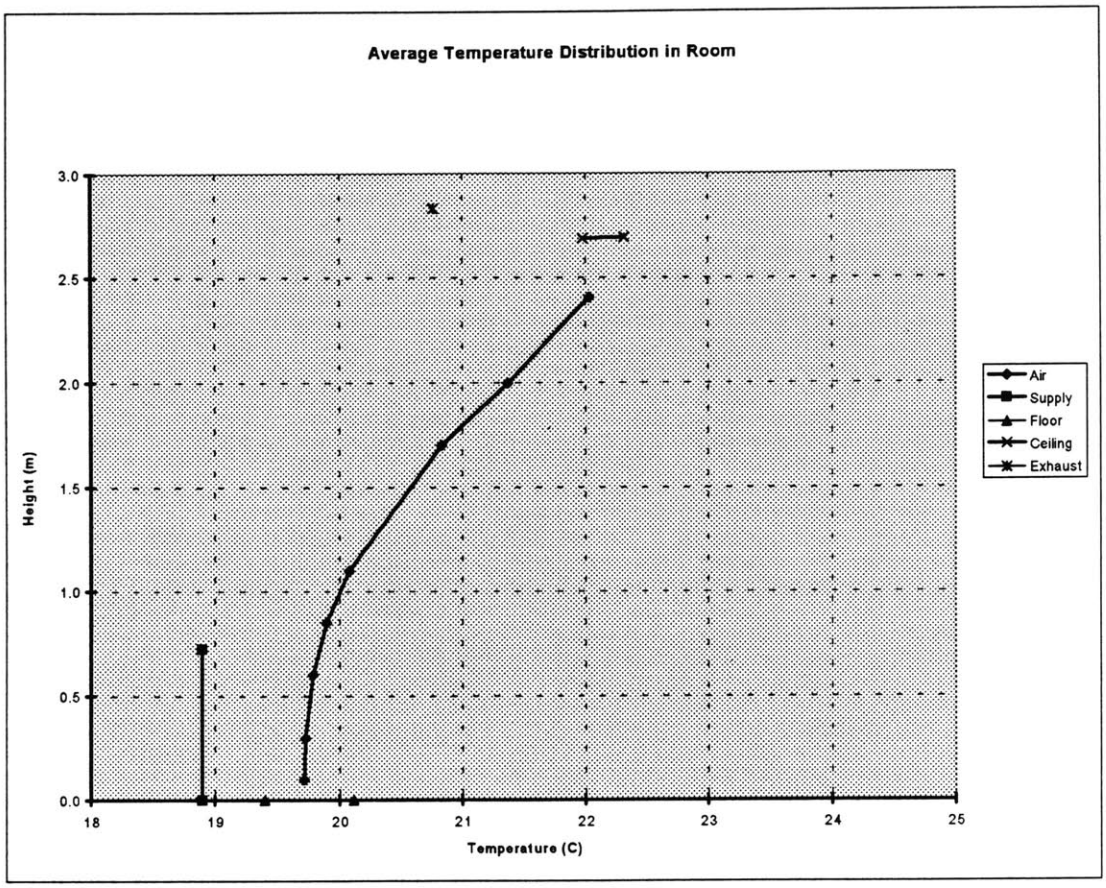

Figure 5.7. Average Temperature Distribution for Experiment 7 (20W/m^2, 596cfm, 16% fans).

The temperature profiles corresponding to each section for the three experiments are shown in Figure 5.2, Figure 5.4 and Figure 5.6. The average profiles for each experiment are given in Figure 5.3, Figure 5.5 and Figure 5.7.

Table 5.4. Summary of Average Temperature Readings for Experiments 5,6,7.

Temperature	Experiment 5	Experiment 6	Experiment 7
T supply	18.9°C	18.9°C	18.9°C
T exhaust	20.9°C	20.8°C	20.8°C
T (0.1m)	19.7°C	20.0°C	19.7°C
T (1.1m)	20.1°C	20.2°C	20.1°C
T (1.7m)	20.9°C	20.9°C	20.8°C
$\Delta T_{(0.1m-1.1m)}$	0.4°C	0.2°C	0.4°C
$\Delta T_{(0.1m-1.7m)}$	1.2°C	0.8°C	1.1°C

5.5. Displacement Ventilation for 27W/m^2 (Experiments 8,9,10)

In this set of experiments, a heat gain of 27W/m^2 was simulated with a supply air flow rate of 0.29m^3/s (626cfm, 9.2 L/s.m^2). The velocity at the supply diffusers was 0.20m/s. The total simulated cooling load in the model (8m x 4m floor area, 2.7m height) was 860W. The heat was dissipated by three occupants, three computer monitors, three photocopiers and the lights at the ceiling. See Table 5.5 and Figure 5.1 for the location and the percentage of contribution of each heat source.

Table 5.5. Heat Sources in Experiments 8,9,10 (27W/m^2).

Heat Source	Symbol	Heat Dissipated (W)	% of total
Occupant 1,2,3	P1,P2,P3	73 x 3	25%
Monitor 1,2,3	S1,S2,S3	66 x 3	23%
Photocopier 1,2,3	X1,X2,X3	120 x 3	42%
Lights	L	77	10%
Total		**860**	100%

R114 concentration during these experiments was 86%. The corrected scaling ratios are summarized in Table 5.6.

Table 5.6. Scaling Ratios for Experiments 8,9,10 ($27W/m^2$).
(Ratios are defined as prototype value / model value)

Geometric Scale Ratio	6.6
Temperature Difference Scale Ratio	0.26
Power Scale Ratio	3.68
Volumetric Flow Rate Scale Ratio	54.78
Mass Flow Rate Scale Ratio	10.18
Velocity Scale Ratio	1.26

The small fans located at the floor level were not used in experiment 8. In experiment 9, the flow through the small fans was 50% of the supply flow rate (air velocity at fan discharge was 0.3m/s). This figure was 15% for experiment 10 (air velocity at fan discharge was 0.09m/s).

The supply air temperature was 18.9°C for these experiments. The summary of the average temperature readings for these experiments can be found in Table 5.7.

Table 5.7. Summary of Average Temperature Readings for Experiments 8,9,10.

Temperature	Experiment 8	Experiment 9	Experiment 10
T supply	18.9°C	18.9°C	18.9°C
T exhaust	20.8°C	20.9°C	20.9°C
T (0.1m)	19.7°C	20.2°C	19.9°C
T (1.1m)	20.6°C	20.8°C	20.7°C
T (1.7m)	22.0°C	22.0°C	22.2°C
$\Delta T_{(0.1m-1.1m)}$	0.9°C	0.6°C	0.9°C
$\Delta T_{(0.1m-1.7m)}$	2.3°C	1.8°C	2.3°C

EXPERIMENT 8

Case	27 W/m^2
Cooling Load	860 W
Heat Sources	P1,P2,P3,S1,S2,S3,X1,X2,X3,L
Flow at fans on floor	0% of total flowrate
Supply air flow rate	626 cfm 0.30 m^3/s
Velocity at diffusers	0.20 m/s

Average Temperature Field Summary	
T supply	18.9 C
T exhaust	20.8 C
T (0.1m)	19.7 C
T (1.1m)	20.6 C
T(1.7m)	22.0 C
delta T (0.1m-1.1m)	0.9 C
delta T (0.1m-1.7m)	2.3 C

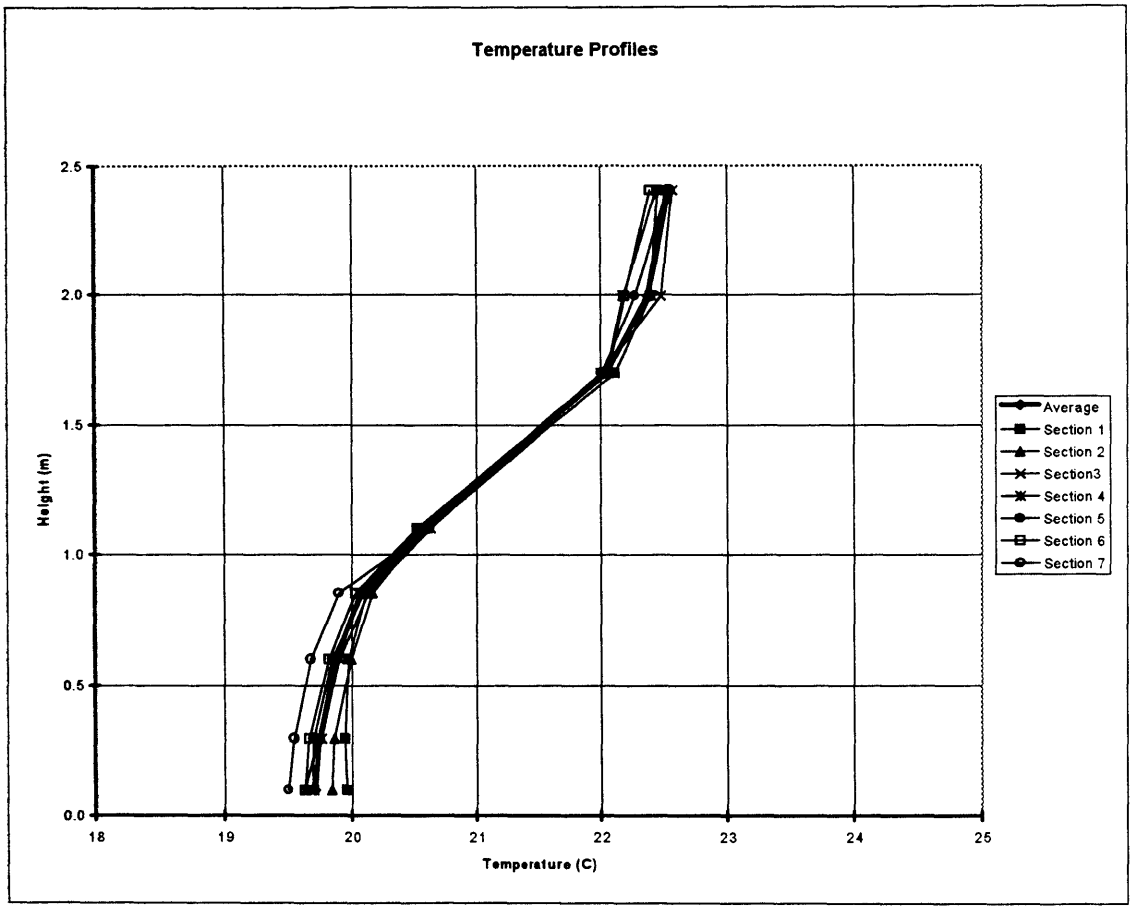

Figure 5.8. Temperature Profiles for Experiment 8 (27W/m^2, 596cfm,0% fans).

EXPERIMENT 8

Case	27 W/m^2
Cooling Load	860 W
Heat Sources	P1,P2,P3,S1,S2,S3,X1,X2,X3,L
Flow at fans on floor	0% of total flowrate
Supply air flow rate	626 cfm 0.30 m^3/s
Velocity at diffusers	0.20 m/s

Average Temperature Field Summary	
T supply	18.9 C
T exhaust	20.8 C
T (0.1m)	19.7 C
T (1.1m)	20.6 C
T(1.7m)	22.0 C
delta T (0.1m-1.1m)	0.9 C
delta T (0.1m-1.7m)	2.3 C

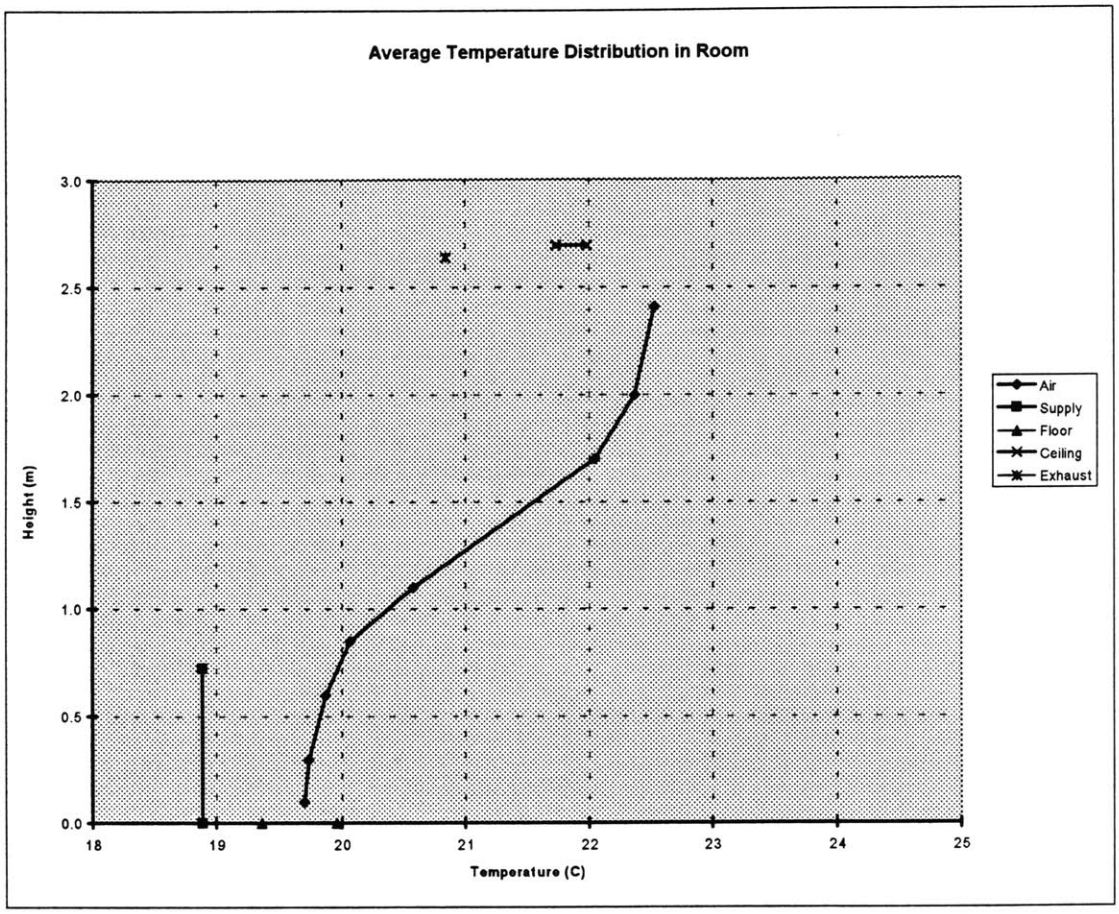

Figure 5.9. Average Temperature Distribution for Experiment 8 (27W/m^2, 596cfm, 0% fans).

EXPERIMENT 9

Case	27 W/m^2
Cooling Load	860 W
Heat Sources	P1,P2,P3,S1,S2,S3,X1,X2,X3,L
Flow at fans on floor	50% of total flowrate
Supply air flow rate	626 cfm 0.30 m^3/s
Velocity at diffusers	0.20 m/s

Average Temperature Field Summary	
T supply	18.9 C
T exhaust	20.9 C
T (0.1m)	20.2 C
T (1.1m)	20.8 C
T(1.7m)	22.0 C
delta T (0.1m-1.1m)	0.6 C
delta T (0.1m-1.7m)	1.8 C

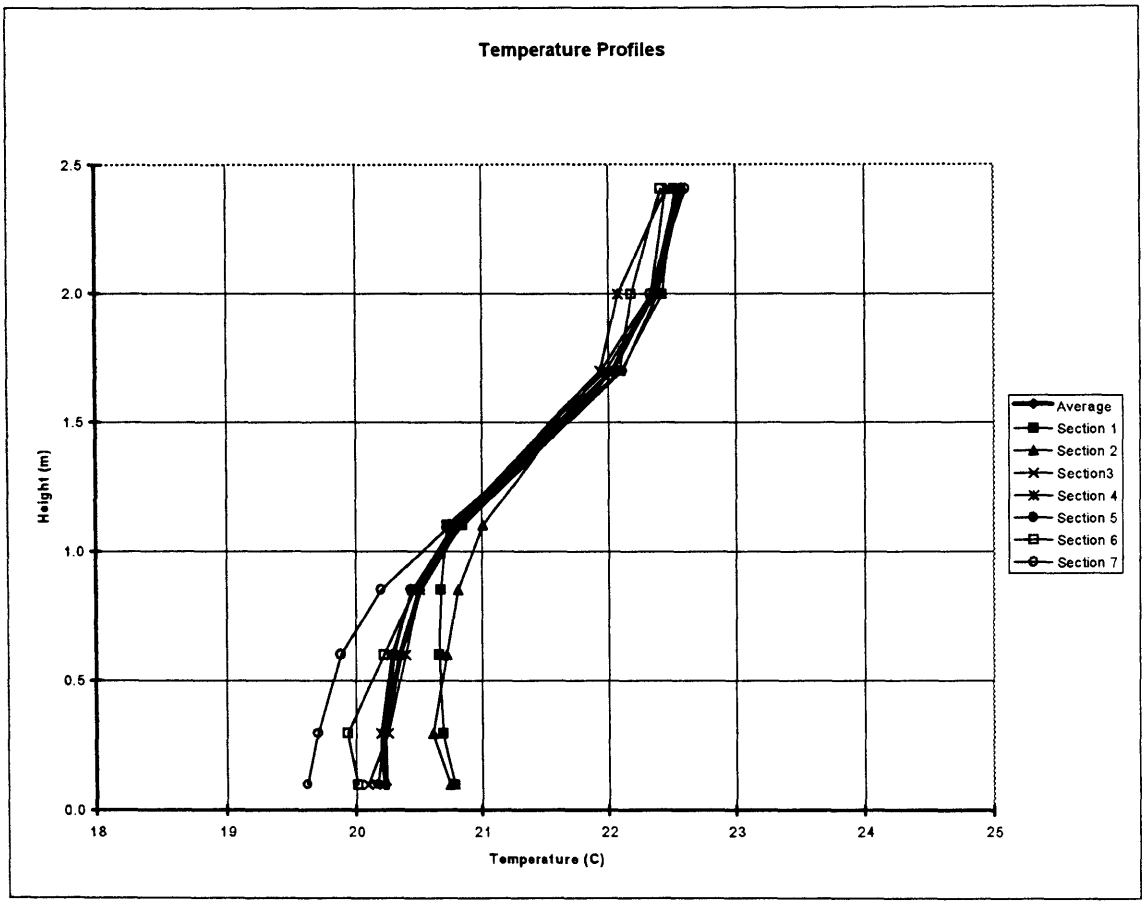

Figure 5.10. Temperature Profiles for Experiment 9 (27W/m^2, 596cfm, 50% fans).

EXPERIMENT 9

Case	27 W/m^2
Cooling Load	860 W
Heat Sources	P1,P2,P3,S1,S2,S3,X1,X2,X3,L
Flow at fans on floor	50% of total flowrate
Supply air flow rate	626 cfm 0.30 m^3/s
Velocity at diffusers	0.20 m/s

Average Temperature Field Summary	
T supply	18.9 C
T exhaust	20.9 C
T (0.1m)	20.2 C
T (1.1m)	20.8 C
T(1.7m)	22.0 C
delta T (0.1m-1.1m)	0.6 C
delta T (0.1m-1.7m)	1.8 C

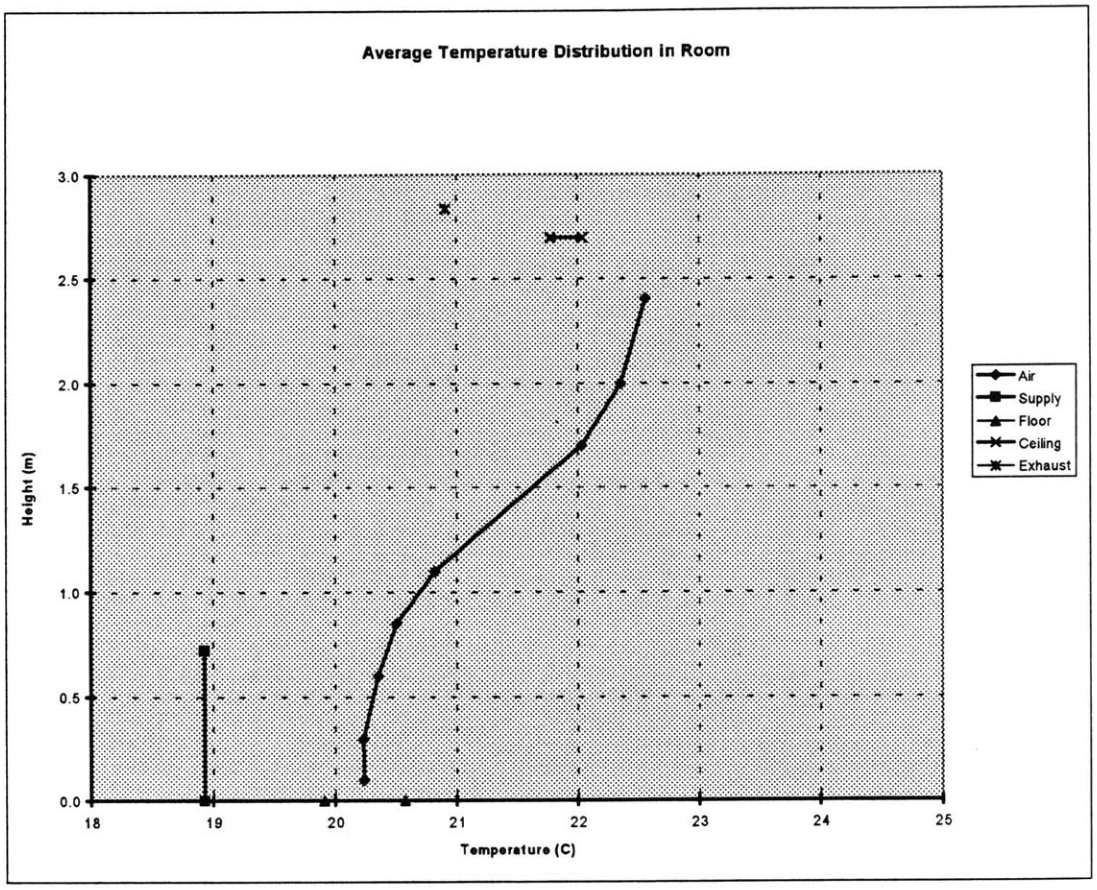

Figure 5.11. Average Temperature Distribution for Experiment 9 (27W/m^2, 596cfm, 50% fans).

EXPERIMENT 10

Case	27 W/m^2
Cooling Load	860 W
Heat Sources	P1,P2,P3,S1,S2,S3,X1,X2,X3,L
Flow at fans on floor	15% of total flowrate
Supply air flow rate	626 cfm 0.30 m^3/s
Velocity at diffusers	0.20 m/s

Average Temperature Field Summary	
T supply	18.9 C
T exhaust	20.9 C
T (0.1m)	19.9 C
T (1.1m)	20.7 C
T(1.7m)	22.2 C
delta T (0.1m-1.1m)	0.9 C
delta T (0.1m-1.7m)	2.3 C

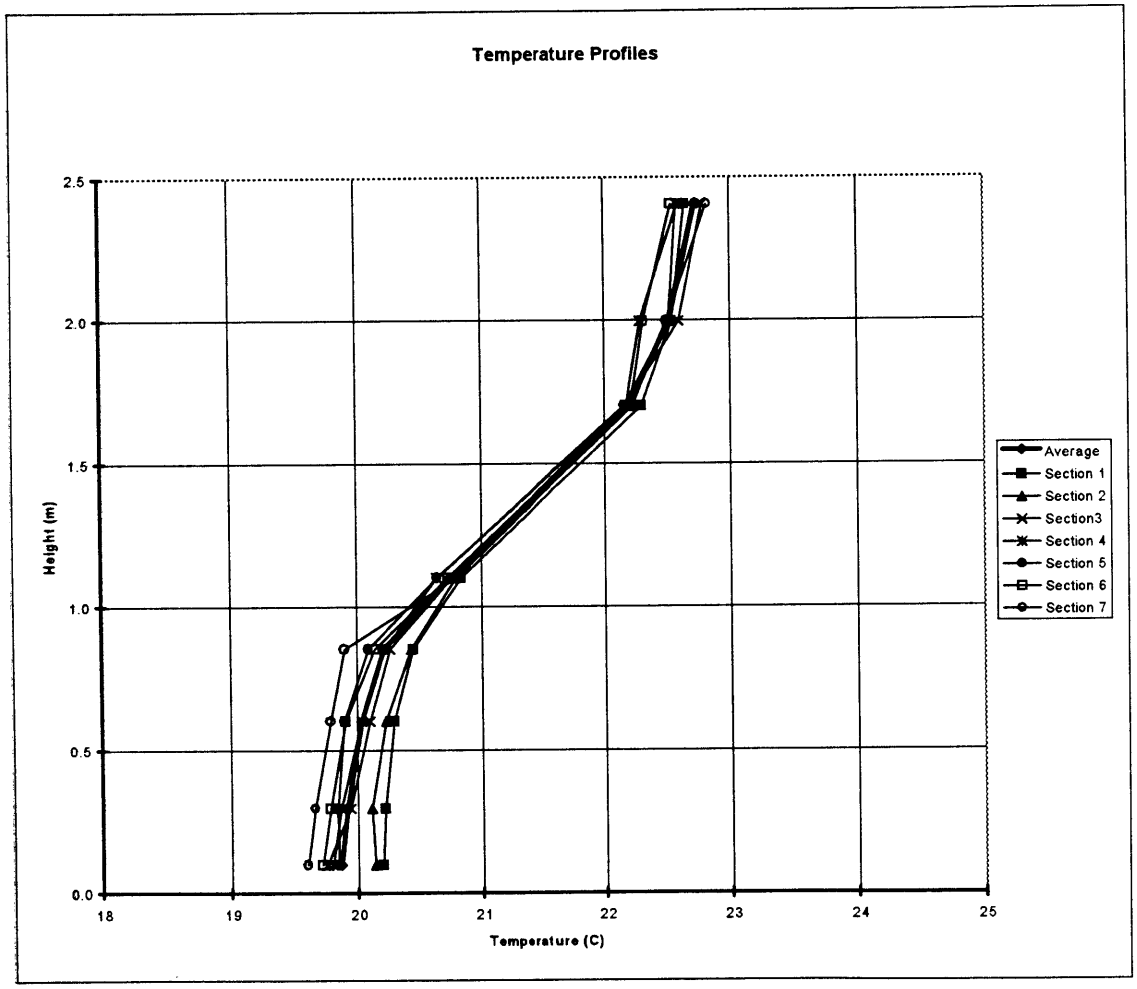

Figure 5.12. Temperature Profiles for Experiment 10 (27W/m^2, 596cfm, 15% fans).

EXPERIMENT 10

Case	27 W/m^2
Cooling Load	860 W
Heat Sources	P1,P2,P3,S1,S2,S3,X1,X2,X3,L
Flow at fans on floor	15% of total flowrate
Supply air flow rate	626 cfm 0.30 m^3/s
Velocity at diffusers	0.20 m/s

Average Temperature Field Summary	
T supply	18.9 C
T exhaust	20.9 C
T (0.1m)	19.9 C
T (1.1m)	20.7 C
T(1.7m)	22.2 C
delta T (0.1m-1.1m)	0.9 C
delta T (0.1m-1.7m)	2.3 C

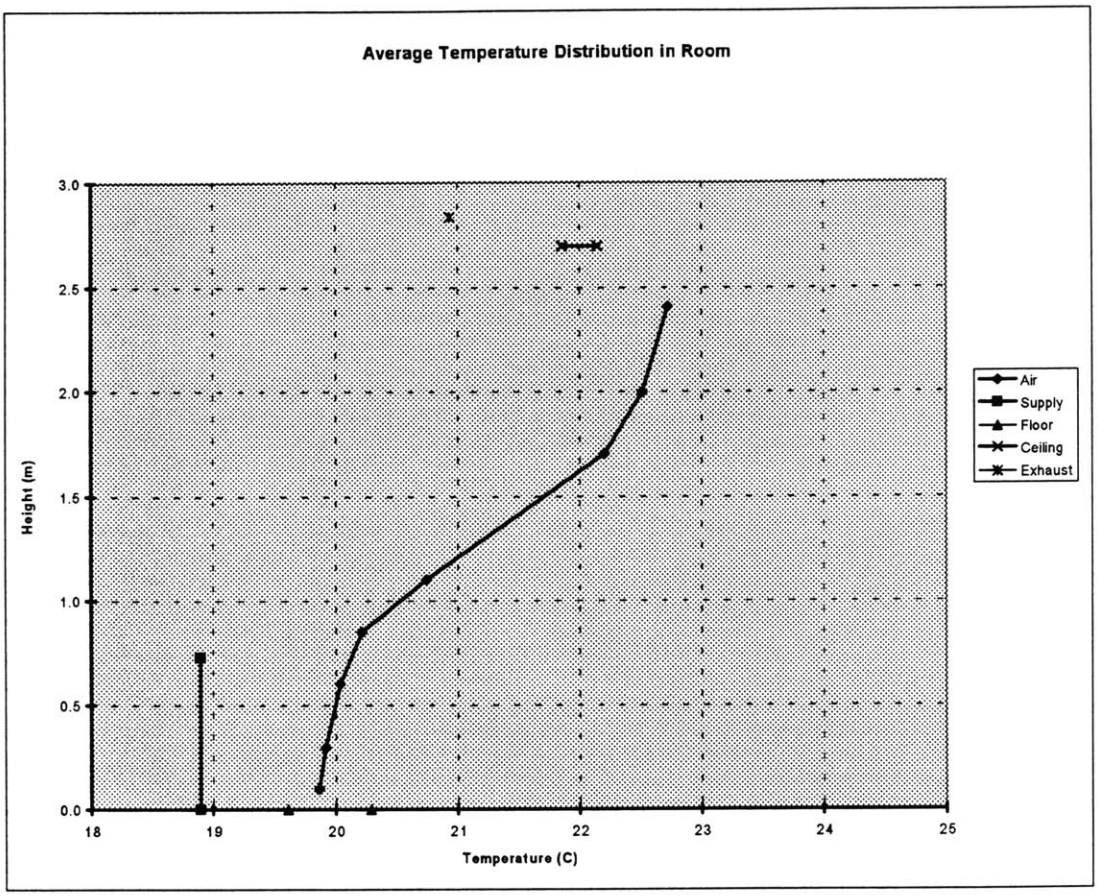

Figure 5.13. Average Temperature Distribution for Experiment 10 (27W/m^2, 596cfm, 15% fans).

The temperature profiles corresponding to each section for the three experiments are shown in Figure 5.8, Figure 5.10 and Figure 5.12. The average profiles for each experiment are given in Figure 5.9, Figure 5.11 and Figure 5.13.

5.6. Displacement Ventilation for 38W/m^2 (Experiments 11,12,13)

In this set of experiments, a heat gain of 38W/m^2 was simulated with a supply air flow rate of 0.29m^3/s (615cfm, 9.1 L/s.m^2). The velocity at the supply diffusers was 0.20m/s. The total simulated cooling load in the model (8m x 4m floor area, 2.7m height) was 1223W. The heat was dissipated by three occupants, three computer monitors, three computer towers, three photocopiers and the lights at the ceiling. See Table 5.8 and Figure 5.1. for the location and the percentage of contribution of each heat source.

Table 5.8. Heat Sources in Experiments 11,12,13 (38W/m^2).

Heat Source	Symbol	Heat Dissipated (W)	% of total
Occupant 1,2,3	P1,P2,P3	69 x 3	17%
Monitor 1,2,3	S1,S2,S3	62 x 3	15%
Tower 1,2,3	T1,T2,T3	62 x 3	15%
Photocopier 1,2,3	X1,X2,X3	113 x 3	28%
Lights	L	302	25%
Total		**1223**	100%

R114 concentration during these experiments was 84%. The corrected scaling ratios are summarized in Table 5.9.

The small fans located at the floor level were not used in experiment 11. In experiment 12, the flow through the small fans was 58% of the supply flow rate (air velocity at fan

discharge was 0.37m/s). This figure was 22% for experiment 13 (air velocity at fan discharge was 0.14m/s).

Table 5.9. Scaling Ratios for Experiments 11,12,13 ($38W/m^2$).
(Ratios are defined as prototype value / model value)

Geometric Scale Ratio	6.6
Temperature Difference Scale Ratio	0.25
Power Scale Ratio	3.44
Volumetric Flow Rate Scale Ratio	53.31
Mass Flow Rate Scale Ratio	10.12
Velocity Scale Ratio	1.23

The supply air temperature was 18.9°C for these experiments. The summary of the average temperature readings for these experiments can be found in Table 5.10.

Table 5.10. Summary of Average Temperature Readings for Experiments 11,12,13.

Temperature	Experiment 11	Experiment 12	Experiment 13
T supply	19.1°C	19.1°C	19.1°C
T exhaust	21.4°C	21.6°C	21.7°C
T (0.1m)	20.1°C	21.0°C	20.6°C
T (1.1m)	22.0°C	22.1°C	22.3°C
T (1.7m)	23.1°C	23.2°C	23.4°C
$\Delta T_{(0.1m-1.1m)}$	1.8°C	1.1°C	1.7°C
$\Delta T_{(0.1m-1.7m)}$	3.0°C	2.2°C	2.8°C

The temperature profiles corresponding to each section for the three experiments are shown in Figure 5.14, Figure 5.16 and Figure 5.18. The average profiles for each experiment are given in Figure 5.15, Figure 5.17 and Figure 5.19.

EXPERIMENT 11

Case	**38 W/m^2**
Cooling Load	1223 W
Heat Sources	P1,P2,P3,S1,S2,S3,T1,T2,T3,X1,X2,X3,L
Flow at fans on floor	**0% of total flowrate**
Supply air flow rate	615 cfm 0.29 m^3/s
Velocity at diffusers	0.20 m/s

Average Temperature Field Summary	
T supply	19.1 C
T exhaust	21.4 C
T (0.1m)	20.1 C
T (1.1m)	22.0 C
T(1.7m)	23.1 C
delta T (0.1m-1.1m)	1.8 C
delta T (0.1m-1.7m)	3.0 C

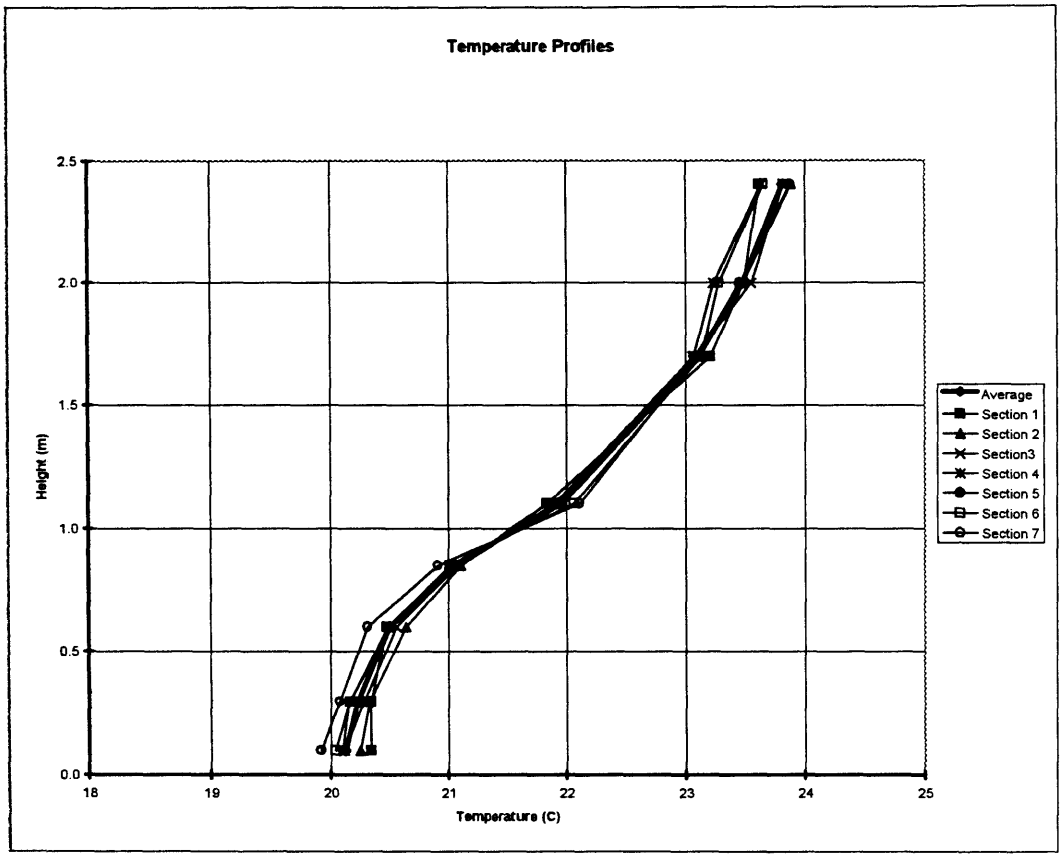

Figure 5.14. Temperature Profiles for Experiment 11 (38W/m^2, 596cfm, 0% fans).

EXPERIMENT 11

Case	38 W/m^2
Cooling Load	1223 W
Heat Sources	P1,P2,P3,S1,S2,S3,T1,T2,T3,X1,X2,X3,L
Flow at fans on floor	0% of total flowrate
Supply air flow rate	615 cfm 0.29 m^3/s
Velocity at diffusers	0.20 m/s

Average Temperature Field Summary	
T supply	19.1 C
T exhaust	21.4 C
T (0.1m)	20.1 C
T (1.1m)	22.0 C
T(1.7m)	23.1 C
delta T (0.1m-1.1m)	1.8 C
delta T (0.1m-1.7m)	3.0 C

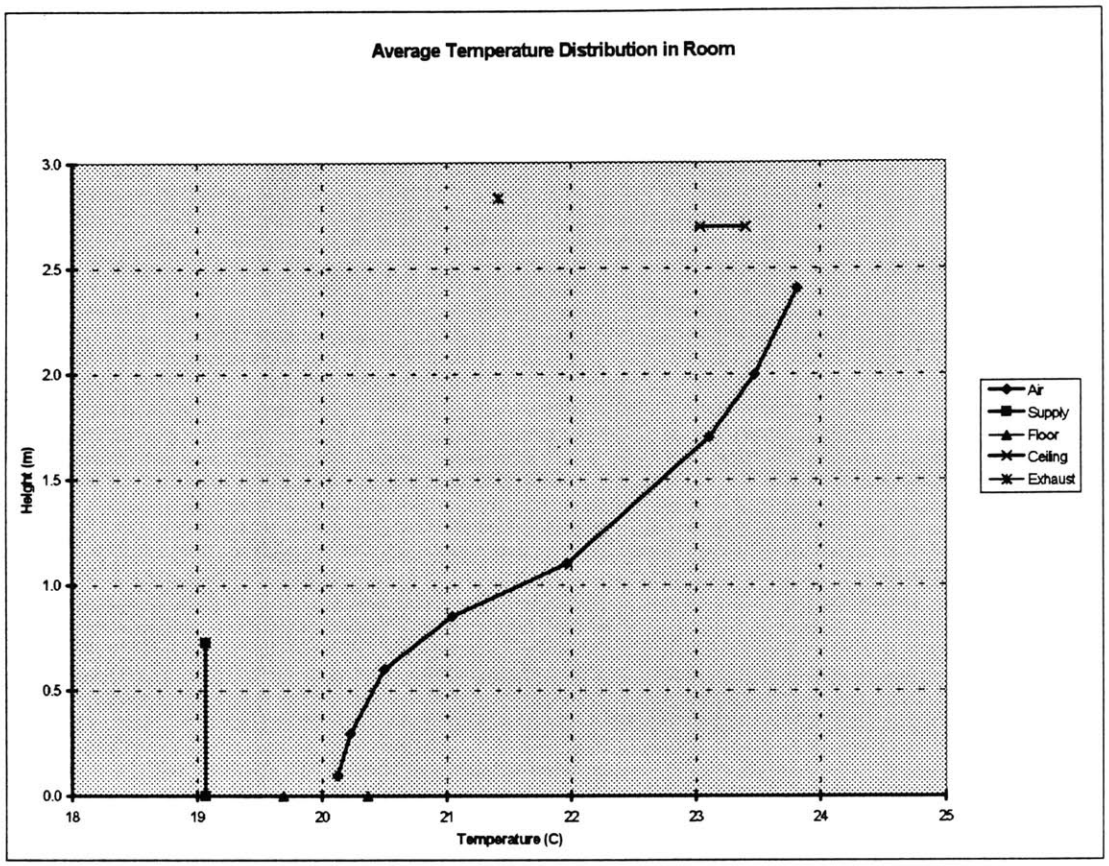

Figure 5.15. Average Temperature Distribution for Experiment 11 (38W/m^2, 596cfm, 0% fans).

EXPERIMENT 12

Case	38 W/m^2
Cooling Load	1223 W
Heat Sources	P1,P2,P3,S1,S2,S3,T1,T2,T3,X1,X2,X3,L
Flow at fans on floor	58% of total flowrate
Supply air flow rate	615 cfm 0.29 m^3/s
Velocity at diffusers	0.20 m/s

Average Temperature Field Summary	
T supply	19.1 C
T exhaust	21.6 C
T (0.1m)	21.0 C
T (1.1m)	22.1 C
T(1.7m)	23.2 C
delta T (0.1m-1.1m)	1.1 C
delta T (0.1m-1.7m)	2.2 C

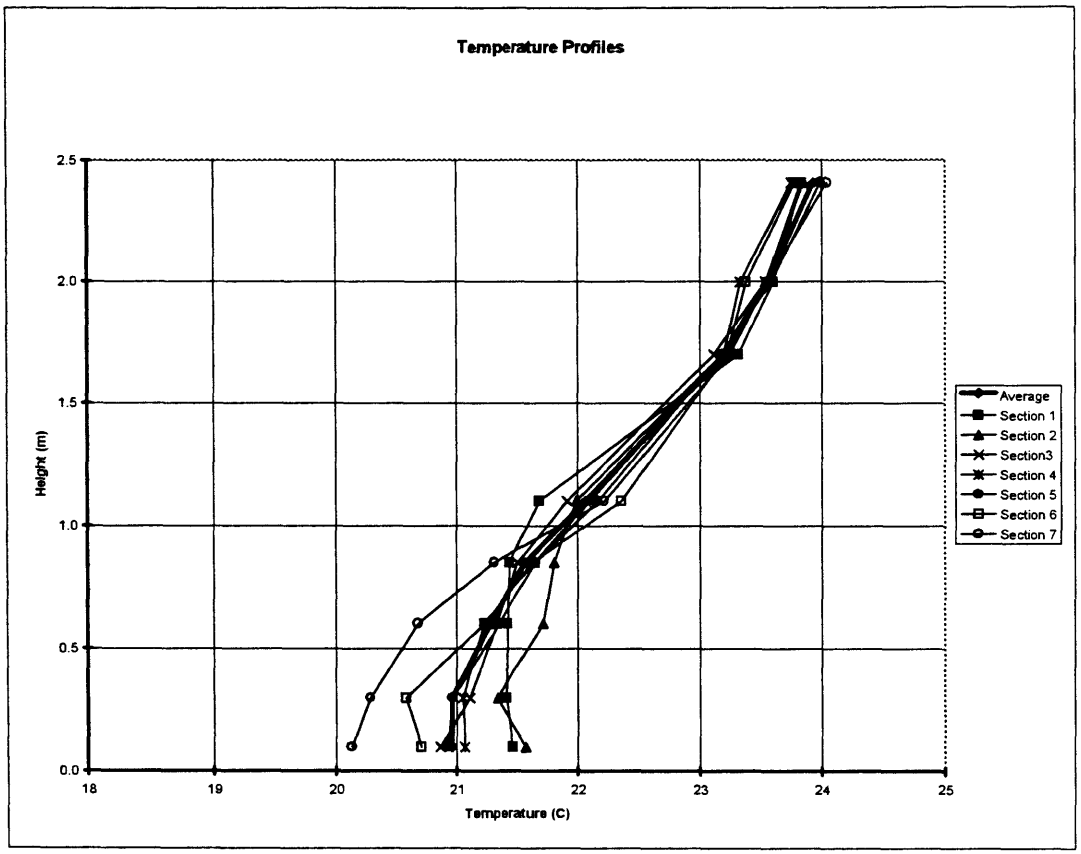

Figure 5.16. Temperature Profiles for Experiment 12 (38W/m^2, 596cfm, 58% fans).

EXPERIMENT 12

Case	38 W/m^2
Cooling Load	1223 W
Heat Sources	P1,P2,P3,S1,S2,S3,T1,T2,T3,X1,X2,X3,L
Flow at fans on floor	58% of total flowrate
Supply air flow rate	615 cfm 0.29 m^3/s
Velocity at diffusers	0.20 m/s

Average Temperature Field Summary	
T supply	19.1 C
T exhaust	21.6 C
T (0.1m)	21.0 C
T (1.1m)	22.1 C
T(1.7m)	23.2 C
delta T (0.1m-1.1m)	1.1 C
delta T (0.1m-1.7m)	2.2 C

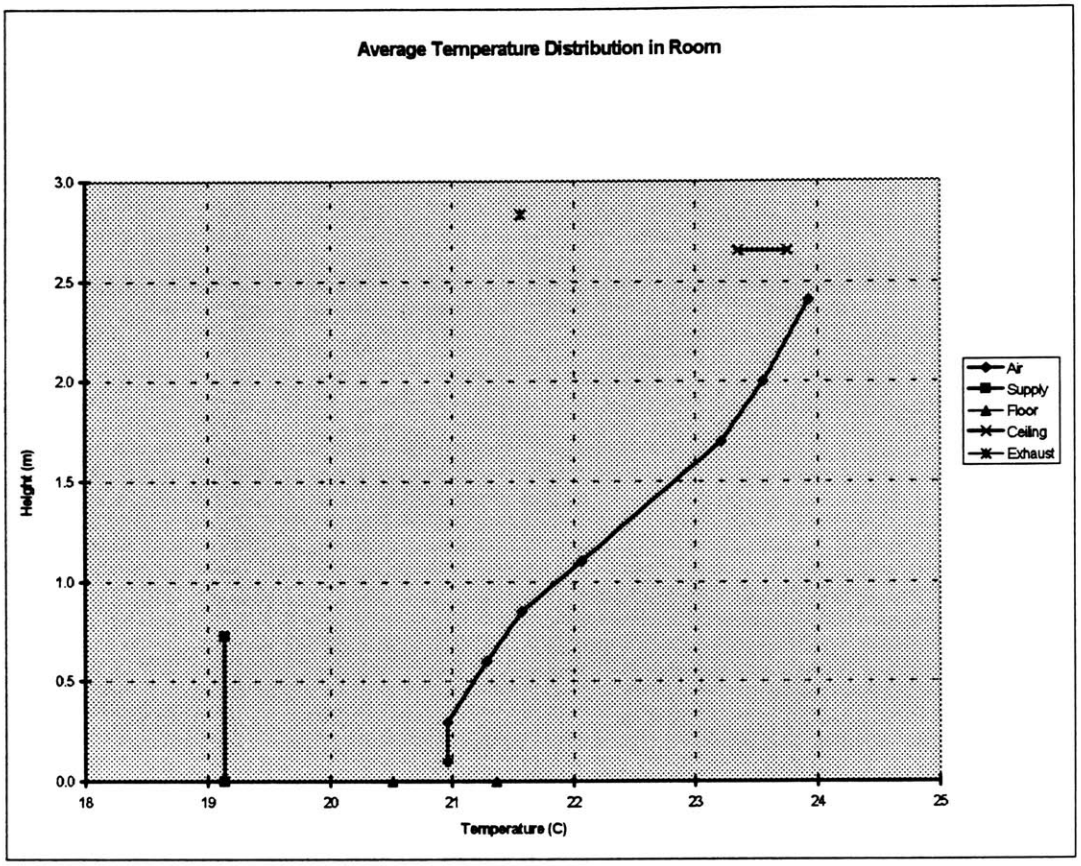

Figure 5.17. Average Temperature Distribution for Experiment 12 (38W/m^2, 596cfm, 58% fans).

EXPERIMENT 13

Case	**38 W/m^2**
Cooling Load	1223 W
Heat Sources	P1,P2,P3,S1,S2,S3,T1,T2,T3,X1,X2,X3,L
Flow at fans on floor	**22% of total flowrate**
Supply air flow rate	615 cfm 0.29 m^3/s
Velocity at diffusers	0.20 m/s

Average Temperature Field Summary	
T supply	19.1 C
T exhaust	21.7 C
T (0.1m)	20.6 C
T (1.1m)	22.3 C
T(1.7m)	23.4 C
delta T (0.1m-1.1m)	1.7 C
delta T (0.1m-1.7m)	2.8 C

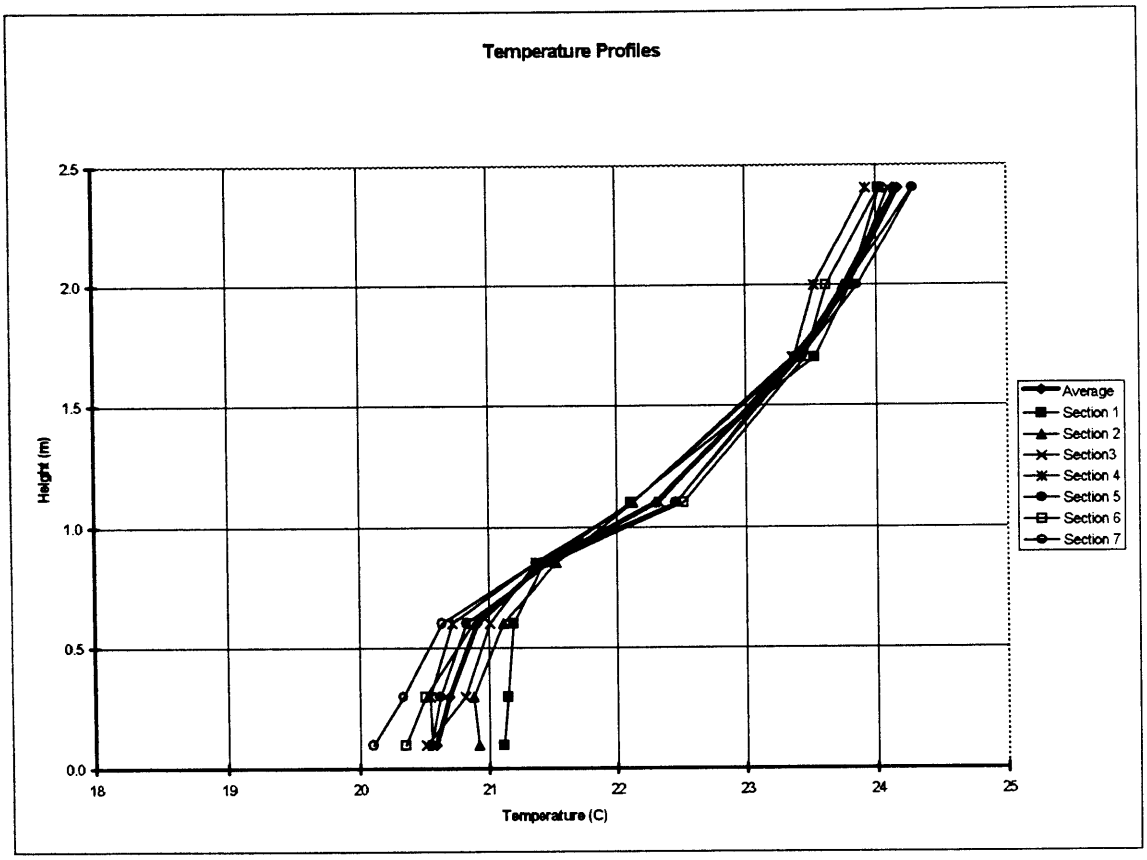

Figure 5.18. Temperature Profiles for Experiment 13 (38W/m^2, 596cfm, 22% fans).

EXPERIMENT 13

Case	38 W/m^2
Cooling Load	1223 W
Heat Sources	P1,P2,P3,S1,S2,S3,T1,T2,T3,X1,X2,X3,L
Flow at fans on floor	22% of total flowrate
Supply air flow rate	615 cfm 0.29 m^3/s
Velocity at diffusers	0.20 m/s

Average Temperature Field Summary	
T supply	19.1 C
T exhaust	21.7 C
T (0.1m)	20.6 C
T (1.1m)	22.3 C
T(1.7m)	23.4 C
delta T (0.1m-1.1m)	1.7 C
delta T (0.1m-1.7m)	2.8 C

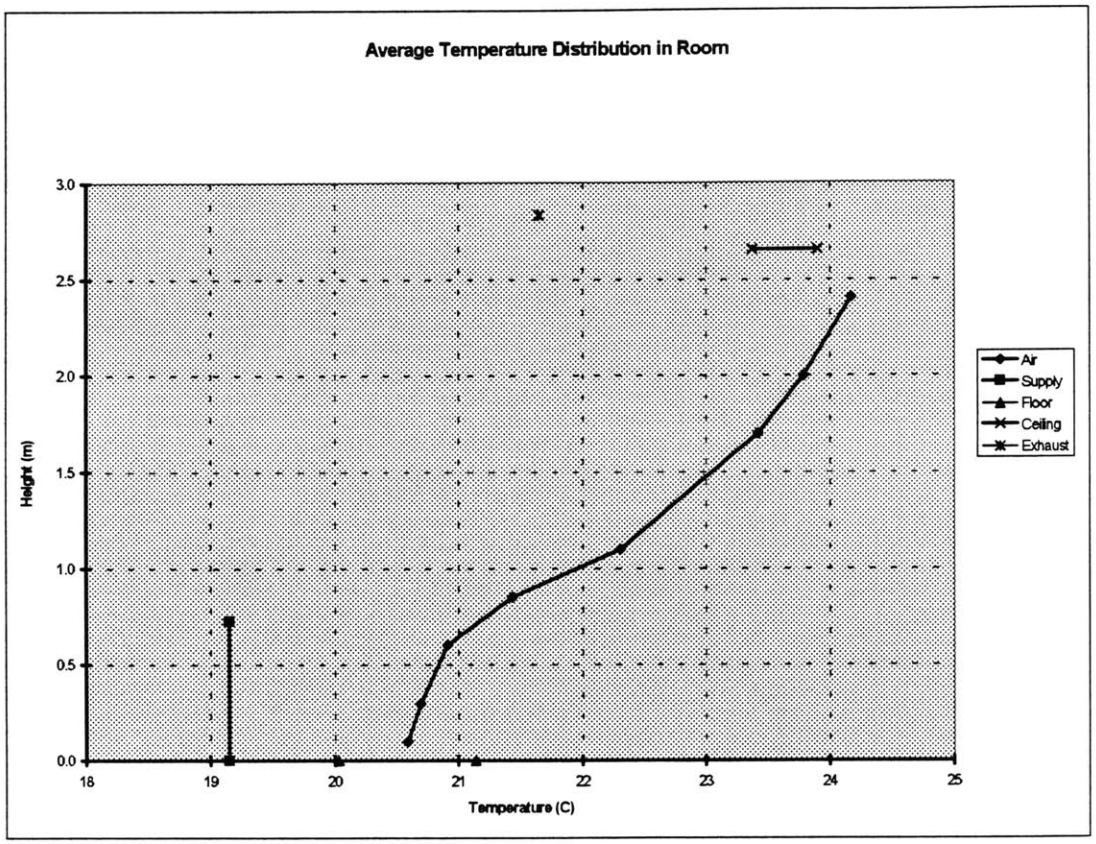

Figure 5.19. Average Temperature Distribution for Experiment 13 (38W/m^2, 596cfm, 22% fans).

5.7. Discussion of the Results

The supply air temperatures simulated are realistic as the supply temperatures are usually close to the room average temperature for displacement ventilation. They typically have values around 19°C. The supply air flow rate simulated in the experiments were quite high (8 L/s.m^2 - 9 L/s.m^2) but within the design limits specified (4 L/s.m^2 to 10 L/s.m^2) for office buildings by ASHRAE. The velocities at the diffusers did not exceed 0.2m/s. The average air temperature inside the office room was always within the comfort limits (21°C to 23°C). The heat gain in the office was reasonable (20W/m^2, 27W/m^2 and 38W/m^2).

Temperature Profiles at Each Section

For each set of conditions considered in experiments, the temperature profiles at each section were different, although the same trend was observed. If the temperature profiles at sections for experiments 5, 8 and 11 (20W/m^2, 27W/m^2 and 38W/m^2 with no small fans) are compared, it can be observed that when the heat gain increases, the difference between temperature profiles is less pronounced at higher levels (see Figure 5.2, Figure 5.8 and Figure 5.14). However the difference in the section profiles at lower levels are similar for all cases. This is probably due to mixing at higher levels resulting from increased plume interaction for greater heat gains. It should also be noted that for the 38W/m^2 case (Experiment 11), the heat sources are uniformly distributed in the room, spreading the effect of the plume interaction to all sections.

There is a consistent temperature asymmetry in the room (see Figures 5.2, 5.4, 5.6, 5.8, 5.10, 5.12, 5.14, 5.16, 5.18) . The lowest temperatures are measured at section 7. The highest temperatures are usually measured at the other end of the room (section 1). This asymmetry is verified by the difference in two end wall temperature readings (0.8°C for 20W/m^2, 1.9°C for 27W/m^2, 3.9°C for 38W/m^2). This can be explained by the different

end wall conditions. The warmer end wall is the Plexiglas wall. There is an empty space (14cm in width) between this wall and the box wall, probably creating a buffer zone against heat loss to outside at this location. The colder end wall is the box wall where the only barrier against heat loss is the wall structure and the insulation. Furthermore, there might be leaks at the location where the Plexiglas false side wall meets the box wall, allowing some of the colder supply refrigerant to leak into the office space close to section 7. Additionally, section 7 is the closest to the exhaust connection at the top of the box. The possible leaks at the location where the false ceiling meets the box walls and unbalanced flow at the exhaust diffusers might be causing different flow patterns at opposite ends, probably causing some stagnation near section 1.

When the small fans operate, the variation in the section temperature profiles is more pronounced at smaller heights (see Figures 5.4, 5.6, 5.10, 5.12, 5.16, 5.18). It is observed that this effect increases when the flow through the small fans is higher when three experiments for each set of heat gain case are compared. For higher heat gains, the variation in section temperature profiles decreases for greater heights. This might be explained by the stronger plume interaction for the higher heat gains, creating a uniformity at higher levels which small fans can not effect.

The effect of small fan operation on the sections are not the same. This is probably because the fans were placed only at three locations, at sections 2, 4 and 6. Also, the flow at the small fan discharge diffusers may not be balanced, causing the fans to direct the flow non uniformly, resulting in different effects at different sections.

Average Temperature Profiles (No Small Fan Operation)

The average temperature profiles typically are not linear (see Figure 5.2 to 5.19). These profiles are similar to the results of some other studies. See Figure 2.1 for comparison of

results with that of Sandberg et al. [18]. It interesting that the experimental results are closer to that reported by Sandberg for higher flow rates (4 L/s.m^2).

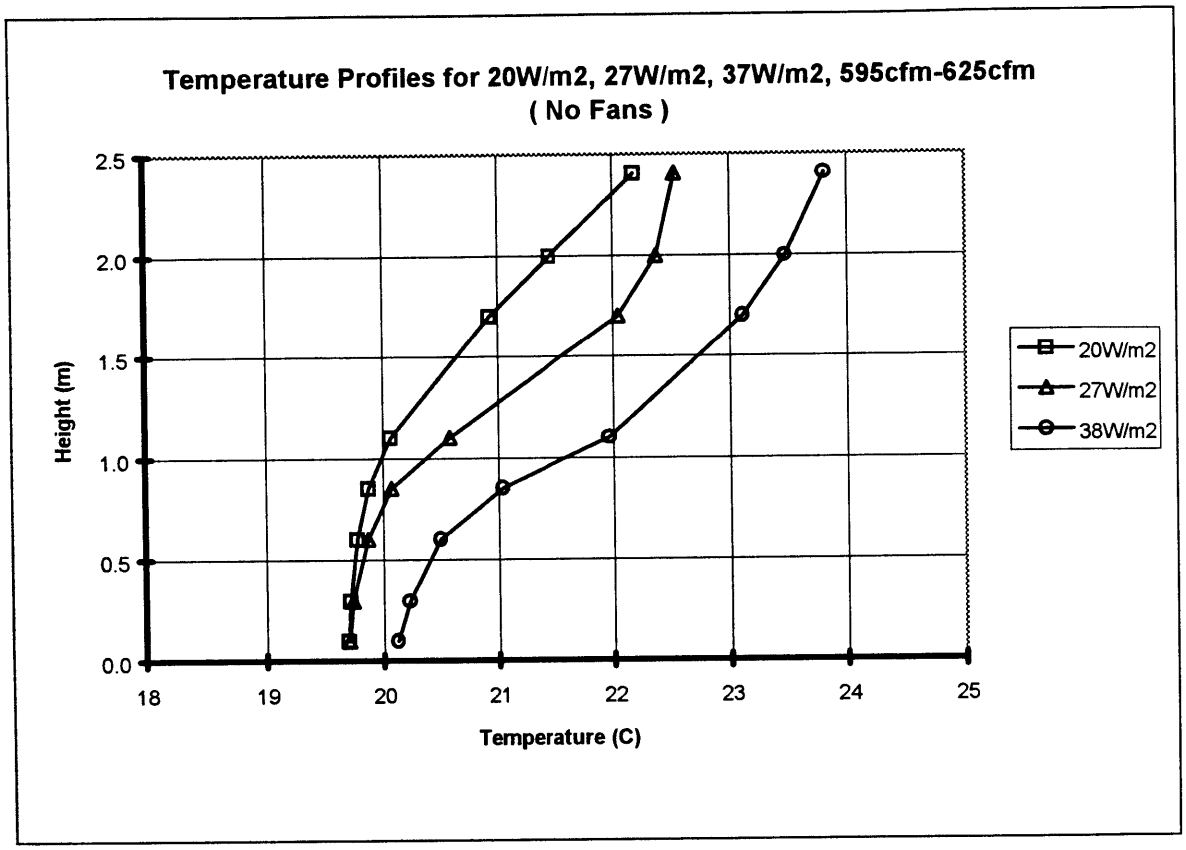

Figure 5.20. Average Temperature Profiles for Experiments 5, 8, 11.

The temperature gradient for 20W/m^2 case (see Figure 5.20) reflects a somewhat constant temperature up to a height of about 0.8m., then temperatures increase rapidly. This is not observed for 38W/m^2 case (see Figure 5.20), air temperatures start to increase at lower heights. Apart from the increase in the total heat gain for the latter case (note that supply flow rate is the same for both cases), this might also be a result of the distribution of the heat sources. In 20W/m^2 case, lights at the ceiling accounts for 38% of the total heat load. On the other hand, in 38W/m^2 case, this value is only 25%. Additionally, computer towers

are operating, 32% of the heat is dissipated at the floor level (combined effect of occupants and towers). In 20W/m^2 case, the only heat sources at the floor level are two occupants accounting for 20% of the total heat load. These results suggest that it might be preferable to place the heat sources at higher levels to keep the stratification at greater heights to improve thermal comfort. An alternative could be putting short chimneys on floor mounted equipment to reduce their affect at lower heights.

Average Temperature Profiles with Slow Mixing at Lower Levels (Small Fans Operating)

When small fans located at the floor level operate, the temperature profiles at lower levels shift to higher temperatures. Two small fan settings for each heat gain were investigated. The results are given in Figure 5.21 for 20W/m^2, Figure 5.22 for 27W/m^2 and Figure 5.23 for 38W/m^2. For all cases, small fans do have a positive effect. They reduce the temperature stratification and increase the temperatures at the floor level (see Figures 5.21, 5.22, 5.23).

Referring to the flow visualization experiments, the plumes from the heat sources accumulate at the top, whereas the cold supplied air accumulates at the floor level. The flow interaction between these two zones are by plumes at the heat sources. At the heat sources located on the floor, air has a chance to go to upper zone immediately. However, at heat sources located on the tables, the plumes start at greater heights, increasing the height of the lower zone at these locations. When small fans located on the floor operate, they start mixing the air at the lower zone. This results in higher temperatures in the lower zone making it good for thermal comfort.

The affect of small fans is more pronounced at lower heights, they reduce the temperature gradient at lower heights. A possible explanation could be: the vertical temperature stratification is more pronounced at high levels and the stratified layers are strong enough

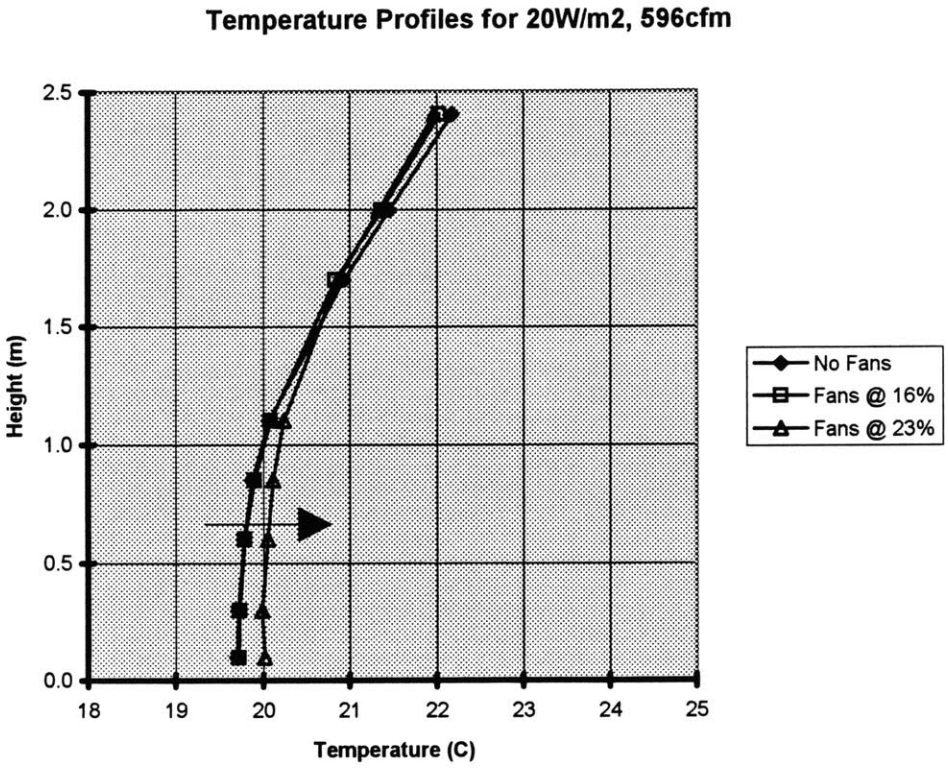

Figure 5.21. The Effect of Slow Mixing at Lower Heights on the Temperature Profile ($20W/m^2$, 596cfm).

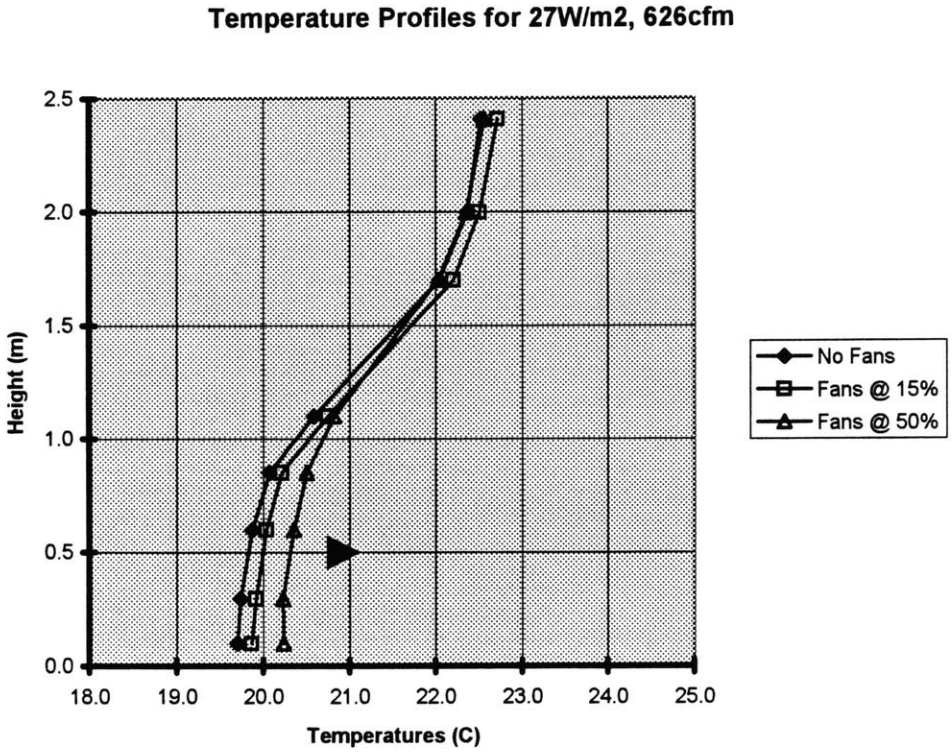

Figure 5.22. The Effect of Slow Mixing at Lower Heights on the Temperature Profile ($27W/m^2$, 626cfm).

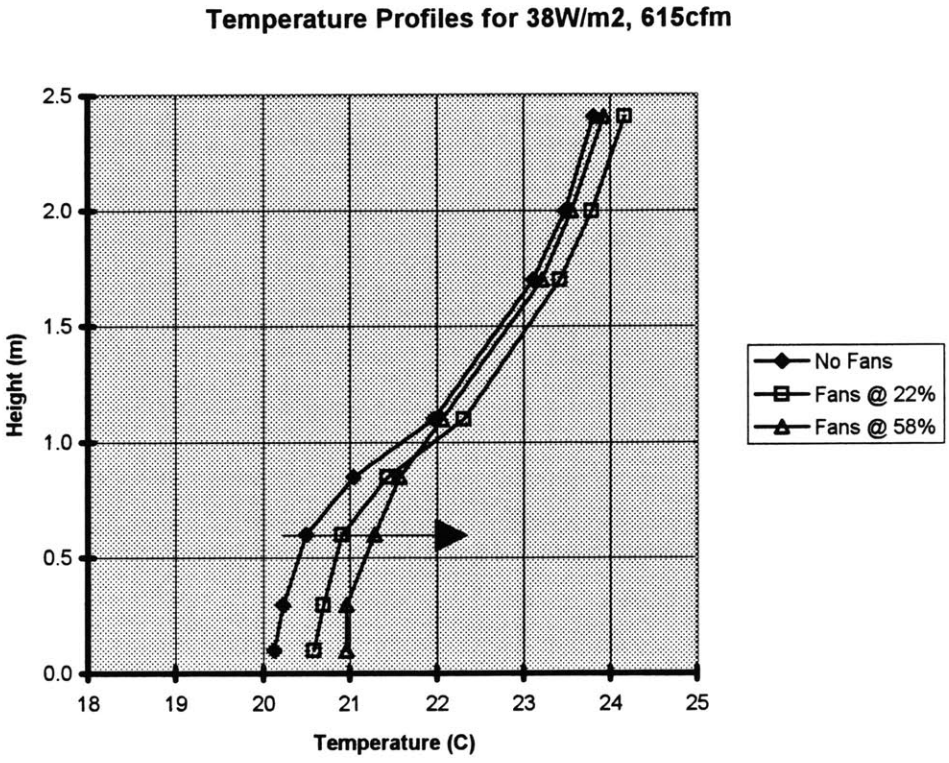

Figure 5.23. The Effect of Slow Mixing at Lower Heights on the Temperature Profile ($38W/m^2$, 615cfm).

to withstand the mixing effect of the fans. Fans can achieve mixing at lower zones, they can not effect the upper zone. This is desirable, because stratification at higher levels are desired for indoor air quality and reduced energy consumption, as mentioned in Chapter 1.

At lower heights (0m-1m), the shift in the temperature profiles resulting from fan operation is roughly the same for all heat gain scenarios, provided that the flow through the fans are kept the same. If $20W/m^2$ and $38W/m^2$ cases are compared (see Figure 5.21 and Figure 5.23), it can be observed that the fan operation with 22-23% of supply air flow rate results in about 0.4°C at 0.1m and 0.3m. For $27W/m^2$ and $38W/m^2$ cases (see Figure 5.22 and Figure 5.23) are compared, the effect of the fan operation with 50-58% of supply air flow rate result in about 0.5°C to 0.7°C at 0.1m and 0.3m.

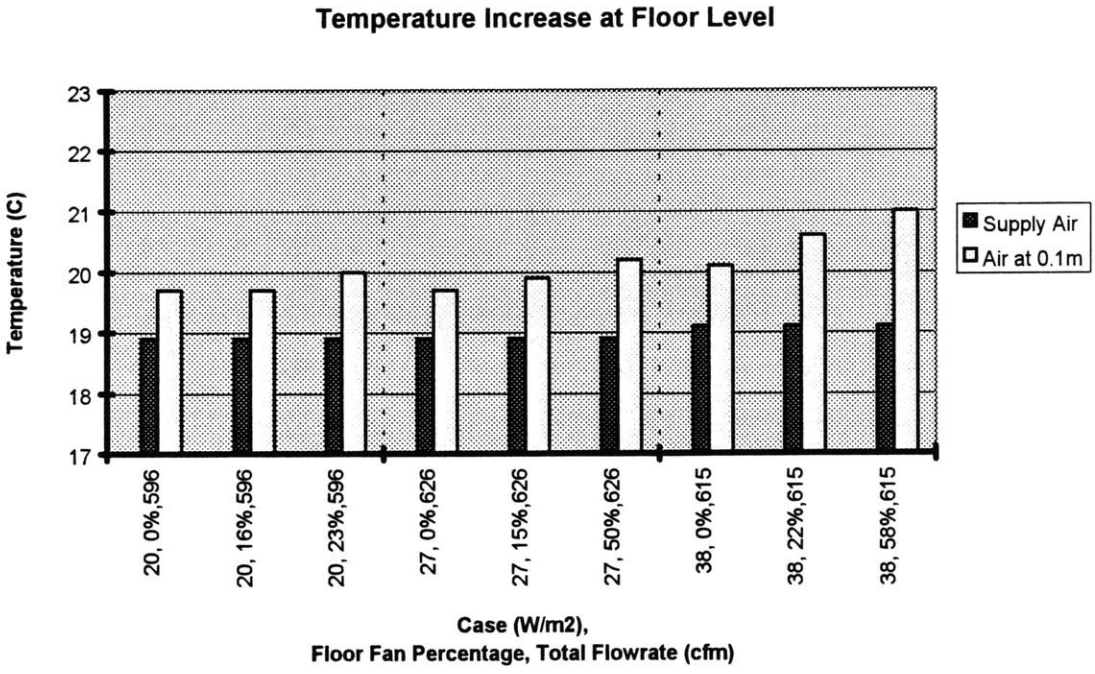

Figure 5.24. Temperature Increase at 0.1m (Experiments 5 to 13).

For all cases, small fan operation results in higher temperatures at floor level, 0.1m (see Figure 5.24). This is good because it might help to accommodate lower air supply temperatures without effecting thermal comfort. If the occupants are not very close to the supply diffusers, small fans on the floor can increase the temperatures at lower levels at the workstations, promoting thermal comfort.

One concern with the fans can be the draft problem if the discharge velocities are high. The fan casings were designed to ensure discharge velocities between 0.1m/s to 0.2m/s. In experiment 12, this figure is 0.37m/s, which might lead to a sensation of draft. However, these fan casings were only experimental. It is possible to come up with better designs with larger discharge areas. The location of the fans are also important. If they are not very close to the occupants, it might be possible to accommodate slightly high velocities. The recommendations on the fan design are given in Chapter 6.

Thermal Comfort Limits

A temperature differential exceeding 3°K between ankle and head levels is considered to be uncomfortable (ASHRAE, 1981). In none of the cases studied is a 3°K difference achieved between temperatures at 0.1m-1.1m (see Figure 5.25). However, in experiment 11 ($38W/m^2$, $9.L/s.m^2$, no fans), the difference between temperatures at heights 0.1m and 1.7m is 3°K where the temperature difference between heights 0.1m and 1.1m is 1.8. This means for a standing occupant vertical temperature difference can be a problem.

Sandberg et al. [18] reports that 3°K limit was exceeded for the heights 0.1m - 1.1m (ankle and head level of a sitting occupant) for $25W/m^2$ for a supply air flow rate of 1.8 $L/s.\ m^2$. The experiments in this study simulate cases with high flow rates. With a flow rate

of 9 L/s.m^2, the vertical temperature difference was not a problem even for high heat gains of 38W/m^2, which is expected.

Small fans located on the floor level help to promote thermal comfort, by achieving slow mixing at the lower levels, without effecting the stratification at higher levels significantly. For all the cases, fans reduce the stratification and increase the air temperatures at the floor level. See Figure 5.25 to compare the effect of fans on thermal comfort in terms of vertical temperature stratification for each case considered.

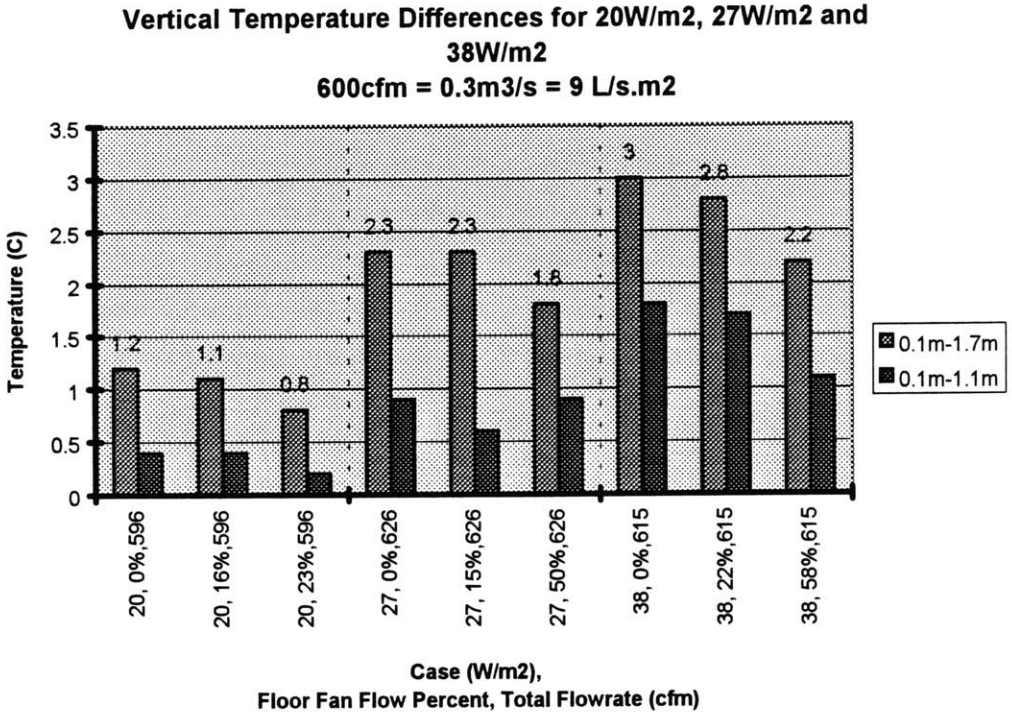

Figure 5.25. Vertical Temperature Differences for Experiments 5 to 13.

5.8. Flow Visualization Results

Flow visualization was performed to investigate the nature of flows inside the office model. Because the experiments were completed in a limited time, it was not possible to analyze the flow field in detail. However, the captured images give an insight to the flow in the model.

It was observed that, the flow at the supply diffusers is quite uniform. As soon as the fluid goes though the diffuser, it drops down and spreads on the floor. There is a cold layer accumulated at the lower levels. At the heat sources, fluid rises to higher levels in the form of plumes. The plumes disintegrate at higher levels and lead to somewhat uniform warm fluid accumulation at the ceiling level. Figure 5.26 shows the fluid entering the office model and rising over the heat sources in workstation 1 (refer to Figure 5.1 for explanation of heat sources. The camera window is placed at the end wall near section 1).

Figure 5.27 shows the stratification observed for experiment 21 ($30W/m^2$, 629 cfm, no fans). The smoke laden supplied fluid stays on the floor, rises as a plume over one of the occupants and accumulates at the top in a less dense manner. The height of the stratification is about 1m, very close to the heat level of the sitting occupant. The stratification is quite stable in terms of height. The relatively clear zone at the upper half is the initial room air before the smoke was injected. The stratification was reduced (the clear zone contained more smoke) when the fans were operated in experiment 23.

The plumes over various heat sources have different character. The occupant is simulated by a long vertical cylinder located on the floor, where as the monitor is simulated by a small box placed on a table. The heat dissipation was about the same for both. The plume over the monitor disintegrates after it leaves the surface. The plume over the occupant was somewhat more stable. This suggests that the geometry of the heat sources might be important in the size and stability of the plumes rising on the surfaces.

Figure 5.26. View of Workstation 1 after Initial Smoke Injection. A Plume Starts Rising over the Occupant (Farthest High Cylinder). Warm Fluid Starts to Accumulate at the Ceiling in a less Dense Manner ($30W/m^2$, 629cfm, no fans).

Unfortunately, further investigation of the flow fields by flow visualization was not possible. The location of the smoke injection probe was not adequate to explore either the plumes over different heat sources in more detail nor the velocities and flows associated with small fan operations. The smoke at these locations was not dense enough to provide better visualization of the flows.

Figure 5.27. Stratification in the Office Model. The Height of the Stratification (Smoke Laden Fluid Accumulation Height) is 1m. (30W/m^2, 629cfm, no fans). (see Figure 5.1. for the explanation of the heat sources).

The slide projector was more useful than the laser for the conditions of these experiments. However, the laser provided a better view of the flow field when whole sections were investigated and the fluid inside the model was very clean. The major problem with laser was the continuous smoke injection caused blurry views from the existing camera window. This suggests a better filtering system must be employed for flow visualization with laser.

CHAPTER 6

CONCLUSIONS

This study investigated the performance of displacement ventilation systems in open plan office environments, focusing on vertical temperature stratification. It explored the possibility of improving the performance of these systems by reducing the temperature stratification at lower levels and allowing the systems to operate with high cooling loads without exceeding the comfort limits.

An experimental setup consisting of a scale model of an office room and equipment necessary to provide the experimental conditions was designed and constructed. Steady state experiments on displacement ventilation were conducted. The experiments simulated a variety of cases in terms of heat gain per area, air supply flow rate and slow mixing at lower levels.

6.1. Summary of the Results

Twenty-three experiments covering various heat gains, supply air flow rates, and slow mixing conditions were conducted. Nine of these experiments were selected for analysis for the reasons mentioned in Chapter 5. These experiments can be considered in three sets simulating three different heat gains ($20W/m^2$, $27W/m^2$ and $38W/m^2$) at the same supply air flow rate ($8.8L/s.m^2$) in an open plan office room (4m x 8m floor area, 2.7m height) with three workstations. Each set consists of three experiments corresponding to different amounts of slow mixing at lower levels.

The temperature profiles in the experiments were similar to the results of other studies [10, 18, 20]. They were not linear for the cases considered. The temperature stratification was more pronounced for greater cooling loads at the same supply air flow rate. The variation in the temperature profiles at different sections of the office room decreased at greater heights when the cooling load increased. The variation at lower levels, however, was very similar for all cooling loads. This was explained by the uniformity achieved at greater heights as a possible result of increased plume interaction with higher heat gains.

When slow mixing was induced at the floor level, the temperature profiles at lower levels shifted to higher temperatures. The temperature stratification was reduced and the temperatures at the floor level increased. During the simulations, slow mixing was achieved by the operation of three small fans located at the floor level in the office model. It was observed that the effect of the fans was more pronounced at lower heights. Fans decreased the temperature gradient at lower levels without significantly affecting the stratification at higher levels. In other words, the stratification at higher levels was strong enough to withstand the mixing of the fans. This was a desirable result; higher exhaust temperatures as a result of stratification may offer energy savings due to longer period of economizer utilization, improved indoor air quality and heat recovery possibilities as mentioned in Chapter 1.

At lower heights (0m-1m), the shift in the temperature profiles resulting from fan operation was roughly the same for all heat gains (for the same supply air flow rate), provided that the flow through the small fans was kept the same. Additionally, small fan operation resulted in higher air temperatures at the floor level (0.1m) for all cases. This was also desirable as it might help to accommodate lower supply air temperatures without adversely affecting the thermal comfort.

Small fan operation may cause draft problems if the fan casing is not adequately designed. In a few experiments, the discharge velocities were high (0.35m/s), although they were usually within acceptable limits (0.1m/s-0.2m/s) in most of the experiments. The fans used in this study were experimental prototypes. Further investigation should go into improved designs.

The thermal comfort limit for vertical temperature stratification ($\Delta T_{0.1m-1.7m}$= 3°K for a standing occupant according to ASHRAE) was exceeded in only the simulated case with the highest heat gain, 38W/m^2 at a supply air flow rate of 9L/s.m^2. The induction of slow mixing at lower levels by small fans on the floor reduced this temperature differential, for all cases studied. This suggests that displacement ventilation may accommodate higher cooling loads with the same supply flow rates if slow mixing is provided at the lower levels, in the office space.

Slow mixing at lower heights has a positive effect. It promotes thermal comfort and allows displacement ventilation to be used for higher cooling loads. It may also allow lower supply air temperatures to be used for displacement ventilation.

6.2. Suggestions for Future Research

The results of this study indicate that slow mixing at lower levels has favorable effects on the performance of displacement ventilation systems. This is clearly an issue to be further investigated. Slow mixing at lower levels was achieved by small fans placed on the floor in this study. The performance of other means, such as swirl diffusers located on the floor, to achieve the same effect should be investigated. Relative costs and the application areas of each should be compared.

The small fans were designed to provide circulation in the lower zone with an air velocity of roughly 0.15m/s to avoid draft problems, but it was not possible to measure the exact velocities. The small fan diffuser structures were only experimental prototypes sufficient for the purposes of this study. The sizing of the fan casings was based on the availability of small axial fans. However, in actual scale, designers would have much more freedom for better designs. Designs with more sophisticated diffusers, say, with a larger discharge diffuser area, with perforated screens to achieve flow uniformity, angled or contoured suction and discharge sections and smaller casing sizes need to be investigated. The effect of spatial distribution of these devices in the office rooms on the performance of displacement ventilation should be studied. Additionally, the flow at fan discharge was horizontal, slightly angled towards the floor. The effect of different flow directions on the slow mixing performance should be explored.

Although a limited number of cases were investigated in this study, the experimental apparatus is able to provide a wide range of experimental conditions. The analysis in this study should be extended to other cases to provide a better understanding of the displacement ventilation performance and effect of slow mixing at different conditions. These conditions could include lower supply air flow rates, higher supply-exhaust temperature differences, different distribution of heat sources and slow mixing devices, effect of occupant motion, location of the supply diffusers, location of the exhaust diffusers, arrangement of the workstations, shape and/or dimensions of the heat sources, other external heat sources and different diffuser designs.

6.3. Recommendations on the Experimental Setup

The major problem encountered with the experimental apparatus was that there were leaks in the box containing the scale model. Therefore, the experiments were completed in a very short time to recover the refrigerant as soon as possible and to simulate cases at

consistent conditions by the experiments. It is strongly recommended to use another enclosure in future studies utilizing the same setup. Special consideration should be given to all removable sections and wiring connections. For wiring connections interface connections specially made for vacuum or high pressure applications should be preferred. Compression fittings should be used whenever applicable.

The heat loss at the box side walls effected some of the experiments considerably. Insulation on the sides, bottom and the top should be improved. The window located at one of the box walls was used for video recordings during flow visualization experiments. It did not provide a sufficiently good view of the flow at the points of interest in the model. It should be replaced with a larger size window for future studies. The flow rate at the gas line was measured by calibration of the pressure drop at the heat exchanger. A more precise flow measurement means at the gas circuit must be provided to reduce the uncertainty in the flow rate measurement.

Flow visualization experiments could not provide a detailed analysis of the flow field. It is recommended to use better filtering system, as the circulating smoke reduced the clarity of the view and was a major problem during the video recordings. Smoke should be injected as close as possible to the points of interest. In this study it was injected at the diffusers. The smoke stream was diluted when it reached the heat sources, making the analysis of the plumes difficult.

6.4. End Note

Office building air conditioning is a large area of research. Displacement ventilation is a promising method of office room air conditioning. There are many issues to be addressed on displacement ventilation. In this study, it is attempted to investigate the performance of these systems focusing on the maximum cooling loads that can be handled by displacement

ventilation, the vertical temperature stratification and the possibility to improve thermal comfort by providing slow mixing at lower levels.

Displacement ventilation has the potential to provide better indoor air quality and lower energy consumption. However, the lack of a proper method to use it with high heat gains makes it difficult to design the systems to promote thermal comfort. Displacement ventilation should be further investigated and extensive design criteria should be established.

BIBLIOGRAPHY

1) H.J. Sauer, R.H. Howell, "Principles of Heating, Ventilating and Air Conditioning", ASHRAE, Missouri, 1992.

2) Roaf S., M. Hancock, "Energy Efficient Building", Blackwell Scientific Publications, Oxford, 1992.

3) Taub S.C., "The Energy Effects of Occupant Controlled Heating, Ventilation and Air Conditioning Systems in Office Buildings", SM Thesis, Department of Mechanical Engineering, MIT, Cambridge, 1994.

4) Spoormaker H.J., "Low Pressure Underfloor HVAC System", ASHRAE Transactions, 1990, vol. 95, part 1.

5) Heinemeier K.E., G.E. Schiller, C.Benton, "Task Conditioning for the Workspace: Issues and Challenges", ASHRAE Transactions, 1990, vol. 95, part 1.

6) Harris L. and Associates, "Comfort and Productivity in the Offices of 80s. The Steelcase National Study of Office Environments, No.2", Steelcase Inc., Grand Rapids, 1980.

7) Brill M., S. Marguilis, "Using Office Design to Increase Productivity", Buffalo Organization for Social and Technological Innovation, Buffalo, 1984.

8) Kraemer, Sieverts and Partners, "Open Plan Offices", McGraw Hill Book Company, London, 1977.

9) Norford L.K., A. Rabl, J. Harris and J. Roturier, "The Sum of Megabytes Equals Gigawatts; Energy Consumption and Efficiency of Office PCs and Related Equipment", ACEEE Summer Study on Energy Efficiency in Buildings, 1988.

10) Alamdari F., K.M. Bennet, P.M. Rose, "Displacement Ventilation Performance", BSRIA, Bourne Press Limited, London, 1993.

11) Sepannen O.A., W.J. Fisk, J. Eto., D.T. Grimsrud, "Comparison of Conventional Mixing and Displacement Air Conditioning and Ventilating Systems in US Commercial Buildings", ASHRAE Transactions, 1989, vol. 95, part 2.

12) ARUP HVAC Applications Guide, Ove Arup Corporation, London, 1993.

13) Svensson A.G.L., "Nordic Experiences of Displacement Ventilation Systems", ASHRAE Transactions, 1989, vol. 95, part 2.

14) Fanger P.O., "Thermal Comfort", McGraw Hill Book Company, New York, 1970.

15) Melikov A.K., J.B Nielsen., "Local Thermal Discomfort Due to Draft and Vertical Temperature Difference in Rooms with Displacement Ventilation", ASHRAE Transactions, 1989, vol. 95, part 2.

16) Kristensson J.A., "Displacement Ventilation Systems in Industrial Buildings", ASHRAE Transactions, 1993, vol. 99, part 2.

17) Mathisen H.M., "Case Studies of Displacement Ventilation in Public Halls", ASHRAE Transactions, 1989, vol. 95, part 2.

18) Sandberg M., C. Blomqvist, "Displacement Ventilation Systems in Office Rooms", ASHRAE Transactions, 1989, vol. 95, part 2.

19) Sandberg M., M. Mattsson, "Displacement Ventilation-Influence of Physical Activity", Royal Institute of Technology, Roomvent, 1994.

20) Mundt E., "Convection Flows above Common Heat Sources in Rooms with Displacement Ventilation", Royal Institute of Technology, Roomvent, 1990.

21) Bauman F.S., D. Faulkner, E.A. Arens, W.J. Fisk, L.P. Johnston, P.J. McNeel, D. Pih, H. Zhang, "Air Movement, Ventilation and Comfort in a Partitioned Office Space", ASHRAE Transactions, 1992, vol. 98, part 1.

22) Kim G., H. Homma, "Possibility for Increasing Ventilation Efficiency with Upward Ventilation", ASHRAE Transactions, 1992, vol. 98, part 1.

23) Hanzawa H., Nagasawa Y., "Thermal Comfort with Underfloor Air Conditioning Systems", ASHRAE Transactions, 1990, vol. 95, part 1.

24) Arnold D., 'Raised Floor Air Distribution-A Case Study", ASHRAE Transactions, 1990, vol. 95, part 1.

25) Shaw C.Y., J.S. Zhang, M.N. Said, F. Vaculik, R.J. Mageee, "Effect of Air Diffuser Layout on the Ventilation Conditions of a Workstation-Part 1: Air Distribution Patterns, ASHRAE Transactions, 1993, vol. 99, part 2.

26) Olson D.A., "Scale Model Studies of Natural Convection in Enclosures at High Rayleigh Number", Ph.D. Thesis, Department of Mechanical Engineering, MIT, Cambridge, 1986.

27) Langhaar H.L., "Dimensional Analysis and Theory of Models", John Wiley & Sons, Inc., New York, 1951.

28) Schuring D.J., "Scale Models in Engineering", Pergamon Press, Oxford, 1977.

29) David F.W., H. Nolle, "Experimental Modelling in Engineering", Butterworths, London, 1982.

30) Isaacson E. de St Q., M. de St Q. Isaacson, "Dimensional Methods in Engineering and Physics", John Wiley & Sons, Inc., New York, 1975.

31) Taylor E., "Dimensional Analysis for Engineers", Clarendon Press, Oxford, 1974.

32) Tritton D.J., "Physical Fluid Dynamics", Van Nostrand Reinhold Company, 1977.

33) Incropera F.P., D.P. DeWitt, "Fundamentals of Heat Transfer and Mass Transfer", John Wiley & Sons, Inc., New York, 1990.

34) Okutan C., "Ic Hava Kalitesinin Enfeksiyon Iliskileri", Tesisat Muhendisleri Dernegi Technical Bulletin, no. 3, 1993, pp. 5-6.

35) Kakac S., W. Aung, R. Viskanta, "Natural Convection", Hemisphere Publishing Corporation, Washington, 1985.

36) Okutan C., "Temiz Oda Teknolojisi", Tesisat Dergisi, no.7, 1991, pp. 38-42.

37) Interview with Camlibel M.E., Civil Engineer, Boston, (10/10/1995).

39) Interview with Kilkis B., Professor at Middle East Technical University, Ankara, (2/10/1994).

40) Kulpmann R. W., "Thermal Comfort and Air Quality in Rooms with Cooled Ceilings-Results of Scientific Investigations", ASHRAE Transactions, 1993, vol. 99, part 2.

41) Aksel M. H., "Notes on Fluid Mechanics", Middle East Technical University, Ankara, 1990.

42) ASHRAE Handbook, "Fundamentals", ASHRAE Publications, Atlanta, 1989.

APPENDIX

SUMMARY OF THE EXPERIMENTAL RESULTS

For each experiment, the measured values for the model are tabulated and graphs for the simulated case are given.

EXPERIMENT # **2**

Results for air operation

Case	**25 W/m^2**
Cooling Load	792 W
Heat Sources	P1,P2,P3,S1,S2,S3,X2,L
Flow at fans on floor	**0% of total flowrate**
Supply air flow rate	412 cfm 0.19 m^3/s
Velocity at diffusers	0.13 m/s

Average Temperature Field Summary	
T supply	19.0 C
T exhaust	20.7 C
T (0.1m)	19.7 C
T (1.1m)	20.3 C
T(1.7m)	21.4 C
delta T (0.1m-1.1m)	0.6 C
delta T (0.1m-1.7m)	1.7 C

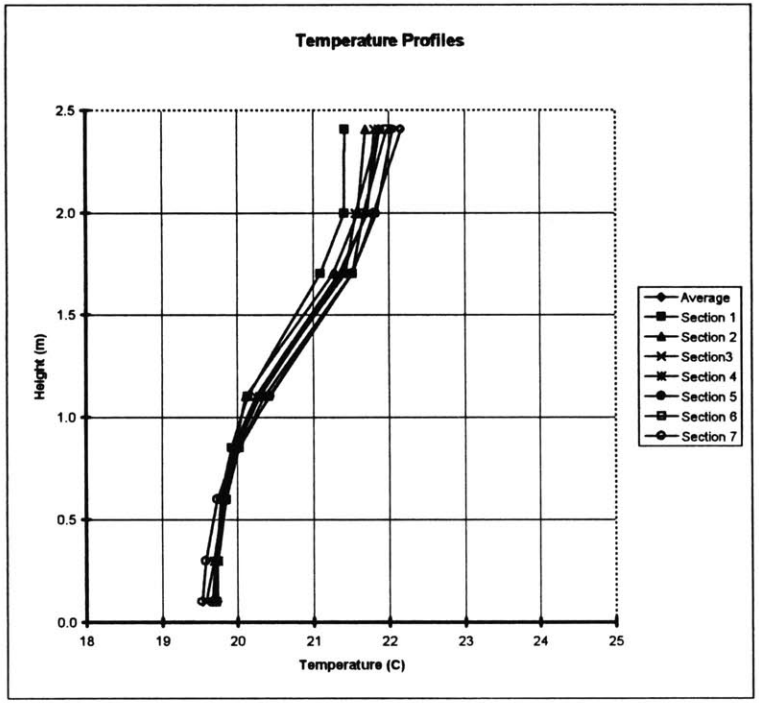

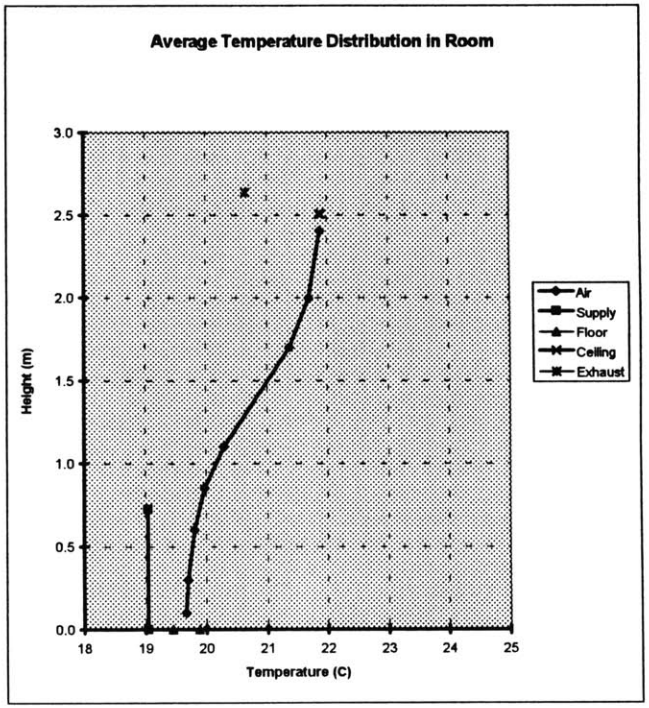

EXPERIMENT # 2

Temps40B.dat

System Data

Considered Case for pure R114	40 W/m2
Actual Case studied	25 W/m2
Oxygen Concentration	3.5%
Air Concentration	17%

Fans	0 V
	0 cfm each
	0 cfm total
	0% of total flowrate

Heat Sources	P1,P2,P3,S1,S2,S3,X2,L
Heat Dissipated	235 W

Monometer Reads	0.05 "wg
Gas Flowrate	7.8 cfm
Velocity at diffuser	0.11 m/s
Water Flowrate	0.27 gpm

Temperature Readings (Average of average readings (x1000) for 7 cases)

T gas in	19.2 C	EXP0,14
T gas out	25.8 C	EXP0,13
T water in	15.6 C	EXP0,12
T water out	19.2 C	EXP0,15

Side wall W1	21.4 C	EXP0,0
Side wall W2	24.5 C	EXP0,1
End wall W3	25.7 C	EXP0,2
Diffuser D1	21.6 C	EXP0,3
Diffuser D2	20.4 C	EXP0,4
Floor F1	20.8 C	EXP0,5
Floor F2	22.6 C	EXP0,6
Ceiling C1	30.9 C	EXP0,7
Ceiling C2	30.8 C	EXP0,8
Wall OWST	26.4 C	EXP0,9
Wall OWSM	20.9 C	EXP0,10
Wall OWET	23.8 C	EXP0,11

Left Rod	Average Temperature	Channel
364mm	31.0 C	EXP1,0
303mm	30.4 C	EXP1,1
258mm	28.9 C	EXP1,2
167mm	24.6 C	EXP1,3
129mm	23.2 C	EXP1,4
91mm	22.4 C	EXP1,5
45mm	22.3 C	EXP1,6
15mm	22.3 C	EXP1,7

Right rod	Average Temperature	Channel
364mm	30.6 C	EXP1,15
303mm	29.7 C	EXP1,14
258mm	28.6 C	EXP1,13
167mm	24.0 C	EXP1,12
129mm	22.9 C	EXP1,11
91mm	22.3 C	EXP1,10
45mm	21.5 C	EXP1,9
15mm	21.1 C	EXP1,8

Average T over height in model

Height	T (C)
36.5 cm	30.8 C
30.3 cm	30.1 C
25.8 cm	28.8 C
16.7 cm	24.3 C
12.9 cm	23.0 C
9.1 cm	22.3 C
4.5 cm	21.9 C
1.5 cm	21.7 C

Scaling Correction		
TEMPERATURE SCALE	>>>>>>	0.24
POWER SCALE	>>>>>>	3.37
VOLUMETRIC FLOWRATE SCALE	>>>>>>	52.82
MASS FLOWRATE SCALE	>>>>>>	10.09
VELOCITY SCALE	>>>>>>	1.22

EXPERIMENT # **3**

Results for air operation

Case	**25 W/m^2**
Cooling Load	792 W
Heat Sources	P1,P2,P3,S1,S2,S3,X2,L
Flow at fans on floor	**39% of total flowrate**
Supply air flow rate	412 cfm 0.19 m^3/s
Velocity at diffusers	0.13 m/s

Average Temperature Field Summary	
T supply	19.2 C
T exhaust	21.0 C
T (0.1m)	20.1 C
T (1.1m)	20.7 C
T(1.7m)	21.8 C
delta T (0.1m-1.1m)	0.6 C
delta T (0.1m-1.7m)	1.7 C

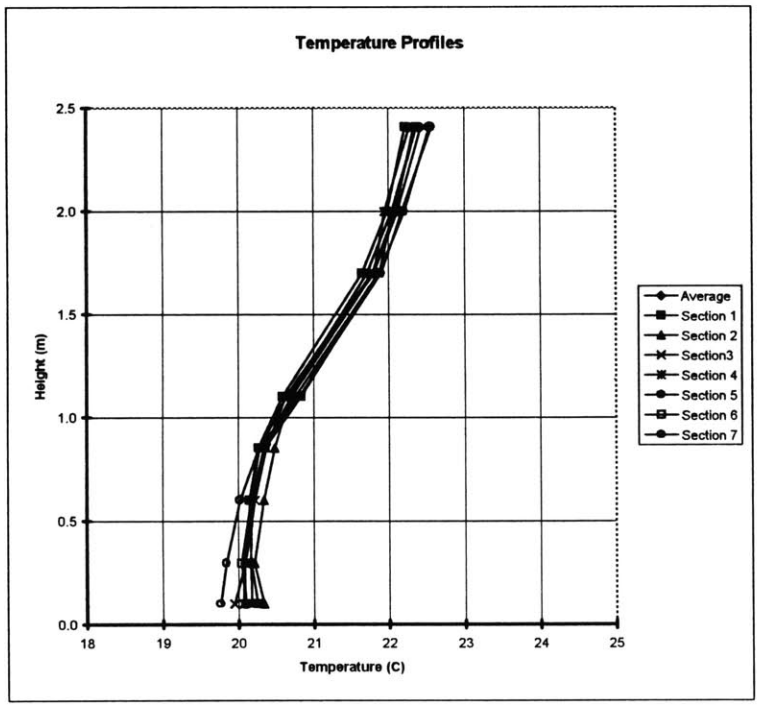

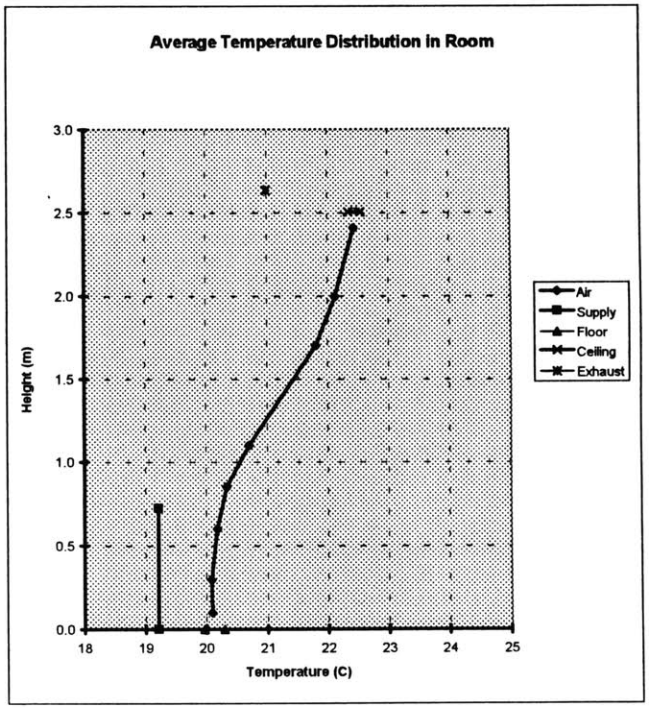

EXPERIMENT # 3

Temps40C.dat

System Data

Considered Case for pure R114	40 W/m2
Actual Case studied	**25 W/m2**
Oxygen Concentration	**3.5%**
Air Concentration	**17%**

Fans	7 V
	1.01 cfm each
	3.03 cfm total
	39% of total flowrate

Heat Sources	P1,P2,P3,S1,S2,S3,X2,L
Heat Dissipated	235 W

Monometer Reads	0.05 "wg
Gas Flowrate	7.8 cfm
Velocity at diffuser	0.11 m/s
Water Flowrate	0.27 gpm

Temperature Readings (Average of average readings (x1000) for 7 cases)

T gas in	19.9 C	EXP0,14
T gas out	27.1 C	EXP0,13
T water in	15.9 C	EXP0,12
T water out	19.5 C	EXP0,15

Side wall W1	22.5 C	EXP0,0
Side wall W2	26.1 C	EXP0,1
End wall W3	27.4 C	EXP0,2
Diffuser D1	23.0 C	EXP0,3
Diffuser D2	21.6 C	EXP0,4
Floor F1	23.0 C	EXP0,5
Floor F2	24.3 C	EXP0,6
Ceiling C1	33.5 C	EXP0,7
Ceiling C2	32.7 C	EXP0,8
Wall OWST	29.0 C	EXP0,9
Wall OWSM	20.9 C	EXP0,10
Wall OWET	25.3 C	EXP0,11

Left Rod	Average Temperature	Channel
364mm	33.3 C	EXP1,0
303mm	32.1 C	EXP1,1
258mm	30.6 C	EXP1,2
167mm	26.0 C	EXP1,3
129mm	24.5 C	EXP1,4
91mm	23.9 C	EXP1,5
45mm	23.9 C	EXP1,6
15mm	24.1 C	EXP1,7

Right rod	Average Temperature	Channel
364mm	32.8 C	EXP1,15
303mm	31.5 C	EXP1,14
258mm	30.4 C	EXP1,13
167mm	26.0 C	EXP1,12
129mm	24.5 C	EXP1,11
91mm	23.7 C	EXP1,10
45mm	22.9 C	EXP1,9
15mm	22.9 C	EXP1,8

Average T over height in model

Height	T (C)
36.5 cm	33.0 C
30.3 cm	31.8 C
25.8 cm	30.5 C
16.7 cm	26.0 C
12.9 cm	24.5 C
9.1 cm	23.8 C
4.5 cm	23.4 C
1.5 cm	23.5 C

Scaling Correction		
TEMPERATURE SCALE	>>>>>>	0.24
POWER SCALE	>>>>>>	3.37
VOLUMETRIC FLOWRATE SCALE	>>>>>>	52.82
MASS FLOWRATE SCALE	>>>>>>	10.09
VELOCITY SCALE	>>>>>>	1.22

EXPERIMENT # **4**

Results for air operation

Case	**25 W/m^2**
Cooling Load	792 W
Heat Sources	P1,P2,P3,S1,S2,S3,X2,L
Flow at fans on floor	**86% of total flowrate**
Supply air flow rate	412 cfm 0.19 m^3/s
Velocity at diffusers	0.13 m/s

Average Temperature Field Summary	
T supply	19.3 C
T exhaust	21.1 C
T (0.1m)	20.6 C
T (1.1m)	21.1 C
T(1.7m)	21.9 C
delta T (0.1m-1.1m)	0.5 C
delta T (0.1m-1.7m)	1.3 C

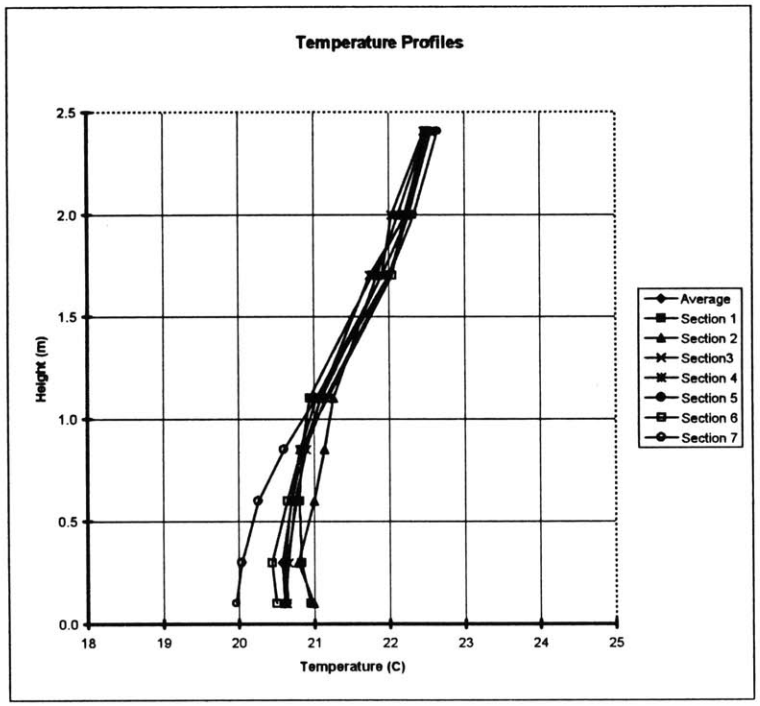

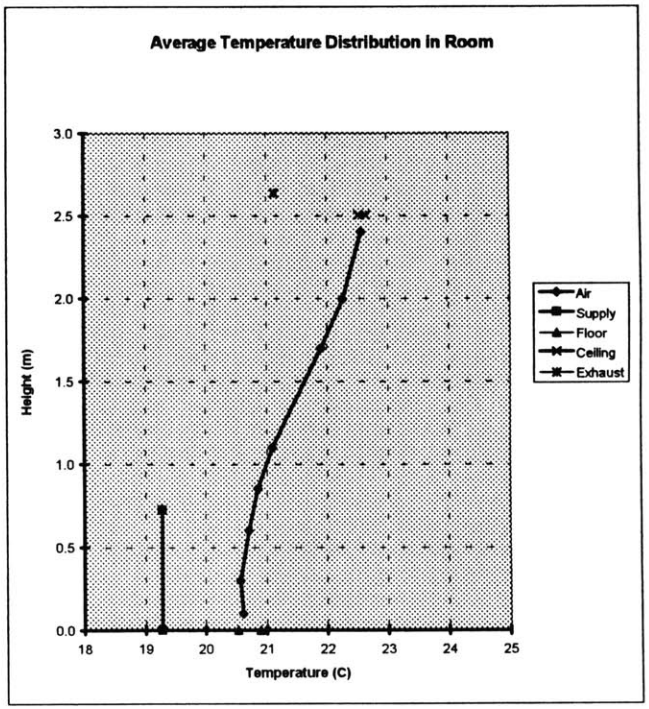

EXPERIMENT # 4

Temps40D.dat

System Data

Considered Case for pure R114	40 W/m2
Actual Case studied	**25 W/m2**
Oxygen Concentration	**3.5%**
Air Concentration	**17%**

Fans	12 V
	2.23 cfm each
	6.69 cfm total
	86% of total flowrate

Heat Sources	P1,P2,P3,S1,S2,S3,X2,L
Heat Dissipated	235 W

Monometer Reads	0.05 "wg
Gas Flowrate	7.8 cfm
Velocity at diffuser	0.11 m/s
Water Flowrate	0.27 gpm

Temperature Readings (Average of average readings (x1000) for 7 cases)

T gas in	20.2 C	EXP0,14
T gas out	27.8 C	EXP0,13
T water in	15.9 C	EXP0,12
T water out	19.6 C	EXP0,15

Side wall W1	23.9 C	EXP0,0
Side wall W2	26.8 C	EXP0,1
End wall W3	28.4 C	EXP0,2
Diffuser D1	23.7 C	EXP0,3
Diffuser D2	22.5 C	EXP0,4
Floor F1	25.2 C	EXP0,5
Floor F2	26.8 C	EXP0,6
Ceiling C1	33.9 C	EXP0,7
Ceiling C2	33.5 C	EXP0,8
Wall OWST	30.5 C	EXP0,9
Wall OWSM	20.7 C	EXP0,10
Wall OWET	26.3 C	EXP0,11

Left Rod	Average Temperature	Channel
364mm	33.6 C	EXP1,0
303mm	32.6 C	EXP1,1
258mm	30.7 C	EXP1,2
167mm	27.7 C	EXP1,3
129mm	26.7 C	EXP1,4
91mm	26.0 C	EXP1,5
45mm	26.1 C	EXP1,6
15mm	26.4 C	EXP1,7

Right rod	Average Temperature	Channel
364mm	33.6 C	EXP1,15
303mm	32.1 C	EXP1,14
258mm	31.0 C	EXP1,13
167mm	27.5 C	EXP1,12
129mm	26.6 C	EXP1,11
91mm	26.0 C	EXP1,10
45mm	24.8 C	EXP1,9
15mm	24.9 C	EXP1,8

Average T over height in model

Height	T (C)
36.5 cm	33.6 C
30.3 cm	32.4 C
25.8 cm	30.9 C
16.7 cm	27.6 C
12.9 cm	26.6 C
9.1 cm	26.0 C
4.5 cm	25.4 C
1.5 cm	25.6 C

Scaling Correction		
TEMPERATURE SCALE	>>>>>>	0.24
POWER SCALE	>>>>>>	3.37
VOLUMETRIC FLOWRATE SCALE	>>>>>>	52.82
MASS FLOWRATE SCALE	>>>>>>	10.09
VELOCITY SCALE	>>>>>>	1.22

EXPERIMENT # **5**

Results for air operation

Case	**20 W/m^2**
Cooling Load	639 W
Heat Sources	P1,P3,S1,S3,X2,L
Flow at fans on floor	**0% of total flowrate**
Supply air flow rate	596 cfm 0.28 m^3/s
Velocity at diffusers	0.19 m/s

Average Temperature Field Summary	
T supply	18.9 C
T exhaust	20.9 C
T (0.1m)	19.7 C
T (1.1m)	20.1 C
T(1.7m)	20.9 C
delta T (0.1m-1.1m)	0.4 C
delta T (0.1m-1.7m)	1.2 C

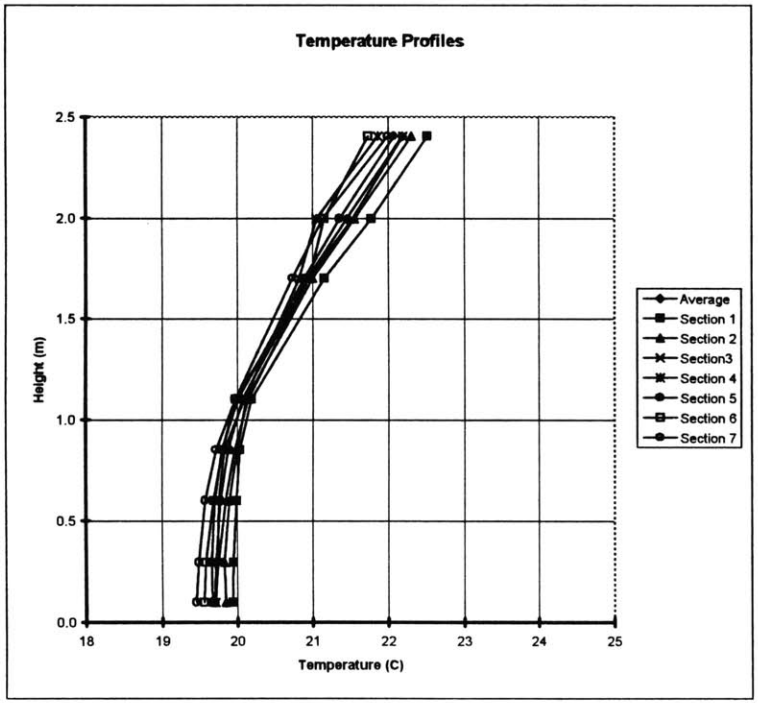

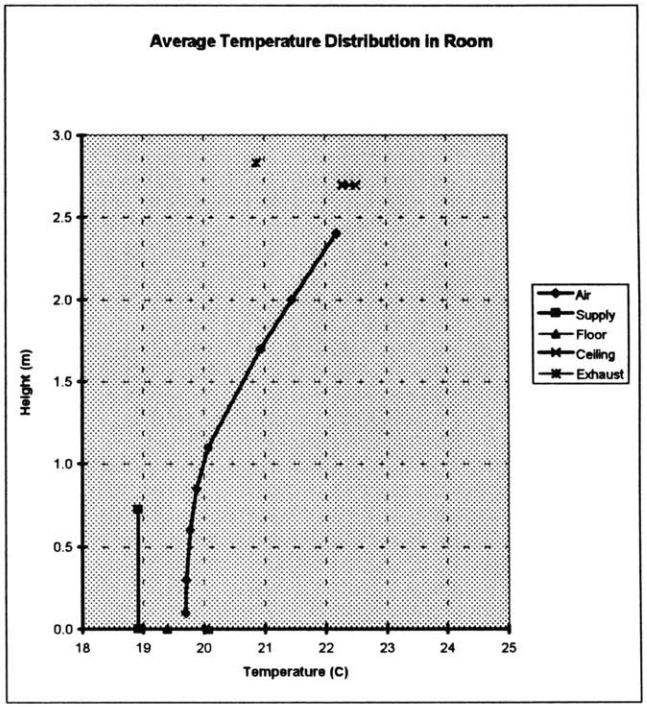

EXPERIMENT # 5

Temps40E.dat (first 3 readings) Temps40F.dat (last 4 readings)

System Data

Considered Case for pure R114	30 W/m2
Actual Case studied	20 W/m2
Oxygen Concentration	3.0%
Air Concentration	14%

Heat Sources	P1,P3,S1,S3,X2,L
Heat Dissipated	175 W

Monometer Reads	0.1 "wg
Gas Flowrate	10.9 cfm
Velocity at diffuser	0.15 m/s
Water Flowrate	0.60 gpm

Fans	
	0 V
	0 cfm each
	0 cfm total
	0% of total flowrate

Temperature Readings (Average of average readings (x1000) for 7 cases)

T gas in	18.7 C	EXP0,14
T gas out	26.2 C	EXP0,13
T water in	14.7 C	EXP0,12
T water out	17.8 C	EXP0,15

Side wall W1	21.2 C	EXP0,0
Side wall W2	23.4 C	EXP0,1
End wall W3	25.7 C	EXP0,2
Diffuser D1	21.2 C	EXP0,3
Diffuser D2	20.4 C	EXP0,4
Floor F1	20.5 C	EXP0,5
Floor F2	23.1 C	EXP0,6
Ceiling C1	32.4 C	EXP0,7
Ceiling C2	31.5 C	EXP0,8
Wall OWST	28.3 C	EXP0,9
Wall OWSM	21.7 C	EXP0,10
Wall OWET	24.9 C	EXP0,11

Left Rod	Average Temperature	Channel
364mm	31.2 C	EXP1,0
303mm	28.6 C	EXP1,1
258mm	26.3 C	EXP1,2
167mm	23.3 C	EXP1,3
129mm	22.5 C	EXP1,4
91mm	22.0 C	EXP1,5
45mm	22.0 C	EXP1,6
15mm	22.1 C	EXP1,7

Right rod	Average Temperature	Channel
364mm	31.2 C	EXP1,15
303mm	28.2 C	EXP1,14
258mm	26.5 C	EXP1,13
167mm	22.9 C	EXP1,12
129mm	22.2 C	EXP1,11
91mm	22.0 C	EXP1,10
45mm	21.5 C	EXP1,9
15mm	21.2 C	EXP1,8

Average T over height in model

Height	T (C)
36.5 cm	31.2 C
30.3 cm	28.4 C
25.8 cm	26.4 C
16.7 cm	23.1 C
12.9 cm	22.3 C
9.1 cm	22.0 C
4.5 cm	21.7 C
1.5 cm	21.7 C

Scaling Correction		
TEMPERATURE SCALE	>>>>>>	0.26
POWER SCALE	>>>>>>	3.65
VOLUMETRIC FLOWRATE SCALE	>>>>>>	54.62
MASS FLOWRATE SCALE	>>>>>>	10.18
VELOCITY SCALE	>>>>>>	1.26

EXPERIMENT # 6

Results for air operation

Case	**20 W/m^2**
Cooling Load	639 W
Heat Sources	P1,P3,S1,S3,X2,L
Flow at fans on floor	**23% of total flowrate**
Supply air flow rate	596 cfm 0.28 m^3/s
Velocity at diffusers	0.19 m/s

Average Temperature Field Summary	
T supply	18.9 C
T exhaust	20.8 C
T (0.1m)	20.0 C
T (1.1m)	20.2 C
T(1.7m)	20.9 C
delta T (0.1m-1.1m)	0.2 C
delta T (0.1m-1.7m)	0.8 C

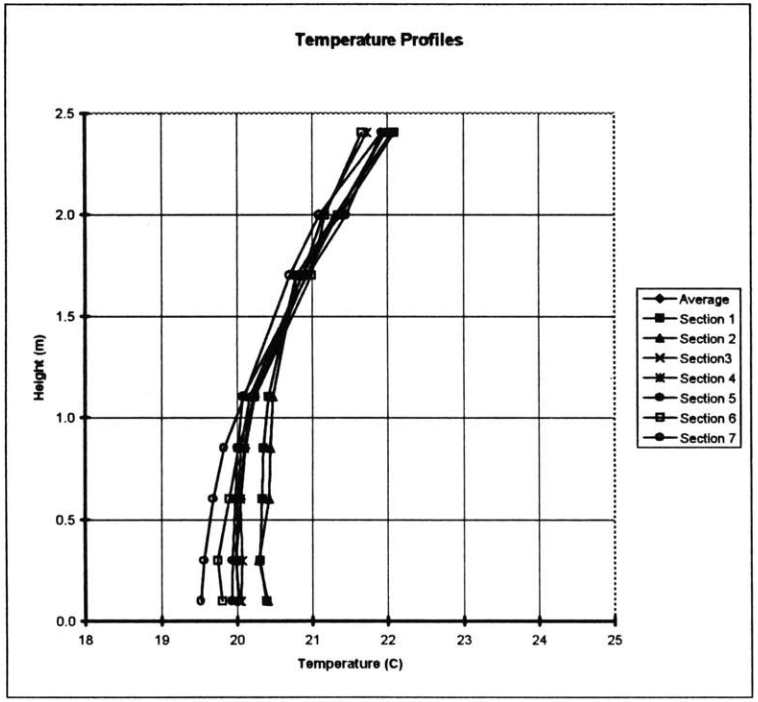

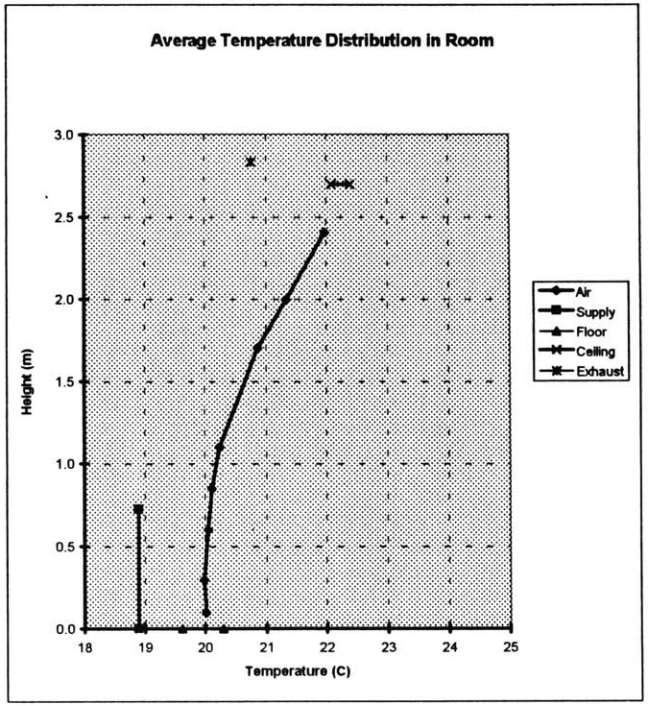

EXPERIMENT # 6

Temps40G.dat

System Data

Considered Case for pure R114	30 W/m2
Actual Case studied	**20 W/m2**
Oxygen Concentration	**3.0%**
Air Concentration	**14%**

Fans	11 V
	0.82 cfm each
	2.46 cfm total
	23% of total flowrate

Heat Sources	P1,P3,S1,S3,X2,L
Heat Dissipated	175 W

Monometer Reads	0.1 "wg
Gas Flowrate	10.9 cfm
Velocity at diffuser	0.15 m/s
Water Flowrate	0.60 gpm

Temperature Readings (Average of average readings (x1000) for 7 cases)

T gas in	18.6 C	EXP0,14
T gas out	25.7 C	EXP0,13
T water in	14.6 C	EXP0,12
T water out	17.6 C	EXP0,15

Side wall W1	21.4 C	EXP0,0
Side wall W2	23.1 C	EXP0,1
End wall W3	25.2 C	EXP0,2
Diffuser D1	20.8 C	EXP0,3
Diffuser D2	20.5 C	EXP0,4
Floor F1	21.4 C	EXP0,5
Floor F2	24.0 C	EXP0,6
Ceiling C1	31.9 C	EXP0,7
Ceiling C2	30.8 C	EXP0,8
Wall OWST	28.3 C	EXP0,9
Wall OWSM	21.7 C	EXP0,10
Wall OWET	24.9 C	EXP0,11

Left Rod	Average Temperature	Channel
364mm	30.2 C	EXP1,0
303mm	27.9 C	EXP1,1
258mm	25.9 C	EXP1,2
167mm	23.7 C	EXP1,3
129mm	23.2 C	EXP1,4
91mm	23.1 C	EXP1,5
45mm	23.2 C	EXP1,6
15mm	23.4 C	EXP1,7

Right rod	Average Temperature	Channel
364mm	30.5 C	EXP1,15
303mm	28.0 C	EXP1,14
258mm	26.3 C	EXP1,13
167mm	23.8 C	EXP1,12
129mm	23.3 C	EXP1,11
91mm	23.0 C	EXP1,10
45mm	22.3 C	EXP1,9
15mm	22.4 C	EXP1,8

Average T over height in model

Height	T (C)
36.5 cm	30.4 C
30.3 cm	27.9 C
25.8 cm	26.1 C
16.7 cm	23.7 C
12.9 cm	23.3 C
9.1 cm	23.0 C
4.5 cm	22.8 C
1.5 cm	22.9 C

Scaling Correction		
TEMPERATURE SCALE	>>>>>>	0.26
POWER SCALE	>>>>>>	3.65
VOLUMETRIC FLOWRATE SCALE	>>>>>>	54.62
MASS FLOWRATE SCALE	>>>>>>	10.18
VELOCITY SCALE	>>>>>>	1.26

EXPERIMENT # **7**

Results for air operation

Case	**20 W/m^2**
Cooling Load	639 W
Heat Sources	P1,P3,S1,S3,X2,L
Flow at fans on floor	**16% of total flowrate**
Supply air flow rate	596 cfm 0.28 m^3/s
Velocity at diffusers	0.19 m/s

Average Temperature Field Summary	
T supply	18.9 C
T exhaust	20.8 C
T (0.1m)	19.7 C
T (1.1m)	20.1 C
T(1.7m)	20.8 C
delta T (0.1m-1.1m)	0.4 C
delta T (0.1m-1.7m)	1.1 C

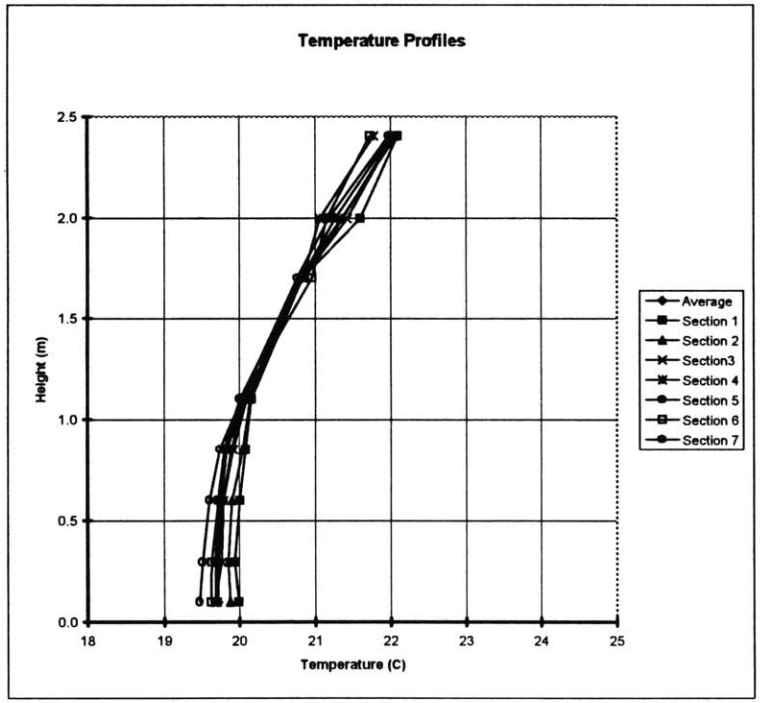

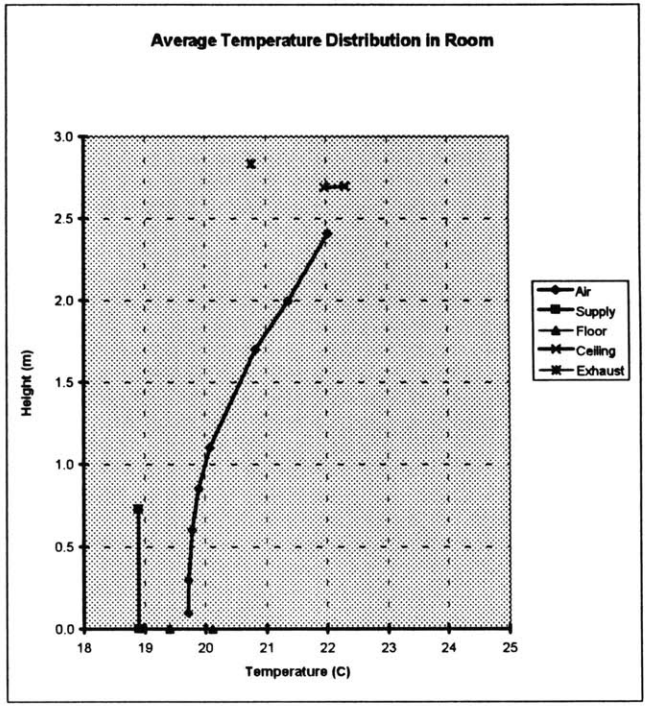

EXPERIMENT # 7

Temps40H.dat

System Data

Considered Case for pure R114	30 W/m2
Actual Case studied	20 W/m2
Oxygen Concentration	3.0%
Air Concentration	14%

Fans	5.11 V
	0.58 cfm each
	1.74 cfm total
	16% of total flowrate

Heat Sources	P1,P3,S1,S3,X2,L
Heat Dissipated	175 W

Monometer Reads	0.1 "wg
Gas Flowrate	10.9 cfm
Velocity at diffuser	0.15 m/s
Water Flowrate	0.60 gpm

Temperature Readings (Average of average readings (x1000) for 7 cases)

T gas in	18.6 C	EXP0,14
T gas out	25.7 C	EXP0,13
T water in	14.5 C	EXP0,12
T water out	17.6 C	EXP0,15

Side wall W1	21.0 C	EXP0,0
Side wall W2	22.8 C	EXP0,1
End wall W3	25.2 C	EXP0,2
Diffuser D1	20.7 C	EXP0,3
Diffuser D2	20.3 C	EXP0,4
Floor F1	20.5 C	EXP0,5
Floor F2	23.3 C	EXP0,6
Ceiling C1	31.7 C	EXP0,7
Ceiling C2	30.4 C	EXP0,8
Wall OWST	28.2 C	EXP0,9
Wall OWSM	21.7 C	EXP0,10
Wall OWET	24.9 C	EXP0,11

Left Rod	Average Temperature	Channel
364mm	30.4 C	EXP1,0
303mm	28.1 C	EXP1,1
258mm	25.8 C	EXP1,2
167mm	23.1 C	EXP1,3
129mm	22.4 C	EXP1,4
91mm	22.0 C	EXP1,5
45mm	22.0 C	EXP1,6
15mm	22.2 C	EXP1,7

Right rod	Average Temperature	Channel
364mm	30.8 C	EXP1,15
303mm	28.0 C	EXP1,14
258mm	26.2 C	EXP1,13
167mm	23.1 C	EXP1,12
129mm	22.4 C	EXP1,11
91mm	22.0 C	EXP1,10
45mm	21.5 C	EXP1,9
15mm	21.3 C	EXP1,8

Average T over height in model

Height	T (C)
36.5 cm	30.6 C
30.3 cm	28.1 C
25.8 cm	26.0 C
16.7 cm	23.1 C
12.9 cm	22.4 C
9.1 cm	22.0 C
4.5 cm	21.8 C
1.5 cm	21.7 C

Scaling Correction

TEMPERATURE SCALE	>>>>>>	0.26
POWER SCALE	>>>>>>	3.65
VOLUMETRIC FLOWRATE SCALE	>>>>>>	54.62
MASS FLOWRATE SCALE	>>>>>>	10.18
VELOCITY SCALE	>>>>>>	1.26

EXPERIMENT # **8**

Results for air operation

Case	**27 W/m^2**
Cooling Load	860 W
Heat Sources	P1,P2,P3,S1,S2,S3,X1,X2,X3,L
Flow at fans on floor	**0% of total flowrate**
Supply air flow rate	626 cfm 0.30 m^3/s
Velocity at diffusers	0.20 m/s

Average Temperature Field Summary	
T supply	18.9 C
T exhaust	20.8 C
T (0.1m)	19.7 C
T (1.1m)	20.6 C
T(1.7m)	22.0 C
delta T (0.1m-1.1m)	0.9 C
delta T (0.1m-1.7m)	2.3 C

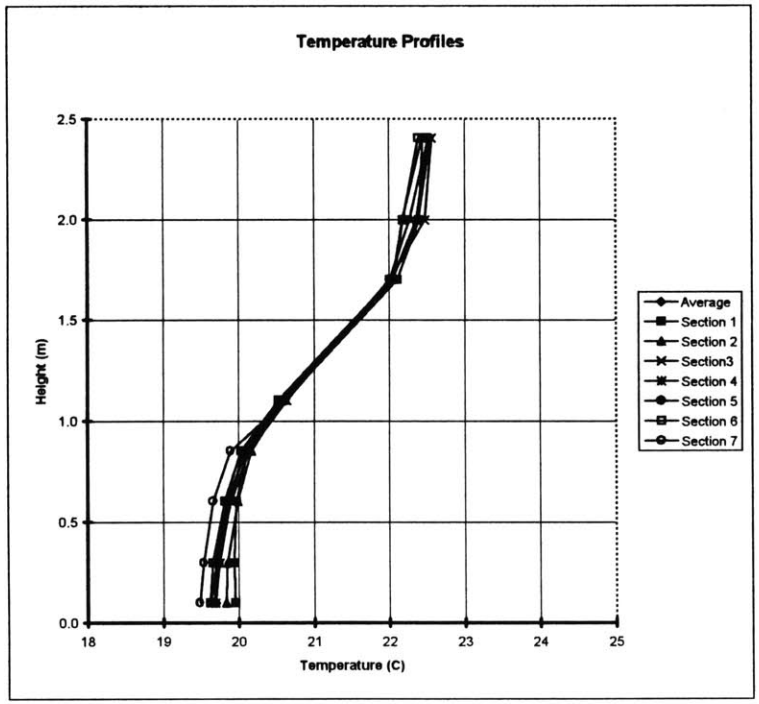

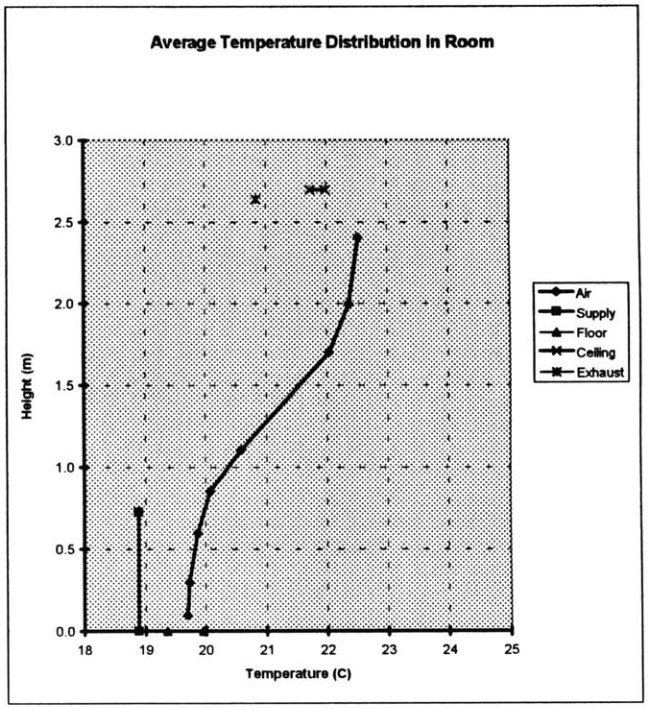

EXPERIMENT # 8

Temps40i.dat

System Data

Considered Case for pure R114	40 W/m2
Actual Case studied	27 W/m2
Oxygen Concentration	2.9%
Air Concentration	14%

Heat Sources	P1,P2,P3,S1,S2,S3,X1,X2,X3,L
Heat Dissipated	234 W

Monometer Reads	0.11 "wg
Gas Flowrate	11.4 cfm
Velocity at diffuser	0.16 m/s
Water Flowrate	0.60 gpm

Fans	0 V
	0 cfm each
	0 cfm total
	0% of total flowrate

Temperature Readings (Average of average readings (x1000) for 7 cases)

T gas in	18.6 C	EXP0,14
T gas out	26.0 C	EXP0,13
T water in	14.5 C	EXP0,12
T water out	17.5 C	EXP0,15

Side wall W1	21.2 C	EXP0,0
Side wall W2	25.4 C	EXP0,1
End wall W3	26.9 C	EXP0,2
Diffuser D1	21.2 C	EXP0,3
Diffuser D2	20.4 C	EXP0,4
Floor F1	20.4 C	EXP0,5
Floor F2	22.6 C	EXP0,6
Ceiling C1	30.3 C	EXP0,7
Ceiling C2	29.4 C	EXP0,8
Wall OWST	29.6 C	EXP0,9
Wall OWSM	21.7 C	EXP0,10
Wall OWET	25.0 C	EXP0,11

Left Rod	Average Temperature	Channel
364mm	32.6 C	EXP1,0
303mm	31.8 C	EXP1,1
258mm	30.3 C	EXP1,2
167mm	25.1 C	EXP1,3
129mm	23.1 C	EXP1,4
91mm	22.1 C	EXP1,5
45mm	21.9 C	EXP1,6
15mm	22.0 C	EXP1,7

Right rod	Average Temperature	Channel
364mm	32.2 C	EXP1,15
303mm	31.7 C	EXP1,14
258mm	30.8 C	EXP1,13
167mm	24.9 C	EXP1,12
129mm	23.1 C	EXP1,11
91mm	22.5 C	EXP1,10
45mm	21.7 C	EXP1,9
15mm	21.3 C	EXP1,8

Average T over height in model

Height	T (C)
36.5 cm	32.4 C
30.3 cm	31.8 C
25.8 cm	30.6 C
16.7 cm	25.0 C
12.9 cm	23.1 C
9.1 cm	22.3 C
4.5 cm	21.8 C
1.5 cm	21.7 C

Scaling Correction		
TEMPERATURE SCALE	>>>>>>	0.26
POWER SCALE	>>>>>>	3.68
VOLUMETRIC FLOWRATE SCALE	>>>>>>	54.78
MASS FLOWRATE SCALE	>>>>>>	10.18
VELOCITY SCALE	>>>>>>	1.26

EXPERIMENT # **9**

Results for air operation

Case	**27 W/m^2**
Cooling Load	860 W
Heat Sources	P1,P2,P3,S1,S2,S3,X1,X2,X3,L
Flow at fans on floor	**50% of total flowrate**
Supply air flow rate	626 cfm 0.30 m^3/s
Velocity at diffusers	0.20 m/s

Average Temperature Field Summary	
T supply	18.9 C
T exhaust	20.9 C
T (0.1m)	20.2 C
T (1.1m)	20.8 C
T(1.7m)	22.0 C
delta T (0.1m-1.1m)	0.6 C
delta T (0.1m-1.7m)	1.8 C

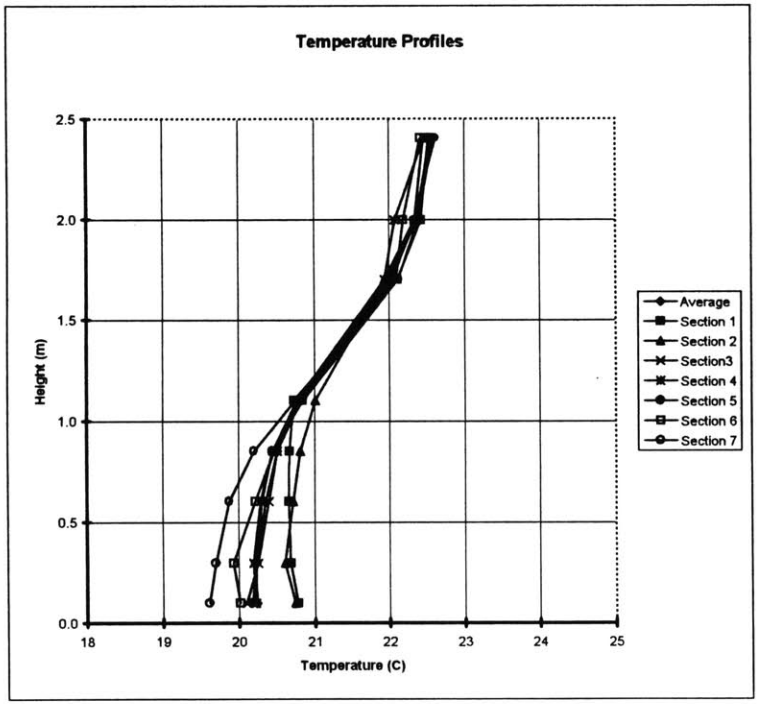

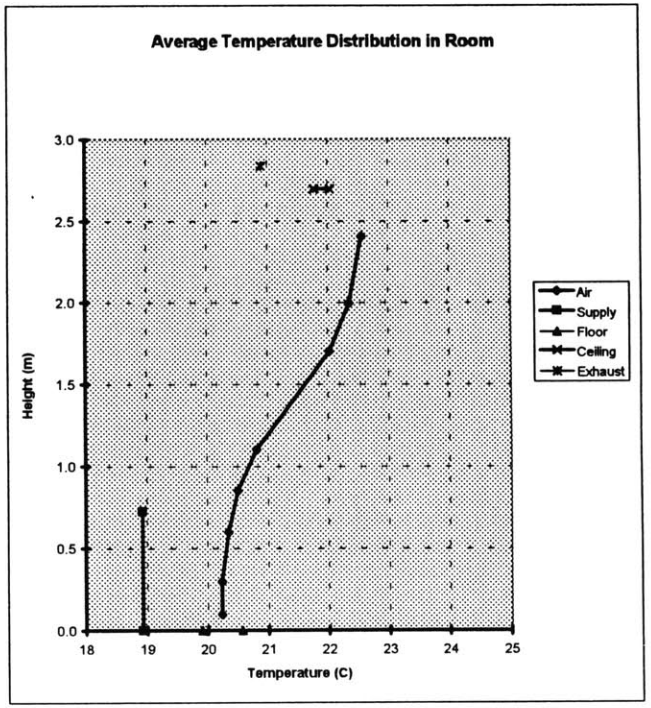

EXPERIMENT # 9

Temps40J.dat

System Data

Considered Case for pure R114	40 W/m2
Actual Case studied	**27 W/m2**
Oxygen Concentration	**2.9%**
Air Concentration	**14%**

Fans	11 V
	1.9 cfm each
	5.7 cfm total
	50% of total flowrate

Heat Sources	P1,P2,P3,S1,S2,S3,X1,X2,X3,L
Heat Dissipated	234 W

Monometer Reads	0.11 "wg
Gas Flowrate	11.4 cfm
Velocity at diffuser	0.16 m/s
Water Flowrate	0.60 gpm

Temperature Readings (Average of average readings (x500) for 7 cases)

T gas in	18.7 C	EXP0,14
T gas out	26.3 C	EXP0,13
T water in	14.6 C	EXP0,12
T water out	17.6 C	EXP0,15

Side wall W1	22.0 C	EXP0,0
Side wall W2	25.7 C	EXP0,1
End wall W3	27.3 C	EXP0,2
Diffuser D1	21.5 C	EXP0,3
Diffuser D2	21.2 C	EXP0,4
Floor F1	22.4 C	EXP0,5
Floor F2	25.0 C	EXP0,6
Ceiling C1	30.6 C	EXP0,7
Ceiling C2	29.5 C	EXP0,8
Wall OWST	30.2 C	EXP0,9
Wall OWSM	21.8 C	EXP0,10
Wall OWET	25.6 C	EXP0,11

Left Rod	Average Temperature	Channel
364mm	32.6 C	EXP1,0
303mm	31.8 C	EXP1,1
258mm	30.2 C	EXP1,2
167mm	25.8 C	EXP1,3
129mm	24.5 C	EXP1,4
91mm	23.9 C	EXP1,5
45mm	24.0 C	EXP1,6
15mm	24.1 C	EXP1,7

Right rod	Average Temperature	Channel
364mm	32.4 C	EXP1,15
303mm	31.6 C	EXP1,14
258mm	30.8 C	EXP1,13
167mm	26.1 C	EXP1,12
129mm	25.0 C	EXP1,11
91mm	24.4 C	EXP1,10
45mm	23.4 C	EXP1,9
15mm	23.2 C	EXP1,8

Average T over height in model

Height	T (C)
36.5 cm	32.5 C
30.3 cm	31.7 C
25.8 cm	30.5 C
16.7 cm	25.9 C
12.9 cm	24.7 C
9.1 cm	24.1 C
4.5 cm	23.7 C
1.5 cm	23.7 C

Scaling Correction		
TEMPERATURE SCALE	>>>>>>	0.26
POWER SCALE	>>>>>>	3.68
VOLUMETRIC FLOWRATE SCALE	>>>>>>	54.78
MASS FLOWRATE SCALE	>>>>>>	10.18
VELOCITY SCALE	>>>>>>	1.26

EXPERIMENT # **10**

Results for air operation

Case	**27 W/m^2**
Cooling Load	860 W
Heat Sources	P1,P2,P3,S1,S2,S3,X1,X2,X3,L
Flow at fans on floor	**15% of total flowrate**
Supply air flow rate	626 cfm 0.30 m^3/s
Velocity at diffusers	0.20 m/s

Average Temperature Field Summary	
T supply	18.9 C
T exhaust	20.9 C
T (0.1m)	19.9 C
T (1.1m)	20.7 C
T(1.7m)	22.2 C
delta T (0.1m-1.1m)	0.9 C
delta T (0.1m-1.7m)	2.3 C

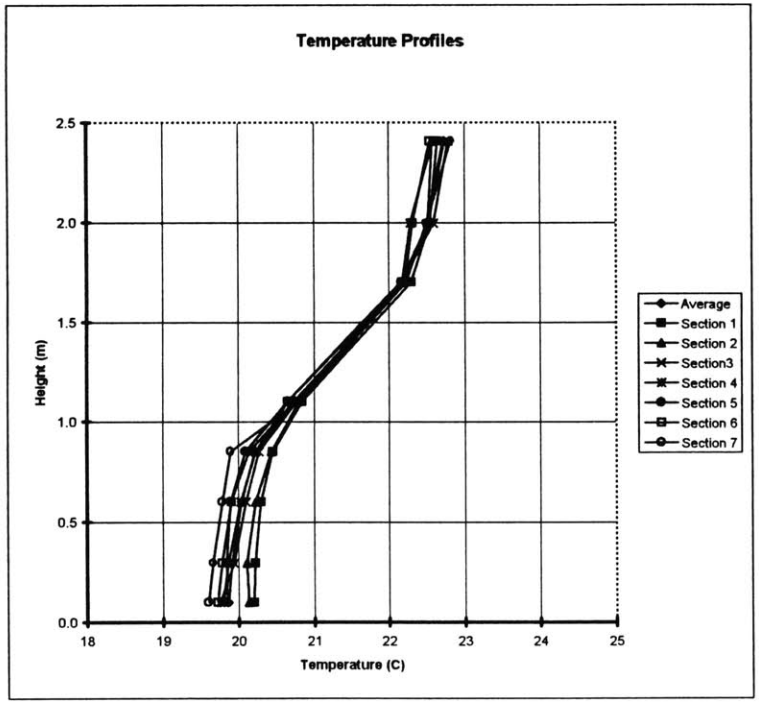

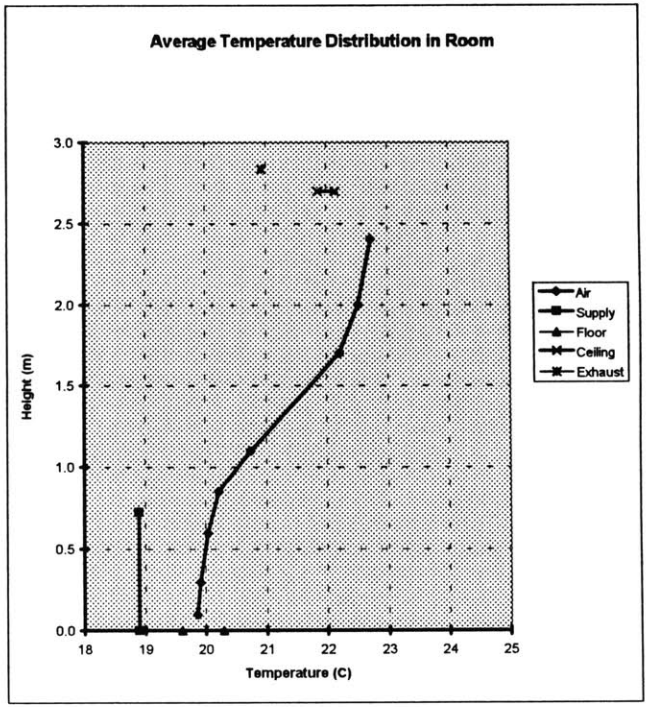

EXPERIMENT # 10

Temps40K.dat

System Data

Considered Case for pure R114	40 W/m2
Actual Case studied	**27 W/m2**
Oxygen Concentration	**2.9%**
Air Concentration	**14%**

Fans	5.2 V
	0.59 cfm each
	1.77 cfm total
	15% of total flowrate

Heat Sources	P1,P2,P3,S1,S2,S3,X1,X2,X3,L
Heat Dissipated	234 W

Monometer Reads	0.11 "wg
Gas Flowrate	11.4 cfm
Velocity at diffuser	0.16 m/s
Water Flowrate	0.60 gpm

Temperature Readings (Average of average readings (x500) for 7 cases)

T gas in	18.6 C	EXP0,14
T gas out	26.4 C	EXP0,13
T water in	14.4 C	EXP0,12
T water out	17.5 C	EXP0,15

Side wall W1	21.4 C	EXP0,0
Side wall W2	25.8 C	EXP0,1
End wall W3	27.6 C	EXP0,2
Diffuser D1	21.5 C	EXP0,3
Diffuser D2	20.8 C	EXP0,4
Floor F1	21.3 C	EXP0,5
Floor F2	23.9 C	EXP0,6
Ceiling C1	30.9 C	EXP0,7
Ceiling C2	29.8 C	EXP0,8
Wall OWST	30.6 C	EXP0,9
Wall OWSM	21.7 C	EXP0,10
Wall OWET	25.8 C	EXP0,11

Left Rod	Average Temperature	Channel
364mm	33.3 C	EXP1,0
303mm	32.4 C	EXP1,1
258mm	30.9 C	EXP1,2
167mm	25.5 C	EXP1,3
129mm	23.4 C	EXP1,4
91mm	22.8 C	EXP1,5
45mm	22.6 C	EXP1,6
15mm	22.6 C	EXP1,7

Right rod	Average Temperature	Channel
364mm	32.9 C	EXP1,15
303mm	32.2 C	EXP1,14
258mm	31.4 C	EXP1,13
167mm	25.8 C	EXP1,12
129mm	23.8 C	EXP1,11
91mm	23.1 C	EXP1,10
45mm	22.3 C	EXP1,9
15mm	21.9 C	EXP1,8

Average T over height in model

Height	T (C)
36.5 cm	33.1 C
30.3 cm	32.3 C
25.8 cm	31.2 C
16.7 cm	25.6 C
12.9 cm	23.6 C
9.1 cm	22.9 C
4.5 cm	22.5 C
1.5 cm	22.3 C

Scaling Correction		
TEMPERATURE SCALE	>>>>>>	0.26
POWER SCALE	>>>>>>	3.68
VOLUMETRIC FLOWRATE SCALE	>>>>>>	54.78
MASS FLOWRATE SCALE	>>>>>>	10.18
VELOCITY SCALE	>>>>>>	1.26

EXPERIMENT # 11

Results for air operation

Case	**38 W/m^2**
Cooling Load	1223 W
Heat Sources	P1,P2,P3,S1,S2,S3,T1,T2,T3,X1,X2,X3,L
Flow at fans on floor	**0% of total flowrate**
Supply air flow rate	615 cfm 0.29 m^3/s
Velocity at diffusers	0.20 m/s

Average Temperature Field Summary	
T supply	19.1 C
T exhaust	21.4 C
T (0.1m)	20.1 C
T (1.1m)	22.0 C
T(1.7m)	23.1 C
delta T (0.1m-1.1m)	1.8 C
delta T (0.1m-1.7m)	3.0 C

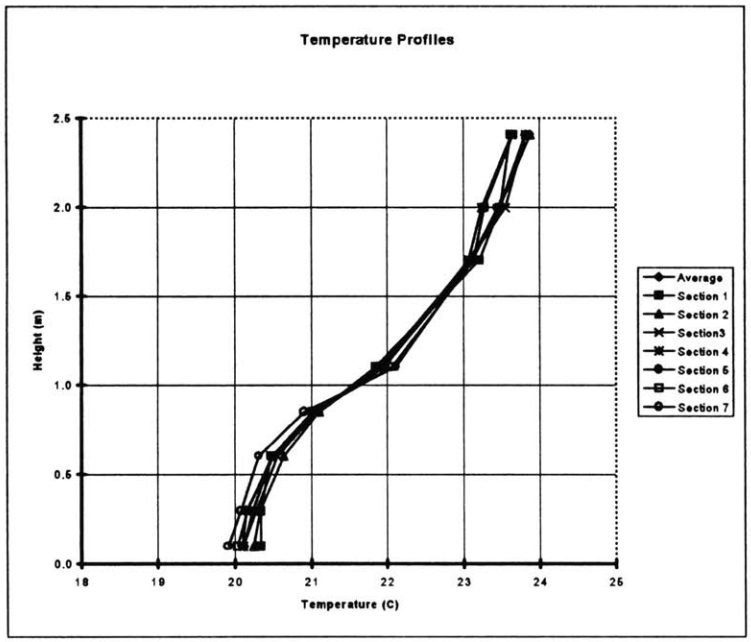

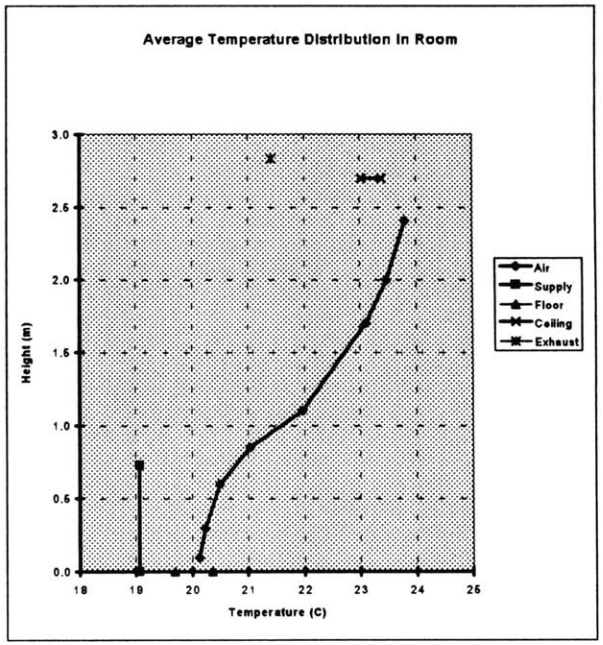

EXPERIMENT # 11

Temps40L.dat

System Data

Considered Case for pure R114	60 W/m2
Actual Case studied	**38 W/m2**
Oxygen Concentration	**3.4%**
Air Concentration	**16%**

Fans	0 V
	0 cfm each
	0 cfm total
	0% of total flowrate

Heat Sources	P1,P2,P3,S1,S2,S3,T1,T2,T3,X1,X2,X3,L
Heat Dissipated	355 W

Monometer Reads	0.11 "wg
Gas Flowrate	11.5 cfm
Velocity at diffuser	0.16 m/s
Water Flowrate	0.60 gpm

Temperature Readings (Average of average readings (x500) for 7 cases)

T gas in	19.3 C	EXP0,14
T gas out	28.7 C	EXP0,13
T water in	14.3 C	EXP0,12
T water out	17.5 C	EXP0,15

Side wall W1	23.7 C	EXP0,0
Side wall W2	28.7 C	EXP0,1
End wall W3	31.3 C	EXP0,2
Diffuser D1	22.9 C	EXP0,3
Diffuser D2	22.4 C	EXP0,4
Floor F1	21.8 C	EXP0,5
Floor F2	24.5 C	EXP0,6
Ceiling C1	36.7 C	EXP0,7
Ceiling C2	35.2 C	EXP0,8
Wall OWST	33.6 C	EXP0,9
Wall OWSM	21.8 C	EXP0,10
Wall OWET	27.4 C	EXP0,11

Left Rod	Average Temperature	Channel
364mm	38.3 C	EXP1,0
303mm	37.0 C	EXP1,1
258mm	35.3 C	EXP1,2
167mm	31.0 C	EXP1,3
129mm	26.9 C	EXP1,4
91mm	24.6 C	EXP1,5
45mm	24.0 C	EXP1,6
15mm	24.0 C	EXP1,7

Right rod	Average Temperature	Channel
364mm	38.4 C	EXP1,15
303mm	36.9 C	EXP1,14
258mm	35.7 C	EXP1,13
167mm	30.8 C	EXP1,12
129mm	27.5 C	EXP1,11
91mm	25.4 C	EXP1,10
45mm	23.8 C	EXP1,9
15mm	23.0 C	EXP1,8

Average T over height in model

Height	T (C)
36.5 cm	38.3 C
30.3 cm	37.0 C
25.8 cm	35.5 C
16.7 cm	30.9 C
12.9 cm	27.2 C
9.1 cm	25.0 C
4.5 cm	23.9 C
1.5 cm	23.5 C

Scaling Correction		
TEMPERATURE SCALE	>>>>>>	0.25
POWER SCALE	>>>>>>	3.44
VOLUMETRIC FLOWRATE SCALE	>>>>>>	53.31
MASS FLOWRATE SCALE	>>>>>>	10.12
VELOCITY SCALE	>>>>>>	1.23

EXPERIMENT # 12

Results for air operation

Case	**38 W/m^2**
Cooling Load	1223 W
Heat Sources	P1,P2,P3,S1,S2,S3,T1,T2,T3,X1,X2,X3,L
Flow at fans on floor	**58% of total flowrate**
Supply air flow rate	615 cfm 0.29 m^3/s
Velocity at diffusers	0.20 m/s

Average Temperature Field Summary	
T supply	19.1 C
T exhaust	21.6 C
T (0.1m)	21.0 C
T (1.1m)	22.1 C
T(1.7m)	23.2 C
delta T (0.1m-1.1m)	1.1 C
delta T (0.1m-1.7m)	2.2 C

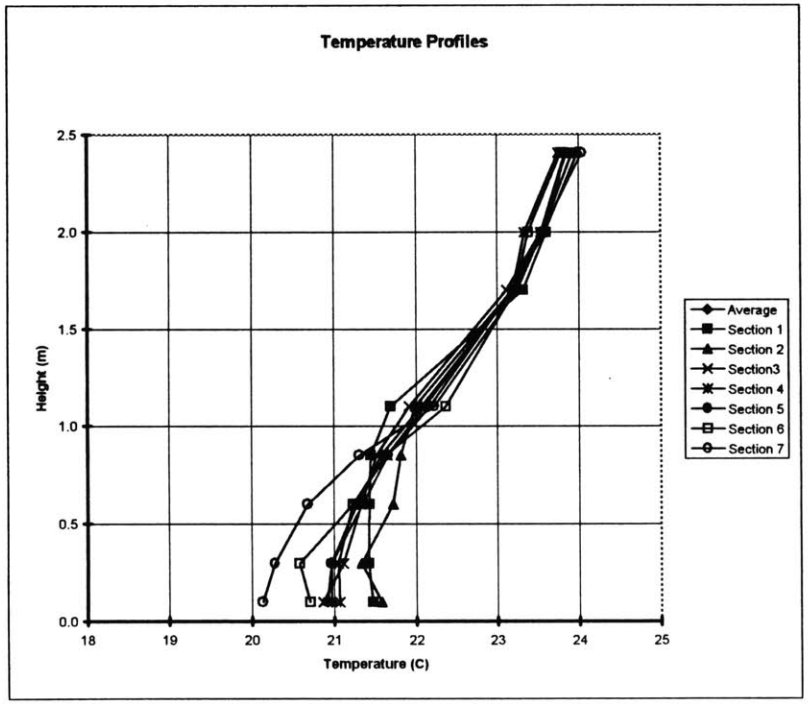

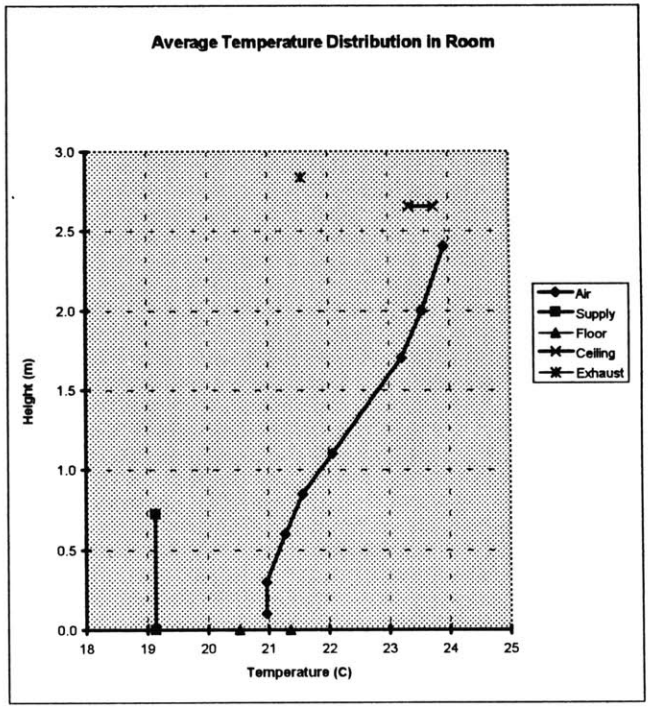

EXPERIMENT # 12

Temps40M.dat

System Data

Considered Case for pure R114	60 W/m2
Actual Case studied	**38 W/m2**
Oxygen Concentration	**3.4%**
Air Concentration	**16%**

Fans	12 V
	2.22 cfm each
	6.66 cfm total
	58% of total flowrate

Heat Sources	P1,P2,P3,S1,S2,S3,T1,T2,T3,X1,X2,X3,L
Heat Dissipated	355 W

Monometer Reads	0.11 "wg
Gas Flowrate	11.5 cfm
Velocity at diffuser	0.16 m/s
Water Flowrate	0.60 gpm

Temperature Readings (Average of average readings (x250) for 7 cases)

T gas in	19.5 C	EXP0,14
T gas out	29.3 C	EXP0,13
T water in	14.3 C	EXP0,12
T water out	17.5 C	EXP0,15

Side wall W1	24.3 C	EXP0,0
Side wall W2	29.2 C	EXP0,1
End wall W3	32.1 C	EXP0,2
Diffuser D1	23.4 C	EXP0,3
Diffuser D2	23.6 C	EXP0,4
Floor F1	25.1 C	EXP0,5
Floor F2	28.5 C	EXP0,6
Ceiling C1	38.1 C	EXP0,7
Ceiling C2	36.5 C	EXP0,8
Wall OWST	34.4 C	EXP0,9
Wall OWSM	21.8 C	EXP0,10
Wall OWET	28.5 C	EXP0,11

Left Rod	Average Temperature	Channel
364mm	38.7 C	EXP1,0
303mm	37.4 C	EXP1,1
258mm	35.9 C	EXP1,2
167mm	30.8 C	EXP1,3
129mm	28.6 C	EXP1,4
91mm	27.6 C	EXP1,5
45mm	27.5 C	EXP1,6
15mm	27.8 C	EXP1,7

Right rod	Average Temperature	Channel
364mm	38.9 C	EXP1,15
303mm	37.2 C	EXP1,14
258mm	35.9 C	EXP1,13
167mm	31.8 C	EXP1,12
129mm	30.1 C	EXP1,11
91mm	28.8 C	EXP1,10
45mm	26.3 C	EXP1,9
15mm	26.0 C	EXP1,8

Average T over height in model

Height	T (C)
36.5 cm	38.8 C
30.3 cm	37.3 C
25.8 cm	35.9 C
16.7 cm	31.3 C
12.9 cm	29.3 C
9.1 cm	28.2 C
4.5 cm	26.9 C
1.5 cm	26.9 C

Scaling Correction		
TEMPERATURE SCALE	>>>>>>	0.25
POWER SCALE	>>>>>>	3.44
VOLUMETRIC FLOWRATE SCALE	>>>>>>	53.31
MASS FLOWRATE SCALE	>>>>>>	10.12
VELOCITY SCALE	>>>>>>	1.23

EXPERIMENT # 13

Results for air operation

Case	**38 W/m^2**
Cooling Load	1223 W
Heat Sources	P1,P2,P3,S1,S2,S3,T1,T2,T3,X1,X2,X3,L
Flow at fans on floor	**22% of total flowrate**
Supply air flow rate	615 cfm 0.29 m^3/s
Velocity at diffusers	0.20 m/s

Average Temperature Field Summary	
T supply	19.1 C
T exhaust	21.7 C
T (0.1m)	20.6 C
T (1.1m)	22.3 C
T(1.7m)	23.4 C
delta T (0.1m-1.1m)	1.7 C
delta T (0.1m-1.7m)	2.8 C

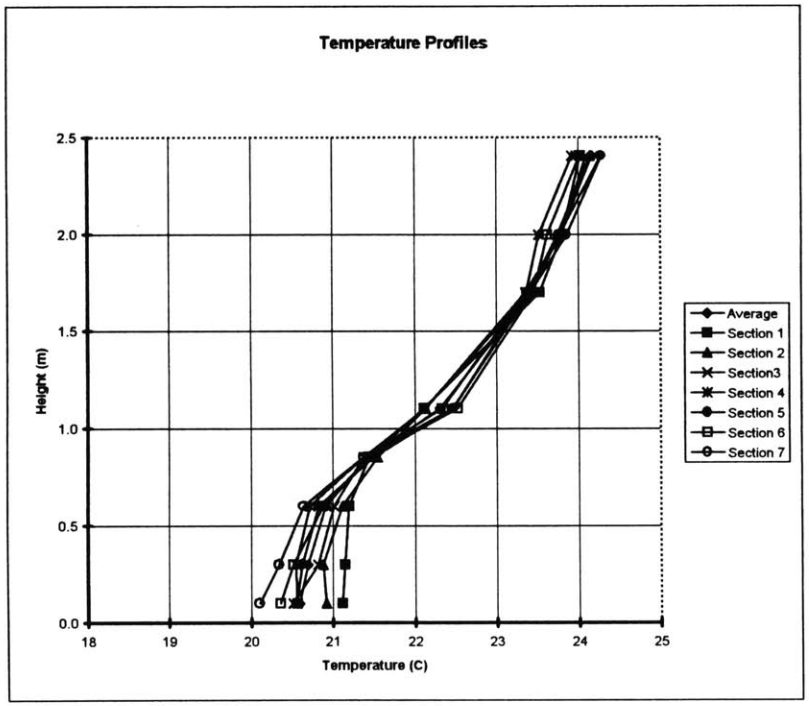

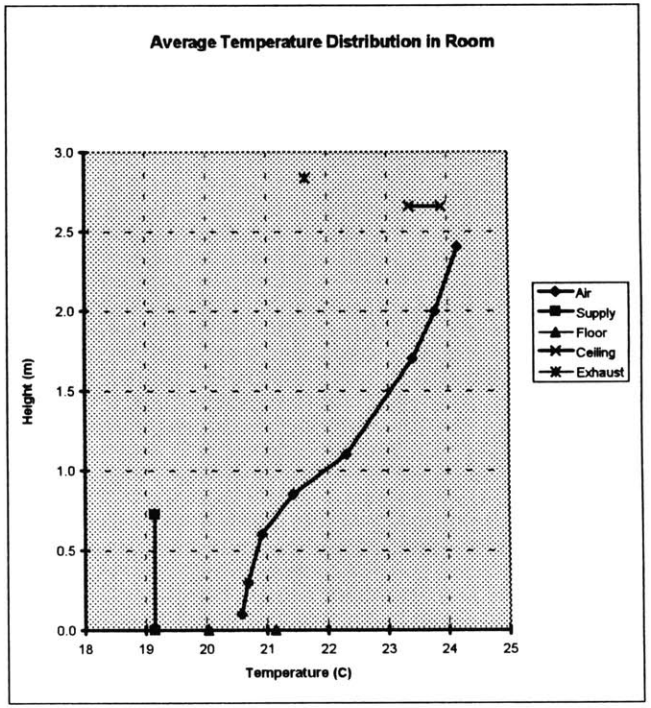

EXPERIMENT # 13

Temps40N.dat

System Data

Considered Case for pure R114	60 W/m2
Actual Case studied	**38 W/m2**
Oxygen Concentration	**3.4%**
Air Concentration	**16%**

Fans	6.1 V
	0.85 cfm each
	2.55 cfm total
	22% of total flowrate

Heat Sources	P1,P2,P3,S1,S2,S3,T1,T2,T3,X1,X2,X3,L
Heat Dissipated	355 W

Monometer Reads	0.11 "wg
Gas Flowrate	11.5 cfm
Velocity at diffuser	0.16 m/s
Water Flowrate	0.60 gpm

Temperature Readings (Average of average readings (x250) for 7 cases)

T gas in	19.6 C	EXP0,14
T gas out	29.7 C	EXP0,13
T water in	14.2 C	EXP0,12
T water out	17.5 C	EXP0,15

Side wall W1	24.8 C	EXP0,0
Side wall W2	29.6 C	EXP0,1
End wall W3	32.9 C	EXP0,2
Diffuser D1	23.7 C	EXP0,3
Diffuser D2	23.3 C	EXP0,4
Floor F1	23.1 C	EXP0,5
Floor F2	27.6 C	EXP0,6
Ceiling C1	38.7 C	EXP0,7
Ceiling C2	36.6 C	EXP0,8
Wall OWST	35.2 C	EXP0,9
Wall OWSM	21.7 C	EXP0,10
Wall OWET	29.0 C	EXP0,11

Left Rod	Average Temperature	Channel
364mm	39.8 C	EXP1,0
303mm	38.3 C	EXP1,1
258mm	36.6 C	EXP1,2
167mm	32.1 C	EXP1,3
129mm	28.2 C	EXP1,4
91mm	26.2 C	EXP1,5
45mm	26.1 C	EXP1,6
15mm	26.0 C	EXP1,7

Right rod	Average Temperature	Channel
364mm	39.8 C	EXP1,15
303mm	38.1 C	EXP1,14
258mm	36.9 C	EXP1,13
167mm	32.5 C	EXP1,12
129mm	29.4 C	EXP1,11
91mm	27.1 C	EXP1,10
45mm	25.6 C	EXP1,9
15mm	24.7 C	EXP1,8

Average T over height in model

Height	T (C)
36.5 cm	39.8 C
30.3 cm	38.2 C
25.8 cm	36.8 C
16.7 cm	32.3 C
12.9 cm	28.8 C
9.1 cm	26.7 C
4.5 cm	25.8 C
1.5 cm	25.4 C

Scaling Correction		
TEMPERATURE SCALE	>>>>>>	0.25
POWER SCALE	>>>>>>	3.44
VOLUMETRIC FLOWRATE SCALE	>>>>>>	53.31
MASS FLOWRATE SCALE	>>>>>>	10.12
VELOCITY SCALE	>>>>>>	1.23

EXPERIMENT # 14

Results for air operation

Case	**10 W/m^2**
Cooling Load	314 W
Heat Sources	P1,P2,S2,L
Flow at fans on floor	**0% of total flowrate**
Supply air flow rate	388 cfm 0.18 m^3/s
Velocity at diffusers	0.13 m/s

Average Temperature Field Summary	
T supply	19.4 C
T exhaust	20.1 C
T (0.1m)	19.6 C
T (1.1m)	19.8 C
T(1.7m)	20.3 C
delta T (0.1m-1.1m)	0.2 C
delta T (0.1m-1.7m)	0.6 C

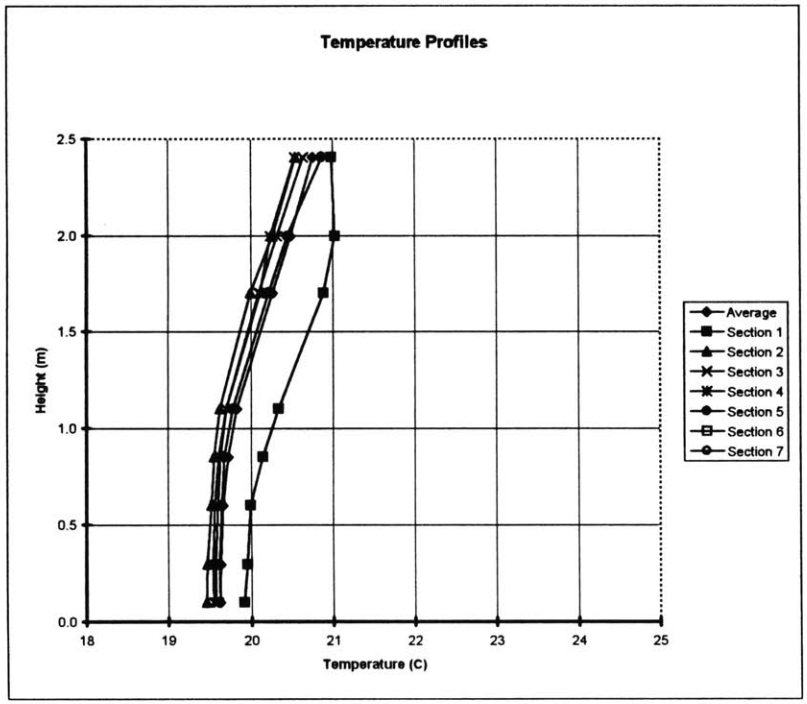

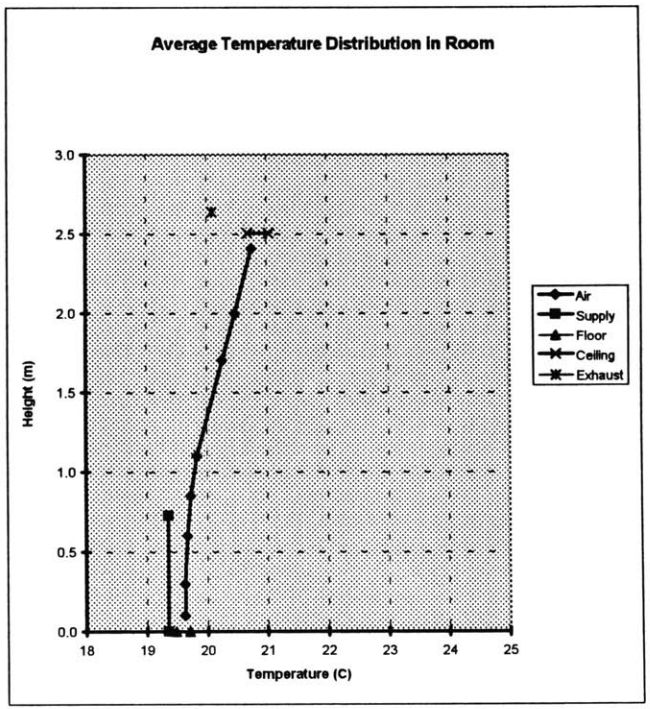

EXPERIMENT # 14

Temps20A.dat

System Data

Considered Case for pure R114	20 W/m2
Actual Case studied	10 W/m2
Oxygen Concentration	5.0%
Air Concentration	24%

Fans	0 V
	0 cfm each
	0 cfm total
	0% of total flowrate

Heat Sources	P1,P2,S2,L
Heat Dissipated	117 W

Monometer Reads	0.05 "wg
Gas Flowrate	8.1 cfm
Velocity at diffuser	0.11 m/s
Water Flowrate	0.11 gpm

Temperature Readings (Average of average readings (x250) for 5 cases)

T gas in	20.8 C	EXP0,14
T gas out	24.5 C	EXP0,13
T water in	15.5 C	EXP0,12
T water out	20.6 C	EXP0,15

Side wall W1	21.6 C	EXP0,0
Side wall W2	22.9 C	EXP0,1
End wall W3	24.2 C	EXP0,2
Diffuser D1	21.8 C	EXP0,3
Diffuser D2	20.9 C	EXP0,4
Floor F1	21.4 C	EXP0,5
Floor F2	22.5 C	EXP0,6
Ceiling C1	29.2 C	EXP0,7
Ceiling C2	27.5 C	EXP0,8
Wall OWST	26.4 C	EXP0,9
Wall OWSM	21.3 C	EXP0,10
Wall OWET	24.0 C	EXP0,11

Left Rod	Average Temperature	Channel
364mm	27.6 C	EXP1,0
303mm	26.1 C	EXP1,1
258mm	25.2 C	EXP1,2
167mm	23.3 C	EXP1,3
129mm	22.8 C	EXP1,4
91mm	22.6 C	EXP1,5
45mm	22.7 C	EXP1,6
15mm	22.9 C	EXP1,7

Right rod	Average Temperature	Channel
364mm	28.0 C	EXP1,15
303mm	26.7 C	EXP1,14
258mm	25.4 C	EXP1,13
167mm	23.0 C	EXP1,12
129mm	22.4 C	EXP1,11
91mm	22.1 C	EXP1,10
45mm	21.6 C	EXP1,9
15mm	21.3 C	EXP1,8

Average T over height in model

Height	T (C)
36.5 cm	27.8 C
30.3 cm	26.4 C
25.8 cm	25.3 C
16.7 cm	23.1 C
12.9 cm	22.6 C
9.1 cm	22.3 C
4.5 cm	22.2 C
1.5 cm	22.1 C

Scaling Correction		
TEMPERATURE SCALE	>>>>>>	0.20
POWER SCALE	>>>>>>	2.68
VOLUMETRIC FLOWRATE SCALE	>>>>>>	47.95
MASS FLOWRATE SCALE	>>>>>>	9.85
VELOCITY SCALE	>>>>>>	1.10

EXPERIMENT # 15

Results for air operation

Case	**10 W/m^2**
Cooling Load	314 W
Heat Sources	P1,P2,S2,L
Flow at fans on floor	**22% of total flowrate**
Supply air flow rate	388 cfm 0.18 m^3/s
Velocity at diffusers	0.13 m/s

Average Temperature Field Summary	
T supply	19.3 C
T exhaust	20.5 C
T (0.1m)	19.7 C
T (1.1m)	19.9 C
T(1.7m)	20.2 C
delta T (0.1m-1.1m)	0.1 C
delta T (0.1m-1.7m)	0.5 C

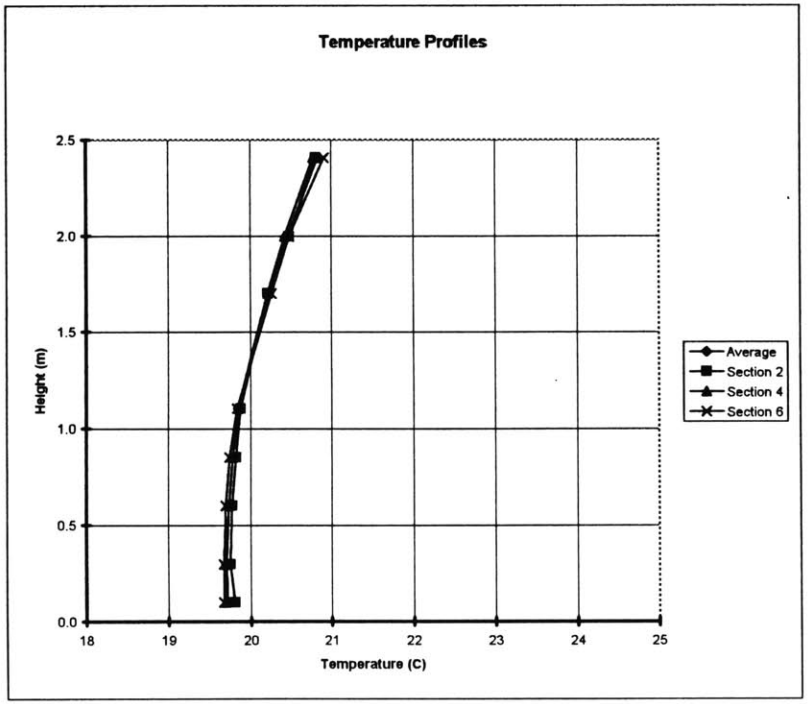

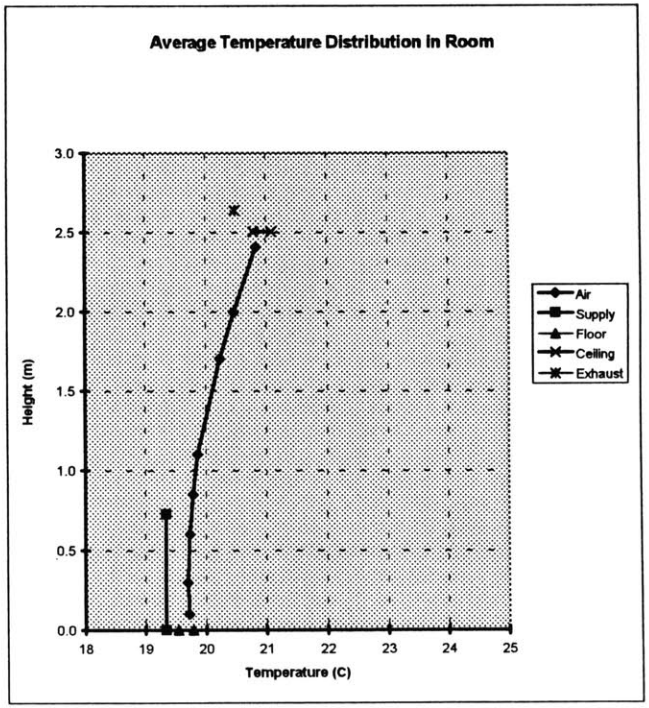

EXPERIMENT # 15

Temps20B.dat

System Data

Considered Case for pure R114	20 W/m2
Actual Case studied	**10 W/m2**
Oxygen Concentration	**5.0%**
Air Concentration	**24%**

Fans	5.02 V
	0.6 cfm each
	1.8 cfm total
	22% of total flowrate

Heat Sources	P1,P2,S2,L
Heat Dissipated	117 W

Monometer Reads	0.05 "wg
Gas Flowrate	8.1 cfm
Velocity at diffuser	0.11 m/s
Water Flowrate	0.11 gpm

Temperature Readings (Average of average readings (x250) for 3 cases)

T gas in	20.7 C	EXP0,14
T gas out	26.5 C	EXP0,13
T water in	16.0 C	EXP0,12
T water out	21.3 C	EXP0,15

Side wall W1	21.8 C	EXP0,0
Side wall W2	23.0 C	EXP0,1
End wall W3	24.5 C	EXP0,2
Diffuser D1	21.9 C	EXP0,3
Diffuser D2	21.2 C	EXP0,4
Floor F1	21.7 C	EXP0,5
Floor F2	22.9 C	EXP0,6
Ceiling C1	29.5 C	EXP0,7
Ceiling C2	28.0 C	EXP0,8
Wall OWST	27.1 C	EXP0,9
Wall OWSM	21.8 C	EXP0,10
Wall OWET	24.6 C	EXP0,11

Left Rod	Average Temperature	Channel
364mm	28.3 C	EXP1,0
303mm	26.2 C	EXP1,1
258mm	25.1 C	EXP1,2
167mm	23.3 C	EXP1,3
129mm	23.1 C	EXP1,4
91mm	22.8 C	EXP1,5
45mm	22.9 C	EXP1,6
15mm	23.1 C	EXP1,7

Right rod	Average Temperature	Channel
364mm	28.0 C	EXP1,15
303mm	26.4 C	EXP1,14
258mm	25.2 C	EXP1,13
167mm	23.2 C	EXP1,12
129mm	22.8 C	EXP1,11
91mm	22.6 C	EXP1,10
45mm	22.1 C	EXP1,9
15mm	22.1 C	EXP1,8

Average T over height in model

Height	T (C)
36.5 cm	28.2 C
30.3 cm	26.3 C
25.8 cm	25.2 C
16.7 cm	23.3 C
12.9 cm	22.9 C
9.1 cm	22.7 C
4.5 cm	22.5 C
1.5 cm	22.6 C

Scaling Correction		
TEMPERATURE SCALE	>>>>>>	0.20
POWER SCALE	>>>>>>	2.68
VOLUMETRIC FLOWRATE SCALE	>>>>>>	47.95
MASS FLOWRATE SCALE	>>>>>>	9.85
VELOCITY SCALE	>>>>>>	1.10

EXPERIMENT # 16

Results for air operation

Case	**10 W/m^2**
Cooling Load	314 W
Heat Sources	P1,P2,S2,L
Flow at fans on floor	**76% of total flowrate**
Supply air flow rate	388 cfm 0.18 m^3/s
Velocity at diffusers	0.13 m/s

Average Temperature Field Summary	
T supply	19.2 C
T exhaust	20.3 C
T (0.1m)	19.9 C
T (1.1m)	20.0 C
T(1.7m)	20.2 C
delta T (0.1m-1.1m)	0.1 C
delta T (0.1m-1.7m)	0.3 C

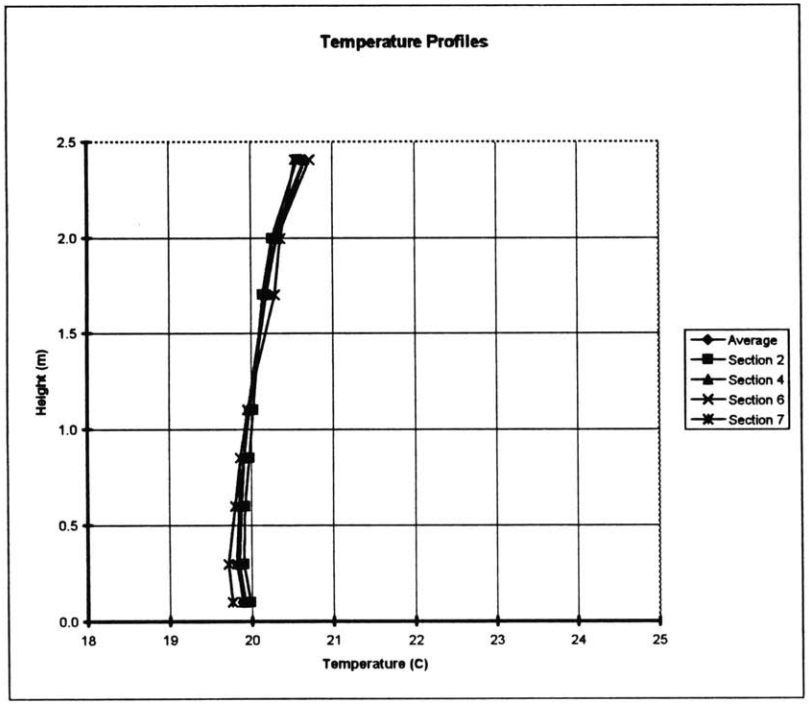

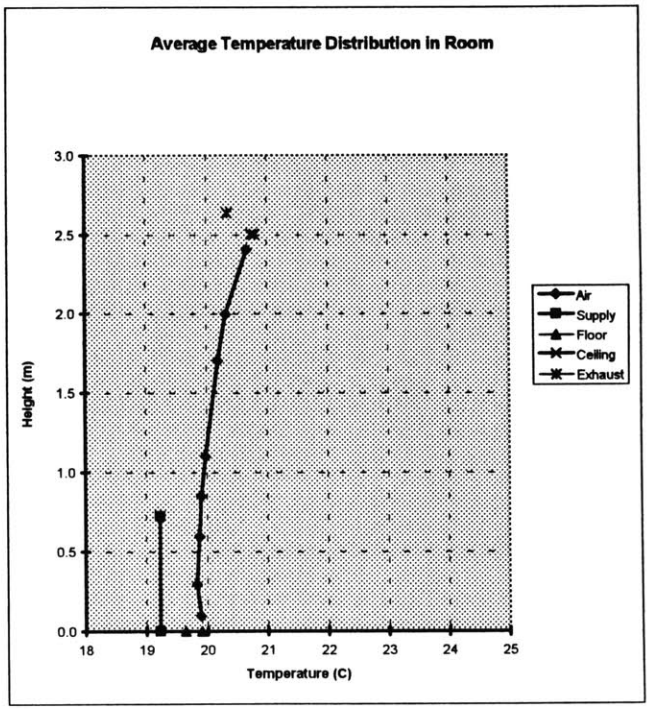

EXPERIMENT # 16

Temps20C.dat

System Data

Considered Case for pure R114	20 W/m2
Actual Case studied	10 W/m2
Oxygen Concentration	5.0%
Air Concentration	24%

Fans	11.02 V
	2.05 cfm each
	6.15 cfm total
	76% of total flowrate

Heat Sources	P1,P2,S2,L
Heat Dissipated	117 W

Monometer Reads	0.05 "wg
Gas Flowrate	8.1 cfm
Velocity at diffuser	0.11 m/s
Water Flowrate	0.11 gpm

Temperature Readings (Average of average readings (x250) for 4 cases)

T gas in	20.1 C	EXP0,14
T gas out	25.8 C	EXP0,13
T water in	15.6 C	EXP0,12
T water out	20.8 C	EXP0,15

Side wall W1	22.0 C	EXP0,0
Side wall W2	22.9 C	EXP0,1
End wall W3	23.9 C	EXP0,2
Diffuser D1	21.6 C	EXP0,3
Diffuser D2	21.0 C	EXP0,4
Floor F1	22.2 C	EXP0,5
Floor F2	23.5 C	EXP0,6
Ceiling C1	28.0 C	EXP0,7
Ceiling C2	27.7 C	EXP0,8
Wall OWST	26.3 C	EXP0,9
Wall OWSM	21.7 C	EXP0,10
Wall OWET	24.2 C	EXP0,11

Left Rod	Average Temperature	Channel
364mm	27.5 C	EXP1,0
303mm	25.6 C	EXP1,1
258mm	25.0 C	EXP1,2
167mm	24.1 C	EXP1,3
129mm	23.7 C	EXP1,4
91mm	23.5 C	EXP1,5
45mm	23.8 C	EXP1,6
15mm	24.2 C	EXP1,7

Right rod	Average Temperature	Channel
364mm	27.2 C	EXP1,15
303mm	25.6 C	EXP1,14
258mm	24.9 C	EXP1,13
167mm	23.7 C	EXP1,12
129mm	23.3 C	EXP1,11
91mm	23.1 C	EXP1,10
45mm	22.5 C	EXP1,9
15mm	22.7 C	EXP1,8

Average T over height in model

Height	T (C)
36.5 cm	27.4 C
30.3 cm	25.6 C
25.8 cm	25.0 C
16.7 cm	23.9 C
12.9 cm	23.5 C
9.1 cm	23.3 C
4.5 cm	23.1 C
1.5 cm	23.5 C

Scaling Correction		
TEMPERATURE SCALE	>>>>>>	0.20
POWER SCALE	>>>>>>	2.68
VOLUMETRIC FLOWRATE SCALE	>>>>>>	47.95
MASS FLOWRATE SCALE	>>>>>>	9.85
VELOCITY SCALE	>>>>>>	1.10

EXPERIMENT # 17

Results for air operation

Case	**27 W/m^2**
Cooling Load	866 W
Heat Sources	P1,P2,P3,S1,S2,S3,X2,L,SW
Flow at fans on floor	**0% of total flowrate**
Supply air flow rate	465 cfm 0.22 m^3/s
Velocity at diffusers	0.15 m/s

Average Temperature Field Summary	
T supply	19.1 C
T exhaust	20.6 C
T (0.1m)	19.7 C
T (1.1m)	20.1 C
T(1.7m)	20.7 C
delta T (0.1m-1.1m)	0.4 C
delta T (0.1m-1.7m)	1.0 C

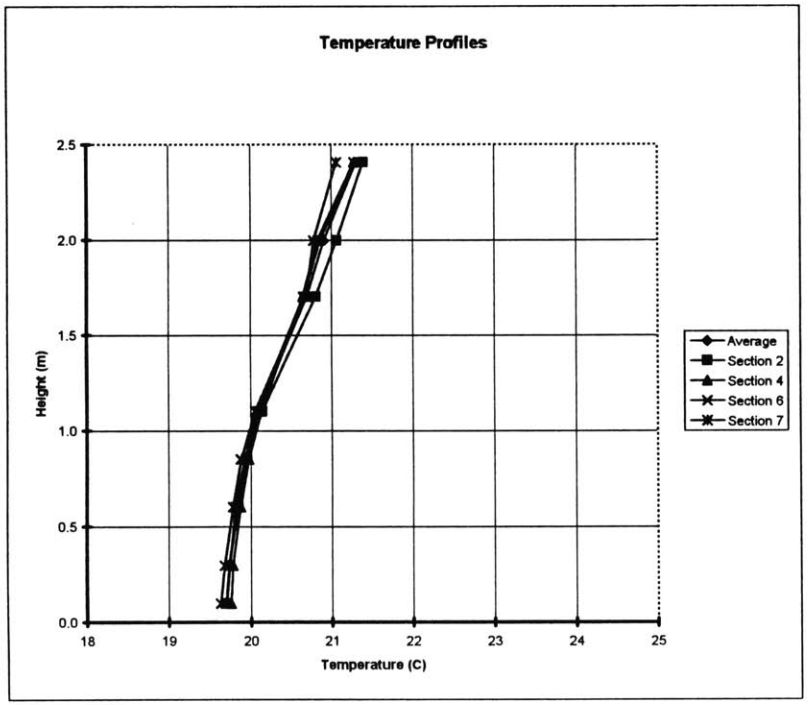

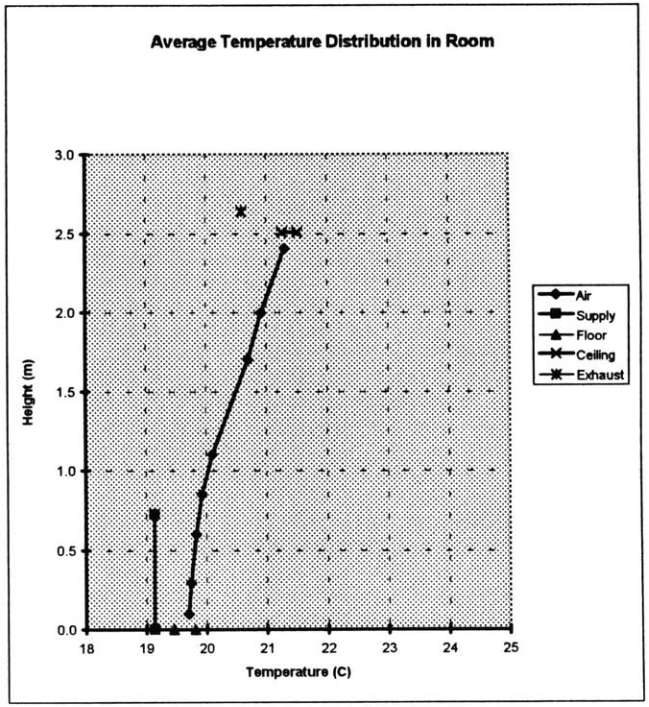

EXPERIMENT # 17

Temps60A.dat

System Data

Considered Case for pure R114	60 W/m2
Actual Case studied	**27 W/m2**
Oxygen Concentration	**5.5%**
Air Concentration	**26%**

Fans	0 V
	0 cfm each
	0 cfm total
	0% of total flowrate

Heat Sources	P1,P2,P3,S1,S2,S3,X2,L,SW
Heat Dissipated	350 W

Monometer Reads	0.075 "wg
Gas Flowrate	10.0 cfm
Velocity at diffuser	0.14 m/s
Water Flowrate	0.35 gpm

Temperature Readings (Average of average readings (x250) for 4 cases)

T gas in	19.7 C	EXP0,14
T gas out	27.6 C	EXP0,13
T water in	15.4 C	EXP0,12
T water out	18.8 C	EXP0,15

Side wall W1	22.5 C	EXP0,0
Side wall W2	25.1 C	EXP0,1
End wall W3	26.8 C	EXP0,2
Diffuser D1	22.3 C	EXP0,3
Diffuser D2	21.5 C	EXP0,4
Floor F1	21.4 C	EXP0,5
Floor F2	23.4 C	EXP0,6
Ceiling C1	32.5 C	EXP0,7
Ceiling C2	31.2 C	EXP0,8
Wall OWST	34.0 C	EXP0,9
Wall OWSM	21.3 C	EXP0,10
Wall OWET	24.9 C	EXP0,11

Left Rod	Average Temperature	Channel
364mm	31.4 C	EXP1,0
303mm	29.3 C	EXP1,1
258mm	28.1 C	EXP1,2
167mm	25.0 C	EXP1,3
129mm	24.0 C	EXP1,4
91mm	23.5 C	EXP1,5
45mm	23.4 C	EXP1,6
15mm	23.5 C	EXP1,7

Right rod	Average Temperature	Channel
364mm	31.4 C	EXP1,15
303mm	29.3 C	EXP1,14
258mm	28.2 C	EXP1,13
167mm	24.9 C	EXP1,12
129mm	23.9 C	EXP1,11
91mm	23.4 C	EXP1,10
45mm	22.5 C	EXP1,9
15mm	22.0 C	EXP1,8

Average T over height in model

Height	T (C)
36.5 cm	31.4 C
30.3 cm	29.3 C
25.8 cm	28.1 C
16.7 cm	24.9 C
12.9 cm	24.0 C
9.1 cm	23.5 C
4.5 cm	23.0 C
1.5 cm	22.7 C

Scaling Correction		
TEMPERATURE SCALE	>>>>>>	0.19
POWER SCALE	>>>>>>	2.48
VOLUMETRIC FLOWRATE SCALE	>>>>>>	46.33
MASS FLOWRATE SCALE	>>>>>>	9.76
VELOCITY SCALE	>>>>>>	1.07

EXPERIMENT # 18

Results for air operation

Case	**27 W/m^2**
Cooling Load	866 W
Heat Sources	P1,P2,P3,S1,S2,S3,X2,L,SW
Flow at fans on floor	**26% of total flowrate**
Supply air flow rate	465 cfm 0.22 m^3/s
Velocity at diffusers	0.15 m/s

Average Temperature Field Summary	
T supply	19.1 C
T exhaust	20.7 C
T (0.1m)	19.8 C
T (1.1m)	20.3 C
T(1.7m)	20.9 C
delta T (0.1m-1.1m)	0.4 C
delta T (0.1m-1.7m)	1.1 C

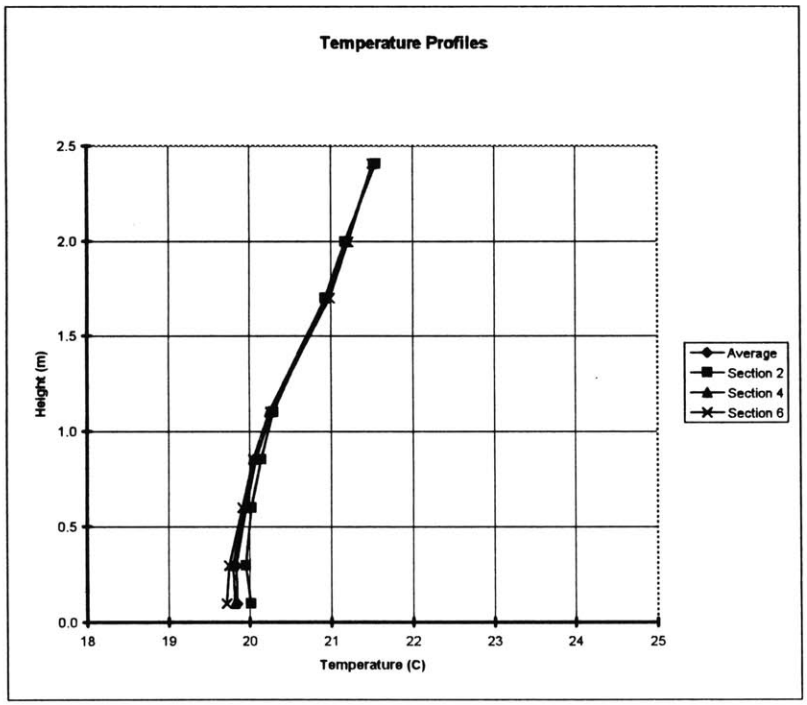

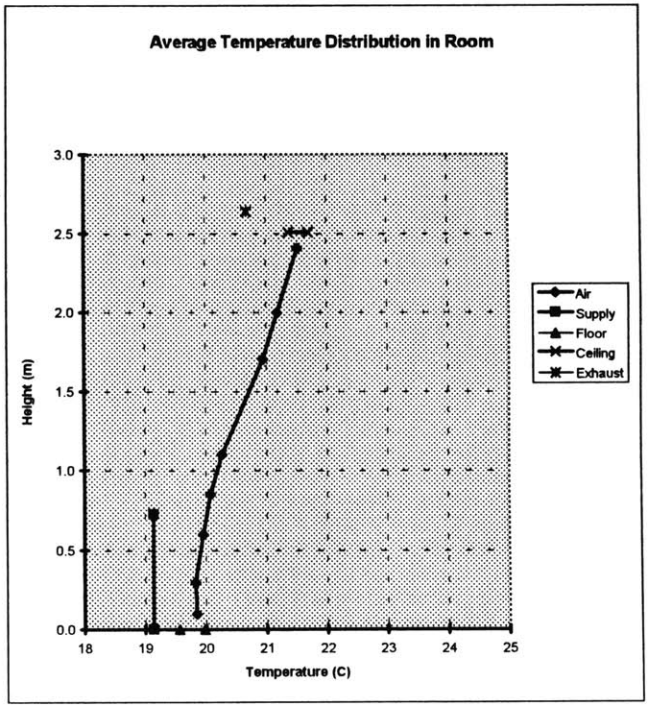

EXPERIMENT # 18

Temps60B.dat

System Data

Considered Case for pure R114	60 W/m2
Actual Case studied	27 W/m2
Oxygen Concentration	5.5%
Air Concentration	26%

Fans	6.06 V
	0.88 cfm each
	2.64 cfm total
	26% of total flowrate

Heat Sources	P1,P2,P3,S1,S2,S3,X2,L,SW
Heat Dissipated	350 W

Monometer Reads	0.075 "wg
Gas Flowrate	10.0 cfm
Velocity at diffuser	0.14 m/s
Water Flowrate	0.35 gpm

Temperature Readings (Average of average readings (x250) for 3 cases)

T gas in	19.7 C	EXP0,14
T gas out	28.0 C	EXP0,13
T water in	15.3 C	EXP0,12
T water out	18.9 C	EXP0,15

Side wall W1	22.3 C	EXP0,0
Side wall W2	25.2 C	EXP0,1
End wall W3	27.1 C	EXP0,2
Diffuser D1	22.2 C	EXP0,3
Diffuser D2	21.7 C	EXP0,4
Floor F1	22.0 C	EXP0,5
Floor F2	24.2 C	EXP0,6
Ceiling C1	33.5 C	EXP0,7
Ceiling C2	31.8 C	EXP0,8
Wall OWST	35.8 C	EXP0,9
Wall OWSM	21.3 C	EXP0,10
Wall OWET	25.3 C	EXP0,11

Left Rod	Average Temperature	Channel
364mm	32.8 C	EXP1,0
303mm	30.9 C	EXP1,1
258mm	29.4 C	EXP1,2
167mm	25.7 C	EXP1,3
129mm	24.7 C	EXP1,4
91mm	24.2 C	EXP1,5
45mm	24.1 C	EXP1,6
15mm	24.2 C	EXP1,7

Right rod	Average Temperature	Channel
364mm	32.3 C	EXP1,15
303mm	30.6 C	EXP1,14
258mm	29.4 C	EXP1,13
167mm	25.9 C	EXP1,12
129mm	24.8 C	EXP1,11
91mm	24.0 C	EXP1,10
45mm	22.8 C	EXP1,9
15mm	22.8 C	EXP1,8

Average T over height in model

Height	T (C)
36.5 cm	32.6 C
30.3 cm	30.8 C
25.8 cm	29.4 C
16.7 cm	25.8 C
12.9 cm	24.8 C
9.1 cm	24.1 C
4.5 cm	23.4 C
1.5 cm	23.5 C

Scaling Correction		
TEMPERATURE SCALE	>>>>>>	0.19
POWER SCALE	>>>>>>	2.48
VOLUMETRIC FLOWRATE SCALE	>>>>>>	46.33
MASS FLOWRATE SCALE	>>>>>>	9.76
VELOCITY SCALE	>>>>>>	1.07

EXPERIMENT # 19

Results for air operation

Case	**27 W/m^2**
Cooling Load	866 W
Heat Sources	P1,P2,P3,S1,S2,S3,X2,L,SW
Flow at fans on floor	**70% of total flowrate**
Supply air flow rate	465 cfm 0.22 m^3/s
Velocity at diffusers	0.15 m/s

Average Temperature Field Summary	
T supply	19.1 C
T exhaust	20.7 C
T (0.1m)	20.2 C
T (1.1m)	20.5 C
T(1.7m)	20.9 C
delta T (0.1m-1.1m)	0.3 C
delta T (0.1m-1.7m)	0.7 C

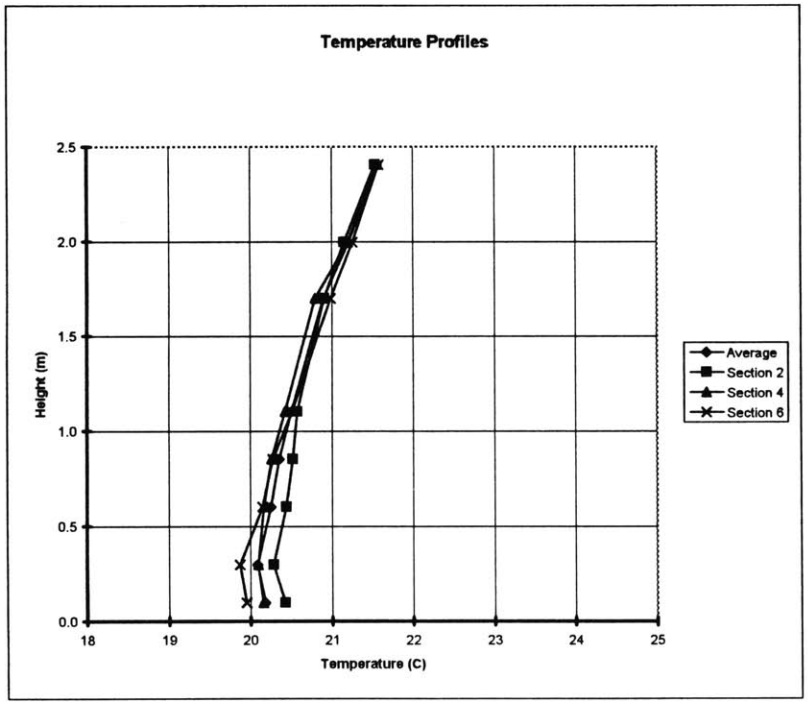

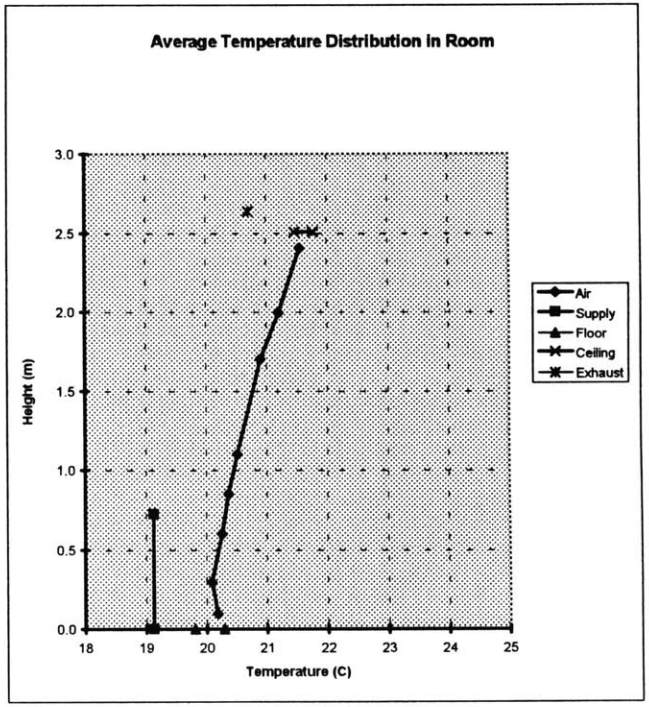

EXPERIMENT # 19

Temps60C.dat

System Data

Considered Case for pure R114	60 W/m2
Actual Case studied	27 W/m2
Oxygen Concentration	5.5%
Air Concentration	26%

Fans	12.04 V
	2.34 cfm each
	7.02 cfm total
	70% of total flowrate

Heat Sources	P1,P2,P3,S1,S2,S3,X2,L,SW
Heat Dissipated	350 W

Monometer Reads	0.075 "wg
Gas Flowrate	10.0 cfm
Velocity at diffuser	0.14 m/s
Water Flowrate	0.35 gpm

Temperature Readings (Average of average readings (x250) for 3 cases)

T gas in	19.7 C	EXP0,14
T gas out	28.1 C	EXP0,13
T water in	15.1 C	EXP0,12
T water out	18.9 C	EXP0,15

Side wall W1	22.8 C	EXP0,0
Side wall W2	25.2 C	EXP0,1
End wall W3	27.3 C	EXP0,2
Diffuser D1	22.2 C	EXP0,3
Diffuser D2	22.1 C	EXP0,4
Floor F1	23.3 C	EXP0,5
Floor F2	25.9 C	EXP0,6
Ceiling C1	34.0 C	EXP0,7
Ceiling C2	32.3 C	EXP0,8
Wall OWST	36.6 C	EXP0,9
Wall OWSM	21.1 C	EXP0,10
Wall OWET	25.3 C	EXP0,11

Left Rod	Average Temperature	Channel
364mm	32.6 C	EXP1,0
303mm	30.8 C	EXP1,1
258mm	29.2 C	EXP1,2
167mm	27.0 C	EXP1,3
129mm	26.2 C	EXP1,4
91mm	25.7 C	EXP1,5
45mm	25.7 C	EXP1,6
15mm	26.3 C	EXP1,7

Right rod	Average Temperature	Channel
364mm	32.8 C	EXP1,15
303mm	30.9 C	EXP1,14
258mm	**** C	EXP1,13
167mm	27.2 C	EXP1,12
129mm	26.3 C	EXP1,11
91mm	25.8 C	EXP1,10
45mm	24.0 C	EXP1,9
15mm	24.4 C	EXP1,8

Average T over height in model

Height	T (C)
36.5 cm	32.7 C
30.3 cm	30.8 C
25.8 cm	29.2 C
16.7 cm	27.1 C
12.9 cm	26.3 C
9.1 cm	25.7 C
4.5 cm	24.8 C
1.5 cm	25.3 C

Scaling Correction		
TEMPERATURE SCALE	>>>>>>	0.19
POWER SCALE	>>>>>>	2.48
VOLUMETRIC FLOWRATE SCALE	>>>>>>	46.33
MASS FLOWRATE SCALE	>>>>>>	9.76
VELOCITY SCALE	>>>>>>	1.07

EXPERIMENT # 20

Results for air operation

Case	**31 W/m^2**
Cooling Load	979 W
Heat Sources	P1,P2,P3,S1,S2,S3,X1,X3,L1,SW
Flow at fans on floor	**60% of total flowrate**
Supply air flow rate	513 cfm 0.24 m^3/s
Velocity at diffusers	0.17 m/s

Average Temperature Field Summary	
T supply	19.2 C
T exhaust	20.6 C
T (0.1m)	20.3 C
T (1.1m)	20.9 C
T(1.7m)	21.3 C
delta T (0.1m-1.1m)	0.6 C
delta T (0.1m-1.7m)	1.0 C

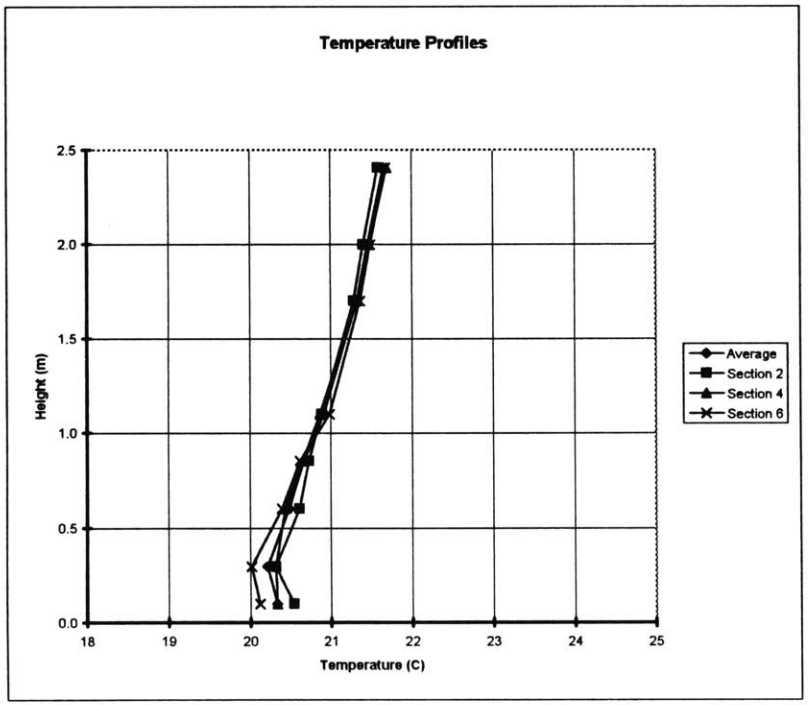

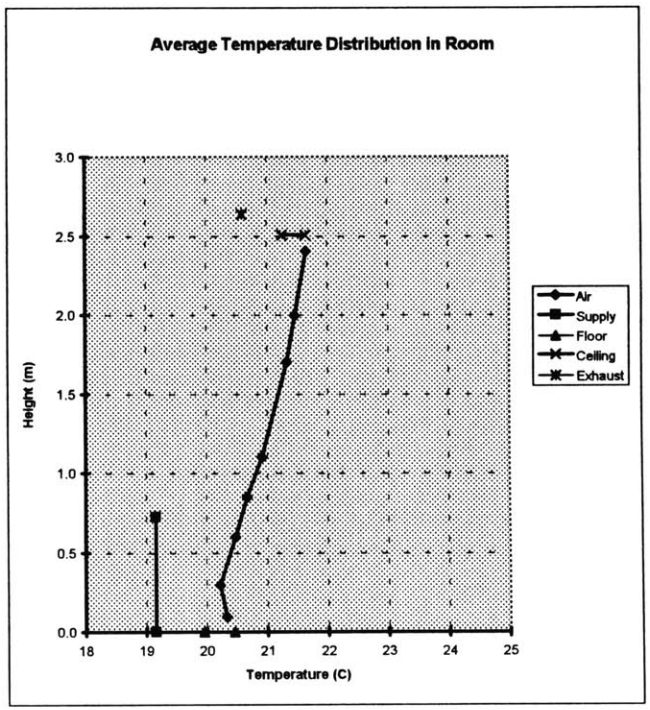

EXPERIMENT # 20

Temps80A.dat (first 3 readings of this file)

System Data

Considered Case for pure R114	80 W/m2
Actual Case studied	**31 W/m2**
Oxygen Concentration	**6.5%**
Air Concentration	**31%**

Heat Sources	P1,P2,P3,S1,S2,S3,X1,X3,L1,SW
Heat Dissipated	467 W

Monometer Reads	0.1 "wg
Gas Flowrate	11.9 cfm
Velocity at diffuser	0.17 m/s
Water Flowrate	0.50 gpm

Fans	
	12.04 V
	2.4 cfm each
	7.2 cfm total
	60% of total flowrate

Temperature Readings (Average of average readings (x250) for 3 cases)

T gas in	20.0 C	EXP0,14
T gas out	29.0 C	EXP0,13
T water in	15.3 C	EXP0,12
T water out	18.7 C	EXP0,15

Side wall W1	23.8 C	EXP0,0
Side wall W2	27.1 C	EXP0,1
End wall W3	29.5 C	EXP0,2
Diffuser D1	22.6 C	EXP0,3
Diffuser D2	23.5 C	EXP0,4
Floor F1	24.9 C	EXP0,5
Floor F2	28.1 C	EXP0,6
Ceiling C1	35.5 C	EXP0,7
Ceiling C2	33.0 C	EXP0,8
Wall OWST	38.7 C	EXP0,9
Wall OWSM	21.4 C	EXP0,10
Wall OWET	25.8 C	EXP0,11

Left Rod	Average Temperature	Channel
364mm	35.5 C	EXP1,0
303mm	34.6 C	EXP1,1
258mm	33.5 C	EXP1,2
167mm	30.4 C	EXP1,3
129mm	28.4 C	EXP1,4
91mm	27.7 C	EXP1,5
45mm	27.6 C	EXP1,6
15mm	28.5 C	EXP1,7

Right rod	Average Temperature	Channel
364mm	35.5 C	EXP1,15
303mm	34.1 C	EXP1,14
258mm	**** C	EXP1,13
167mm	31.4 C	EXP1,12
129mm	30.4 C	EXP1,11
91mm	28.7 C	EXP1,10
45mm	25.5 C	EXP1,9
15mm	26.1 C	EXP1,8

Average T over height in model

Height	T (C)
36.5 cm	35.5 C
30.3 cm	34.3 C
25.8 cm	33.5 C
16.7 cm	30.9 C
12.9 cm	29.4 C
9.1 cm	28.2 C
4.5 cm	26.6 C
1.5 cm	27.3 C

Scaling Correction		
TEMPERATURE SCALE	>>>>>>	0.16
POWER SCALE	>>>>>>	2.10
VOLUMETRIC FLOWRATE SCALE	>>>>>>	43.12
MASS FLOWRATE SCALE	>>>>>>	9.58
VELOCITY SCALE	>>>>>>	0.99

EXPERIMENT # 21

Results for air operation

Case	**31 W/m^2**
Cooling Load	979 W
Heat Sources	P1,P2,P3,S1,S2,S3,X1,X3,L1,SW
Flow at fans on floor	**0% of total flowrate**
Supply air flow rate	629 cfm 0.30 m^3/s
Velocity at diffusers	0.20 m/s

Average Temperature Field Summary	
T supply	19.2 C
T exhaust	20.7 C
T (0.1m)	20.0 C
T (1.1m)	20.9 C
T(1.7m)	21.5 C
delta T (0.1m-1.1m)	0.9 C
delta T (0.1m-1.7m)	1.5 C

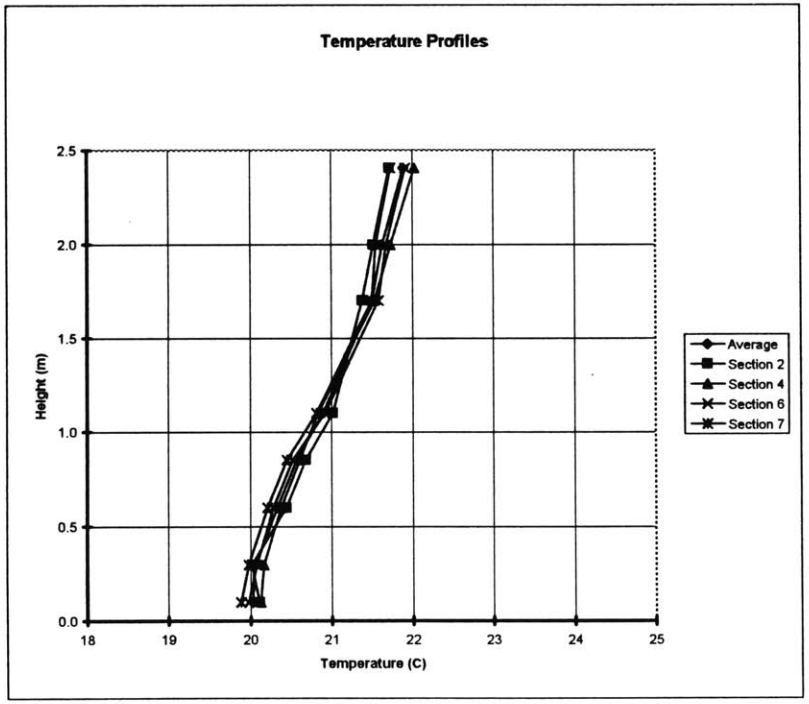

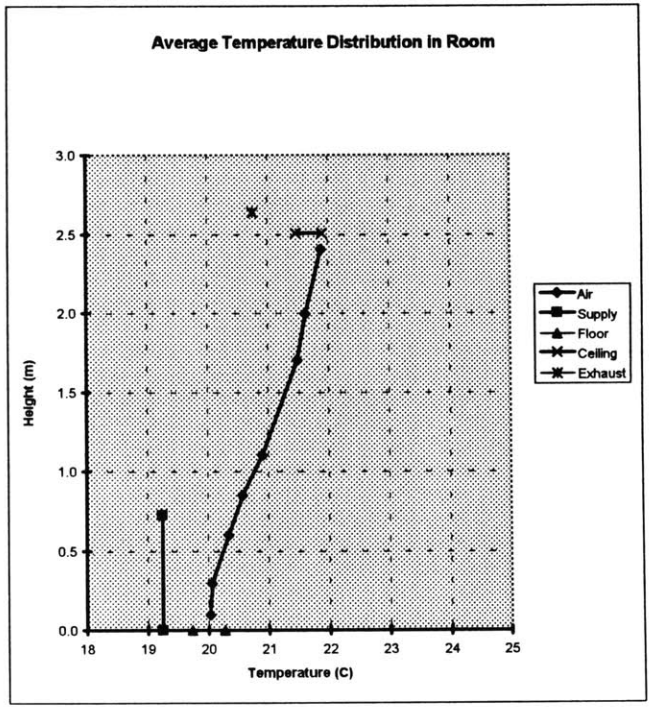

EXPERIMENT # 21

Temps80A.dat (last 4 readings of this file)

System Data

Considered Case for pure R114	80 W/m2
Actual Case studied	31 W/m2
Oxygen Concentration	6.5%
Air Concentration	31%

Fans	0 V
	0 cfm each
	0 cfm total
	0% of total flowrate

Heat Sources	P1,P2,P3,S1,S2,S3,X1,X3,L1,SW
Heat Dissipated	467 W

Monometer Reads	0.15 "wg
Gas Flowrate	14.6 cfm
Velocity at diffuser	0.20 m/s
Water Flowrate	0.75 gpm

Temperature Readings (Average of average readings (x250) for 4 cases)

T gas in	20.5 C	EXP0,14
T gas out	29.9 C	EXP0,13
T water in	15.3 C	EXP0,12
T water out	18.6 C	EXP0,15

Side wall W1	24.7 C	EXP0,0
Side wall W2	28.1 C	EXP0,1
End wall W3	31.1 C	EXP0,2
Diffuser D1	23.2 C	EXP0,3
Diffuser D2	24.0 C	EXP0,4
Floor F1	23.5 C	EXP0,5
Floor F2	26.9 C	EXP0,6
Ceiling C1	37.1 C	EXP0,7
Ceiling C2	34.4 C	EXP0,8
Wall OWST	40.9 C	EXP0,9
Wall OWSM	21.4 C	EXP0,10
Wall OWET	26.6 C	EXP0,11

Left Rod	Average Temperature	Channel
364mm	37.2 C	EXP1,0
303mm	35.5 C	EXP1,1
258mm	34.6 C	EXP1,2
167mm	30.8 C	EXP1,3
129mm	28.2 C	EXP1,4
91mm	26.8 C	EXP1,5
45mm	26.1 C	EXP1,6
15mm	26.3 C	EXP1,7

Right rod	Average Temperature	Channel
364mm	36.8 C	EXP1,15
303mm	35.2 C	EXP1,14
258mm	**** C	EXP1,13
167mm	30.9 C	EXP1,12
129mm	29.4 C	EXP1,11
91mm	27.8 C	EXP1,10
45mm	25.1 C	EXP1,9
15mm	24.5 C	EXP1,8

Average T over height in model

Height	T (C)
36.5 cm	37.0 C
30.3 cm	35.4 C
25.8 cm	34.6 C
16.7 cm	30.8 C
12.9 cm	28.8 C
9.1 cm	27.3 C
4.5 cm	25.6 C
1.5 cm	25.4 C

Scaling Correction		
TEMPERATURE SCALE	>>>>>>	0.16
POWER SCALE	>>>>>>	2.10
VOLUMETRIC FLOWRATE SCALE	>>>>>>	43.12
MASS FLOWRATE SCALE	>>>>>>	9.58
VELOCITY SCALE	>>>>>>	0.99

EXPERIMENT # 22

Results for air operation

Case	**31 W/m^2**
Cooling Load	979 W
Heat Sources	P1,P2,P3,S1,S2,S3,X1,X3,L1,SW
Flow at fans on floor	**18% of total flowrate**
Supply air flow rate	629 cfm 0.30 m^3/s
Velocity at diffusers	0.20 m/s

Average Temperature Field Summary	
T supply	19.3 C
T exhaust	20.8 C
T (0.1m)	20.2 C
T (1.1m)	20.9 C
T(1.7m)	21.5 C
delta T (0.1m-1.1m)	0.7 C
delta T (0.1m-1.7m)	1.3 C

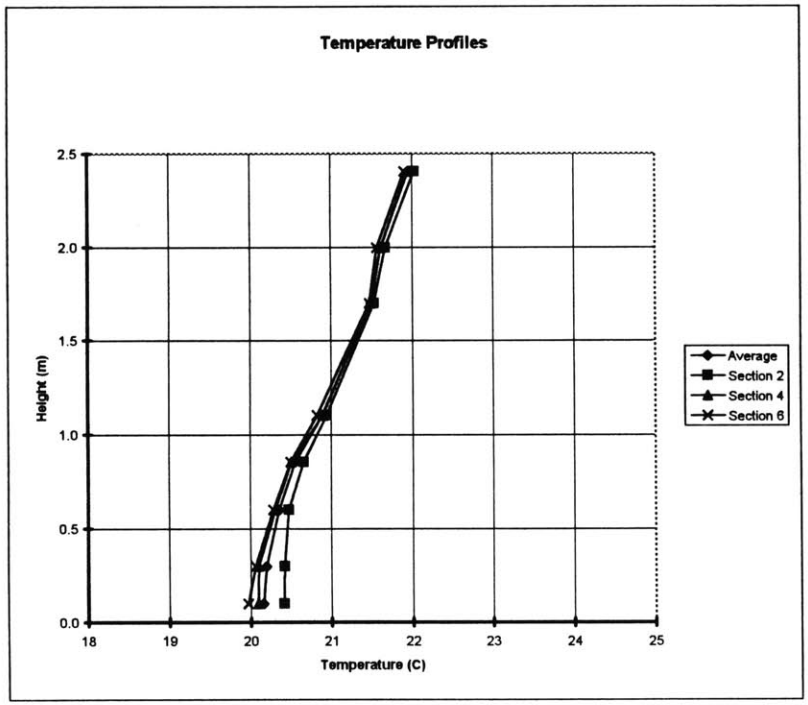

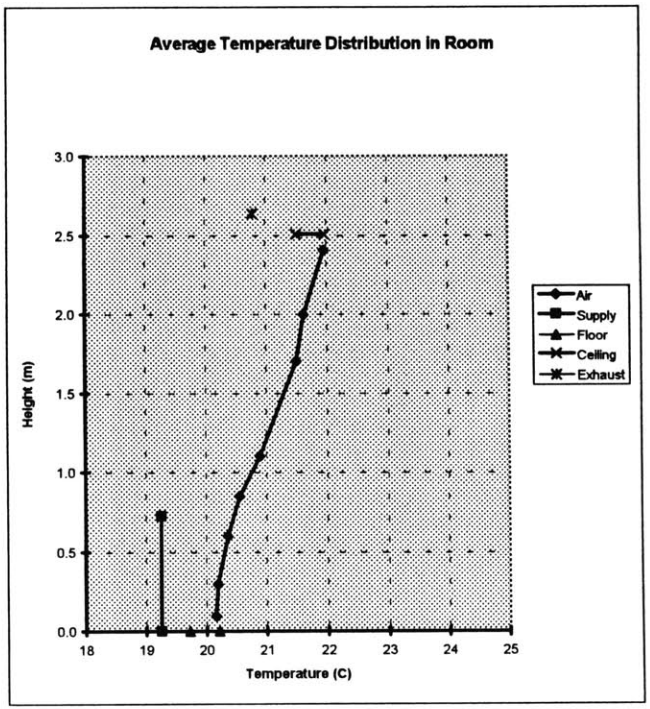

EXPERIMENT # 22

Temps80B.dat

System Data

Considered Case for pure R114	80 W/m2
Actual Case studied	31 W/m2
Oxygen Concentration	6.5%
Air Concentration	31%

Fans	6 V
	0.89 cfm each
	2.67 cfm total
	18% of total flowrate

Heat Sources	P1,P2,P3,S1,S2,S3,X1,X3,L1,SW
Heat Dissipated	467 W

Monometer Reads	0.15 "wg
Gas Flowrate	14.6 cfm
Velocity at diffuser	0.20 m/s
Water Flowrate	0.75 gpm

Temperature Readings (Average of average readings (x250) for 3 cases)

T gas in	20.6 C	EXP0,14
T gas out	30.1 C	EXP0,13
T water in	15.3 C	EXP0,12
T water out	18.5 C	EXP0,15

Side wall W1	24.6 C	EXP0,0
Side wall W2	28.2 C	EXP0,1
End wall W3	31.3 C	EXP0,2
Diffuser D1	23.3 C	EXP0,3
Diffuser D2	24.2 C	EXP0,4
Floor F1	23.5 C	EXP0,5
Floor F2	26.5 C	EXP0,6
Ceiling C1	37.5 C	EXP0,7
Ceiling C2	34.6 C	EXP0,8
Wall OWST	41.9 C	EXP0,9
Wall OWSM	21.6 C	EXP0,10
Wall OWET	27.1 C	EXP0,11

Left Rod	Average Temperature	Channel
364mm	37.7 C	EXP1,0
303mm	35.6 C	EXP1,1
258mm	34.6 C	EXP1,2
167mm	30.4 C	EXP1,3
129mm	28.0 C	EXP1,4
91mm	26.8 C	EXP1,5
45mm	26.5 C	EXP1,6
15mm	26.5 C	EXP1,7

Right rod	Average Temperature	Channel
364mm	37.2 C	EXP1,15
303mm	35.0 C	EXP1,14
258mm	**** C	EXP1,13
167mm	31.1 C	EXP1,12
129mm	29.4 C	EXP1,11
91mm	28.0 C	EXP1,10
45mm	26.4 C	EXP1,9
15mm	25.9 C	EXP1,8

Average T over height in model

Height	T (C)
36.5 cm	37.4 C
30.3 cm	35.3 C
25.8 cm	34.6 C
16.7 cm	30.7 C
12.9 cm	28.7 C
9.1 cm	27.4 C
4.5 cm	26.4 C
1.5 cm	26.2 C

Scaling Correction		
TEMPERATURE SCALE	>>>>>>	0.16
POWER SCALE	>>>>>>	2.10
VOLUMETRIC FLOWRATE SCALE	>>>>>>	43.12
MASS FLOWRATE SCALE	>>>>>>	9.58
VELOCITY SCALE	>>>>>>	0.99

EXPERIMENT # 23

Results for air operation

Case	**31 W/m^2**
Cooling Load	979 W
Heat Sources	P1,P2,P3,S1,S2,S3,X1,X3,L1,SW
Flow at fans on floor	**49% of total flowrate**
Supply air flow rate	629 cfm 0.30 m^3/s
Velocity at diffusers	0.20 m/s

Average Temperature Field Summary	
T supply	19.2 C
T exhaust	20.7 C
T (0.1m)	20.4 C
T (1.1m)	20.9 C
T(1.7m)	21.3 C
delta T (0.1m-1.1m)	0.5 C
delta T (0.1m-1.7m)	0.9 C

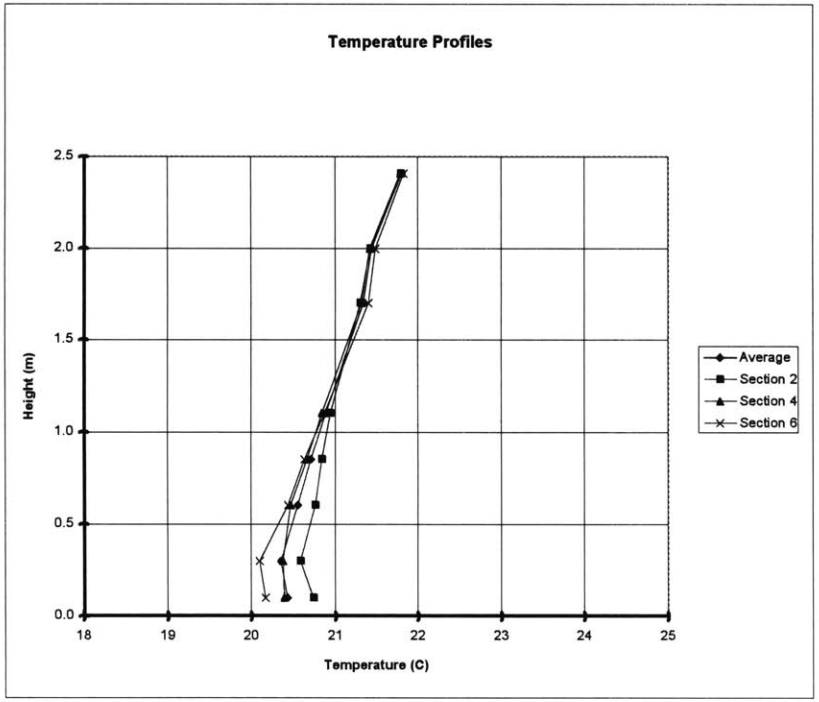

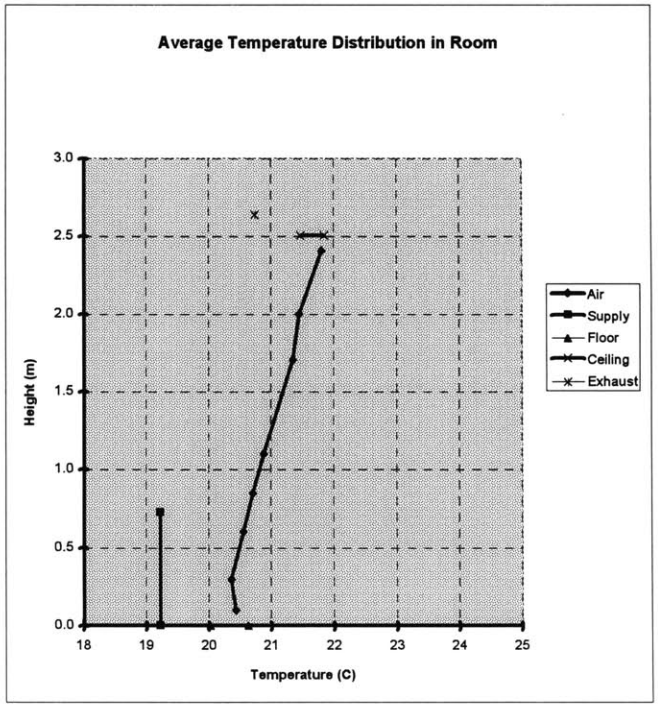

EXPERIMENT # 23

Temps80C.dat

System Data

Considered Case for pure R114	80 W/m2
Actual Case studied	31 W/m2
Oxygen Concentration	6.5%
Air Concentration	31%

Fans	12 V
	2.4 cfm each
	7.2 cfm total
	49% of total flowrate

Heat Sources	P1,P2,P3,S1,S2,S3,X1,X3,L1,SW
Heat Dissipated	467 W

Monometer Reads	0.15 "wg
Gas Flowrate	14.6 cfm
Velocity at diffuser	0.20 m/s
Water Flowrate	0.75 gpm

Temperature Readings (Average of average readings (x250) for 3 cases)

T gas in	20.3 C	EXP0,14
T gas out	29.9 C	EXP0,13
T water in	15.0 C	EXP0,12
T water out	18.5 C	EXP0,15

Side wall W1	24.7 C	EXP0,0
Side wall W2	28.0 C	EXP0,1
End wall W3	31.1 C	EXP0,2
Diffuser D1	23.6 C	EXP0,3
Diffuser D2	24.4 C	EXP0,4
Floor F1	25.3 C	EXP0,5
Floor F2	29.1 C	EXP0,6
Ceiling C1	36.7 C	EXP0,7
Ceiling C2	34.4 C	EXP0,8
Wall OWST	41.4 C	EXP0,9
Wall OWSM	21.3 C	EXP0,10
Wall OWET	27.3 C	EXP0,11

Left Rod	Average Temperature	Channel
364mm	36.5 C	EXP1,0
303mm	34.6 C	EXP1,1
258mm	33.6 C	EXP1,2
167mm	30.2 C	EXP1,3
129mm	29.0 C	EXP1,4
91mm	28.5 C	EXP1,5
45mm	28.6 C	EXP1,6
15mm	29.2 C	EXP1,7

Right rod	Average Temperature	Channel
364mm	36.4 C	EXP1,15
303mm	33.9 C	EXP1,14
258mm	**** C	EXP1,13
167mm	31.3 C	EXP1,12
129mm	30.3 C	EXP1,11
91mm	28.9 C	EXP1,10
45mm	26.3 C	EXP1,9
15mm	26.7 C	EXP1,8

Average T over height in model

Height	T (C)
36.5 cm	36.5 C
30.3 cm	34.2 C
25.8 cm	33.6 C
16.7 cm	30.7 C
12.9 cm	29.7 C
9.1 cm	28.7 C
4.5 cm	27.4 C
1.5 cm	27.9 C

Scaling Correction

TEMPERATURE SCALE	>>>>>>	0.16
POWER SCALE	>>>>>>	2.10
VOLUMETRIC FLOWRATE SCALE	>>>>>>	43.12
MASS FLOWRATE SCALE	>>>>>>	9.58
VELOCITY SCALE	>>>>>>	0.99